NASA CR-
144439

Oak Ridge Associated Universities

STUDIES RELATIVE TO THE RADIOSENSITIVITY OF MAN: BASED ON RETROSPECTIVE EVALUATIONS OF THERAPEUTIC AND ACCIDENTAL TOTAL-BODY IRRADIATION

FINAL REPORT

T-88566

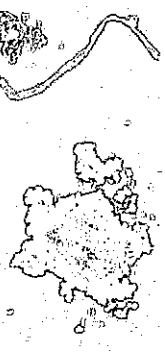

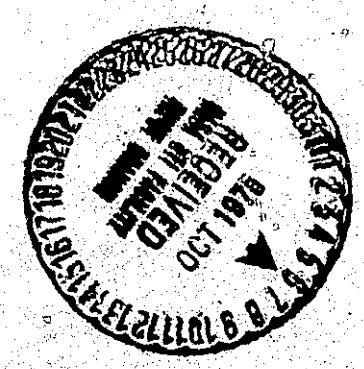

Report written and compiled by R. C. Ricks and C. C. Lushbaugh.

Study Completion Date: June 30, 1975

Report Completed: September 1, 1975

CHAPTER I

SUMMARY AND COMMENTS

This report compiles in a somewhat abbreviated fashion the bulk of the radiobiologic studies carried out with joint (AEC) ERDA and NASA support during the years 1964 to 1974 at the Medical Division of Oak Ridge Associated Universities. Their termination was directed by a decreased urgency on the part of NASA for broadly focused human radiobiologic data and on the part of ERDA for a redirection of ORAU's Medical Division efforts away from radiotherapy toward occupational medical problems that are being generated by the increasing demands for energy from non-nuclear sources.

The physiologic data generated by this study were similar in many ways to those previously observed in other medical radiobiologic experiences. They differed, however, in the methods of data acquisition and analysis. Instead of more conventional analytical methods, pulmonary impedance was recorded and quantitated as a measure of radiation-induced gastrointestinal distress and fatiguability.

While refinements in dose response related to gastrointestinal distress were accomplished we also found that through the use of Fourier analysis of pulmonary impedance waveform GI distress could easily be recognized and quantified even when the initial stages of nausea were below the subjects subjective level of recognition. Our results demonstrate that change in pulmonary impedance waveform closely parallel well-defined stages of GI distress, i.e., initial nausea, a progressive increase in nausea, and finally vomiting episodes. These stages of GI distress are

similar when induced chemically or by exposure to ionizing radiations although that induced by radiation is often sudden in onset and little nausea may proceed the actual emetic episode. Throughout the study period, pulmonary impedance waveform analysis never failed to recognize radiation-induced GI distress. Finally, these data demonstrate that real-time analysis of GI status with continuous data update can be accomplished using Fourier analysis of the pulmonary impedance waveform monitored from a remote, isolated environment.

Attempts to measure and quantify radiation-induced physical deconditioning using pulmonary impedance waveform analysis were not as clearly delineated as in the case of gastrointestinal distress. Pulmonary impedance measured before, during, and after controlled exercise stress (ergometry) correlated very well with periods of physical stress. Increased respiratory demand during submaximal exercise stress was accompanied by increased pulmonary impedance variance and within stress periods an increase or decrease in workload was accompanied by respective shifts in pulmonary impedance waveform. However, exposure to ionizing radiations resulted in amplified (increased) pulmonary impedance variance in over 80% of those humans studied although the ergometric workload remained unchanged. Thus, it would appear that exposure to radiation resulted in increased respiratory demand to perform at a constant, non-varying workload. Analysis of cardiac rate during controlled exercise stress in control volunteers and therapeutically likewise demonstrated increased response in over 70% of those patients who participated in the study. We believe that these amplified cardiac rates are indicative of diminished cardiovascular efficiency since workloads were non-varying

throughout each patient study period. Since some radiobiologists believe that venodilation and decreased venous compliance occur during early postirradiation periods (hours to several days) a pooling of blood in the venous system could account for increased cardiac rates and increased pulmonary impedance (increased mediastinal blood mass) postirradiation.

Efforts to model these data with those of other physical deconditioning experiments led to O_2 consumption measurements. Using bedrest as a typical model we found that a remarkable similarity exists between the decrement cause by 21 days of bedrest and exposure to 100 R irradiation. Unfortunately, we were able to study only one therapy patient in the time period between developing our capability for O_2 consumption measurement and the termination of the inpatient therapy program of our Division.

The important question remains unanswered as to whether or not radiation-induced physical deconditioning and that induced by bedrest (weightlessness) are additive. If they are the threshold radiation dose would be lowered as mission length was increased unless strong countermeasures were used to prevent or retard zero-G deconditioning. Another facet of this physiologic problem that remains to be considered is whether the level of physical training (vigorous in astronauts) can affect the degree of physical deconditioning. Some studies, needing to be confirmed, suggest that the well-conditioned individual may react more strongly and recover more slowly than a non-conditioned person. Our study of performance after radiation exposure using controlled exercise stress in physically trained and untrained ponies supports this suggestion in that the conditioned animals responded with a greater degree of decrement than the

unconditioned ones. The biochemical mechanisms underlying this phenomenon need to be studied without necessarily any reference to radiation exposure because of its general applicability to everyday life as well as to disease.

Our hematologic studies concerning the changing patterns of peripheral blood cell numbers after irradiation produced significant improvement in the quantitative aspects of the problem, particularly in defining the doubling times for human leukocytes in terms of repair kinetics.

The laboratory studies showed that rapid cell sizing techniques provided an additional parameter to hematologic studies that improved speed of quantitation and diagnosis. In polycythemia rubra vera, for example, changes in RBC morphology proved to be extremely useful in appraising the relative sizes of the iron and erythroblastic pools after radiation exposure. The unique observation of serum CPK rise after a large accidental radiation exposure in a man could not be confirmed in subsequent study in animals. Nevertheless, it led us to evaluate serum CPK levels before and after radiation exposure. The results of this study suggested that changes in muscle CPK as reflected in serum CPK levels may be related to fatigue and ability to perform physical work. This lead needs to be pursued further.

The simultaneous studies of human and mouse hemic responses to the same low dose rates and daily dose point up the threefold greater radiation resistance of mouse over man while suggesting what the basic lethal mechanisms may be for man under various conditions of low dose-rate irradiation as it approaches about one rad per day.

These studies are, of course, not to be considered definitive and without need for substantiation and extension. Only changing priorities places them, in our opinion, on "the back burner" for the moment.

R. C. Ricks

C. C. Lushbaugh

CHAPTER II

OBJECTIVES AND SCOPE

The objective of this study was to glean from human accidental and therapeutic irradiation case histories all pertinent radiobiologic information for reappraising and improving our knowledge of man's radiosensitivity. This study was cooperative with an ERDA supported study of total-body irradiation as a therapeutic modality for human blood dyscrasias. Where the AEC/ERDA study concerned itself with clinical aspects, this NASA study was directed toward extracting measurable information on biologic endpoints of radiation effects. Study areas that received major emphasis were: hematology, gastrointestinal side effects, dosimetry, and physiologic monitoring for performance decrement.

The need for more quantitative information on the effects of low radiation doses and low-dose-rate exposures was generated by NASA program planning that involved manned space flights. The plans for space laboratories expanded the number of persons at risk from the low doses of natural space radiation and included the possibility that an additional risk might arise from manmade radiation associated with the use of nuclear power generating systems. Our studies were intended to strengthen the confidence we presently have in our knowledge of man's ability to repair radiation damage so that ERDA, NRC, NASA, and other governmental agencies could establish nonoccupational permissible radiation exposure levels and continually review and update NASA occupational career limits for radiation exposure of astronauts as required for engineering design of advanced systems. While knowledge of the effects of larger radiation exposures at

high and low dose rates is growing substantially, it is as yet inadequate for deriving dose/response equations that allow high-confidence predictions of the amount of acute and chronic damage that can be expected from small doses to the total body or its parts. Extrapolations that estimate effects from extremely low exposures accumulated over long periods of time on the basis of studies of high exposure sustained in short periods of time, derive all of their justification from radiobiological studies of lower mammals (chiefly mice). Some observations indicate that after a 5 to 10 rad dose, for example, the probability of a serious consequence occurring in an individual's lifetime is so low that a threshold concept is valid for practical regulatory purposes. Confidence was limited on previous conjectures concerning the levels of radiation that could cause detrimental human reactions. The inherent difficulties in evaluating voluminous clinical data containing numerous variables however have now been largely overcome. Modern research methods using computers with large memory storage capacity have enabled us to construct a human radiation injury data bank containing clinical data from more than 3000 human total body irradiation exposures in the United States. These charts have been extracted, encoded, and were analyzed by modern mathematical electronic computer methods. The Oak Ridge Associated Universities (ORAU) patient studies obtained in a radiotherapeutic program since 1957 and additional human studies ($\sim$ 3000 cases) obtained from other hospital centers with similar studies were incorporated into a study to determine dose relationships in man for anorexia, nausea, vomiting, diarrhea, fatigue, weight loss, fever, erythema, epilation, lymphopenia, granulocytopenia, anemia, thrombocytopenia, cytogenetic damage, decreased

resistance to infection, decreased antibody synthesis, increased aging, and carcinogenesis. The values were assessed for degree of clinical and mathematical confidence to permit their use in predicing man's reaction to the ambient radiations of space, and to direct further clinical exploration on the effect of ionizing radiation upon cancerous and normal processes.

Additionally, there were multiple reasons for this study overall. Therapeutic total-body irradiation is efficacious in controlling some cases of leukemia and lymphoma and ameliorating symptoms in others. The possibility that low dose rates may favor repair of normal tissue in contrast to malignant processes had not been evaluated in the present modern era of radiotherapy and radiobiology; we proposed to test this hypothesis with a radiation facility producing an isotropic flux of uniform radiation giving low rates of exposure. This irradiator was large enough for patients to live in comfortably for several weeks. Because of expanding programs in nuclear energy and space exploration, the need was more acute than ever for data derived directly by observation of man's reaction rather than assumed from animal studies. The retrospective accumulation of such data as was available showed that the old data suffered from lack of modern dosimetry, tissue depth dose knowledge, biased recording of symptomatology, and incomplete and inaccurate records. Finally, these additional unbiased clinical observations were sorely needed to defend existing environmental and occupational radiation exposure constraints from attack by well-meaning, but impractical, theorists.

CHAPTER III

RETROSPECTIVE STUDIES

A. Human Radiation Effects Data Bank

Initial efforts were directed at establishing a case origin for human radiobiologic experiences from therapeutic or accidental exposures. Contacts were made through the University of Cincinnati and City of Hope (Duarte, California) Hospitals to secure human radiotherapy data to compliment the 100 case experiences previously accumulated at the ORAU Medical Division. This data base of cases of human clinical experiences was ultimately expanded to over 2500 therapeutic exposure experiences from 45 contributing institutions (see Appendix A). In addition, data were accumulated from reports of ORAU staff medical assistance in accidental radiation exposures at both national and foreign levels.

The actual clinical data recorded in all human whole body radiation exposures obtained was extracted and encoded in such a form that the volume of data and its complexity was minimized by modern mathematical electronic computer methods. First, emphasis was placed on developing an analytical system basic to probit analysis to determine where apparent dose-response relationships existed that could be used in probit regression equations and effective doses (ED_{50}) with acceptable fiducial confidence limits. Although probit analysis was neither designed nor intended to be used in retrospect so that deviations from implied assumptions are not ascertainable with it, our use of it appears justified by its widespread use in experimental radiobiology and allowed relative comparisons to be made between sick and well persons and various species of small and large animals. We applied methods used in testing of inanimate engineering components for reliability

and durability. The Weibull density function that describes wear out failure, predicting the time that any rate of failure will be evident, seemed promising, since most symptoms and signs of biological distress can be considered as evidence for "wear out" of a homeostatic physiologic system. These data were then used to appraise the extent to which probability estimates of what doses, rates, and quality of radiation of energies will be met during two-week to two-year missions.

B. Dosimetry

The single most important factor affecting the validity of our retrospective determination of human dose-response relations was the accuracy of each dose estimate. The statistical analysis commonly used in such studies contains the assumption that the independent variable, dose, is known precisely while the biological response may not be accurately measured.

The retrospective study was divided into four phases. Phase I was a pilot study of only 100 single exposures of less than 24 hr in patients at the Medical Division. Phase II was an extension of this study to test the feasibility of using data from other hospitals and also included only single radiation exposures. Phase III included single and fractionated exposures (greater than one day and less than eight days). Phase IV evaluated protracted exposures where exposure time was greater than eight days.

Phase I. Phase I was composed of 93 single-exposure cases of therapeutically administered total-body irradiation (TBI) and seven cases of accidental TBI (Y-12 accident). Eighty-four of these were treated

with the Division's medium-exposure-rate total body irradiator (METBI) and the other nine were treated with the Division's cobalt-60 irradiator (Barnes teletherapy unit).

The dose estimates for the 93 patients were based on a dosimetry study by Hayes et al. (Int. J. Appl. Radiat. 15: 313-318, 1964). The dosimetric system consisted of an aqueous ferrous sulfate solution (Fricke dosimeter) within a plexiglass phantom. The absorbed dose to the solution was taken as the patient's dose when he was exposed to the same amount of radiation.

Using this technique we determined the whole-body average dose (WBAD) and the midepigastric dose for all 93 patients. The WBAD is an estimate of the average energy absorbed per gram of tissue, where the average is taken for every gram of tissue in the body. The midepigastric dose is an estimate of the average energy absorbed per gram in the upper abdominal compartment.

The dose estimates for the seven Y-12 accident cases were determined by a mock-up of the accident at its site (a complete description of this accident can be found in several reports relating to various catagorical aspects).

Phase II. Phase II extended the pilot study by the addition of 11 new ORAU cases, 29 from Cincinnati General Hospital, Cincinnati, Ohio and 23 from the City of Hope Medical Center, Duarte, California, bringing the total number of patients in the study to 163.

The dose estimates for the new ORAU cases were made with the same technique described in Phase I. However, all the ORAU dose estimates were modified for patient size. The size-correction factors were determined

from the experimental measurements of the absorbed dose in three phantoms representative of an adult, an adolescent, and a child.

The dose estimates for the Cincinnati and City of Hope cases were based on a comparison of phantom depth-dose measurements made at each facility.

Phase III. The addition of about 600 patients from 24 institutions with both single and fractionated exposures brought the total number under study to more than 750. Approximately 50 treatment techniques were used and 'dosage' was recorded in more than 15 different units. To make these doses comparable to those in Phase I and II it was necessary to convert the variously reported doses to total-body average dose.

Table 1 shows the dose distribution of the 504 cases for whom total-body average dose were originally estimated.

Of the 600 new cases only 66 were treated with gamma rays from isotopic sources and 39 of these were from institutions included in Phase II. We estimated the absorbed dose for 40 of these on the basis of experimental phantom measurements made at each facility. No dose estimates for the other 26 patients could be made owing to lack of phantom data.

Doses were estimated for 310 of 535 cases of X-ray TBI with the use of a method developed by Mayneord (1). Mayneord's method was experimentally verified by phantom measurements before its use. With it we estimated the total-body average dose for all cases of bilateral X-ray TBI having qualities expressed as half-value layers of from 0.5 mm to 4.2 mm of copper. For most of the other cases of X-ray TBI, the free-air exposure is the only 'dosage' parameter available.

TABLE 1

Dose Distribution of 504 Cases

Whole-Body Average Dose (in rads)	Number of Cases
0-25	149
26-50	108
51-75	90
76-100	19
101-125	17
126-150	36
151-200	19
201-250	26
251-300	4
301-400	15
401-500	7
501-700	7
701-900	2
901-1100	3
1101-1300	2
	504

There were only 34 cases of the 757 single exposures to be considered in Phase III for whom we were not able to estimate either the total-body average dose or the free-air exposure, less than a 5% loss of cases due to insufficient dosimetry data.

Since the completion of these early effects to establish a human radiobiologic data bank efforts have continued to add to an update information for future retrieval. Considerable additional therapy experience at ORAU Medical Division and data from radiation accidents have resulted in a data bank containing information on 2063 cases of radiation exposure. Of these, 16 are cases of accidental exposures and are encoded as single exposures. The remaining 2047 cases are therapeutic exposures and these data were obtained from the records of the hospitals identified in Appendix A.

There are five types of exposures in the data bank. A "single exposure" was defined as any number of short exposures within a 24 hr period with any number of time intervals between exposures or any exposure of a continuous nature lasting less than 36 hr. A single or continuous exposure was generally a "Heublein exposure" if it was greater than 36 hr in duration. A "multiple exposure" was any treatment which the patient was treated with more than one single exposure within a six-week period. The isotope and portal exposure data was taken only from ORAU patients.

The NASA Retrospective Data Bank is composed of multiple records keyed by record type, hospital number, patient number, date, and hour. Because of the retrospective nature of the data collection (some treatments go back to 1931), all possible data are not available on every case or treatment. The data are stored on six magnetic tapes and may be described as follows:

Tape 1--Identification (87,343 records)

A0 Patient name, sex, race, etc. (1,803 records)

A1 Total body exposure data (19,928 records)

I2 Isotope exposure data (432 records)

D0 Death information (1,076 records)

T0 General exposure information such as source, distance, etc. (10,016 rec.)

T1 General exposure information (18,995 records)

T2 Original dose reported & alternate calculated doses (19,001 records)

T3 Heublein type dose information (207 records)

P1 General portal exposure dose information (5,777 records)

P2 Portal site exposure information (1,108 records)

Tape 2--Nursing Notes (168,455 records)

These records contain data on appetite, nausea, emesis, bowel movement, and strength.

Tape 3--Vital Signs (172,346 records)

These records contain information on temperature, pulse, respiration, height, weight, and blood pressure.

Tape 4--Clinical Data (145,180 records)

C0 Clinical chemistry (37,330 records)

C5 Cytology (126 records)

H0,H2,H3 Hematology (85,305 records)

U0 Urology (4,615 records)

S0 Serology (1,855 records)

M0 Microbiology (3,663 records)

A5 Antibiotic sensitivity (6,816 records)

B5 Blood transfusions (5,470 records)

Tapes 5 and 6--Medications (277,235 records)

These records contain information on all patient medications from dressings to drugs.

The data are so voluminous (850,559 records) that composite information is kept on a separate tape. This tape is used to produce summary reports and to judge availability of data for specific studies. The tape contains abbreviated case identification, dose information, and frequency of other records such as nursing notes in the time vacinity of each treatment.

C. Dose/Response Models

1. Prodromal syndrome

Nausea and vomiting are not considered a significant clinical problem in patients who have received less than 200 r to the abdomen, as partial or total-body therapeutic irradiation. Most radiologists and radiobiologists would not debate the view that an exposure of about 200 r is required to cause nausea and vomiting in man but few, if any, can predict with any stated degree of certainty for man what the probability is that any exposure to less than 200 r of total body irradiation will elicit nausea or vomiting. Recently it has become urgent to obtain such information as precisely as possible to predict the probability of total mission failure for manned space flight because of detrimental physiologic responses of the astronaut. Vomiting, per se, or nausea if severe enough, is conceivably an effect of radiation exposure, which, if not anticipated, could be disastrous in space flight.

The case histories of 94 patients who had received total-body irradiation in the course of therapy, or as the result of a criticality accident (Y-12 accident), were encoded and processed to determine the incidence of anorexia, nausea, and vomiting. As shown in Table 2, the patients were divided into five dosage groups for which geometric mean doses of 49.6, 105.2, 300, 370.3, and 540.5 r were determined. In Table 3 the percentage of cases in each group that showed anorexia, nausea, and vomiting are shown. Probability (probit) analyses were then done with these data to estimate the total-body irradiation dose required to produce the particular response in 50% of the patients. Table 4 contains the probit equations, the chi-square confidence limits, and the effective dose (ED_{50}) for these responses. The values are expressed as common logarithm to define the standard deviations of the estimates and the midline air dose (roentgens) and the absorbed dose (rads) to the gastrointestinal tract.

These results appear to indicate that, if it is true that the chance of an astronaut in space receiving 10 rads to the abdomen is less than 1 in 1000, the chance that radiation-induced severe nausea and vomiting will occur is less than 1:100,000.

The studies were refined by the collection of additional observations of human total-body irradiation and were extended to include similar estimates of the occurrence of diarrhea, fatiguability, erythema, alopecia, hematologic injury, infections, cataracts, and death.

TABLE 2

Distribution of Single-exposure Patients in the Division's Radiotherapy Study Including Those in the Y-12 Accident

Dose Group	Dose (r)	Number Cases	Geometric Mean Dose (r)
I	35*	1	49.6
	49	1	
	50	24	
	60	1	
II	100	34	105.2
	104*	2	
	162	1	
	200	1	
	206	1	
III	300	12	300.0
IV	349	1	370.3
	350	1	
	357	1	
	358*	1	
	360	1	
	362	1	
	384	1	
	409*	1	
	410	1	
V	473	1	540.5
	495*	1	
	514*	1	
	527	1	
	553*	1	
	616	1	
	624	1	

*Y-12 accident patients.

TABLE 3

Frequency of Anorexia, Nausea, and Vomiting in the Division's Radiotherapy Study of Single-exposure Patients, Including Division's Therapeutic and Y-12 Accident Patients

Geometric Mean Dose (r)	Total Cases	Anorexia Yes	Anorexia %	Nausea Yes	Nausea %	Vomiting Yes	Vomiting %
49.6	27	4	14.8	4	14.8	2	7.4
105.2	39	19	48.7	13	33.3	9	23.1
300.0	12	11	91.7	8	66.7	7	58.3
370.3	9	9	100.0	7	77.8	5	55.5
540.5	7	7	100.0	7	100.0	6	85.7

TABLE 4

Estimate of Effective Doses for Gastrointestinal Responses To Total-body Irradiation in Man

Response	Equation P = a (dose) + b		Chi-square Confidence
	(a)	(b)	(%)
Anorexia	3.389	-1.849	91.2
Nausea	2.244	+0.066	82.4
Vomiting	2.102	-0.005	87.6

	ED_{50} ± S.D.	Midline Air Dose	Absorbed Dose to GI Tract
	(Log_{10})	(r)	(rads)
Anorexia	2.0208 ± 0.2951	104.9	69.2
Nausea	2.1984 ± 0.4455	157.9	104.2
Vomiting	2.3810 ± 0.4758	240.5	158.7

Of particular importance in this retrospective analysis was onset time for occurrence of anorexia, nausea, and vomiting, the systemic responses to irradiation manifested by patients who received portal radiation therapy. These symptoms constitute a syndrome that has been called radiation sickness or in those exposed in radiation accidents, the prodromal syndrome. In this retrospective analysis based on 194 patients who were irradiated on 346 different occasions (each treatment being regarded as a separate entity) we attempted to establish quantitative estimates on the onset of each type response in the radiation syndrome. These patients were selected according to the following criteria: (1) They were irradiated between 1956 and 1965. (2) They were hospitalized at Oak Ridge Associated Universities Medical Division. (3) Irradiation was given to one part of the body only, excluding total-body irradiation. (4) Observations were available for the duration of the treatment course plus three days before and three days after the irradiation.

The basic information was coded from nurses' notes. For instance, a recorded observation like "patient ate poorly" or "refused supper" was encoded as anorexia: YES. Nausea, another subjective symptom, was recorded from the nursing notes when the patient had told the nurse that he was nauseated, either by volunteering the information or by being asked. Vomiting was accompanied by liquid objective evidence, and it was recorded with greatest faithfulness to actual occurrence. All information for each patient on any one day was reduced to either YES or NO for

anorexia, nausea, and vomiting, no matter how many times a particular response occurred on that day.

The question we wanted to answer was: When, in the course of a treatment series, will the patient first complain of anorexia, of nausea, and of vomiting? Any contributing factor other than time and his preirradiation status was ignored, specifically the kind of disease, where he was treated, and how much radiation he was given. The data for anorexia are summarized in Table 5. This table was prepared in a manner to permit an acturial analysis, as is done to calculate survival rates. The first column lists the days which irradiation was given, including any pauses for weekends or any other reason. Day 1 is the first irradiation day. The second column, headed N, recorded the number of patients that on the designated days had not yet responded. Each entry is the number of nonresponders on the preceding day minus those who the preceding day either first responded or were withdrawn from observation. The third column, R, is the number of patients who first responded on the designated day. Patients withdrawn from observation, W, are those who were followed up to the designated day without responding. The number at risk was obtained by subtracting one half of W from N. The 6th column is probability or response for each day (R/at risk), and the 7th column the probability of not responding for each day. Next to it is the cumulative probability of not responding, which is obtained by transmultiplying all the entries in the preceding column. Finally, the 9th column is the cumulative probability of responding, calculated by subtracting each entry on the preceding

TABLE 5

Onset of Anorexia
All Cases

Treatment Day	N	R	W	At risk	P(R)	1-P(R)	Cum 1-P(R)	Cum P(R)
1	346	155	-	346	.4480	.5520	.5520	.4480
2	191	36	-	191	.1885	.8115	.4480	.5520
3	155	27	-	155	.1742	.8258	.3699	.6301
4	128	13	-	128	.1016	.8984	.3324	.6676
5	115	8	1	114.5	.0699	.9301	.3091	.6909
6	106	11	-	106	.1038	.8962	.2771	.7229
7	95	7	1	94.5	.0741	.9259	.2565	.7435
8	87	5	5	84.5	.0592	.9408	.2414	.7586
9	77	2	6	74	.0270	.9730	.2348	.7652
10	69	9	2	68	.1324	.8676	.2038	.7962
11	58	3	-	58	.0517	.9483	.1932	.8068
12	55	2	1	54.5	.0367	.9633	.1861	.8139
13	52	2	6	49	.0408	.9592	.1785	.8215
14	44	1	-	44	.0227	.9773	.1745	.8255
15	43	2	-	43	.0465	.9535	.1664	.8336
16	41	1	6	38	.0263	.9737	.1620	.8380
18	34	2	5	31.5	.0635	.9365	.1517	.8483
21	27	1	2	26	.0385	.9615	.1459	.8541
22	24	2	1	23.5	.0851	.9149	.1334	.8666
26	21	1	8	17	.0588	.9412	.1256	.8744
29	12	2	2	11	.1818	.8182	.1028	.8972
30	8	1	1	7.5	.1333	.8667	.0891	.9109
40	6	1	4	4	.2500	.7500	.0668	.9332
49	1	-	1	-	-	-	-	-

column from 1. The information contained in the last column is better visualized if plotted graphically (Fig. 1) where the treatment day is plotted on a logarithmic scale and the cumulative probability of responding is plotted on a probability scale. In this fashion all data points arranged themselves along a straight line.

The high incidence of anorexia on the first day of treatment might not represent a radiation effect, but rather continuation of a preexisting condition. Many of the treated patients actually had anorexia because of their illnesses. Conceivably these patients responded differently to irradiation; they might respond to a greater degree because they were already prone to become anoretic, or they might respond less because irradiation partially relieved the pathological condition that made them anoretic.

We decided, therefore, to subdivide the patient into two groups: those who had anorexia before irradiation and those who did not. The first group includes all patients who on any of the three days preceding irradiation had been anoretic one or more times. There were 176 patients in the first group and 170 patients in the second group. The cumulative incidences are graphed in Fig. 2.

The response of nausea was analyzed in the same fashion as anorexia. First, all patients were taken together and then two groups were treated separately: patients who had nausea before irradiation and those who had not. Again, a patient was included in the first group if he had had nausea at any time during the three

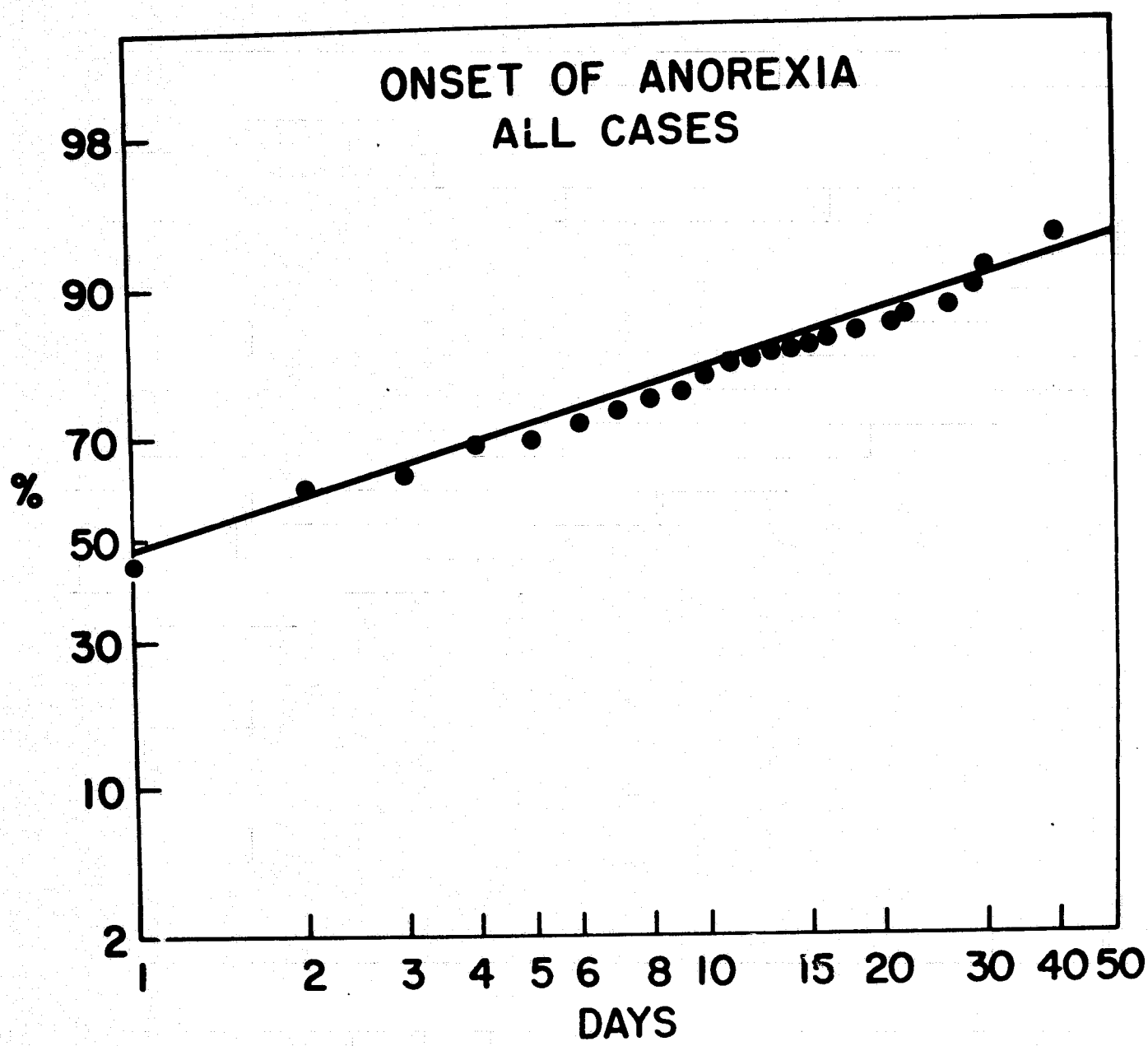

Fig. 1

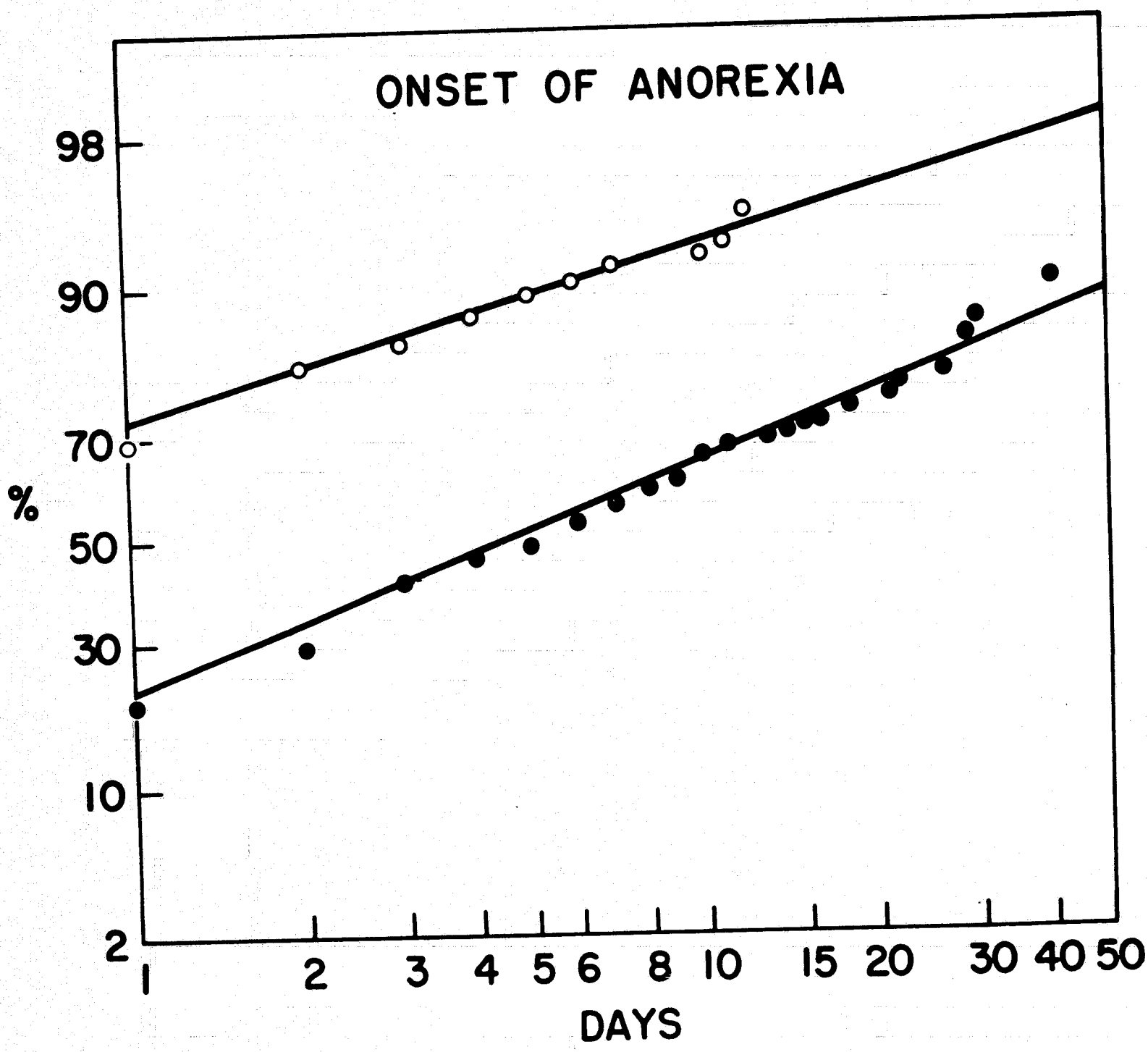
ONSET OF ANOREXIA
98
90
70
50
30
10
2
%
1
2
3
4
5
6
8
10
15
20
30
40
50
DAYS

Fig. 2

days preceded the beginning of the radiation course. The data are summarized in Fig. 3.

The vomiting response was evaluated as in the two preceding sections. The data are summarized in Fig. 4.

Of the three symptoms of radiation sickness, anorexia appeared earliest, next nausea, and vomiting last. The time of onset for each response depends considerably on whether the patient had any of those symptoms before irradiation. If he did, his chances of having more of the same during the treatment course are very high and if the treatment time lasts as long as two weeks the majority of patients will respond. Patients free of these symptoms before irradiation fare better. Yet their risk of having anorexia, nausea, or vomiting, at least once, is high. It is highest for anorexia; at 40 days, 88% of the patients will have had this symptom at least once.

Nausea generally appears later and the risk of developing it does not increase as fast as for anorexia. Still, at the 40th day of treatment, 60% of the patients will have experienced it.

Initially the risk of vomiting is only slightly below that of nausea, but as time passes the increment rate for vomiting is less than for nausea. At the 40th day 43% will have vomited sometime since irradiation was started (Figs. 5 and 6).

It should be underscored that the tables and graphs present cumulative probabilities. On a day-to-day basis, the probability of response decreases with time. For instance, for previously

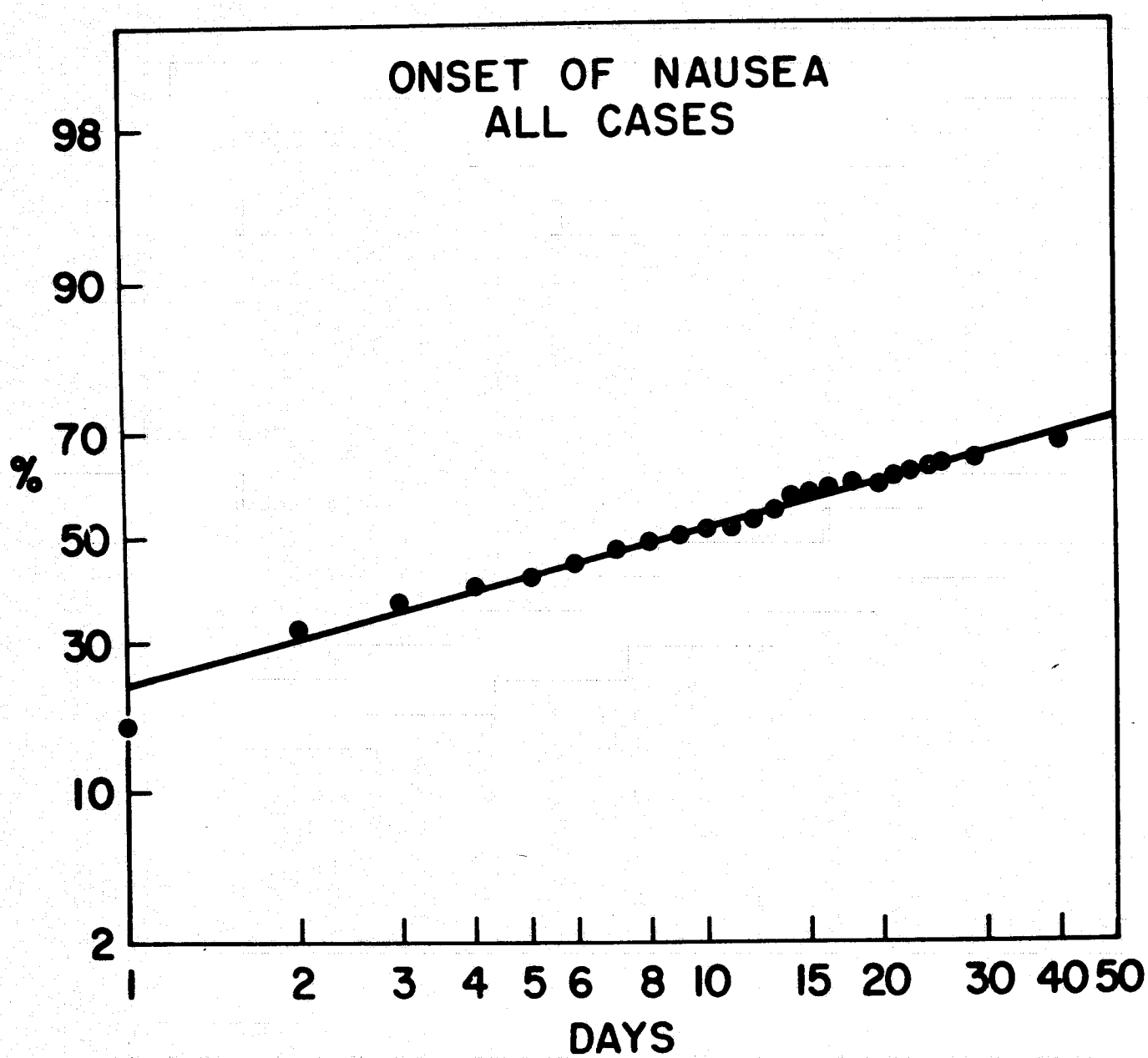

Fig. 3

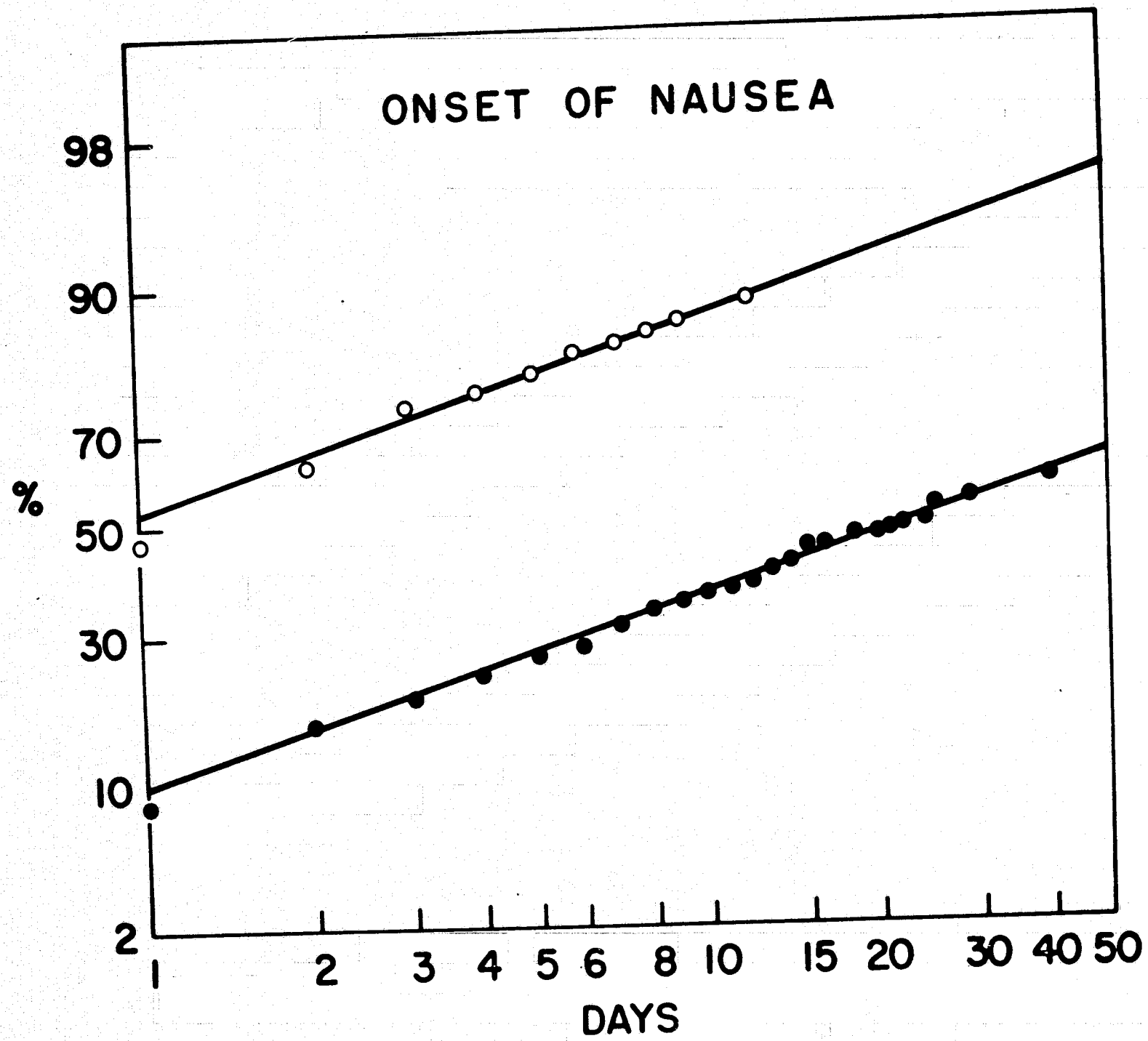

Fig. 4

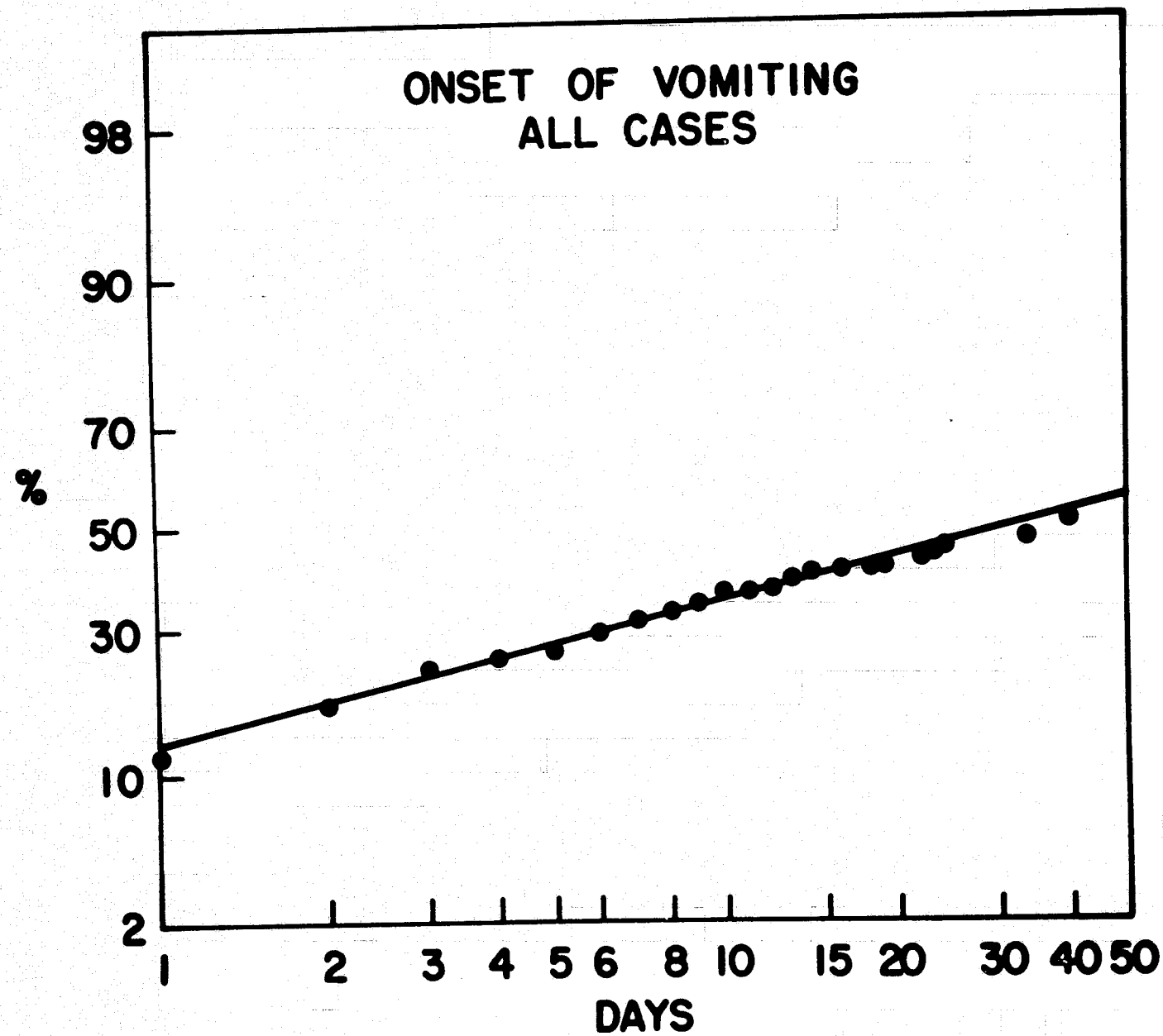
ONSET OF VOMITING
ALL CASES
98
90
70
50
30
10
2
%
1
2
3
4
5
6
8
10
15
20
30
40
50
DAYS

Fig. 5

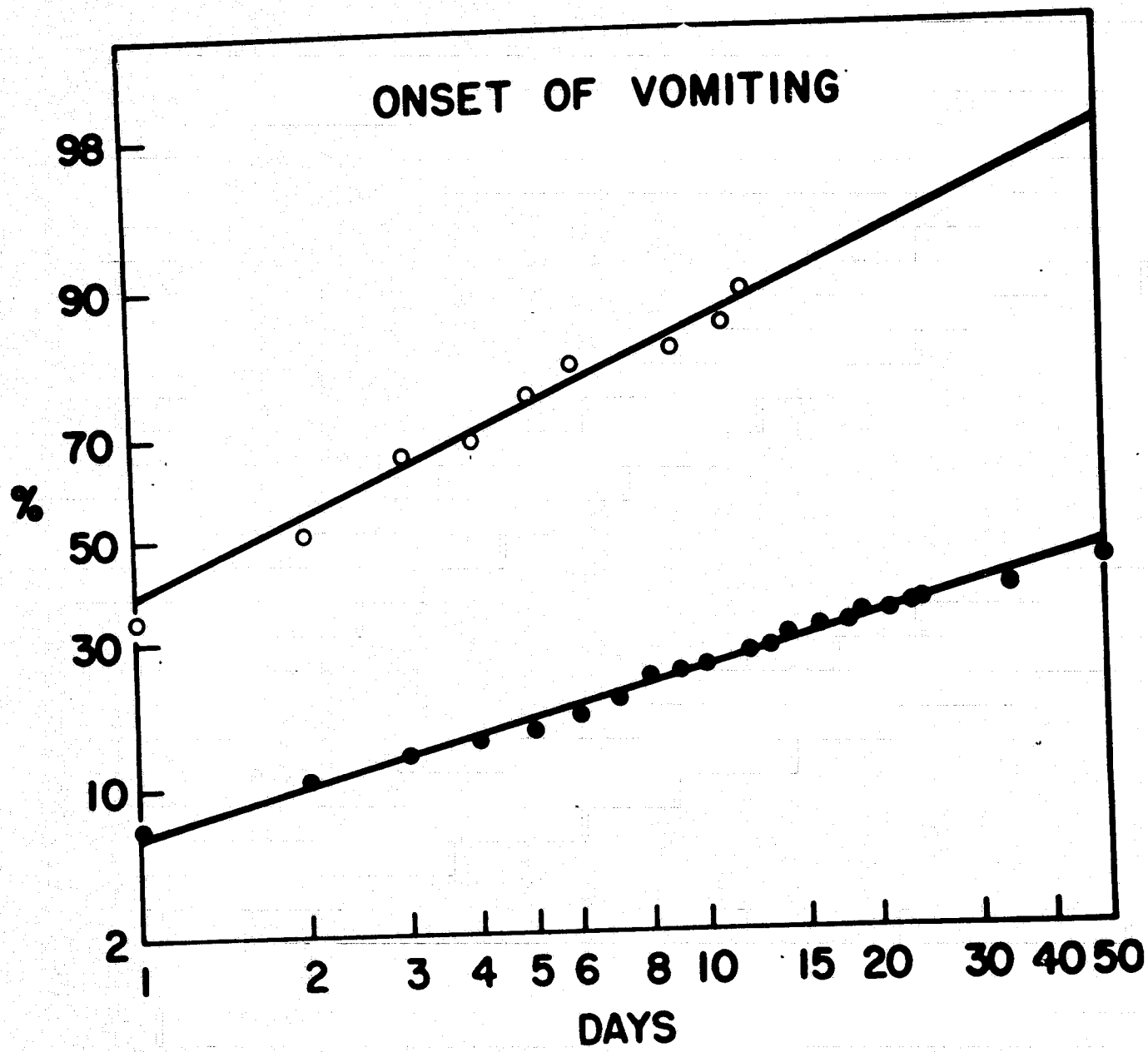
ONSET OF VOMITING
98
90
70
50
30
10
2
%
1
2
3
4
5
6
8
10
15
20
30
40
50
DAYS

Fig. 6

nonresponders the risk of developing anorexia on the first day is 0.18, on the second day it is 0.12 (0.18 + 0.12 = 0.30), on the third day it is 0.08, etc.

The time scale, in effect, is proportional to radiation dose. Longer treatment times tend to correspond to high total radiation doses, although the clinical data include high single doses and low-dose fractionated courses. The remarkably good fit of most of the curves, however, indicates that there is, indeed, a good correlation between onset of symptoms of radiation sickness and length of radiation course. It should be stressed that we have commented only on the onset of symptoms.

Further analysis of these data indicated that the patterns of response can be well described by a Weibull distribution of the form

$$f_{(t)} = \alpha\beta t^{\beta-1} e^{-\alpha t^{\beta}} \qquad (1)$$

Although these data were fitted to a logit or probit distribution the Weibull distribution was used here because of somewhat greater mathematical simplicity and especially because the beta exponent in equation 1 indicates, without further calculations, the rate of change in probability of response as a function of time. When beta was less than 1 (as in most of our data) the probability of response decreases with time.

In a Weibull distribution the cumulative probability of response is given by

$$e^{-\alpha t^{\beta}} \qquad (2)$$

where alpha and beta are parameters of the equation and t represents days after beginning of treatment. Figure 7 shows that the values calculated by equation 2 fit well the experimental data.

Of greater interest than the cumulative probabilities were the conditional probabilities defined as the probability that a response will occur at a certain time provided that it has not occurred before. The conditional probabilities were calculated by subtracting the cumulative probabilities of occurrence in two successive days and dividing by the cumulative probability that the response had not yet occurred in the earlier of the two days being compared. Equation 2 was used to compare the cumulative probabilities. Figure 8 shows the conditional probabilities for the onset of anorexia, nausea, and vomiting. It clearly shows that an irradiated patient is more apt to respond on the very first day of treatment than at any other time. If no response occurs on the first day, the risk of responding on the next 10 to 20 days steadily decreases and beyond that time is almost constant.

This analysis can also be carried out for responses other than the first one. For instance one may wish to determine what is the probability that a certain response will occur provided it has already occurred once and only once before. Figure 9 shows the conditional probability for an irradiated patient to develop anorexia, nausea, or vomiting for the second time during a radiation treatment course. It is clear that if the patient previously responded he is at a much greater risk to respond again than if he had not had anorexia, nausea, or vomiting once before. Yet, the

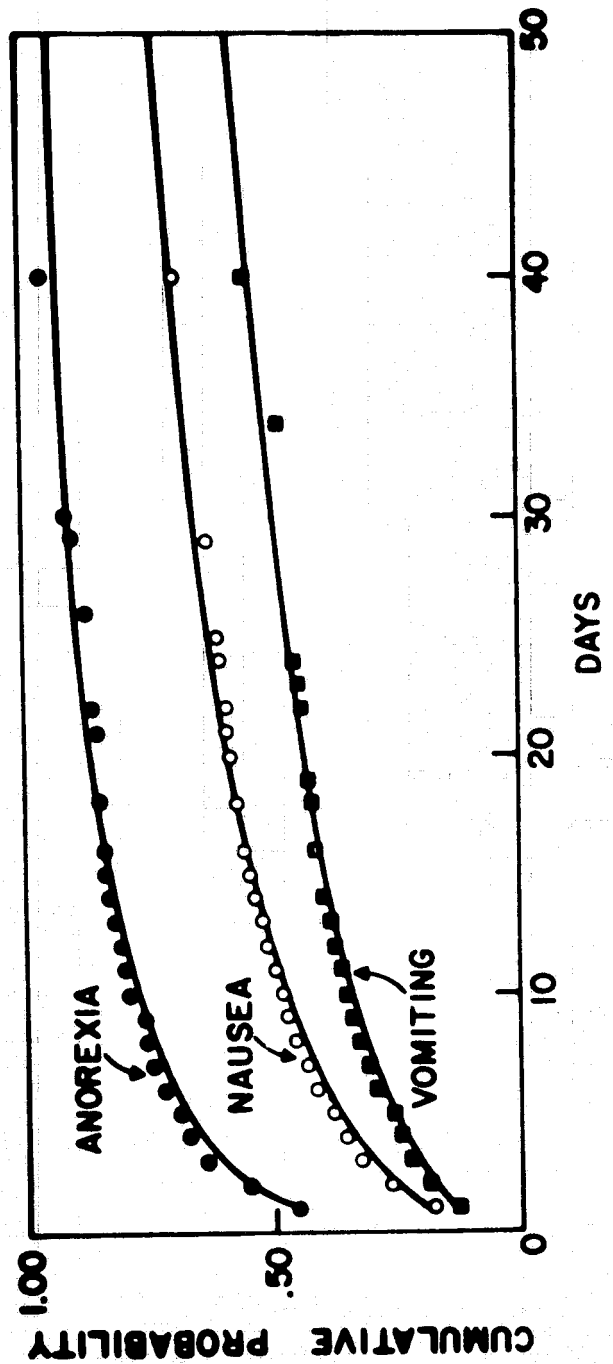

PRECEDING PAGE BLANK NOT FILMED

Fig. 7

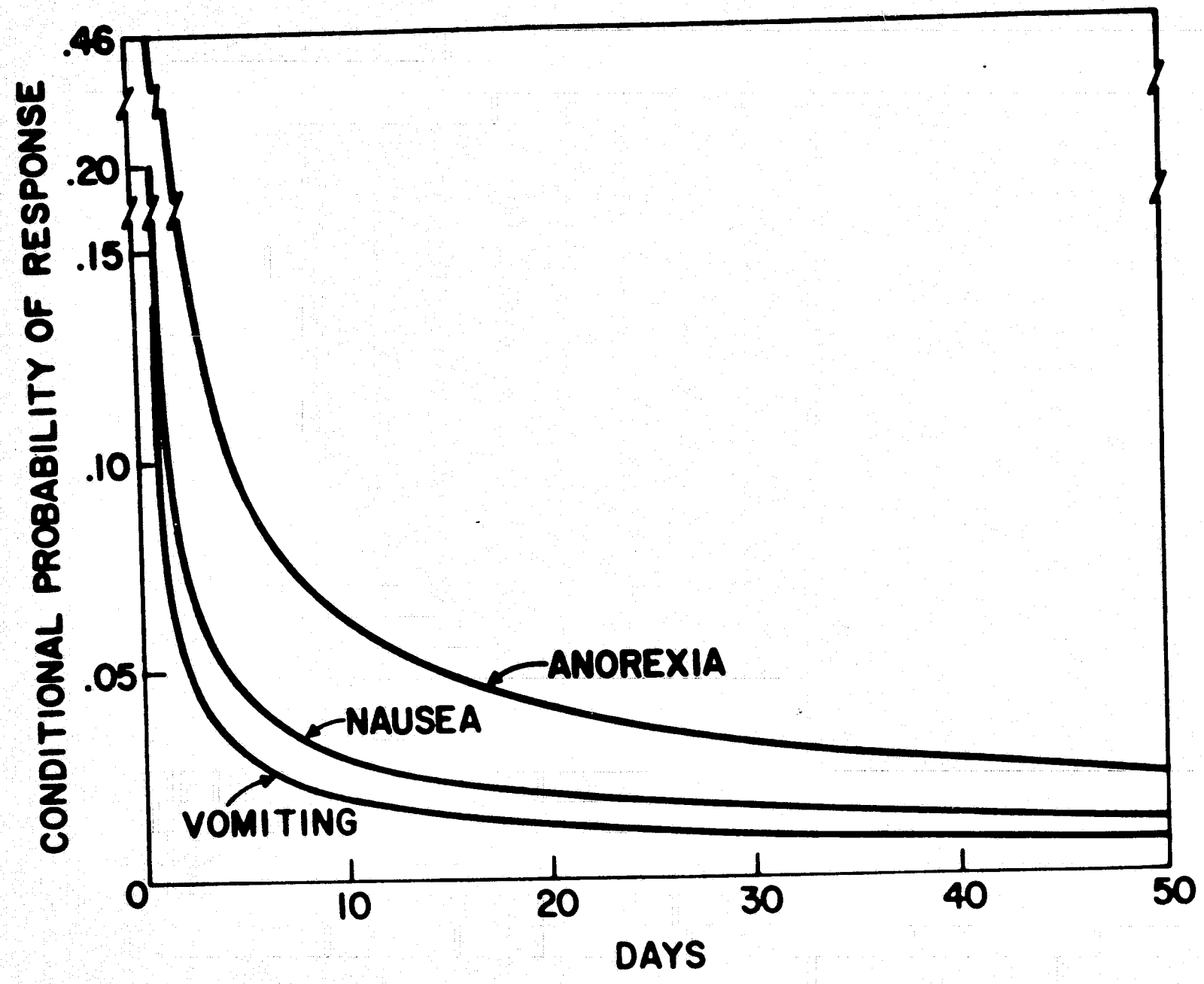
CONDITIONAL PROBABILITY OF RESPONSE
.46
.20
.15
.10
.05
0
10
20
30
40
50
DAYS
ANOREXIA
NAUSEA
VOMITING

Fig. 8

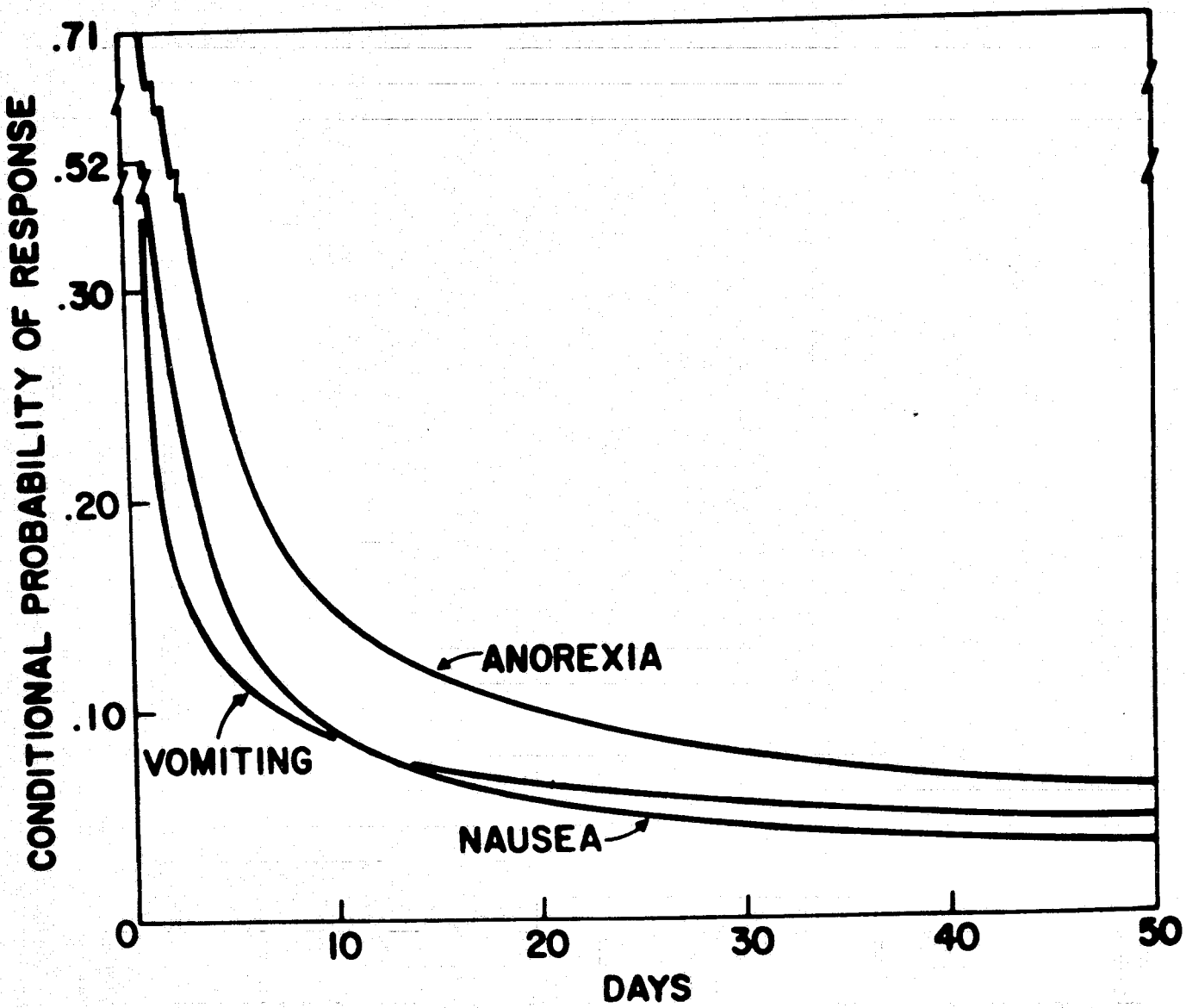
CONDITIONAL PROBABILITY OF RESPONSE
.71
.52
.30
.20
.10
0
10
20
30
40
50
DAYS
ANOREXIA
VOMITING
NAUSEA

Fig. 9

conditional probability of responding for the second time also decreases with time. In general, this is true for any response number, either first, second, or nth.

The overall pattern of responses in a population receiving radiation therapy is shown in Fig. 10, where the conditional probabilities of responding for the first, second, or nth time have been summated for each day, weighing those conditional probabilities by the relative number of people that at any one day are responding for the first, second, or nth time. Figure 10 shows that the overall probability of response decreases little with time. This is not in contradiction with the earlier conclusion that a patient's risk of manifesting a response steadily decreases with time. That is true so long as we consider a certain response number (first, second, nth) by itself. However, with the passage of time, patients are exposed to new risks which increase the overall probability of responding. For instance, the risk of vomiting for the 10th time does not begin until the 10th treatment day and only for those who have vomited daily for the past 9 days. For these patients the risk of vomiting again is very great, although overall this is an uncommon occurrence. To put it another way, after a few days of radiation treatments, almost all the patients who vomit consist of a rather small population of patients who have vomited several times earlier and who have high risks of vomiting again.

The results of these studies on prodromal responses were incorporated within the text of *Radiobiological Factors in Manned Space Flight* of which Wright Langham (2) was the editor and are discussed

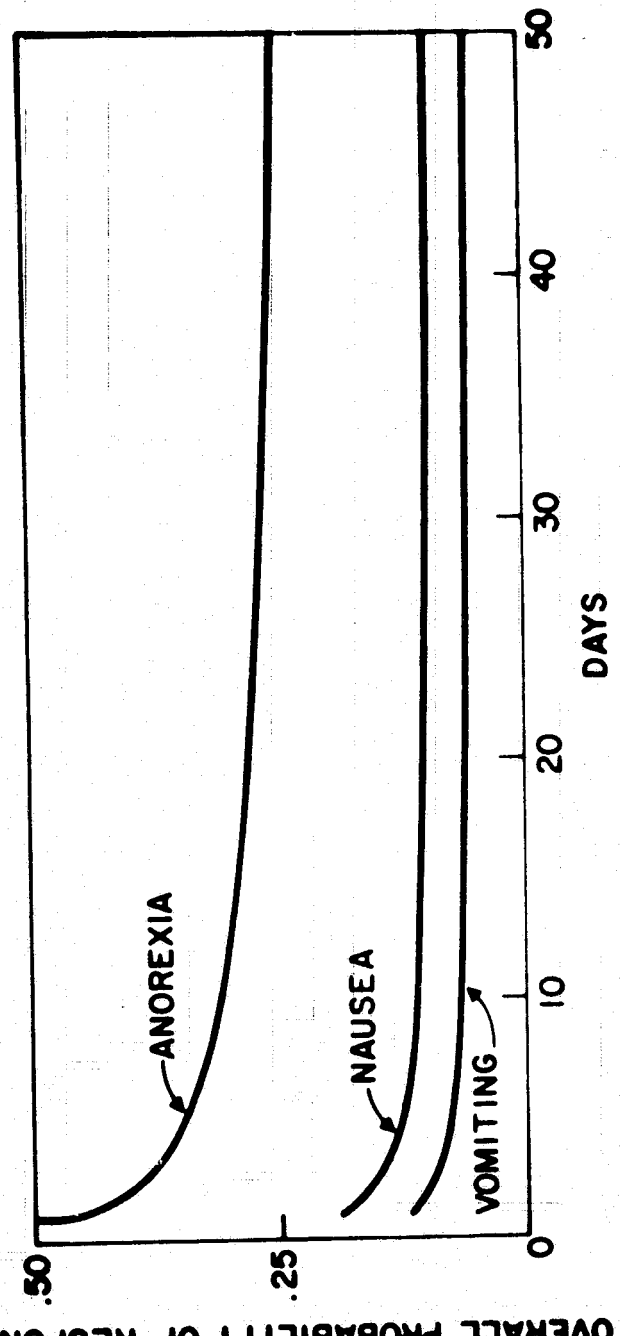

Fig. 10

at length in Chapter X, Human Radiation Tolerance (3).

2. Acute hematopoietic damage

We have attempted to make quantitative analyses of the radiation-induced hematologic responses of patients who received total-body irradiation at some time during the course of therapy for neoplastic diseases. Our results have not yet been any more quantitative or less narrative than those of numerous other investigators working on this problem. The need for quantitating these effects does not stem from any immediate clinical problems since available descriptions of the time-course of radiation-induced hematologic events afford abundant information to aid in the medical management of any patient irradiated either accidentally or therapeutically. Quantitative formulae are needed, however, to help predict, with some known level of precision, how hematologic damage may be caused by chronic low-dose-rate exposures of normal men.

We collected the clinical case histories of 2310 patients from hospitals in the United States and Canada, encoded these records for manipulation and programmed retrieval by computer, graphed the time-course of the changes in peripheral blood cell counts after each TBI and determined the percent survival of leukocytes and platelets after specific single and multiple radiation exposures. Our efforts concentrated on studying only the most complete hematologic records, culling out those having uncertainties about exposure (total roentgens, fractional doses, total treatment time, intervals between exposures, etc.) and with blood studies insufficient

to determine the nadir of peripheral blood cell values and its time of occurrence. We found that at least seven blood cell counts done at weekly intervals for 6 weeks are needed to estimate the percent survival of most blood cells after an exposure, to be certain that a true nadir was observed. Many patients were too ill to afford hematologic data that were not biased heavily by their diseases and terminal infections; these were identified by these data searches and eliminated. In addition, we evaluated the clinical and laboratory evidence that defined the diagnosis in order to group together only patients with the same disease. Only four general disease categories were found that contained sufficiently numerous patients who had received single or multiple exposures to form groups for study. Second and third series of exposure were not included since the responses might be influenced by the previous irradiations. In these ways the single-exposure cases that total 1085 in our data bank were reduced to only 151; the 1225 multiple-exposure cases to 395. Table 6 shows the composition of this study material divided into the four hematologic-disease groups and according to single and multiple types of exposures. The average doses and the exposure duration of the multiple exposures are shown for each diagnostic group. The isolation of a so-called "normal" group was a fundamental need of this problem. The patients in this normal group, however, were not actually normal but either had disseminated solid (but not hematologic) tumors or were in late stages of nonmalignant diseases of the bone, joints, and the genitourinary system. However, in the absence of recorded hemato-poietic abnormalities the patients in this group were considered to

TABLE 6

Diagnostic Group	Number of Patient Studies (#)		Average Total Exposures (R)		Average Length of Multiple Exposures (Days)
	Single	Multiple	Single	Multiple	
"Normal"	92	29	195	232	27
Chronic myelogenous leukemia	15	116	117	152	28
Chronic lymphatic leukemia	28	200	*	116	36
Lymphosarcoma	16	50	108	217	31

*Incomplete

have "normal" (nonleukemic) marrow and lymphatic systems. The presence in this "normal" group of serious systemic diseases, even though not primarily hematologic, makes our apparent assumption of the existence of completely normal peripheral blood-cell kinetics unquestionably naive. The implication should not be accepted unequivocally that the mathematical description of the response pattern of this "normal" group can be used to describe exactly that or normal young men in the prime of life. It is difficult, however, to believe that normal young men would respond worse than this group did rather than better.

In the first step of the statistical analyses of this data, we chose to ignore the influence of the number of fractions of exposure, for the time being, to simplify our confirming the applicability of multivariant analysis to this problem. Accordingly, we related the individual nadir (%S) of the total leukocyte counts (expressed as percent of the initial total that survived) with the total exposure in R and the total time (days) required for the total exposure to be made. Slope constants (b_1) and (b_2) for a multivarient regression formula were computed first for the single exposures and then for the multiple exposures for each disease group. No radiation dosage groupings within these four diagnostic groups were needed with this method of computation and fitting the regression. In the equation

$$\%S = \qquad \cdot 100\ (D)^{lb_1} \cdot (T)^{b_3} \qquad \ldots\ldots\ldots\ldots (3)$$

K is the constant required for the regression line for percent survival to intercept the ordinate at zero dose. This interception

point is greater than 100% of initial WBC survival because no effect was observed on cell survival after exposures of less than 50 R; D is exposure in roentgens; T is total length of exposure time in whole days; F is the number of fractional exposures made. For the purpose of this initial analysis the variable F was not used. In single exposures, T by definition is ignored and the equation becomes

$$\%S = \frac{K \cdot 100 \cdot T^{b2}}{(D)} \tag{4}$$

For exposures longer than one day (as multiple exposures are defined here) the equation is then

$$\%S = \frac{K \cdot 100 \cdot T^{b2}}{(D)} \tag{5}$$

The computed slope constants for the four diagnostic types of hematologic statuses analyzed here are listed in Table 7 along with the test values for the significance of the first of the data to the equations 4 and 5.

These results seemed encouraging. They showed that this method of analysis is applicable to our problem and that the data were statistically well described by the equations. These multiple regression correlation coefficients were exceptionally good for analyses of clinical data. The values for the slope constants appear to have interesting biological implications that are medically logical and acceptable. For example, in Table 7 the negativity of b_1 indicates that as dose increases the percent survival by peripheral WBC decreases. The correspondence of this value for each group to 1.0 may indicate that in the leukocytic systems difference in

TABLE 7

Slope Constants and Tests of the Statistical Significance of the Models

Diagnostic Group	Single Exposures		Multiple Exposures		
	b_1	Correlation Coefficients	b_2	Correlation Coefficients	P Value
"Normal"	1.04	0.57	0.63	0.535	<0.025
CML	0.999	0.82	0.392	0.569	<0.0001
CLL	0.91?	-	0.221	0.583	<0.0001
LS	1.119	0.42	0.231	0.567	<0.0005

radiosensitivity is not a significant factor. This result is surprising in view of the widely-held clinical belief that the leukocytes in chronic lymphocytic leukemia, for example, are much more radiosensitive than the cells comprising the WBC in chronic granulocytic leukemia or in "normal" persons. This apparent deviation from clinical "fact," however, can be explained by the significant differences found in the values of b_2. The larger this positive slope constant is, the more effective is the length of protraction of exposure in increasing the level of cellular survival; according to these values, in the "normal" the white blood cell level is protected by dose protraction three-fold over that afforded to it in CLL and lymphosarcoma. According to this analysis, dose protraction in the latter groups should not decrease the effectiveness of the total dose as much as in the "normal" group or in the CGL group. These interpretations are in agreement with most clinical observations and suggest, in keeping with experimental observations, that dose protraction aids normal tissue to recover and regenerate more rapidly than pathologic tissues. This concept is, in fact, the rationale for fractionation and protraction of radiation therapy of malignant tissues. Clinically observed differences in WBC survival after the same radiation exposure result more from difference efficiencies of recovery mechanisms than they do from inately different cellular radiosensitivities in these diseases.

CHAPTER IV

PROSPECTIVE STUDIES

A. Irradiation Facilities and Dosimetry

During the operation of a clinical/medical facility for the care and treatment of patients with leukemia, lymphoma, and related disorders the Medical Division of ORAU had operable two total-body therapeutic irradiation facilities. One, built in 1960, was a room with eight cesium-137 sources initially capable of exposures ranging from 300 R/hr down to 1.8 R/hr. This facility was generally operated at exposure rates of 1.5 R/min (90 R/hr) for therapeutic irradiation and is identified as METBI (Medium-Exposure-Rate Total-Body Irradiator). Another, built in 1967, consisted of 10 cobalt-60 sources geometrically arranged so to produce an isodose level of 1.5 R/hr anywhere within the treatment room and is identified as LETBI (Low-Exposure-Rate Total-Body Irradiator). The total number of patients treated in these facilities is shown in Table 7a.

1. METBI

Figure 11 shows a cutaway model of the total-body irradiation room. A 2 x 2 x 6 ft virtual volume was suspended over a bed by four posts that are out of the exposure field. The bed was made of two sheets of 1/32 in aluminum separated by approximately an inch and a half of honeycomb cardboard. The material is usually used for the extreme strength necessary in airplane fuselage construction and has no sag when a patient is placed on the bed. The bed is slightly trough-shaped so that patients cannot easily roll off. A nylon net surrounded the bed. A television set with remote controls was placed so that a patient lying on the bed can view television.

TABLE 7a

TBI TREATMENTS OF 50 R AND GREATER THROUGH 1974

Exposure per treatment (R_x)	METBI (1.5 R/min)					LETBI I (1.5 R/hr)		LETBI II (0.8/hr)	Totals
	Single acute exposures	10 R/day (3 days/ week)	10 R day	30 R day	60 R day	10 R day	30 R day	16 R day	
Chronic Lymphocytic Leukemia									
50	15								15
100	20					1	4	2	27
120		1							1
150		1							1
Lymphosarcoma and Lymphosarcoma Cell Leukemia									
50	5	1*	1						7
100	22	1†	1			1	3‖	3¶	31
150		1		1		2‡			4
250				1			4¶		5
Chronic Granulocytic Leukemia									
50	8								8
60					3				3
100	4			1§			6		11
120							1		1
150				16		1	9	1	27
200						2			2
250				1			8°		9
Polycythemia Rubra Vera									
100	7						5	1	14
150				5			8	1	14
250							4✓		4
Idiopathic Thrombocythemia									
100	1						1		2
150				2			7		9
Totals	82	5	2	27	3	7	60	8	194

* Patient received 60 R
† Patient received only 90 R
‡ One patient received only 140 R
§ 25 R/day
‖ One patient had lymphosarcoma cell leukemia
¶ Two patients had lymphosarcoma cell leukemia
° One patient received only 222 R
✓ One patient received 230 R

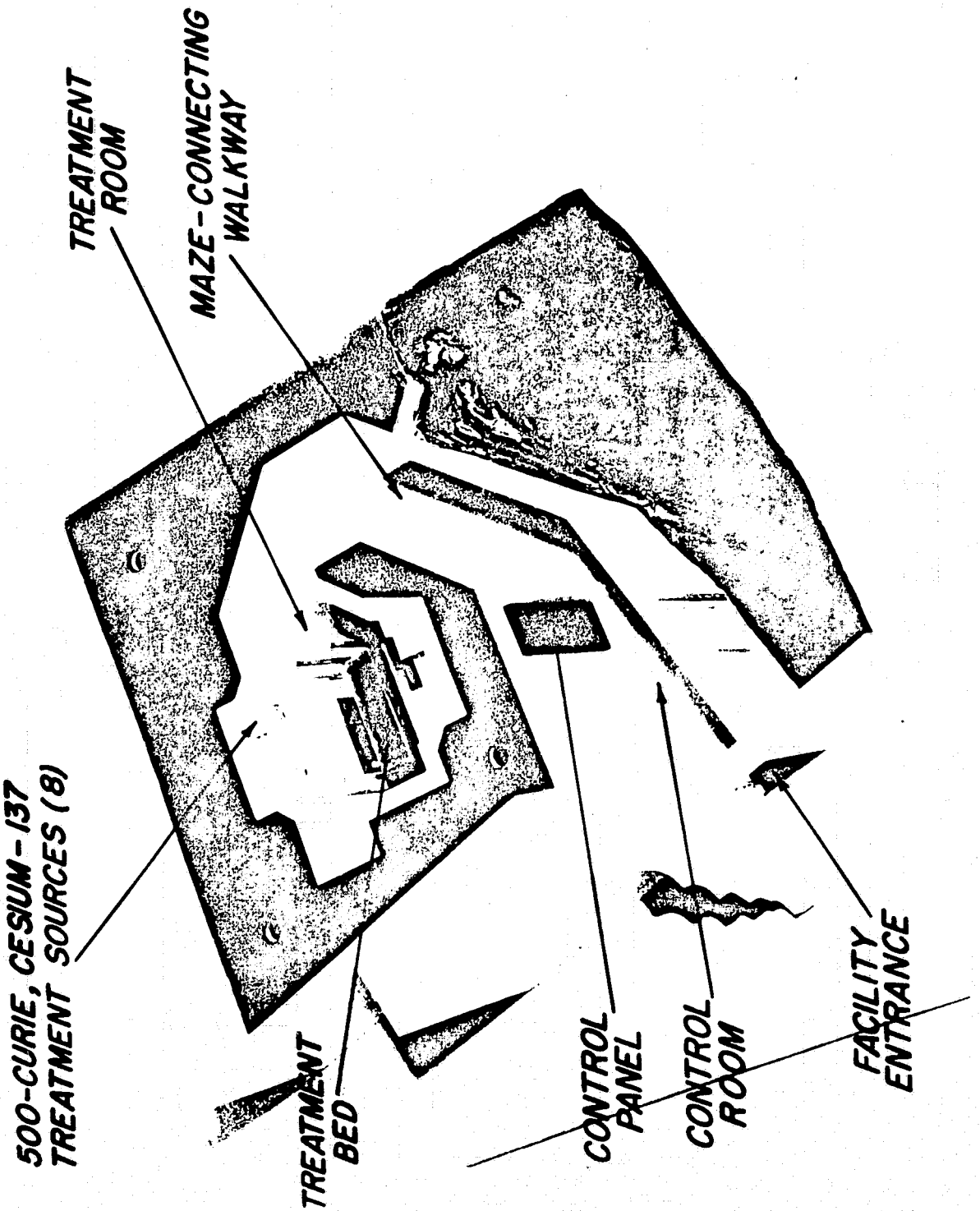

PRECEDING PAGE BLANK NOT FILMED

Fig. 11

The room is constructed of poured concrete, but the inside wall is covered with an acoustic tile, which has no effect on the radiation characteristics. The floor is of vinyl tiles. Ventilation is arranged so that the air enters through the maze and leaves through a ventilator funnel on the wall opposite. Heating is done with electric wall heaters. In summer, air is drawn through a louvered door from an air-conditioned corridor. Two steel rails at the ceiling over the bed support an instrument trolly. The instrument cables go through a conduit in the ceiling. Preliminary investigations showed no appreciable scatter from the accessories.

The bed is placed in the center of an 8 ft (plus entry) cubical room. Eight teletherapy machines (four each side of the therapy space, near the corners) all point toward the center of the irradiation volume. Each source contains 500 ± 0.5 c of cesium-137. With all sources "ON" the exposure to the 2 x 2 x 6 ft irradiation volume ranges from 308 to 318 r/hr without the final filter covers in place. The exposure rate drops off slowly (about 8 r/hr) at the very head and foot ends of the bed but more quickly outside the irradiation volume.

The room is approached through a semispiral maze. At the end of this maze is a wrought-iron gate that must be closed for the machine to be turned on. Opening the gate automatically shuts off the machine. Any person going through the gate will shut off the machine before he can receive a significant exposure. The maze is sufficiently wide for patients' beds to be wheeled through, but patients are usually carried on a travelling cart.

Each of the sources can be turned on separately (Fig. 12). While this might be of value in later treatment problems, its primary purpose was to allow for dosimetry testing. These separate controls were covered and the only control necessary for the clinician is a clock and the master control button.

METBI Dosimetry. After initial background experiments were concluded the eight 500 c ^{137}Cs sources were loaded into the shields. One of the design features of this installation was to try for as uniform an exposure field to the patient as possible. Therefore, the eight sources were aimed to irradiate the subject from many different angles, each ported to expose the entire bed length. It was realized that scatter off the room walls and other variable factors might alter the desired uniformity, and a series of measurements was undertaken to investigate this possibility. The ion chamber was suspended at a point 12 cm above the bed center and was moved toward each end in 10 cm steps. The readings obtained are reproduced in intensity toward each end of the bed. The maximum rate of 7.4 r/min at the bed center would allow an exposure of 444 r/hr - a good deal more than the 250 r/hr originally thought possible.

With an excess of exposure rate available, the suggestion was made to attempt to even the exposure field. For this purpose stacks of metal strips were made and installed to give an attenuated portion in the center of each beam. A pyramidal stack for each source with the thickest portion in the beam center gave the lower curve in Fig. 13. As illustrated, this curve is more uniform throughout its length and gives an exposure rate of about 300 r/hr.

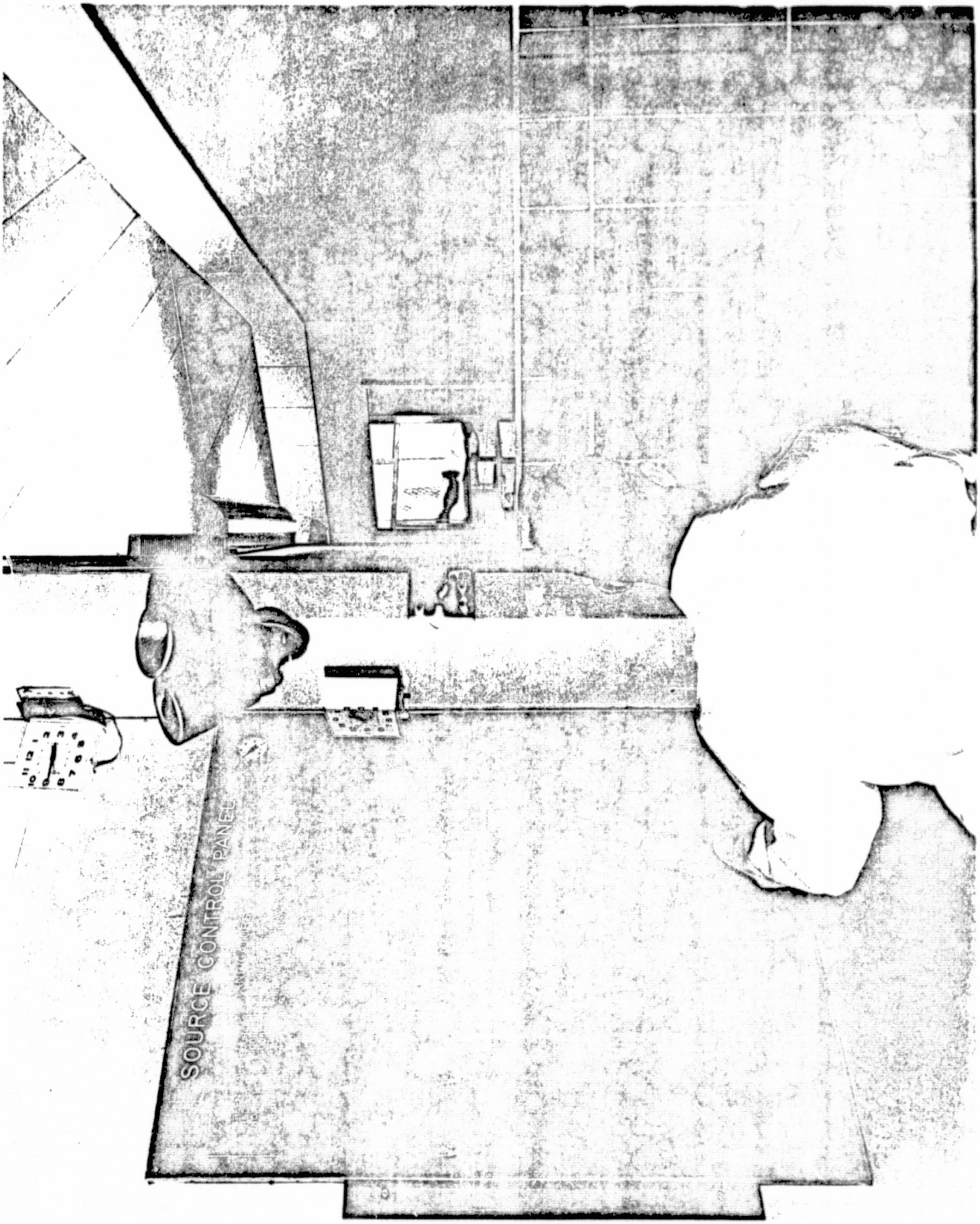

ORIGINAL PAGE IS
OF POOR QUALITY

Fig. 12

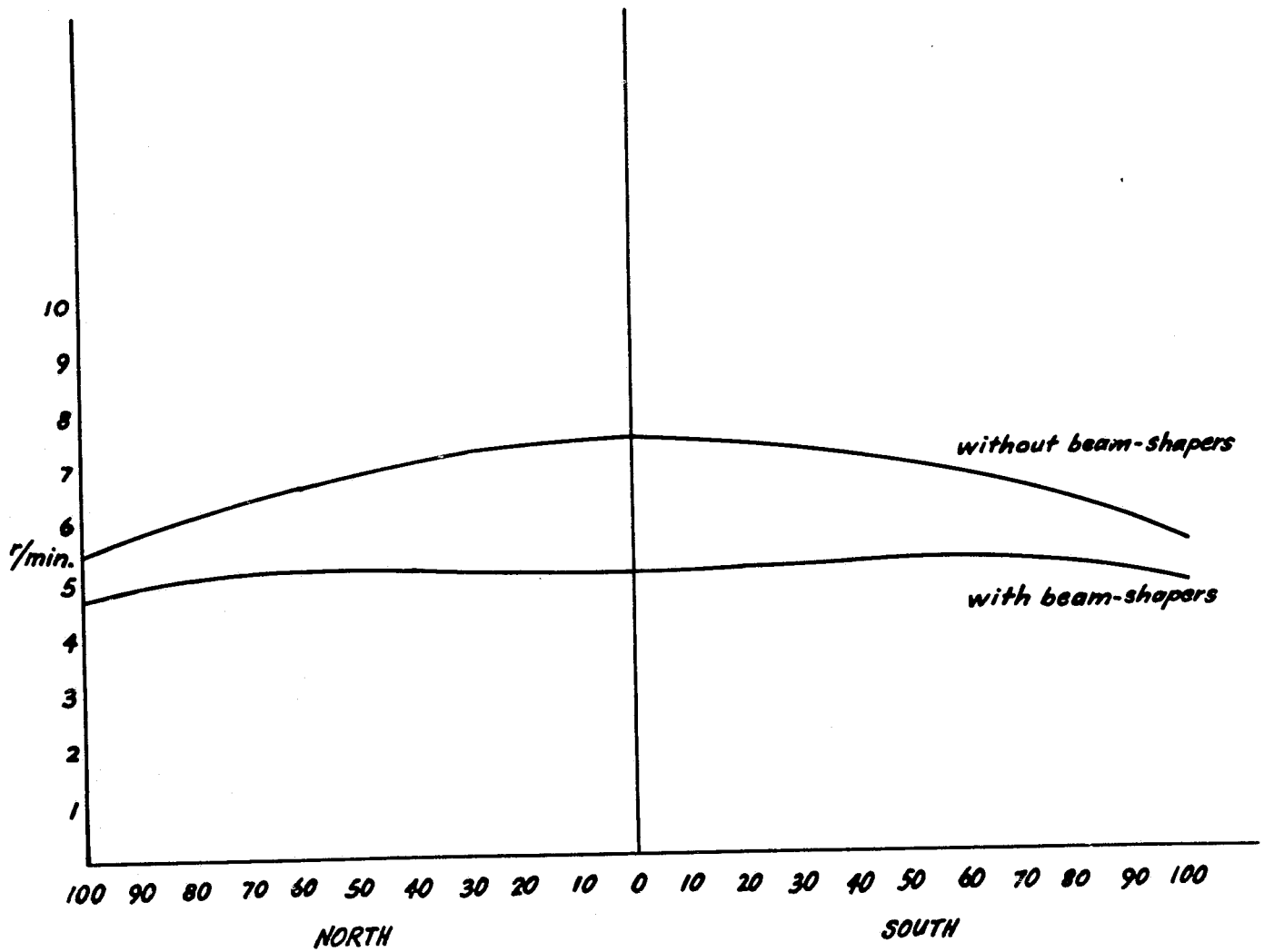
10
9
8
7
6
r/min.
5
4
3
2
1
without beam-shapers
with beam-shapers
100 90 80 70 60 50 40 30 20 10 0 10 20 30 40 50 60 70 80 90 100
NORTH
SOUTH

Fig. 13

Studies were also made in the lateral and vertical directions in the volume immediately above the bed. The variations of the field in these positions were not found to be large enough to require further compensation.

Attenuating the rate of exposure to the patient by using increasing filter thicknesses proved to be an excellent means of making these adjustments. Nevertheless, the question of spectral changes resulting from the introduction of these filters was an important one to examine because of possible changes in the depth-dose relationships in the patient.

The variations in spectrum with exposure rate were investigated using weak (2 mc) mock sources, in order to keep the intensity down to a reasonable level. The background for such measurements, however, is not the "natural" background investigated earlier, but rather that existing when the 500 c sources are present but are turned to the "off" position. The count rates for these backgrounds (and later for the gross counts) were found to be very low, to such an extent that recording of the count with a meter system was impractical. Therefore, 17 spectral points of interest were selected and cumulative counts were made at each point for each filter setting. Some of these counts took as much as 10-20 min to complete, and a rather lengthy procedure resulted from the checking of 32 filter positions for 17 spectral points. This process was repeated again for the gross counts and the background counts were subtracted.

After computation of the net counts, a series of curves was drawn representing the spectrum for each filter position. These curves

were transferred to and cut out of wooden sheets of uniform thickness. Incorporating the 32 resulting curves into a solid model gave the three-dimensional representation of Fig. 14. The three axes in this model represent energy (X), count rate (Y), and filter thickness (Z). The two black lines running down the face of the curves denote the primary ^{137}Cs peak at 660 keV and the 120 keV scatter peak. The 660 keV primary radiation falls off in the smooth exponential fashion expected from increasing incremental filter thickness. The scatter components do not follow this smooth fall-off so well. The scatter starts off as a double-peak function, which drops rapidly in the first few filtrations to become a single-peaked curve at lower intensities. The initial rapid fall-off in the scatter component later becomes slow, whereas the attenuation of the primary peak continues unabated. This causes the scatter to persist even at the weakest intensities, where the primary peak is no longer visable. This residual scatter present may be the result of leakage around the edges of the filter, which is not tight against the source shield; or it may represent the degraded components of the primary radiation that finally trickles through the filters.

Generally speaking, the relative shape of these curves is reasonably constant except when the heaviest filter sections are in position. Unless treatments are to be given at very low dose rates, no corrections for spectral changes are anticipated.

The last series of measurements made before release of the facility for clinical use was to determine the exposure rates available for treatment. The ionization chamber was positioned 12 cm above the

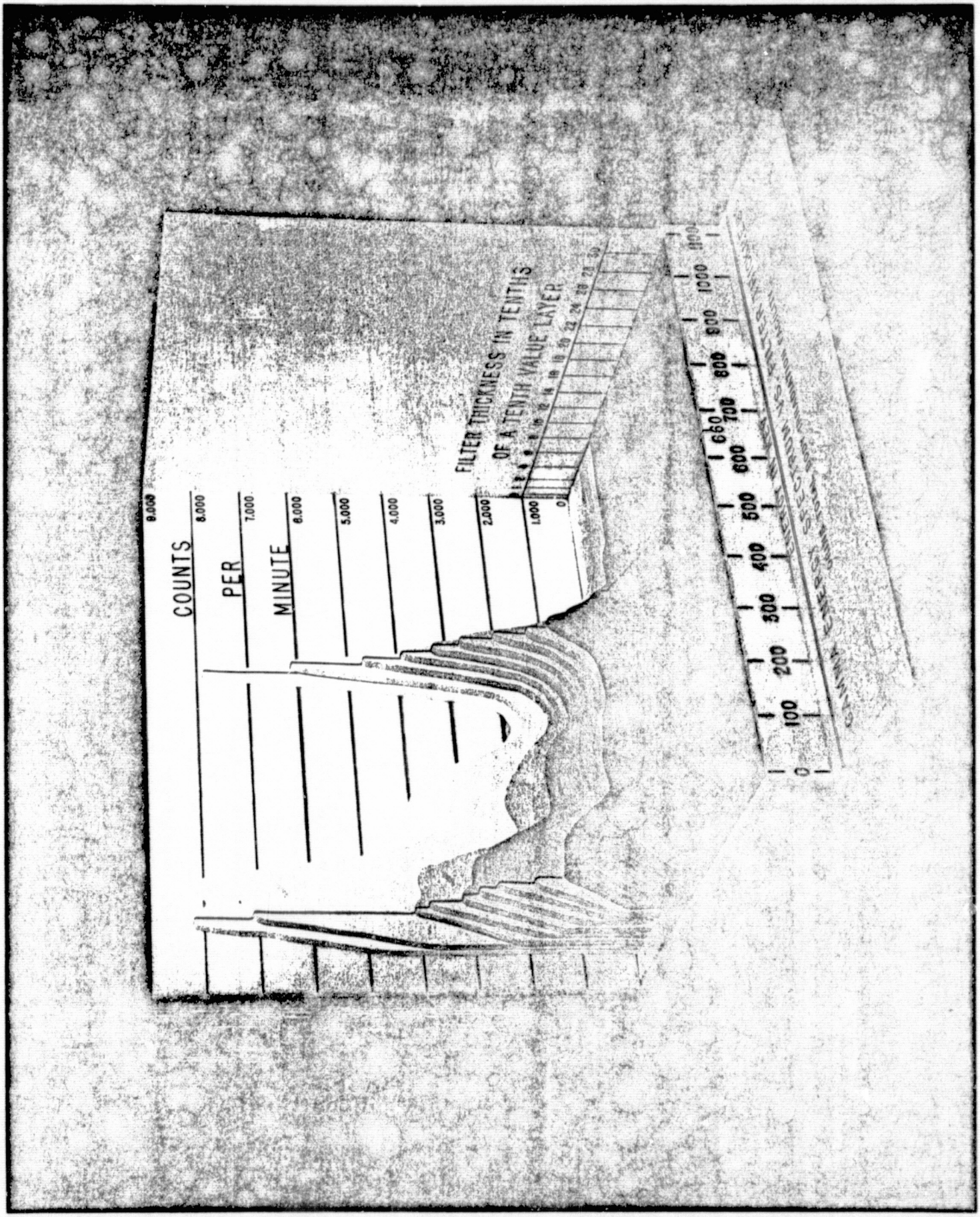

Fig. 14

center of the bed and successive readings were taken for each filter thickness. Figure 15 illustrates the result of this investigation by plotting exposure rate against increasing filter thickness. The actual curve deviates substantially from the calculated attenuation line at heavier filtrations. Probably this results from the leakage of radiation around the sides of the filter and, moreover, from the scattered component, which is not considered in calculating the theoretical attenuation line, that leaks through the filter.

The attenuating filters provided an intensity range of about 160:1, which was more than adequate for clinical studies. For the convenience of the operators, a chart was prepared showing the treatment times required to deliver various total exposures (corrected for decay) with any desired filter thickness. If a slow rate of treatment was desired, more filtration was added and the time lengthened. This relieved the technician of the responsibility of making a separate time calculation for each treatment, and thus minimized the chance of error.

Initial therapeutic protocols called for midline exposures of 50-100 R given within 1.5 hrs. The exposure rate was 1.5 R/min except in a few instances where the clinical course of disease required larger total doses at higher rates. These protocols were later expanded to include fractionated therapy that called for 30 R/day, at 1.5 R/min for five consecutive days (total exposure 150 R), as well as either 30 R or 10 R (1.5 R/min) on a prn basis as mandated by disease progression.

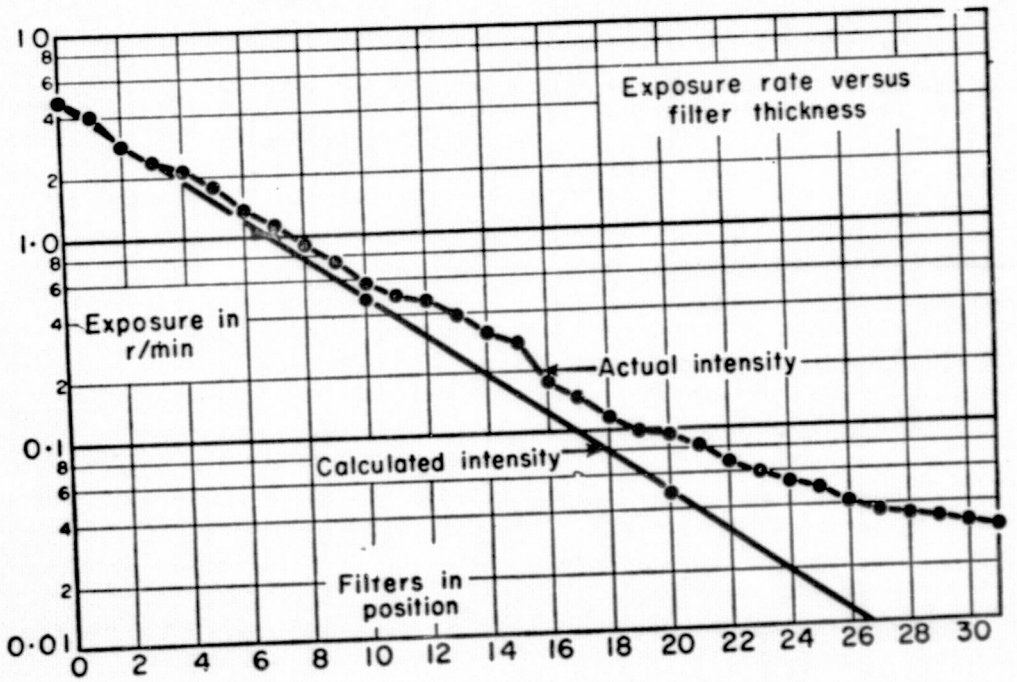
Exposure rate versus filter thickness
Exposure in r/min
Actual intensity
Calculated intensity
Filters in position
10
8
6
4
2
1·0
8
6
4
2
0·1
8
6
4
2
0·01
0
2
4
6
8
10
12
14
16
18
20
22
24
26
28
30

Fig. 15

2. LETBI

Radiobiologic observations on dose fractionation and protraction in animals and man suggest that beneficial effects of TBI in chronic leukemia and other myeloproliferations may be augmented by low-exposure rates or dose fractionation. These observations provide the experimental and clinical rationale for this new low-exposure-rate facility.

The low-exposure-rate total-body irradiation facility (LETBI) diagramed in Fig. 16 consists primarily of a large concrete outer room in which a smaller inner exposure room is centrally positioned. The ^{60}Co sources located in the outer room, as shown, irradiate the inner room from all sides.

The resulting radiation field enabled the inner room to be made sufficiently large (16 ft x 16 ft x 8 ft) for two patients to live in, as in a two-bed ward, for an extended time (days) during their exposure to 1.5 R/hr (Fig. 17). The eight corner sources (Fig. 16) initially consisted of 26 curies each of ^{60}Co and the central ceiling and floor sources of 4 curies each. These sources are operated and monitored remotely from an instrument console (Fig. 18) located in an adjacent control room (Fig. 16C), that also contains closed circuit TV monitors, an intercommunication system for patient surviellance, and a physiologic monitoring system described elsewhere in this report. All these instruments, operational relays, safety interlock switches, interrupt circuits are wired to an IBM 1800 computer in another adjacent room (Fig. 16D) for data storage and processing on a constant real-time basis during the facility's operation. Switches on the console permit the various interrupt levels in the IBM 1800 computer, located in the room below, to be activated so that prearranged programs for analysis

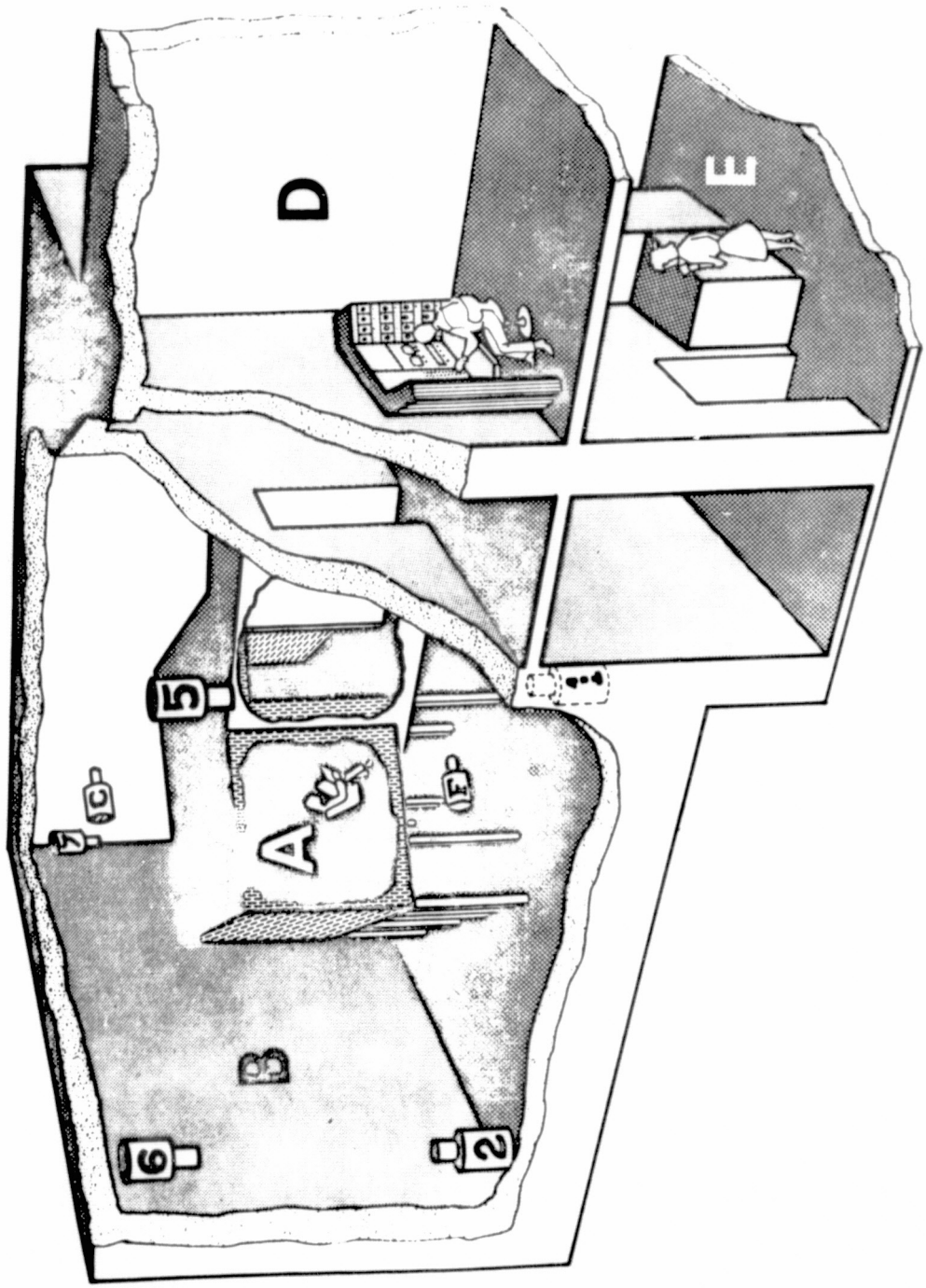

Fig. 16

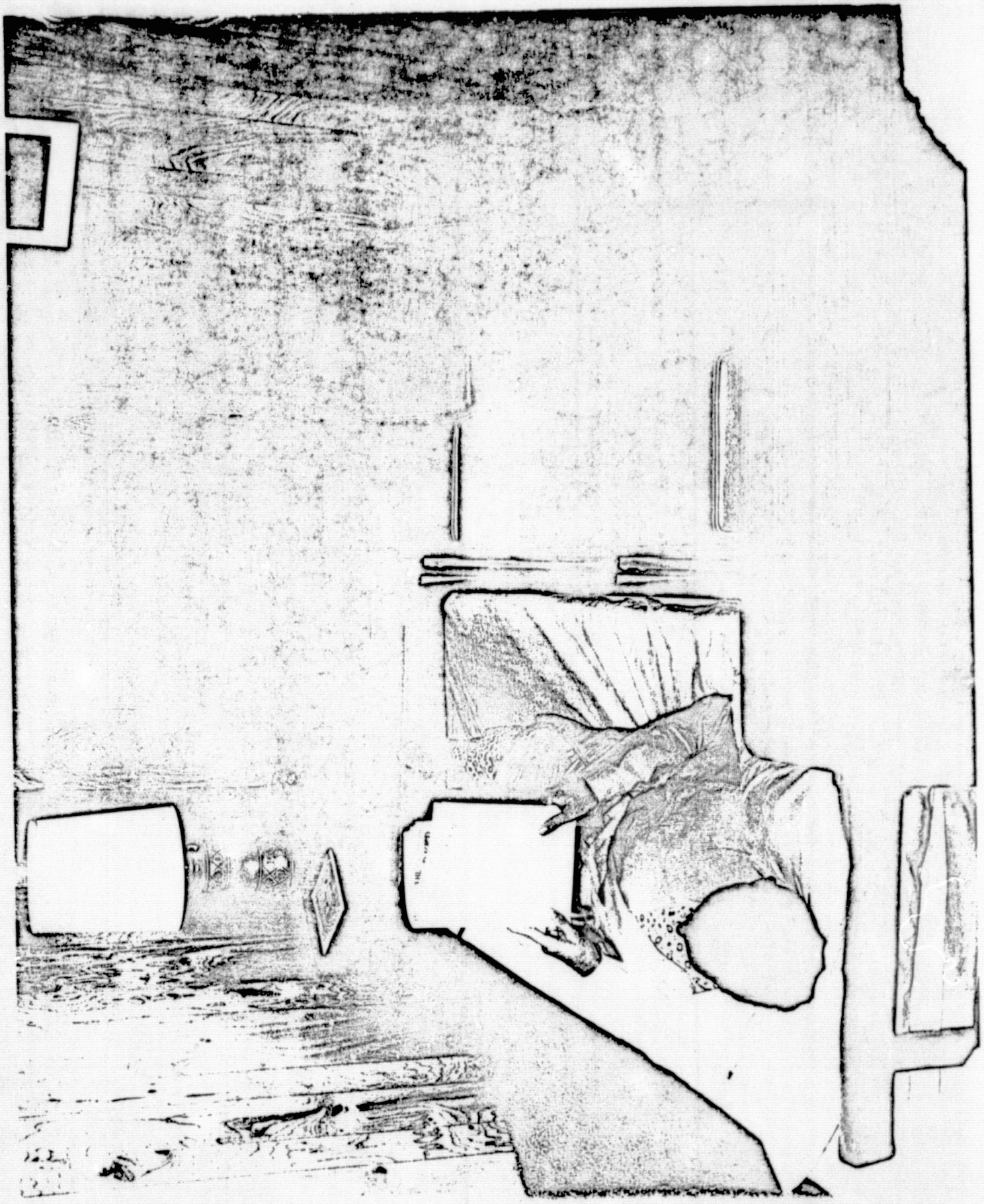

Fig. 17

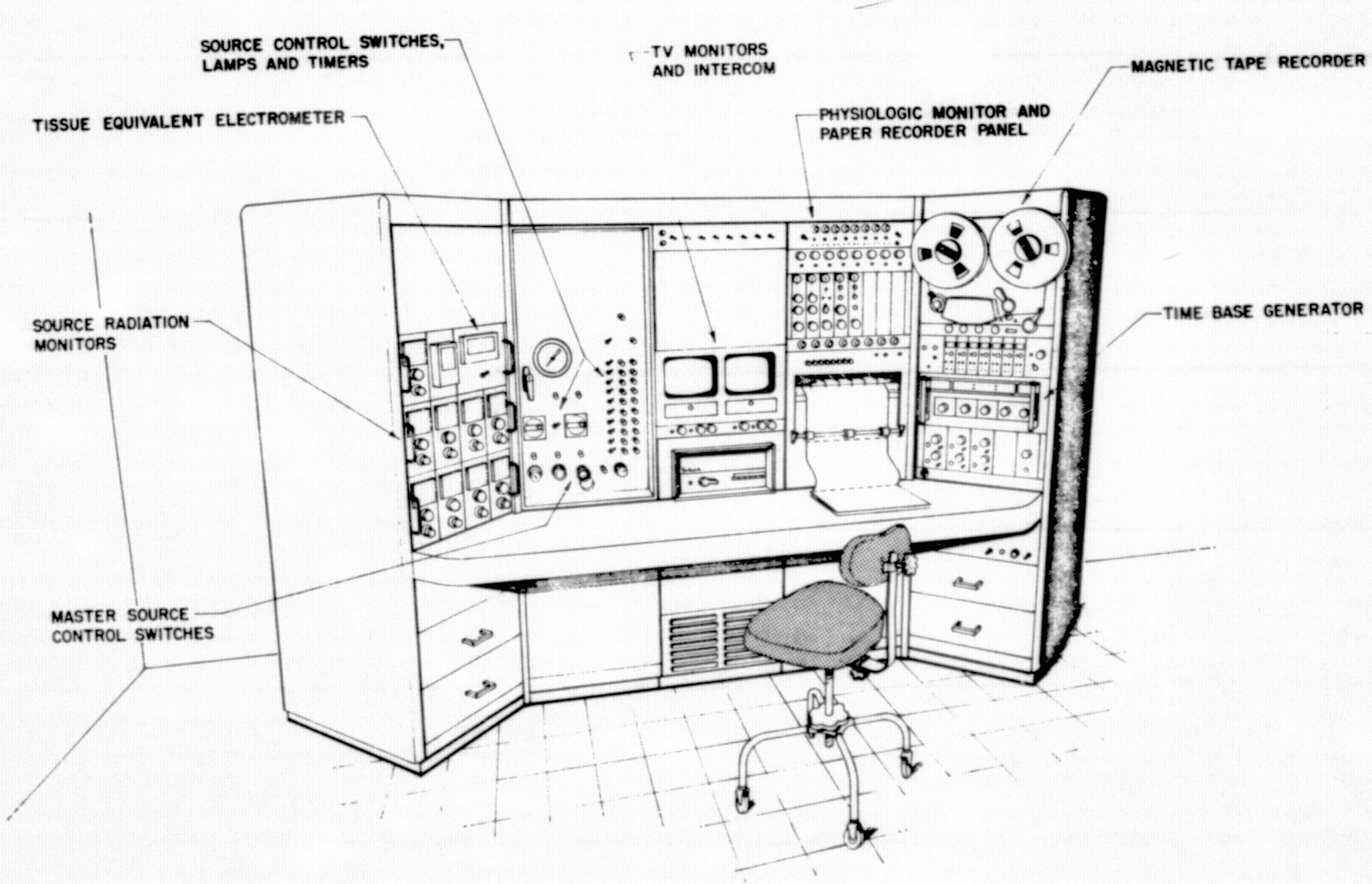
SOURCE CONTROL SWITCHES, LAMPS AND TIMERS
TV MONITORS AND INTERCOM
MAGNETIC TAPE RECORDER
TISSUE EQUIVALENT ELECTROMETER
PHYSIOLOGIC MONITOR AND PAPER RECORDER PANEL
SOURCE RADIATION MONITORS
TIME BASE GENERATOR
MASTER SOURCE CONTROL SWITCHES

Fig. 18

of physiological signals can be called and executed. Figure 19 shows the signals that are now being fed into the computer. On the analog side, calibrated voltages in the ± 10 millivolt range are being supplied from the conditioned physiologic monitor outputs. Other analog signals from the radiation monitor report on the operation of the individual sources. All these signals are recorded and analyzed by the computer programs. The computer is programmed to check the values of all analog signals and to signal an alarm if any physiologic signals or radiation levels stray outside preset limits or source-containing pistons fail to return to their shields on demand. Digital switch closure signals (Fig. 19) from the console enable the computer to record when the sources are raised and lowered and the reasons interruptions in exposure occurred.

The radiation is turned off automatically whenever the patient leaves the treatment room or when anyone enters the interlock-controlled area. When the patient leaves to visit the bathroom located off the entrance hall to the treatment room but does not leave the controlled area itself, the radiation devices are turned on automatically upon his return to the treatment room. If the exposure is interrupted for nursing care, meals, and other reasons, the radiation devices must be turned on by the nurse who records the reason for the interruption. These events and exposure times are recorded by the computer and nursing and technical staff (Fig. 20) for use in retrospective studies of therapeutic effectiveness and evaluation of possible radiation-induced effects. Hematologic studies and a system of dosimetry based on the use of tissue equivalent humanoid phantoms in LETBI are described elsewhere in this report.

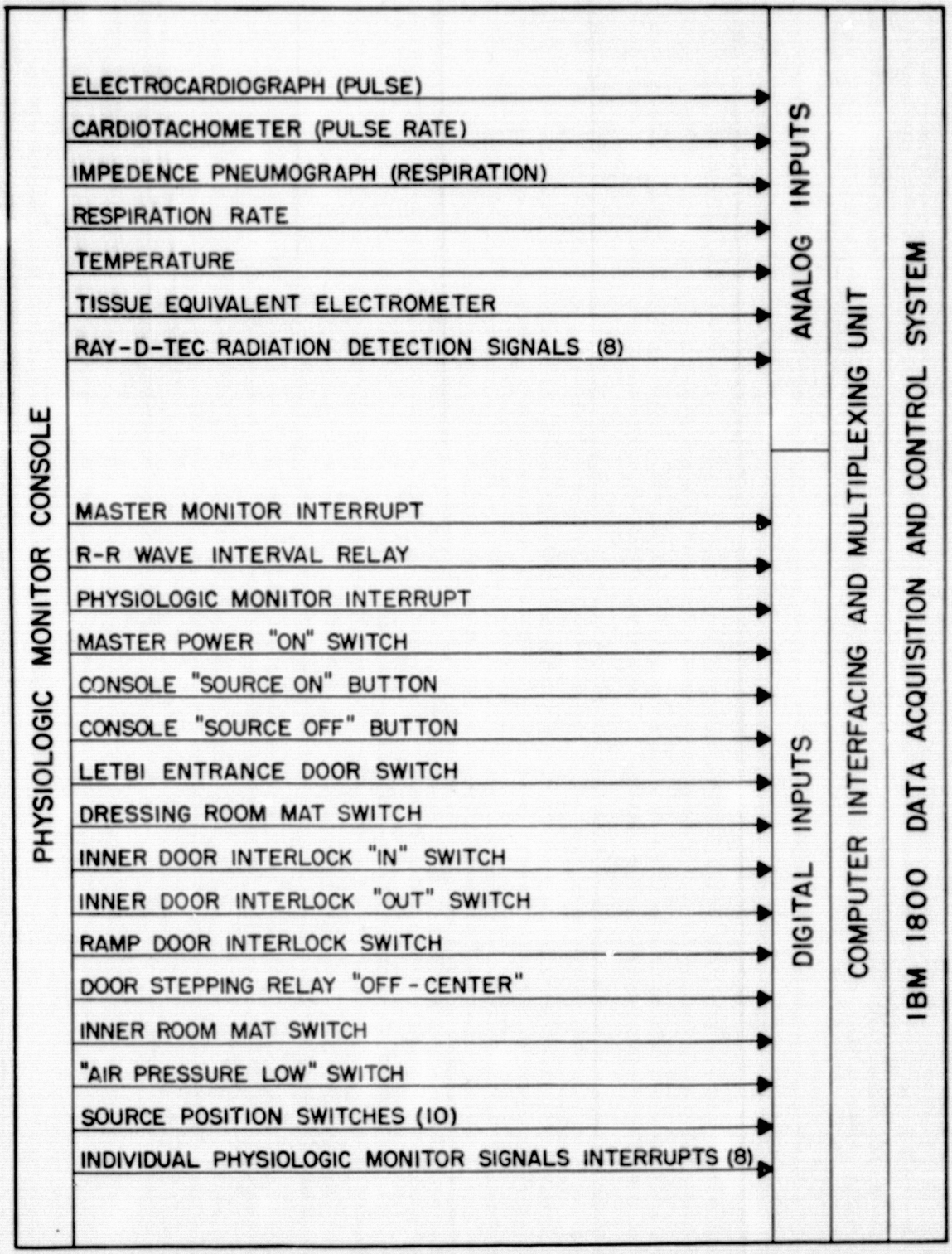
PHYSIOLOGIC MONITOR CONSOLE
ELECTROCARDIOGRAPH (PULSE)
CARDIOTACHOMETER (PULSE RATE)
IMPEDENCE PNEUMOGRAPH (RESPIRATION)
RESPIRATION RATE
TEMPERATURE
TISSUE EQUIVALENT ELECTROMETER
RAY-D-TEC RADIATION DETECTION SIGNALS (8)
MASTER MONITOR INTERRUPT
R-R WAVE INTERVAL RELAY
PHYSIOLOGIC MONITOR INTERRUPT
MASTER POWER "ON" SWITCH
CONSOLE "SOURCE ON" BUTTON
CONSOLE "SOURCE OFF" BUTTON
LETBI ENTRANCE DOOR SWITCH
DRESSING ROOM MAT SWITCH
INNER DOOR INTERLOCK "IN" SWITCH
INNER DOOR INTERLOCK "OUT" SWITCH
RAMP DOOR INTERLOCK SWITCH
DOOR STEPPING RELAY "OFF-CENTER"
INNER ROOM MAT SWITCH
"AIR PRESSURE LOW" SWITCH
SOURCE POSITION SWITCHES (10)
INDIVIDUAL PHYSIOLOGIC MONITOR SIGNALS INTERRUPTS (8)
ANALOG INPUTS
DIGITAL INPUTS
COMPUTER INTERFACING AND MULTIPLEXING UNIT
IBM 1800 DATA ACQUISITION AND CONTROL SYSTEM

Fig. 19

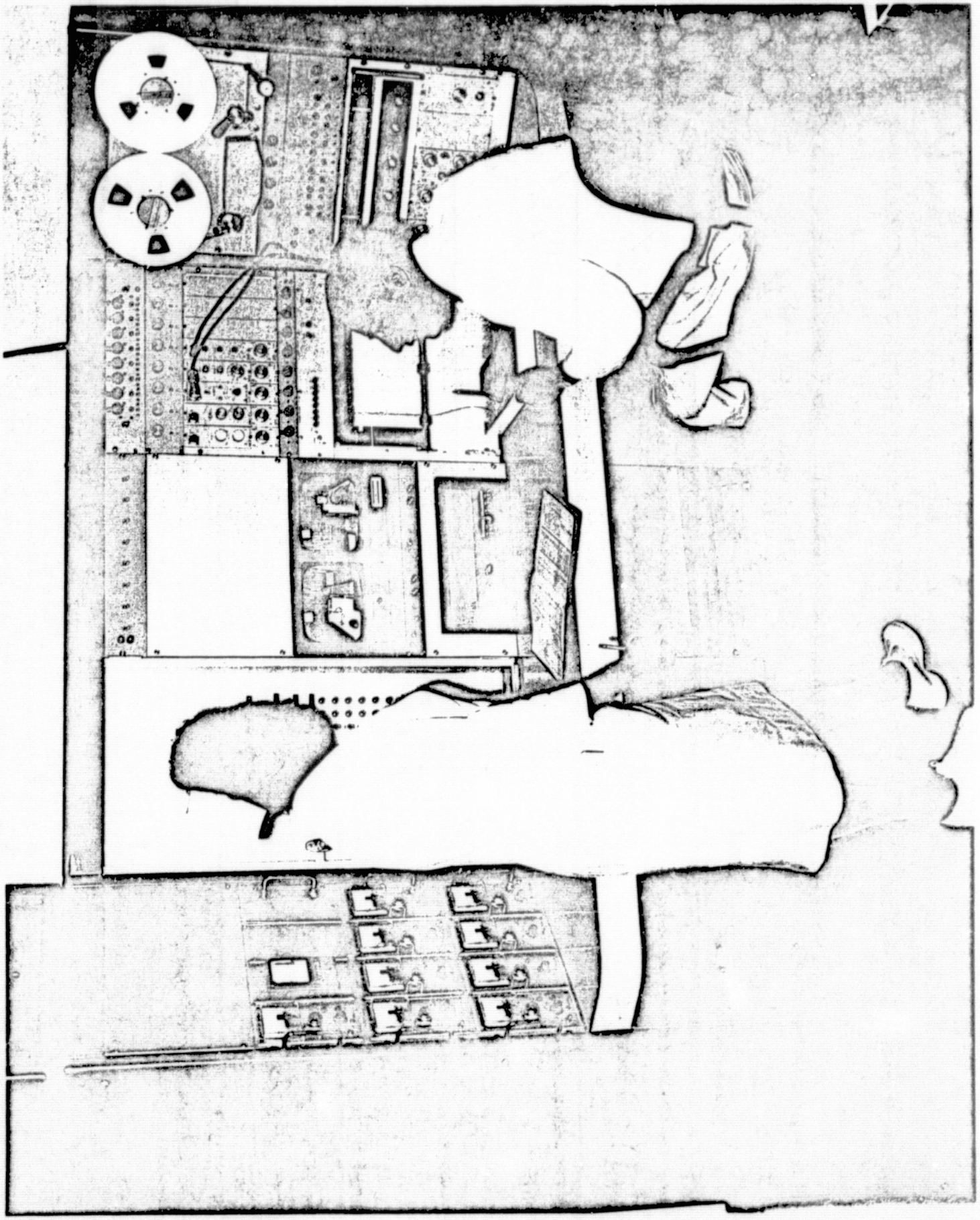

Fig. 20

Therapy protocols for this low-exposure-rate irradiation facility were designed so that patients received 30 R/day (1.5 R/hr) based upon a 20 hr day. Total exposures ranged from 30 R to 250 R. After establishment of a clinical hematologic data base, some patients were treated with only 10 R/day (∿6.7 hrs). After source decay resulted in alteration of isodose configurations, the exposure rate was dropped (via source shielding) to 0.8 R/hr or total daily exposures of 16 R.

A physiologic monitoring system was developed for use in the LETBI facility to study vital functions of patients undergoing radiation treatment. The basic monitoring system is illustrated in the block diagram of Fig. 21. The system was initially developed to record the following six variables:

1. EKG waveform (frequency response: 0.01 to 250 Hz).
2. Heart or pulse rate (range: 0 to 200 beats/min).
3. Respiration waveform (frequency response: 0.01 to 10 Hz).
4. Respiration rate (range: 0 to 60 breaths/min).
5. Rectal temperature (range 34° to 42°C).
6. Time base (from start of irradiation).

As shown in Fig. 22, signals from the patients were conducted through a flexible umbilical cable in the irradiation room and a 65-ft long signal cable running to the monitor console. The remote console location was necessary because of the gamma radiation field. Signals from the patient were conditioned by the monitor electronics and then transmitted for recording and analysis through cables to the computer room located below the monitor. We investigated a number of electrode and sensor arrangements to obtain the most information with the least

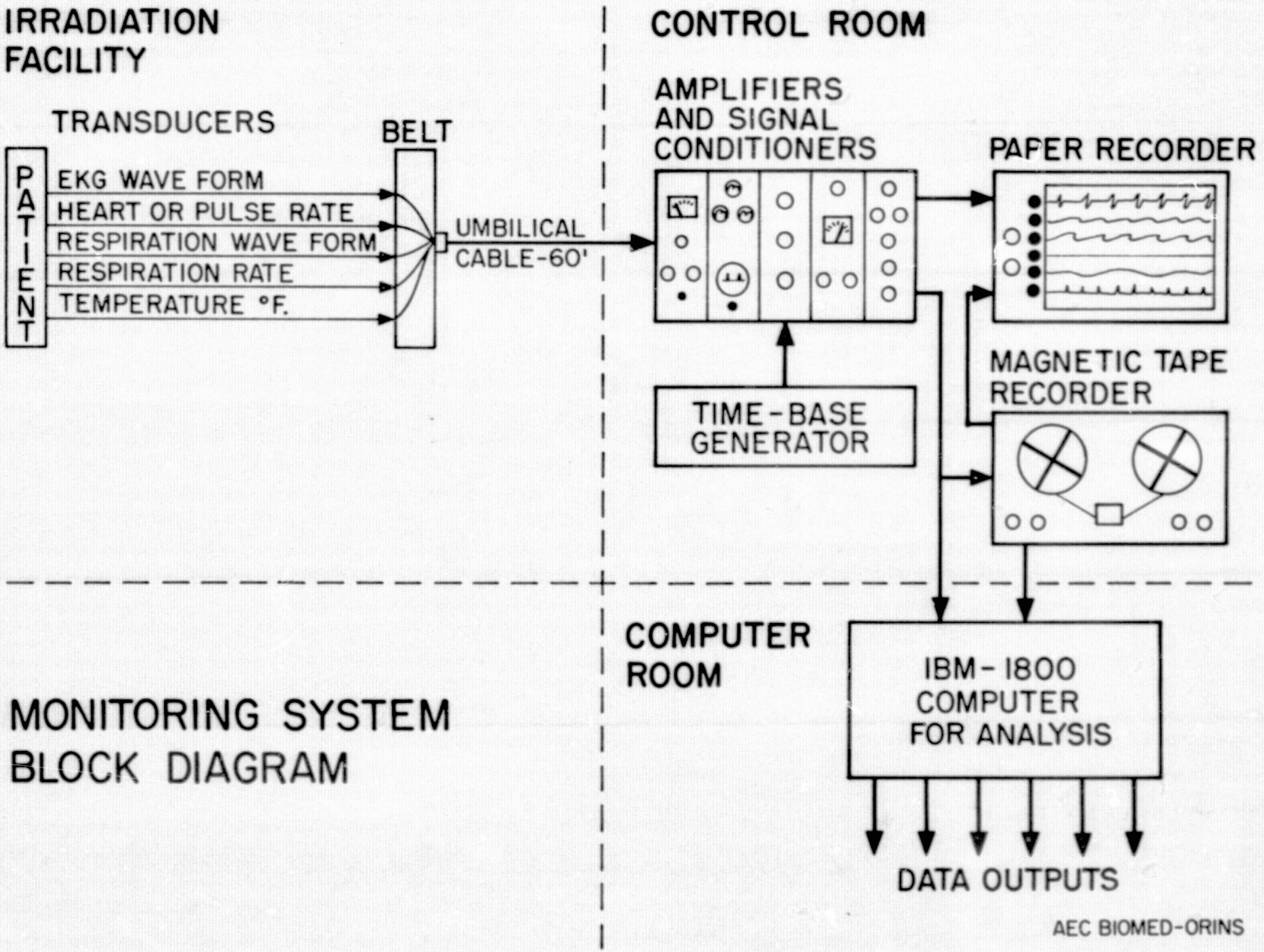

MONITORING SYSTEM
BLOCK DIAGRAM

Fig. 21

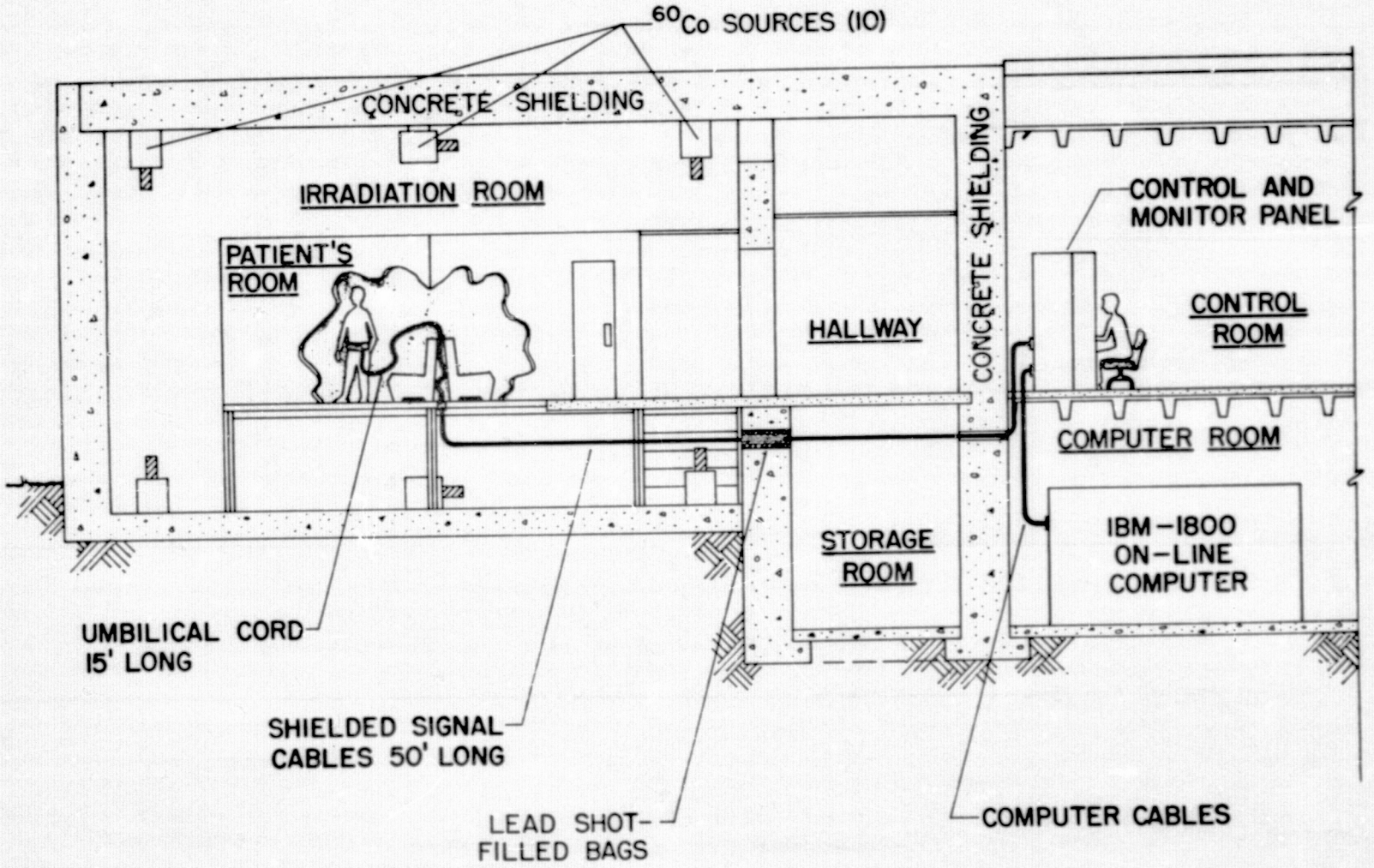
^{60}Co SOURCES (10)
CONCRETE SHIELDING
IRRADIATION ROOM
PATIENT'S ROOM
HALLWAY
CONCRETE SHIELDING
CONTROL AND MONITOR PANEL
CONTROL ROOM
COMPUTER ROOM
STORAGE ROOM
IBM-1800 ON-LINE COMPUTER
UMBILICAL CORD 15' LONG
SHIELDED SIGNAL CABLES 50' LONG
LEAD SHOT-FILLED BAGS
COMPUTER CABLES

Fig. 22

inconvenience to the patient. The configuration shown in Fig. 23 permitted us to record the first four of the listed variables with the use of only three electrodes attached to the patient. The EKG waveform and pulse rate were obtained with the use of a differential amplifier and a cardiotachometer of standard manufacture. The respiration waveform and breathing rate were obtained, however, at a frequency of 50 khz so that the two types of information from the same set of electrodes will not mutually interfere. Wiring for future monitoring of galvanic skin resistance (GSR) was included in the cables.

One of the problems with using the monitor is that radiation treatments were planned to last a week or more. Difficulties have been experienced in getting the electrodes applied for minimum irritation and in arranging the interconnecting belt and umbilical cord for least discomfort and restraint for an ambulatory patient. The electrode, belt, and cable arrangement shown in Fig. 24 overcame these problems. Usually the patient wore the belt over his hospital clothing as shown in Fig. 25 and guided the umbilical cord with his hands as he moved about the room. The umbilical cord contained a set of quick-disconnect connectors near the belt so that the patient or attendant could uncouple and reestablish the monitoring circuits without the need for removing the electrodes.

Power-frequency interference was a major problem in recording low-level bipotential measurements and the physiologic measurements we made in the low-exposure-rate total-body irradiation facility were not exempt from this difficulty. The interference on our recording charts resulted from the fact that electric currents and voltages can

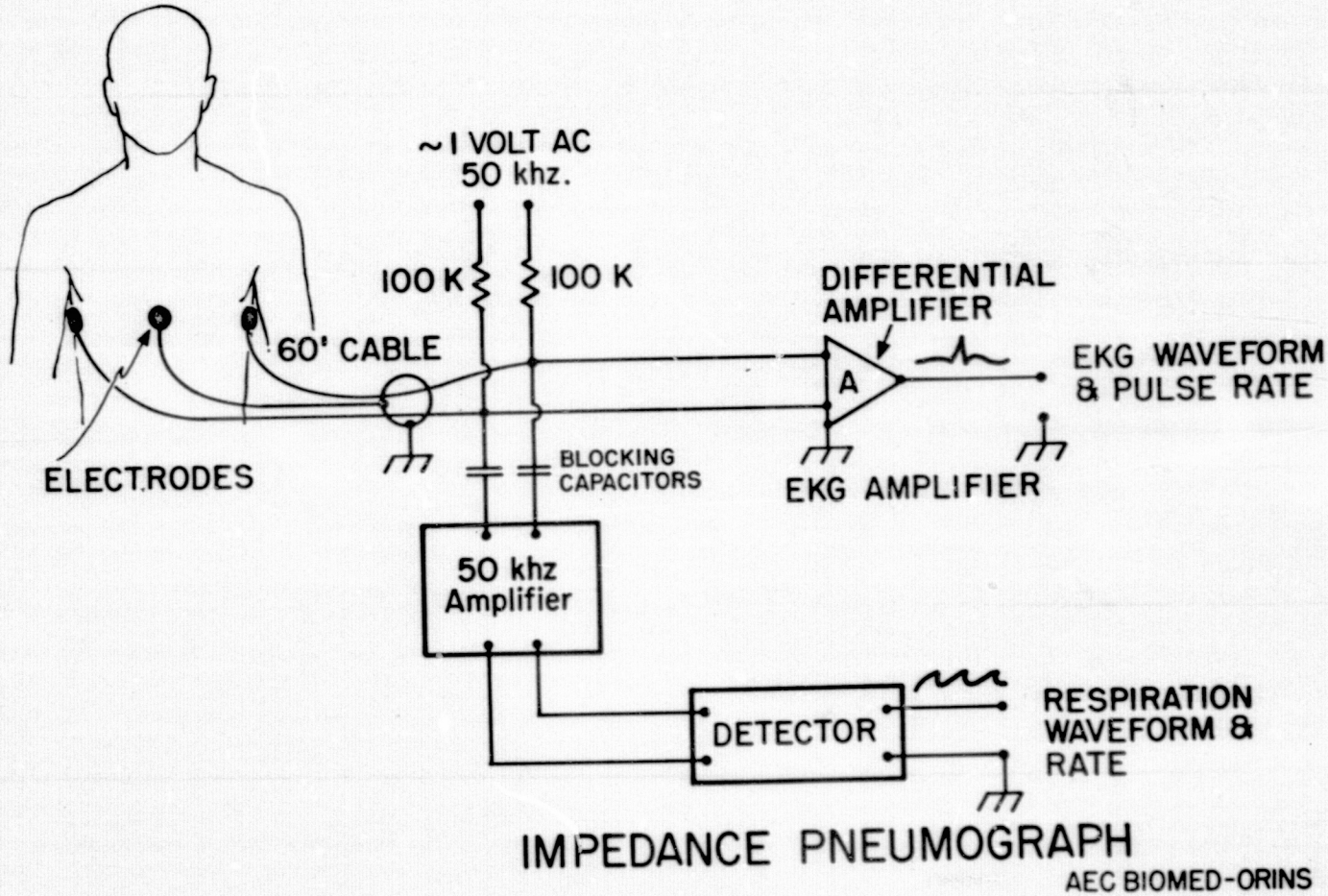
~1 VOLT AC
50 khz.
100 K
100 K
DIFFERENTIAL
AMPLIFIER
60' CABLE
A
EKG WAVEFORM
& PULSE RATE
ELECTRODES
BLOCKING
CAPACITORS
EKG AMPLIFIER
50 khz
Amplifier
DETECTOR
RESPIRATION
WAVEFORM &
RATE
IMPEDANCE PNEUMOGRAPH
AEC BIOMED-ORINS

Fig. 23

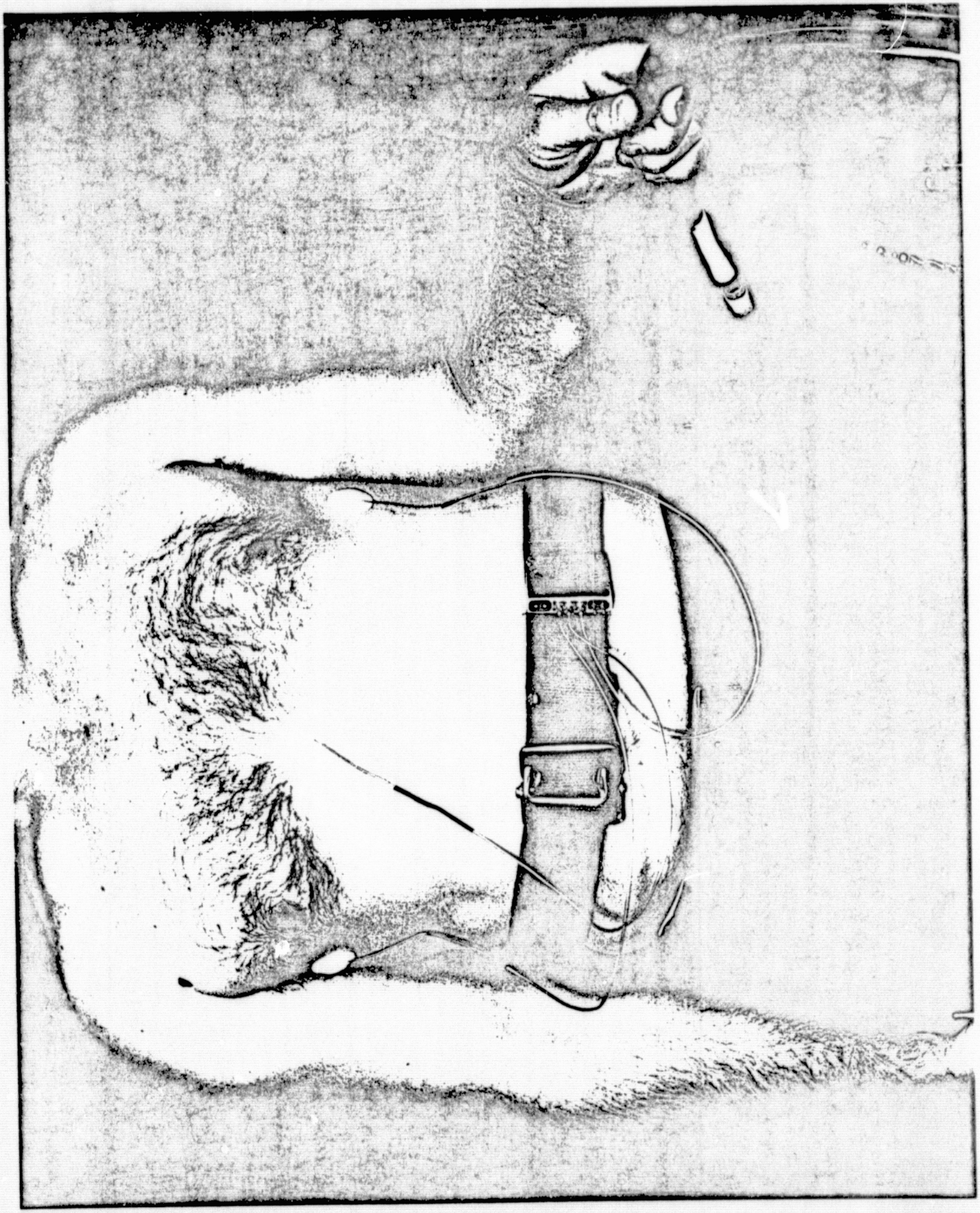

Fig. 24

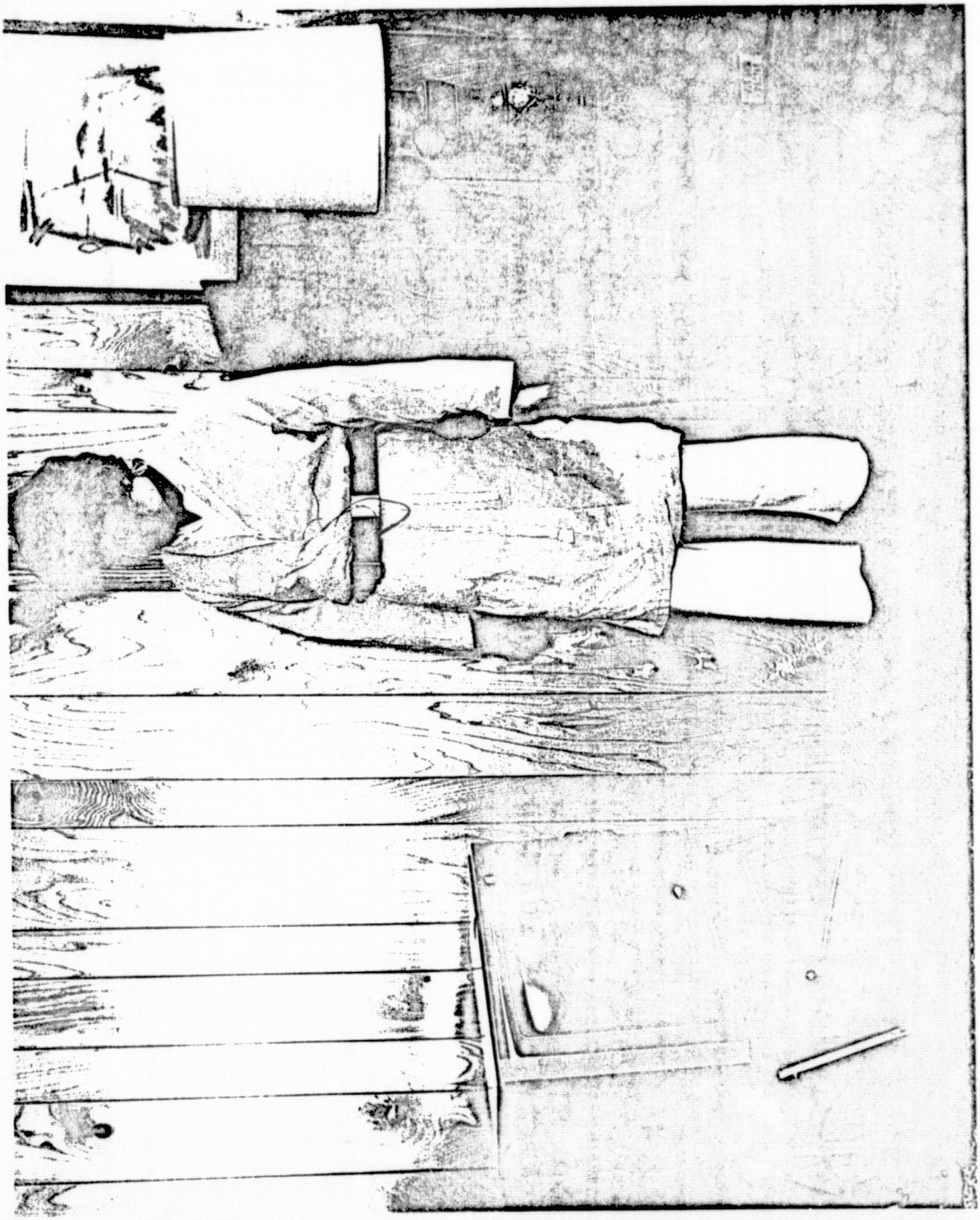

Fig. 25

be induced in a patient from nearby equipment powered from the commercial supply system. These artifacts show up most frequently in the EKG trace, and other traces derived from it, because the information frequently bandwidth for the EKG ranges from 0.01 to 250 Hz and the 60-Hz power-line frequency falls in the middle of this band. The respiration signals were derived, however, from a 50-kHz, 100-microampere constant-current supply and were much less affected by signals at the power-line frequency.

The interference in the EKG trace is coupled to the patient in two ways, similar to the broadcast and reception of radio signals. The first mode is by electric flux coupling, where charges in the subject are set in motion by moving charges in wiring and nearby electrical devices. This type of coupling is illustrated in Fig. 26. In the upper portion of the figure a single-ended amplifier is shown with capacitive coupling to a patient from a fluorescent lamp. Interference occurs because an AC voltage is induced through the lower resistor R_E to ground. This is picked up by the amplifier at terminal A and produces an output voltage E_o heavily contaminated with the power-frequency component. The lower portion of Fig. 26 shows how this 60-Hz component can be greatly attenuated through the use of a differential amplifier. The common-mode 60-Hz voltage is cancelled out by the differential amplifier characteristic. At the same time the differential EKG voltage is amplified properly and the output voltage E_o is interference free. In operation, with the differential amplifier connected, we found that by making low resistance electrode connections and positioning them carefully on the patient good recordings could be

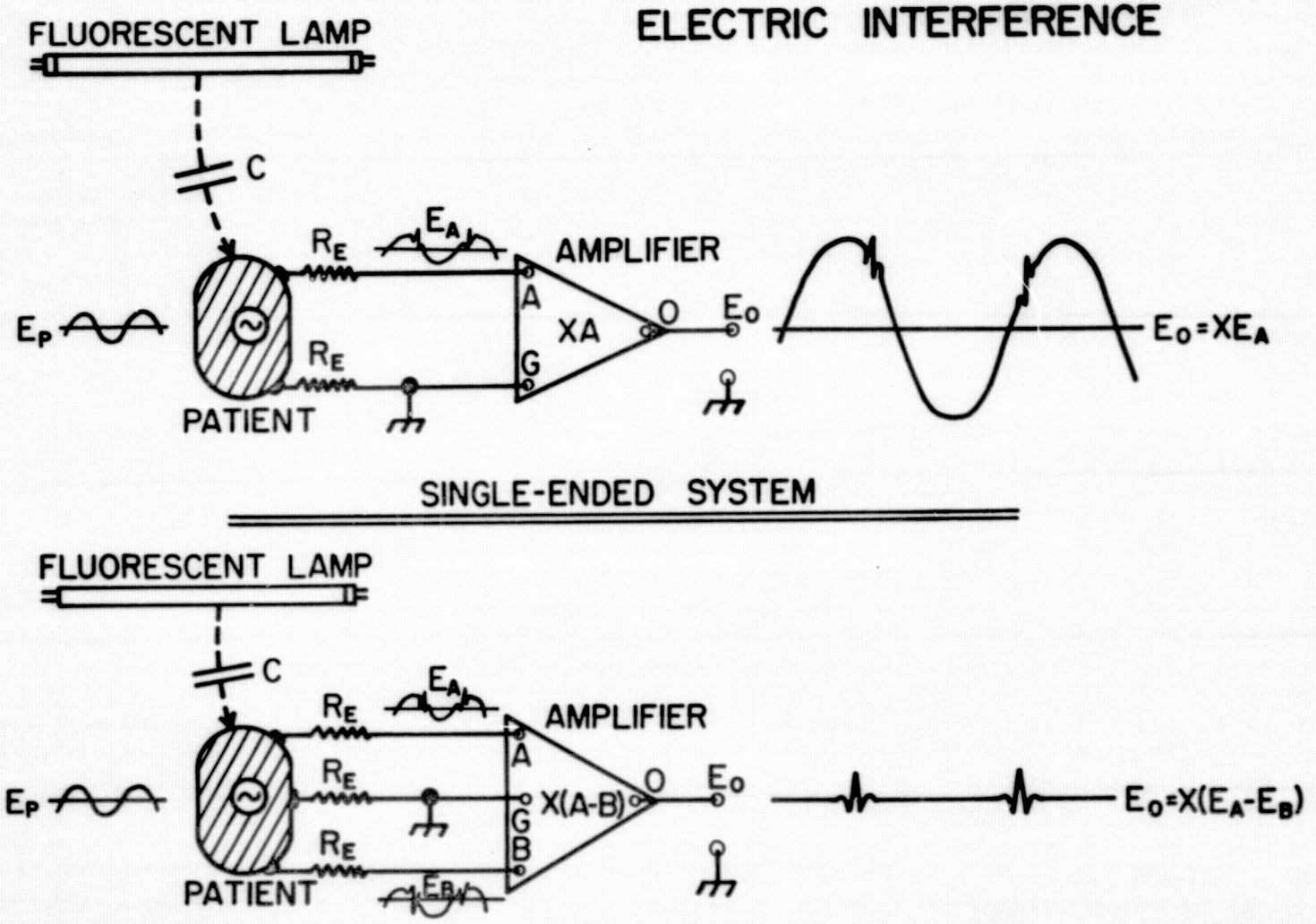
ELECTRIC INTERFERENCE
FLUORESCENT LAMP
C
R_E
E_A
AMPLIFIER
A
XA
O
E_o
E_P
R_E
G
PATIENT
$E_o = XE_A$
SINGLE-ENDED SYSTEM
FLUORESCENT LAMP
C
R_E
E_A
AMPLIFIER
A
R_E
X(A-B)
O
E_o
E_P
G
B
R_E
PATIENT
E_B
$E_o = X(E_A - E_B)$
DIFFERENTIAL AMPLIFIER SYSTEM

Fig. 26

obtained. Our interference-free recording of a 1-millivolt EKG voltage in the presence of a 60-Hz signal, many factors higher in magnitude, demonstrated the efficacy of the differential amplifier circuit.

The second mode of interference transfer is by magnetic flux coupling, where currents are induced in the patient through a transformer-like action by currents and magnetic fluxes in nearby power wiring and electrical equipment. Figure 27 shows how our present three-electrode patient connections act as two, one-turn secondary loops of a transformer coil through the patient; an electrical device acts as the primary circuit and air is the transformer core. If there is am imbalance in the flux coupling between the source and the two patient loops, a differential current and voltage will exist as terminals A and B that will be detected and amplified. Because this kind of signal is not rejected by the differential amplifier circuit we have been particularly interested in locating and mapping the magnetic field sources and intensities in the LETBI facility.

To explore these magnetic fields a resonant probe was constructed as shown in Fig. 28. The probe consisted of a coil wound on an iron core that is made resonant to 60 Hz with a parallel capacitor. An oscilloscope with a high-sensitivity preamplifier was used as a read-out device (Fig. 29). The volume contained within the LETBI room was measured off in 2-ft increments and every electrical device was turned on to provide a "worst case" condition. Measurements were then made holding the probe axis vertical and with the oscilloscope located in

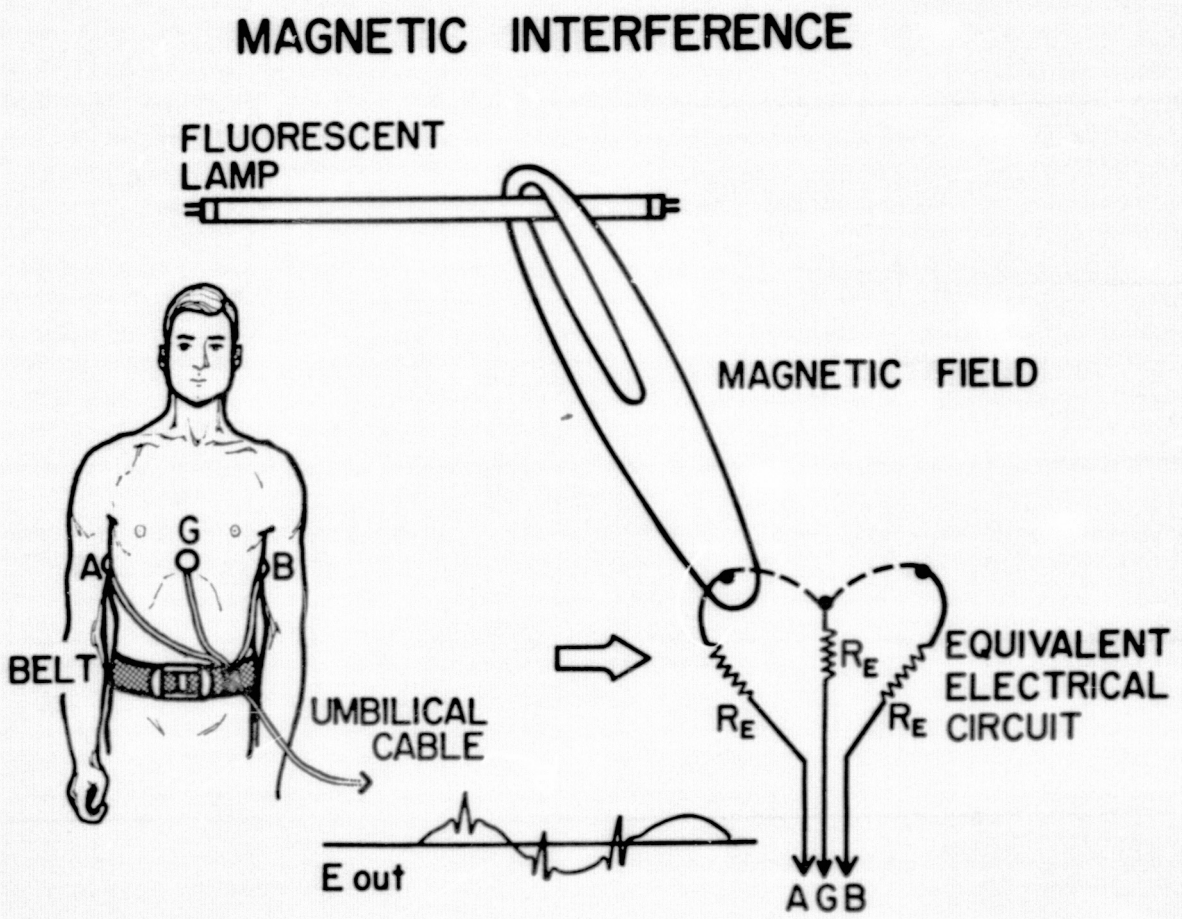
MAGNETIC INTERFERENCE
FLUORESCENT LAMP
MAGNETIC FIELD
G
A
B
BELT
UMBILICAL CABLE
E out
R_E
R_E
R_E
EQUIVALENT ELECTRICAL CIRCUIT
A G B

Fig. 27

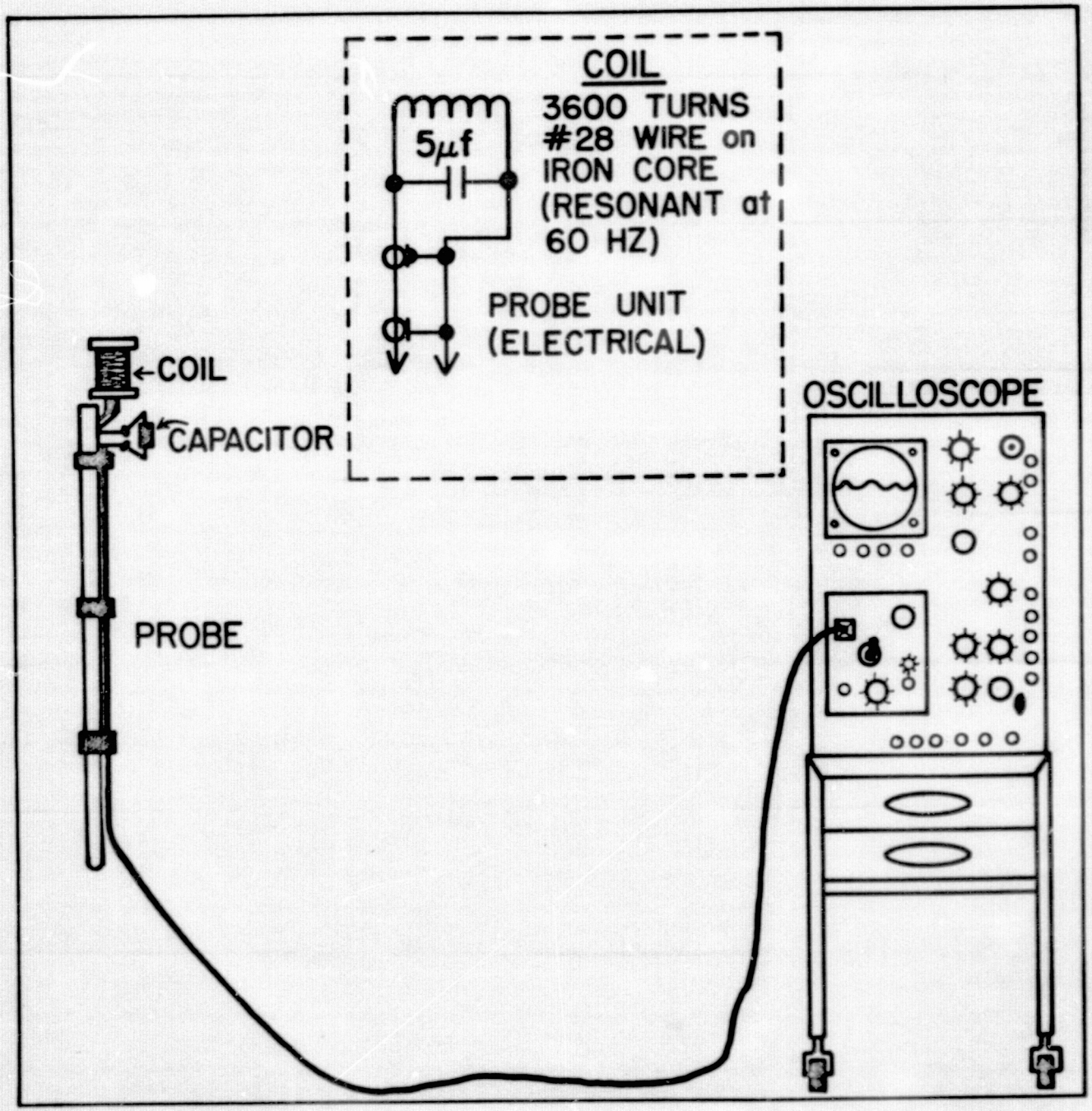
COIL
3600 TURNS
#28 WIRE on
IRON CORE
(RESONANT at
60 HZ)
5μf
PROBE UNIT
(ELECTRICAL)
COIL
CAPACITOR
PROBE
OSCILLOSCOPE

Fig. 28

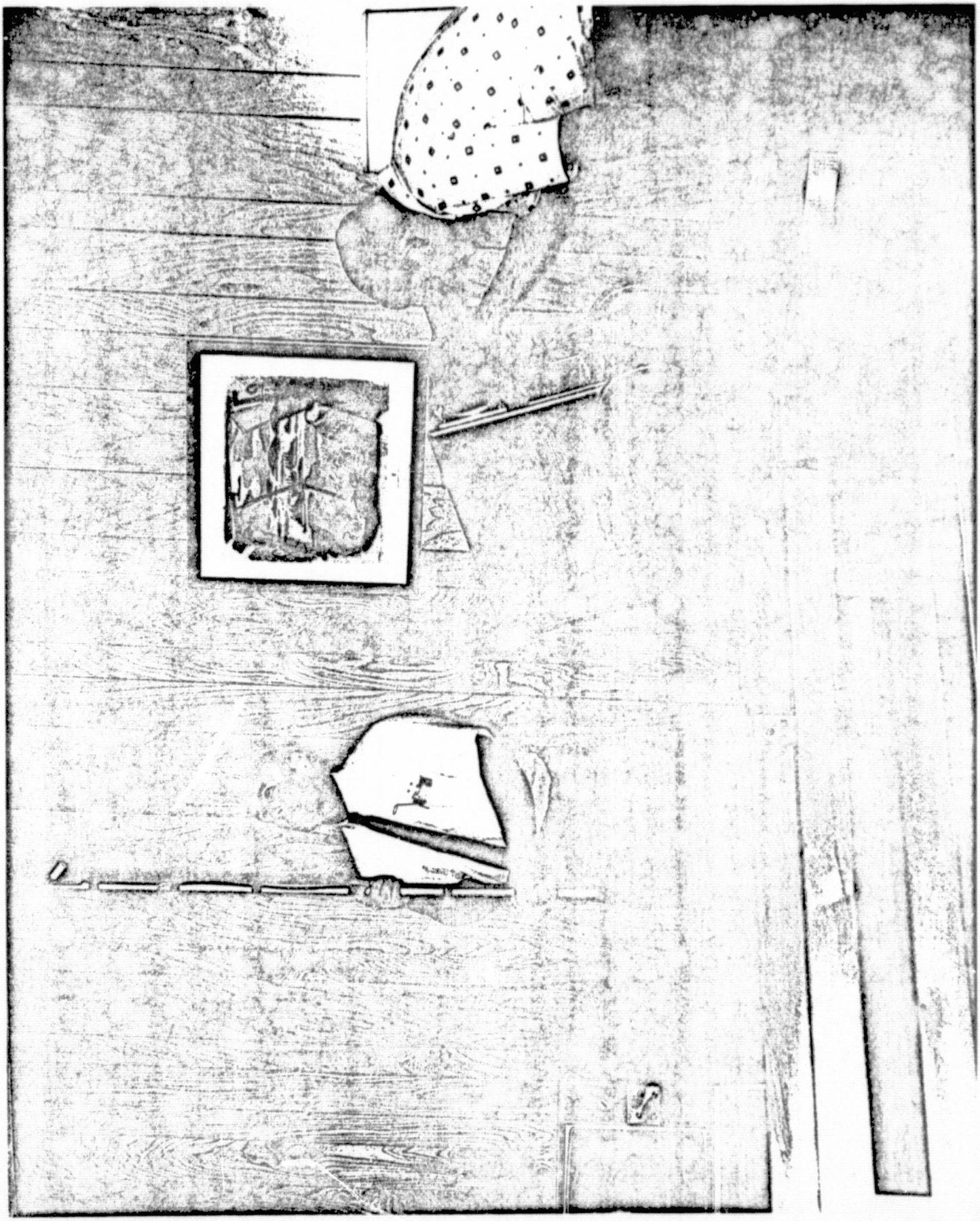

Fig. 29

the outside hall with an interconnecting cable between the two. Values were recorded for planes parallel to the floor, ceiling, four walls, a vertical cross section 3-3/4 ft from the west wall, and a horizontal cross section 3 ft above the floor.

Figure 30 shows a flux map made on a plan 3 ft above the floor. The flux was concentrated near the color TV set and near the wall corners and door where wiring is present. A magnetic flux map of the east wall (Fig. 31) showed two intense flux areas. One was located at the intercom and power switch panels and the other (highest intensity recorded in the room was 50 millivolts) located in the floor corner directly above some fluorescent-lighting ballast circuits. Figure 32 shows the flux pattern obtained in a vertical cross section taken directly beneath a row of fluorescent lamps. These lamp fixtures give off an appreciable amount of magnetic flux and, as seen in the figure, this field falls off with distance.

To determine the magnitude of the magnetic coupling, a two-loop wire probe was constructed similar in shape to the equivalent circuit shown in Fig. 27. This probe was held near one of the fluorescent lamps on the ceiling, positioned with one loop toward the lamps and the other loop pointed away. The unequal flux coupling produced a differential voltage of 50 microvolts on our measuring instruments. Although this intensity of magnetically coupled voltage was not detrimental to our present EKG measurements, it would have serious effects on EEG or other low-level physiologic signals which we might attempt to record in the future.

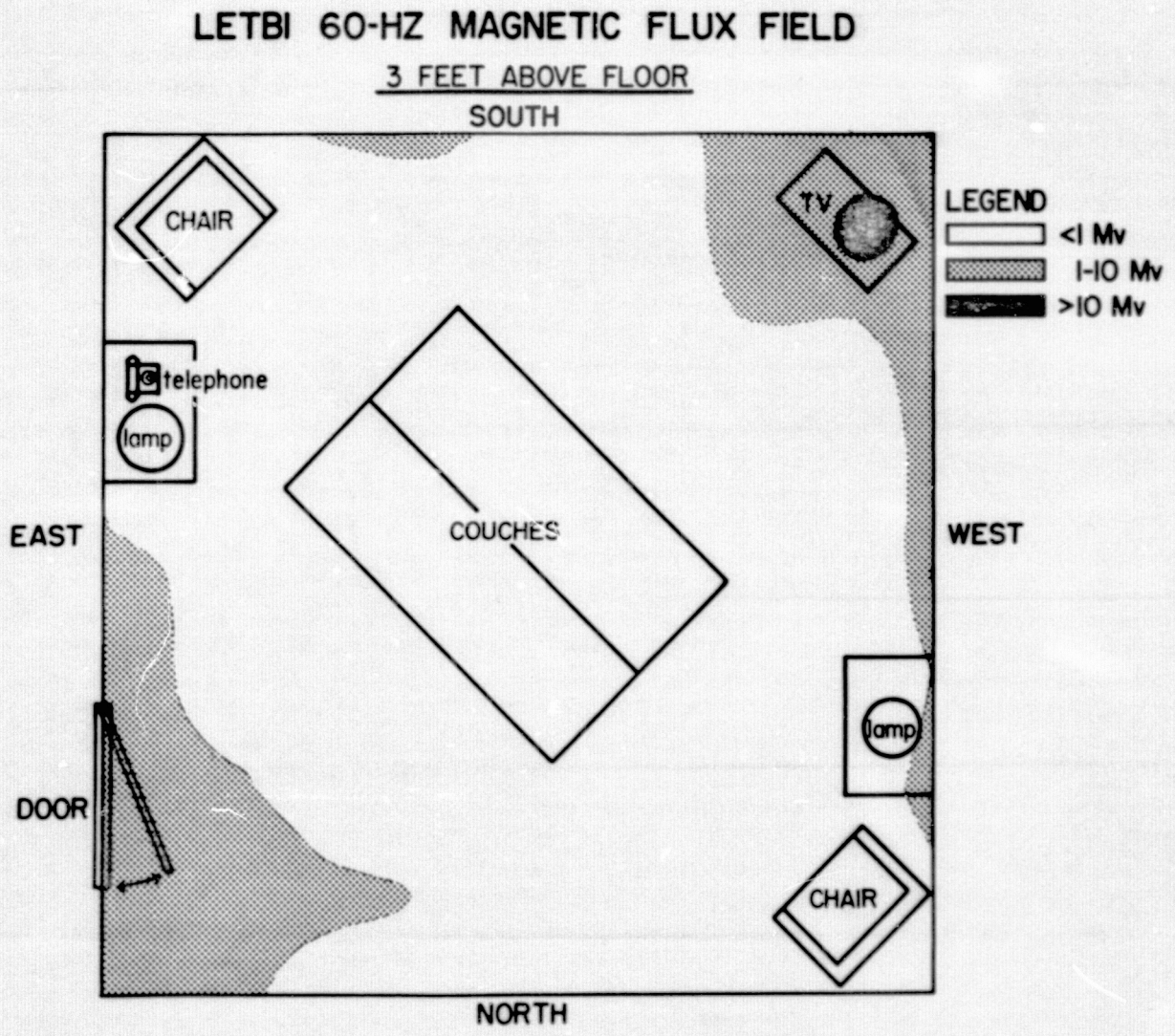
LETBI 60-HZ MAGNETIC FLUX FIELD
3 FEET ABOVE FLOOR
SOUTH
CHAIR
TV
LEGEND
<1 Mv
1-10 Mv
>10 Mv
telephone
lamp
COUCHES
EAST
WEST
DOOR
lamp
CHAIR
NORTH

Fig. 30

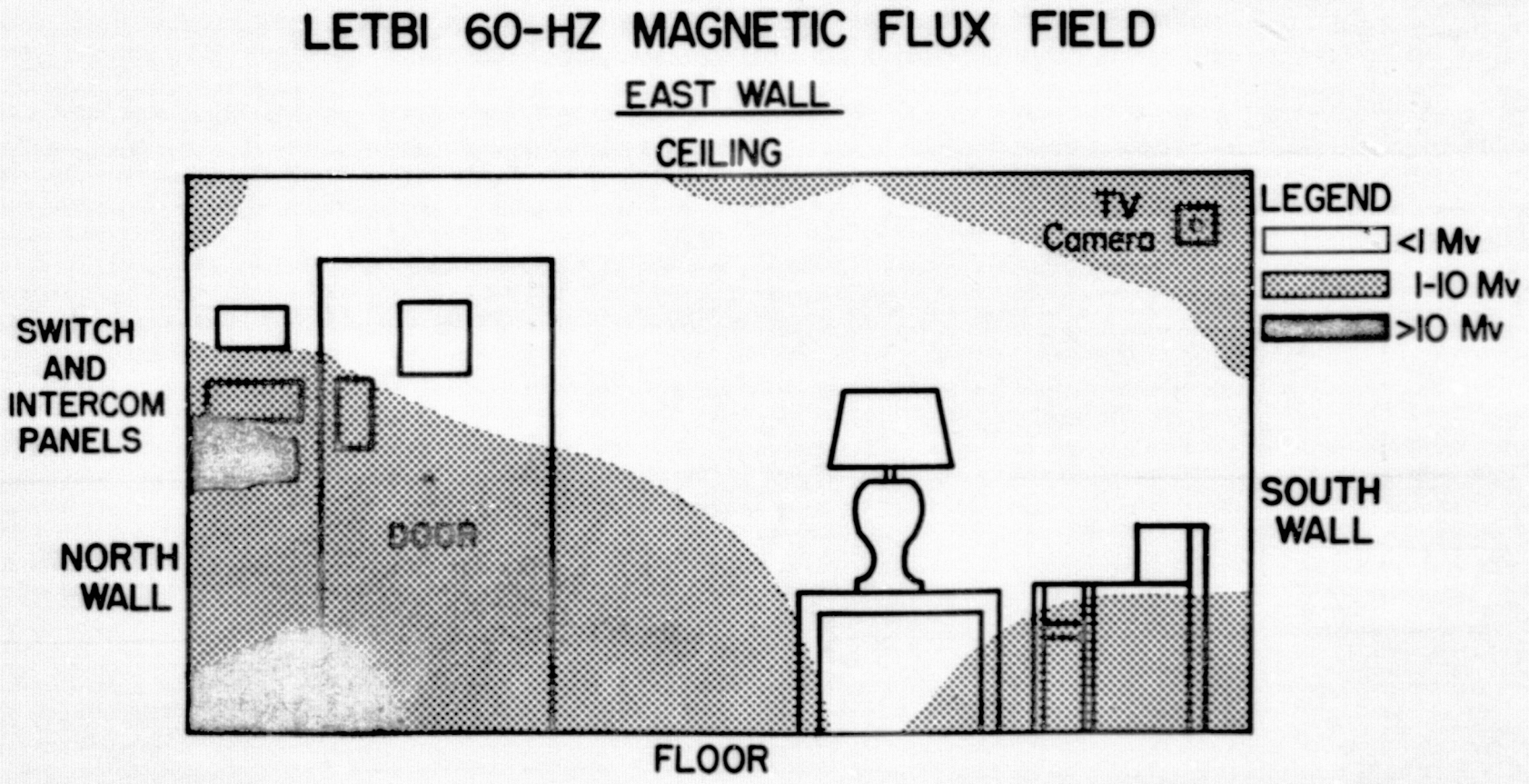
LETBI 60-HZ MAGNETIC FLUX FIELD
EAST WALL
CEILING
TV Camera
LEGEND
<1 Mv
1-10 Mv
>10 Mv
SWITCH AND INTERCOM PANELS
DOOR
NORTH WALL
SOUTH WALL
FLOOR

Fig. 31

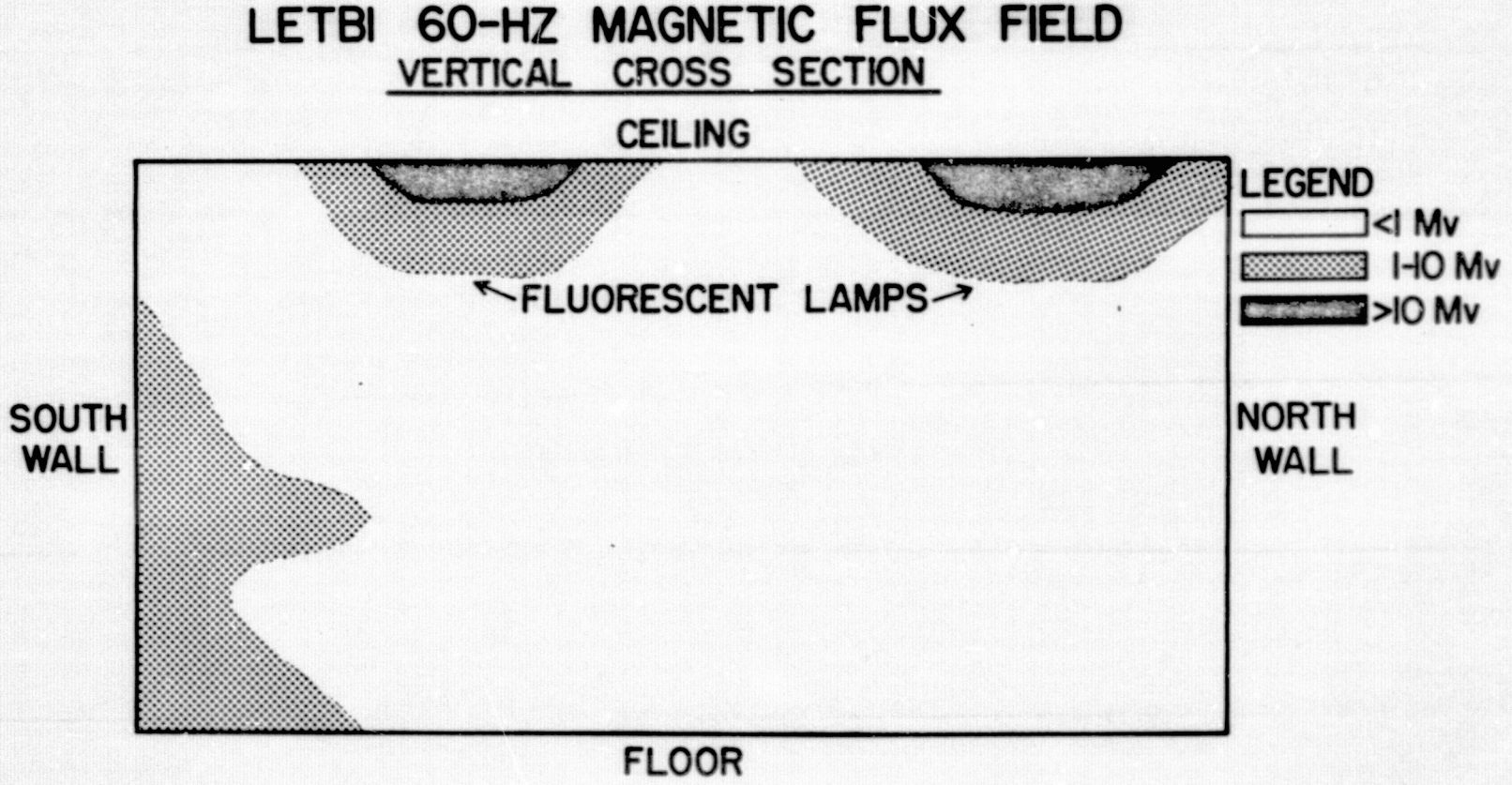
LETBI 60-HZ MAGNETIC FLUX FIELD
VERTICAL CROSS SECTION
CEILING
FLUORESCENT LAMPS
SOUTH WALL
NORTH WALL
FLOOR
LEGEND
<1 Mv
1-10 Mv
>10 Mv

Fig. 32

In light of these flux and voltage values we experimented with some convenient shielding materials to reduce the magnetic fields. Our search probe was positioned inside a two-foot cubic box of fine copper screen. This gave no reduction in the probe signal so a second box of galvanized hardware cloth was built over the first one. Even with this double-screen shield the probe signal was not reduced. We then placed a search probe in a canister of Conetic foil (a material having a high magnetic permeability) and again the signal was not reduced. We have concluded from these tests that any successful magnetic shielding of the room would involve covering all room surfaces with thick ferrour metal sheets - an impractical arrangement because of the needed gamma-ray exposure field coming through the room walls. A grounded screen shield would probably help reduce the electric field and might well be considered for future installation, but it would be ineffectual for the magnetic fields.

During the course of these experiments we have found that electrode placement patterns for best signals and minimum power-line interference varies considerably with the condition of the patient. The patients to be irradiated and monitored in the facility frequently have enlarged abdominal organs that congest the thoracic cavity and change the cardiac electrical surface patterns. Usually preliminary care in securing a good, low-resistance sternal ground electrode connection, together with trying the two active electrodes at various chest test sites, gave optimum results.

LETBI Dosimetry. The objectives of the low-exposure-rate total-body irradiator dosimetry study were to produce a large, uniform

exposure field with an exposure rate of approximately 1 R/hr and to accurately determine a patient's absorbed dose.

The initial step in this study was an investigation of the various source arrangements that would provide the desired exposure field. The basic requirements were that the field be uniform (± 5%) throughout a treatment volume large enough to provide two patients with comfortable living quarters for extended exposure periods.

The calculations made to find an optimum source configuration incorporated two major assumptions: that the sources could be considered "point" sources and that variations in the exposure rate are produced by produced by the inverse square law. Attenuation or scattering were not taken into account. Calculations were done for a single source arrangement and several multiple-source configurations.

A configuration of 10 sources in a rectangular array was selected because the predicted exposure field was uniform within ±5% throughout a treatment volume of 14' x 14' x 6'. This arrangement provided the greatest percentage of usable treatment volume per volume of shielding-superstructure and consequently proved to be the most economical structure to build.

Figure 33 compares the isodose or relative exposure lines predicted theoretically for the horizontal midplane of the volume to be occupied by the treatment room and the corresponding measured isodose lines. These results indicate that the horizontal variations in the field were predicted very well by theory. The measured vertical variation, however, was ± 15% compared to a predicted value of only ± 5%.

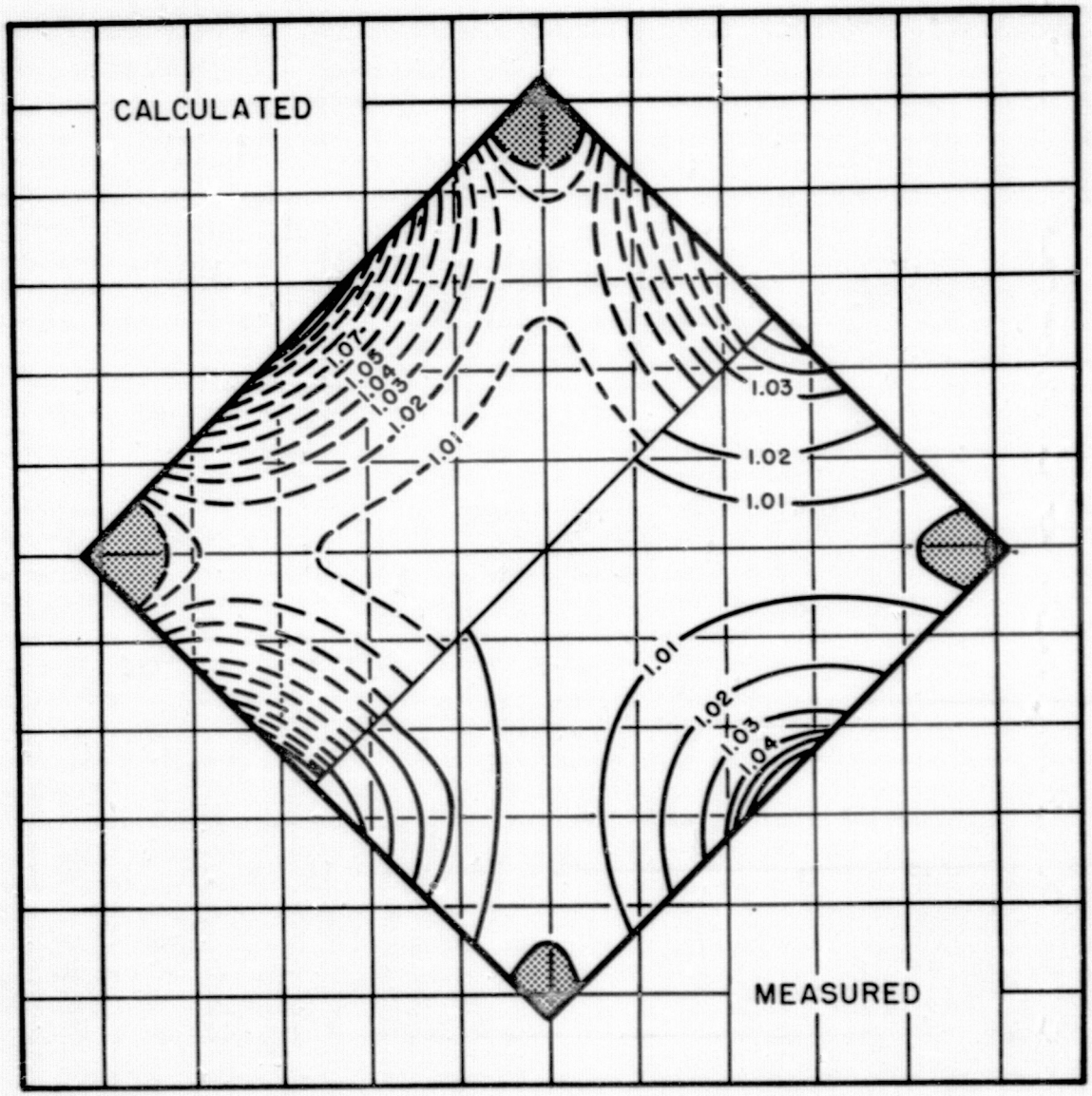
CALCULATED
1.07
1.05
1.04
1.03
1.02
1.01
1.03
1.02
1.01
1.01
1.02
1.03
1.04
MEASURED

Fig. 33

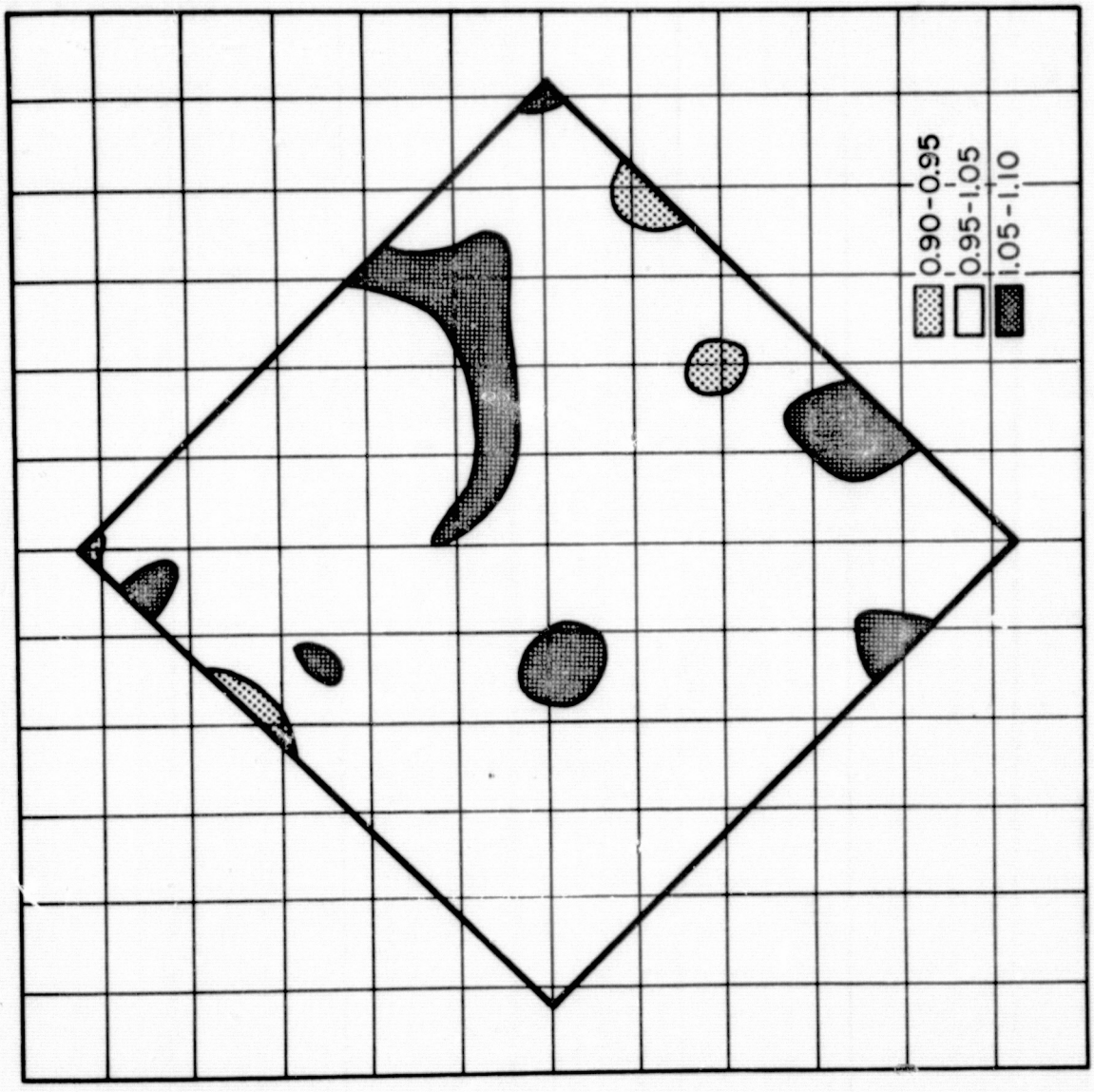

Fig. 34

The source manipulators were designed to vary the exposure rate by changing the fraction of the 3-in long source positioned in the beam portal. Operating the manipulator with only a fraction of the source exposed was found to be the primary factor contributing to the vertical field gradient. The vertical gradient was reduced by positioning the entire source in the beam portal. The exposure rate was reduced to the desired value by placing cylindrical lead attenuators over the beam portal.

The variation in the exposure field through the midplane of the completely furnished treatment room is shown in Fig. 34. Except for the small shaded areas, all measurements are between ± 5% and only one measurement in 289 varied by more than ± 10% of the exposure at the center of the room. Within 90% of the treatment volume the exposure rates varied by no more than ± 10% and furniture placement restricts the patient from occupying most of these areas.

All the exposure measurements were made with a miniature Geiger detector with a selective shield, chosen for its sensitivity, reproducibility, energy independence, and small size. This instrument was also desirable because it could be operated remotely from the control area.

Calibration was accomplished by measuring the exposure rate at the center of the room with a Victoreen condenser R-meter. On June 1, 1967 the exposure rate at the center of the treatment room was 1.50 R/hr. The exposure rate was kept approximately constant by decreasing the thickness of the lead attenuators to compensate for the ^{60}Co decay.

Spectral measurements made with a NaI (Tl) detector at several positions within the treatment volume showed no significant variations in energy distribution.

Patient and Phantom Dosimetry. During patient treatment thermoluminescent dosimeters are worn on the patient's wrists, ankles, and chest. The patient's absorbed dose is determined by correlating the measurements with surface-depth dose ratios obtained from phantom studies. Table 8 shows the comparison of surface exposures measured on the first eight patients treated in the facility and the phantom measurements. The surface exposures are less than the exposure measured in the center of the room (100 R) due to attenuation by the patient's body.

An extensive phantom dosimetry study was undertaken to determine the average whole-body dose as well as the doses to individual organs for patients receiving TBI in all three of our TBI facilities. In this study a tissue equivalent phantom (complete with skeleton and density adjusted lung spaces, etc.) was used as a patient analog and individually calibrated thermoluminescence dosimeters were used to measure dose. To locate organ volumes, we compared radiographs of the 34 transverse sections of the phantom with bone structure and organ location of anatomy reference works. Individually calibrated LiF dosimeters were placed in all available sites within the volumes defined as organs. Then we reassembled the phantom and exposed it in the same manner as a patient. The rad dose measured by each dosimeter was determined by analysis techniques previously reported (USAEC Report CONF-680920, 1969, p. 976). With the exception of the bone marrow we

TABLE 8

LETBI Patient Dosimetry for Initial Year of Facility Operation

Relative Exposures

Position	Phantom	Pt #1	Pt #2	Pt #3	Pt #4	Pt #5	Pt #6	Pt #3*	Pt #7	Average	S.D.
Room Center	100	100	100	100	100	100	100	100	100	100	-
Chest	78	67	75	73	81	-	70	71	69	73.0	±4.75
Left Wrist	76	69	81	78	84	74	75	75	78	76.7	±4.30
Right Wrist	82	71	81	72	81	74	73	78	75	76.3	±4.24
Left Ankle	76	82	77	72	77	74	77	76	71	75.8	±3.23
Right Ankle	76	-	78	78	78	74	77	75	70	75.7	±2.15

*The second treatment of Patient No. 3 and the treatment of Patient No. 7 were administered simultaneously.

assume that the average rad response of all dosimeters in an organ equals the organ dose.

In Table 9 the organ dose and their ranges are given for all three irradiators. Predictably, the bone marrow dose ranges are the most variable since the bone marrow is both near the midline and near the surface of the body. In LETBI, on comparing the dose distribution with the other two facilities, we find that organs in the head and neck receive about 10% more, in the upper and central chest about 10% less, and in the lower part of the torso about 15 to 30% less. In METBI, as compared with the variable-dose-rate irradiation facility* (VDRIF), the organ doses are slightly higher in the head, about the same in the upper chest, and lower in the abdominal and pelvic regions.

Since the active marrow is not uniformly distributed within the body in a simple, well-defined volume, it was necessary to know the spatial distribution of the marrow to determine average marrow dose. The distribution of active marrow for normal adults is expressed as the percent of the total amount located in a particular anatomical marrow compartment, e.g., the ribs or skull. The distribution of the dosimeters in the marrow comparments was not proportionate to the amount of marrow therein. For example, 19% of the 137 dosimeters were located in ribs which contained only about 8% of the total active marrow. Therefore, average total dose to marrow had to be calculated by first determining the average dose for a specific compartment and then using its percentage of total marrow as a weighting factor. Table 10 lists the average compartment dose and its range per 100 R of exposure from each of the three irradiators. Table 11 summarizes the average marrow dose calculations.

*A facility owned by the University of Tennessee Comparative Animal Research Laboratory and used by ORAU for therapeutic exposures in patients prior to bone marrow transplantation.

TABLE 9

Organ Doses in Three Total-body Irradiation Facilities
In Rads Per 100 R at Centerline of Patient

Organ	Facility					
	LETBI		METBI		VDRIF	
	Dose	Range	Dose	Range	Dose	Range
Bone marrow	60	42-94	64	53-86	72	61-83
Cerebellum	79	75-81	77	74-81	71	66-75
Cerebrum	82	77-87	75	70-79	70	66-74
Heart	66	61-74	66	58-70	73	65-83
Intestines	57	48-64	67	54-76	68	59-75
Kidneys	54	53-57	66	62-70	68	61-78
Lenses of eyes	94	93-96	87	85-90	72	70-74
Liver	62	55-71	67	61-78	72	67-81
Lungs	67	59-81	67	58-77	77	65-90
Skin (above sternum)	86	84-87	73	72-75	78	72-84
Skin (front waist)	77	76-79	74	72-75	79	73-84
Spleen	58	55-60	69	69-73	73	68-79
Stomach	54	49-61	64	59-69	71	66-76
Thyroid	82	80-84	76	75-77	74	73-76

TABLE 10

Marrow Compartment Average Dose in Rads/100 R

Marrow Compartment	IRRADIATORS					
	LETBI		METBI		VDRIF	
	Average Dose	Range	Average Dose	Range	Average Dose	Range
Head	82	73-89	78	71-85	68	61-74
Upper Limb Girdle	69	58-75	66	58-73	78	70-82
Sternum	75	73-77	69	65-71	77	74-77
Ribs	63	46-76	68	62-72	75	70-84
Vertebrae	58	47-75	65	59-80	70	63-78
Sacrum	45	41-46	54	50-56	75	67-83
Lower Limb Girdle	52	44-62	59	52-71	72	63-77

TABLE 11

Calculations of Average Bone Marrow Dose in Rads/100 R

Bone Marrow Compartment	Percent Active Bone Marrow	LETBI Average Dose	LETBI Weighted* Factor	METBI Average Dose	METBI Weighted* Factor	VDRIF Average Dose	VDRIF Weighted* Factor
Head	13.1	82	1074	78	1022	68	891
Upper Limb Girdle	6.4	69	442	66	422	78	499
Sternum	2.3	75	173	69	159	77	177
Ribs	7.9	63	498	68	537	75	593
Vertebrae	28.4	58	1647	65	1846	70	1988
Sacrum	13.9	45	626	54	751	75	1043
Lower Limb Girdle	26.1	52	1357	59	1570	72	1879
Totals	98.1†		5820		6277		7070
Average Weighted Dose‡		59		64		72	

*Weighted factor = average dose x percent marrow.

†Average weighted dose = Σ weighted factors / total percent active bone marrow.

‡Total percent is 98.1 because 1.9% of the marrow is located in the heads of the humeri where no measurements could be made.

Because most studies of total-body irradiation, both in humans and animals, relate response to some "average-body dose," we have estimated the average torso-dose also. Our estimates are: LETBI, 67 rads/100 R; METBI, 68 rads/100 R; and VDRIF, 74 rads/100 R.

The importance of using absorbed dose as the basis of comparison is clear from Table 9, i.e., if two patients were exposed to 100 R, one in LETBI and the other in VDRIF, the VDRIF patient would receive about a 20% greater marrow dose but his dose to the lenses of the eyes would be 20% smaller than the LETBI patient. Depending upon whether the biological endpoint was marrow suppression or cataract formation, we would either overestimate or underestimate by 20% the effectiveness of equal exposures given in these different irradiators.

C. Physiologic Studies

Irradiation therapy, regardless of its modality, requires shielding to protect hospital personnel from exposure during patient treatment. Low levels of total body irradiation therapy presented additional problems since patients could be isolated for considerable periods (days or weeks) during which physiologic contact for vital signs monitoring generate considerable volumes of physiologic data daily that require analysis and reduction in their content. In our facility large volumes of cardiac (EKG waveform and rate) and pulmonary data were recorded real time (strip chart) and on analog tape for retrospective analysis. Each of these physiologic parameters presented special problems concerning data analysis, storage, and retrieval.

1. Pulmonary Impedance

At the present state-of-the-art, the pulmonary impedance pneumograph is used to study respiratory patterns physiologically and to monitor respiratory function in remotely located persons, e.g., astronauts in space (4-7). We attempted to use this system of impedance pneumography to measure pulmonary functions in patients undergoing total body irradiation therapy. However, no data-reduction system was available to facilitate medical interpretation of changes in pulmonary impedance pneumography as used clinically in remote monitoring. We made a preliminary study of the feasibility of using power spectral analysis for this purpose. Pulmonary impedance wave-form was recorded on a Beckman Dynagraph (previously described) utilizing an electrode configuration described previously by others (8-13) using it to monitor the physiologic status of astronauts in space flight or in simulated tests.

We found that the pulmonary impedance changed periodically with time in a way that was remarkably consistent and typical of any one subject, if he was in an unstressed steady state in a well-controlled, constant environmental situation. Any physiologic demand that required a respiratory response caused a change in this periodicity. Visual inspection of the impedance pneumography wave form (Fig. 35) indicated that the cyclic nature of the respiratory response was considerably more complex and difficult to describe and measure.

Many other time series known to the physical sciences, engineering, and economics have an underlying periodic structure. These phenomena are amenable to statistical analysis using the mathematical technique

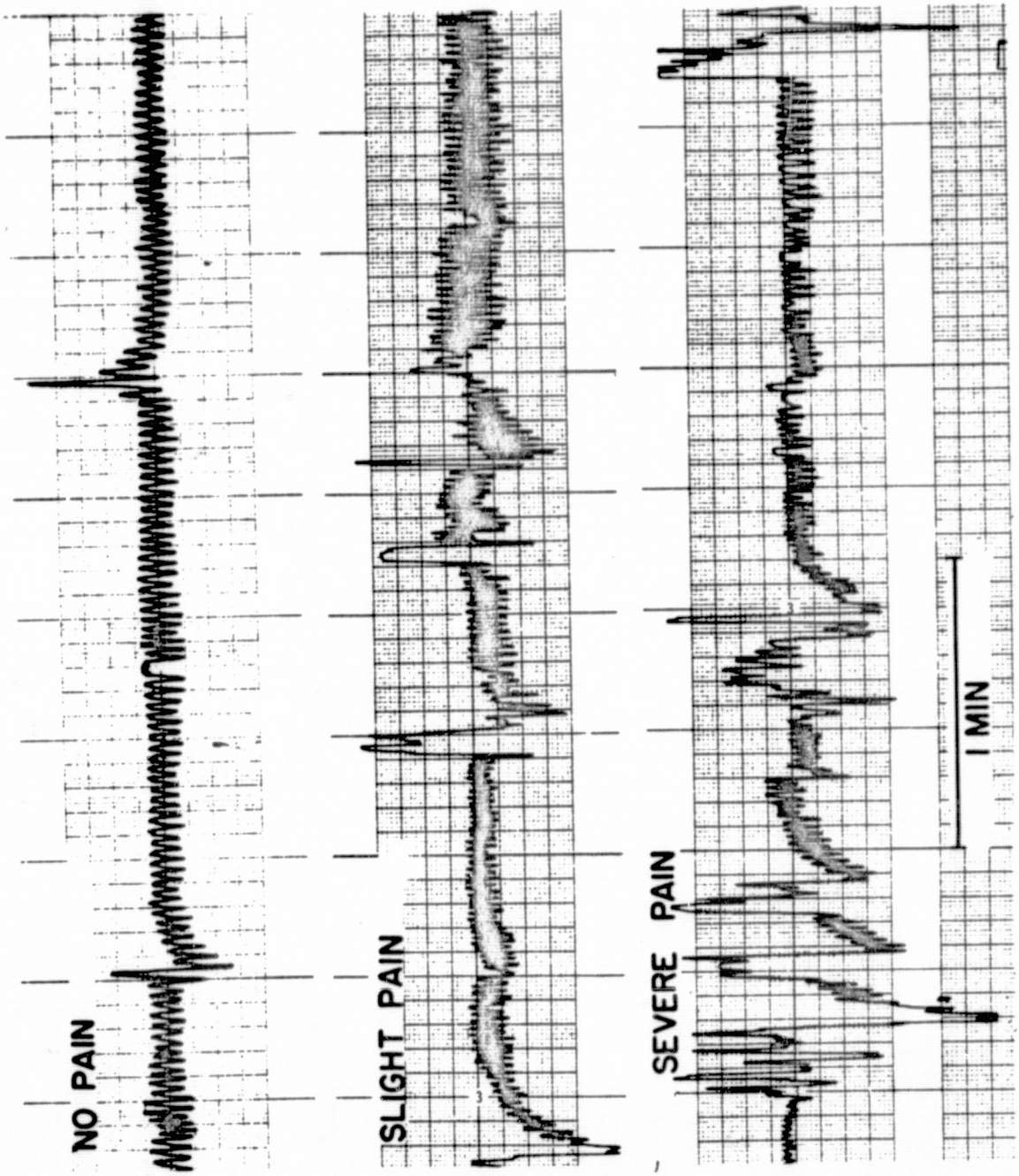

PRECEDING PAGE BLANK NOT FILMED

Fig. 35

of power spectrum analysis (14-15). Interpretation of the results of such an analysis is not difficult, and it is possible to develop testing procedures to determine whether a change has occurred. Although power-spectrum analysis is commonly used in communications engineering, seismology, radio-astronomy, and other physical sciences, its application in biology is new. Walter (16) has proposed spectral analysis as a method for analyzing EEG data and has demonstrated its use in experimental electroencephalography. Our preliminary study showed that power spectral analysis is a natural system for reducing the vast amount of data in the analog tracings obtained in impedance pneumography. It minimizes the interpretive workload and produces a measurement that is unique in respiratory physiology that seems related in some way to the physical work involved in breathing and meeting respiratory demands.

Mathematically, the impedance pneumograph measured by Pacella's technique (17) can be considered as a trace of length T from an arbitrary origin and designated $X_i(t)$ where i refers to the ith trace and t is time ($0 \leq t < T$). The function of $X_i(t)$ is sampled at n equally spaced intervals of width $\Delta t (\Delta t = T/n)$. The resulting series X_{it}, t-1,..., n is the subject of the present analysis.

If X(t) could be considered as a deterministic periodic function of time, then classical harmonic analysis would lead to the following Fourier representation of n equally spaced points from the trace.

$$X_t = \mu + \sum_{j=1}^{m} \{\alpha_j \cos(\omega_j t) + \beta_j \sin(\omega_j t)\} \qquad (6)$$

where

$m = (n/2) - 1$,

$\omega_j = 2\pi j/n$,

$j = 1,\ldots,m$.

Then ω_j is the slowest cosine wave with a period of one cycle per T minutes.

The least squares estimates of the α_j's and β_j's are

$$a_j = \frac{2}{n} \sum_{t=1}^{n} X_t \cos(2\pi jt/n) \quad b_j = \frac{2}{n} \sum_{t=1}^{n} X_t \sin(2\pi jt/n) \qquad (7)$$

Since the energy in a wave if proportional to the square of its amplitude, we can obtain the following relation (Parseval's Identity) between the power (energy†) in one cycle and the Fourier coefficients.

$$\sum_{t=1}^{n} X_t^2 = \sum_{t=1}^{n} \{\bar{x} + \sum_{j} \{a_j \cos(\omega_j t) + b_j \sin(\omega_j t)\}\}^2$$

$$= n\bar{x}^2 + \frac{n}{2} \sum_{j} (a_j^2 + b_j^2)$$

$$\text{or} \quad \frac{1}{n} \sum (X_t - \bar{x})^2 = \frac{1}{2} \sum_{j} (a_j^2 + b_j^2) = \text{Var} X_t \qquad (8)$$

---

†This energy concept is not specified physically and the implication is not intended that energy here is linearly related to the energy involved in the respiratory effort that produces the pulmonary impedance traces.

The quantity $1/2\ (a_j^2 + b_j^2)$ may be considered as the contribution to the total power from the jth frequency band, the width of which is $2\pi/n$. Then,

$$I_n\ (\omega_j) = \Delta t \cdot n\ (a_j^2 + b_j^2)/4\pi$$

defines the Schuster periodogram. A plot of $I_n(\omega_j)$ vs. frequency is known as a harmonic analysis. Jenkins (18) shows that

$$\lim_{n \leftrightarrow \infty} E\ I_n(\omega_j) = P(\omega_j)$$

and discusses the difference between this approach to time-series analysis and the statistical approach, which considers X(t) as a sample function from a stochastic process. The harmonic analysis breaks down completely when applied to a statistical fluctuation, since $I_n(\omega)$ does not converge to $p(\omega)$ as n becomes larger.

However, if X(t) is a stationary time series and $E\{X(t)\} = 0$, then $C(\tau) = E\{X(t)\ x\ (t + \tau)\}$ is the autocovariance function, (9)

and its Fourier transform

$$P(f) = \int_{-\infty}^{\infty} e^{-i2\pi f\tau} C(\tau)d\tau = \int_{0}^{\infty} 2\tau\cos(2\pi f\tau)\ c\ (\tau)d \qquad (10)$$

is the power spectrum of X(t). Then if

$$\tau = 0 \text{ in eq. } 1$$

$$C(0) = \text{var}\{X(t)\} = 2\int_{0}^{\infty} P(f)df$$

so that $2P(f)df$ represents the contribution to the power of the process from frequencies between f and (f + df), where only positive frequencies are considered.

When a record of X(t) of length T is available and is sampled at equally spaced intervals of time, the discrete time series X_t, $t = 1,\ldots,n$ may be used to estimate the autocovariance and the power spectrum. The value of Δt and T chosen will depend primarily upon two factors:

1. The Nyquist frequency, $\omega_n = \pi/\Delta t$ radians/minute or $1/2\Delta t$ cycles/minute. All frequencies above ω_n will be aliased with those in the range $(0,\omega_n)$.

2. The resolution required in the estimated range $(0,\omega_n)$ and the lowest frequencies of interest.

The aim of our analysis is to estimate the aliased spectrum for frequencies from 0 to $1/2\Delta t$ cycles/minute. To obtain estimates that converge, it is necessary to use a lag window in the time domain or the equivalent spectral window in the frequency domain.

We use here the Blackman-Tukey estimation procedure (19) with hamming. The calculations may be briefly summarized as follows:

1. Calculate estimates of the autocovariance function:

$$C_r = \frac{1}{n - r} \sum_{t=1}^{n-r} X_t X_{t+r} \qquad r = 0, 1, \ldots m$$

2. Calculate raw power-spectrum estimates:

$$V_r = \frac{2\Delta t}{\pi} \{C_o + 2 \sum_{k=1}^{m-1} C_k \cos(kr/m) + C_m \cos(r\pi)\}$$

3. Calculate the smoothed power-spectrum estimates (hamming):

$$P(f) = P_r = .23V_{r-1} + .54V_r + .23V_{r+1}$$

$$\text{Where } f = \frac{r}{2m\Delta t} \text{ cycles/minute}$$

The smoothed estimate P(f) may also be interpreted as the contribution from the jth frequency band to var $\{X_t\}$ (19).

Thus, it is possible to consider respiration in the frequency domain that is physically more meaningful than the trace in the time domain.

Figure 35 shows the pulmonary impedance traces produced while a patient was experiencing different subjective degrees of pain expressed as none, slight, and severe. The power spectra produced by the analysis of these three traces are presented in Fig. 36. They indicate that as pain increased the amplitude of the low frequency cycles showed a substantial increase. Complete results of these initial efforts are summarized in a report by Lushbaugh et al. (20).

Prodromal Syndrome. Later we applied these techniques of pulmonary impedance power spectral analysis on patients undergoing total-body irradiation therapy. The purpose of this study was to see if pulmonary impedance power spectral analysis could be used to detect the onset and course of gastrointestinal distress induced pharmacologically or by total body irradiation.

Traces of pulmonary impedance were obtained before, during (in the case of exposure protraction), and after therapeutic levels of total-body irradiation of leukemic patients with ^{137}Cs or ^{60}Co gamma rays. The radiation facilities used have been previously described. Briefly, fractionated exposures of 30 R/day were carried out in a ^{137}Cs total body irradiator at a rate of 1.5 R/min, while protracted (30 R/day) and fractionated (10 R/day) exposures were administered utilizing a ^{60}Co total body irradiator at the rate of 1.5 R/hr. The voltage changes in

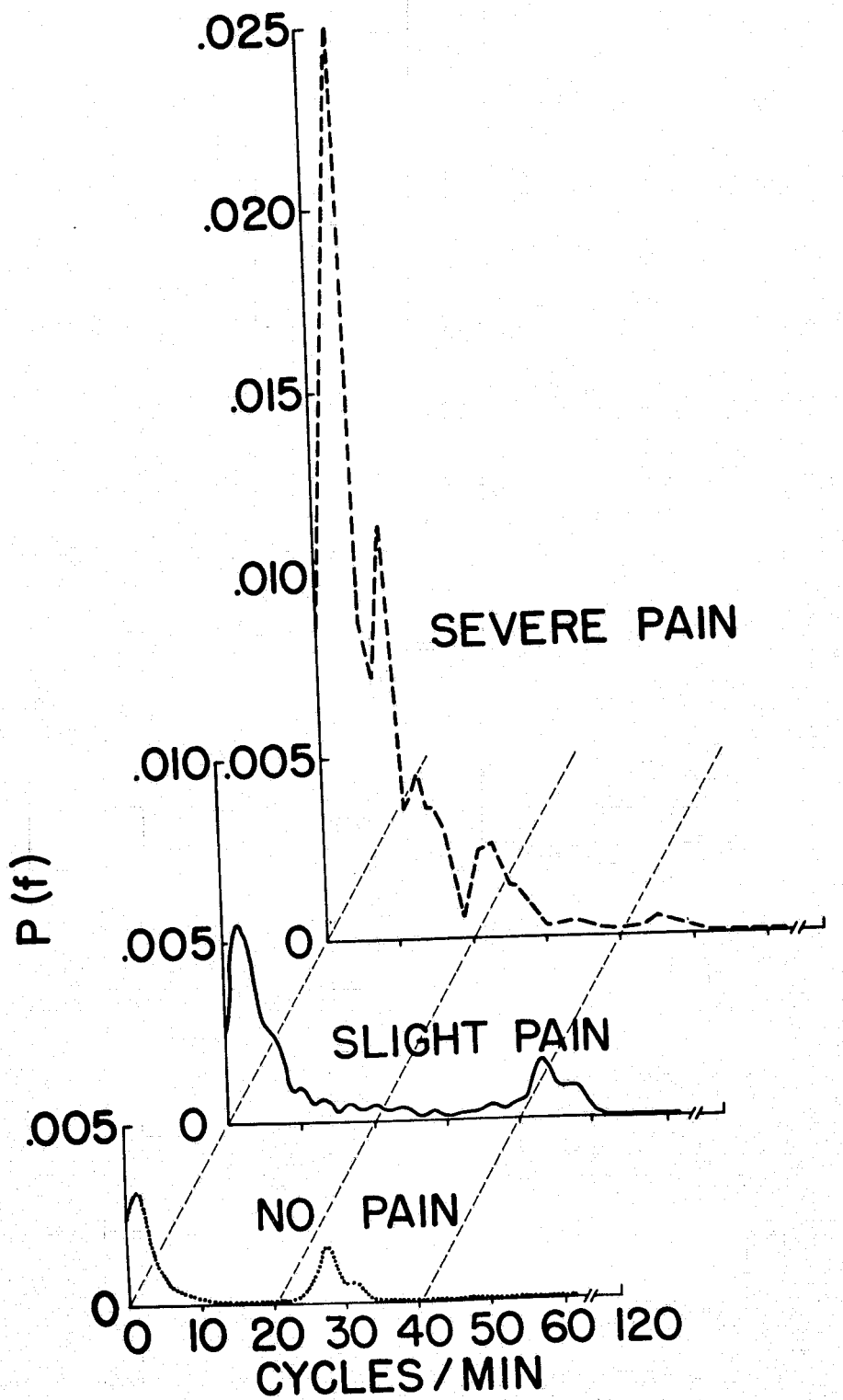

PRECEDING PAGE BLANK NOT FILMED

Fig. 36

pulmonary impedance were recorded on strip chart and on analog tape from which 4-minute data segments were selected, converted into digital form and analyzed using an IBM-1800 computer. In our system, in its present stage of development, digital data processing can be done in real time or in retrospect. After digital conversion, the data were processed with a power spectral analysis program which computed power spectral estimates and respiratory variances that were graphed automatically.

Selected impedance pneumograph traces obtained from a patient receiving 30 R/20 hr day at an exposure rate of 1.5 R/hr are shown in Fig. 37. The total exposure was 250 R over an 8-day period. These traces illustrate that normal, regular breathing occurred throughout all monitoring periods. The regularity of these impedance pneumographs is reflected by low-power spectra and nonvarying frequencies as shown in Fig. 38. During the entire exposure the patient, who had received no previous radiation therapy, felt well and did not develop nausea or loss of appetite. In Fig. 39 the pre- and postexposure pulmonary impedance traces from a patient receiving 30 R/day (1.5 R/min), total exposure 150 R, became increasingly irregular postexposure with increasing exposure accumulation up through day 4. The effect of the last fractional dose (30 R) appears to have been suppressed by 20 mg chlorpromazine administered prior to exposure. The changes in pulmonary impedance are more easily visualized in the power spectra computed from them (Fig. 40). All five postexposure pulmonary impedance traces were obtained within 30 min after irradiation. Subjective levels of postexposure gastrointestinal distress experienced by the patient are shown in Table 12. These symptoms correlated well

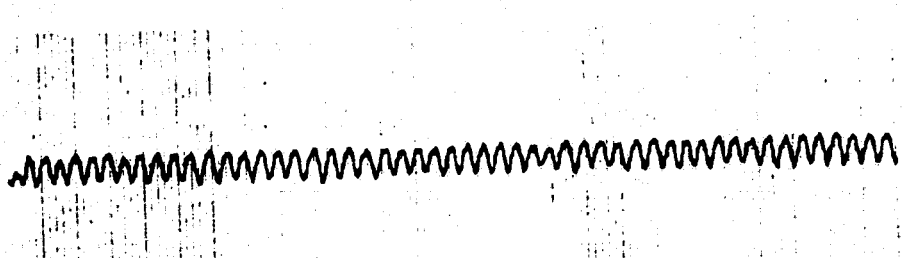

BEFORE TREATMENT

DURING TREATMENT

AFTER TREATMENT

| 1 MIN |

Fig. 37

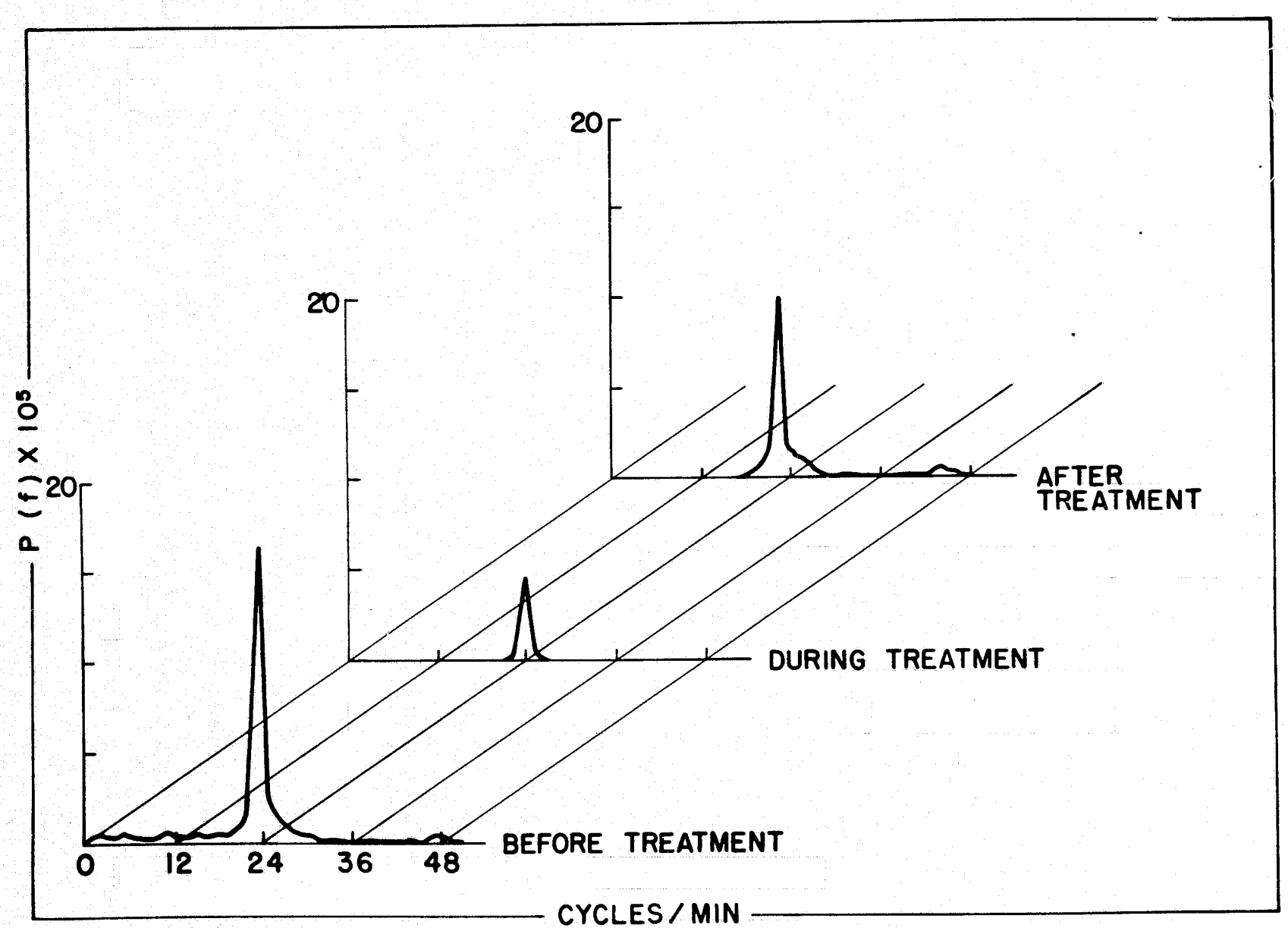
20
20
20
P (f) X 10⁵
AFTER TREATMENT
DURING TREATMENT
BEFORE TREATMENT
0
12
24
36
48
CYCLES / MIN

Fig. 38

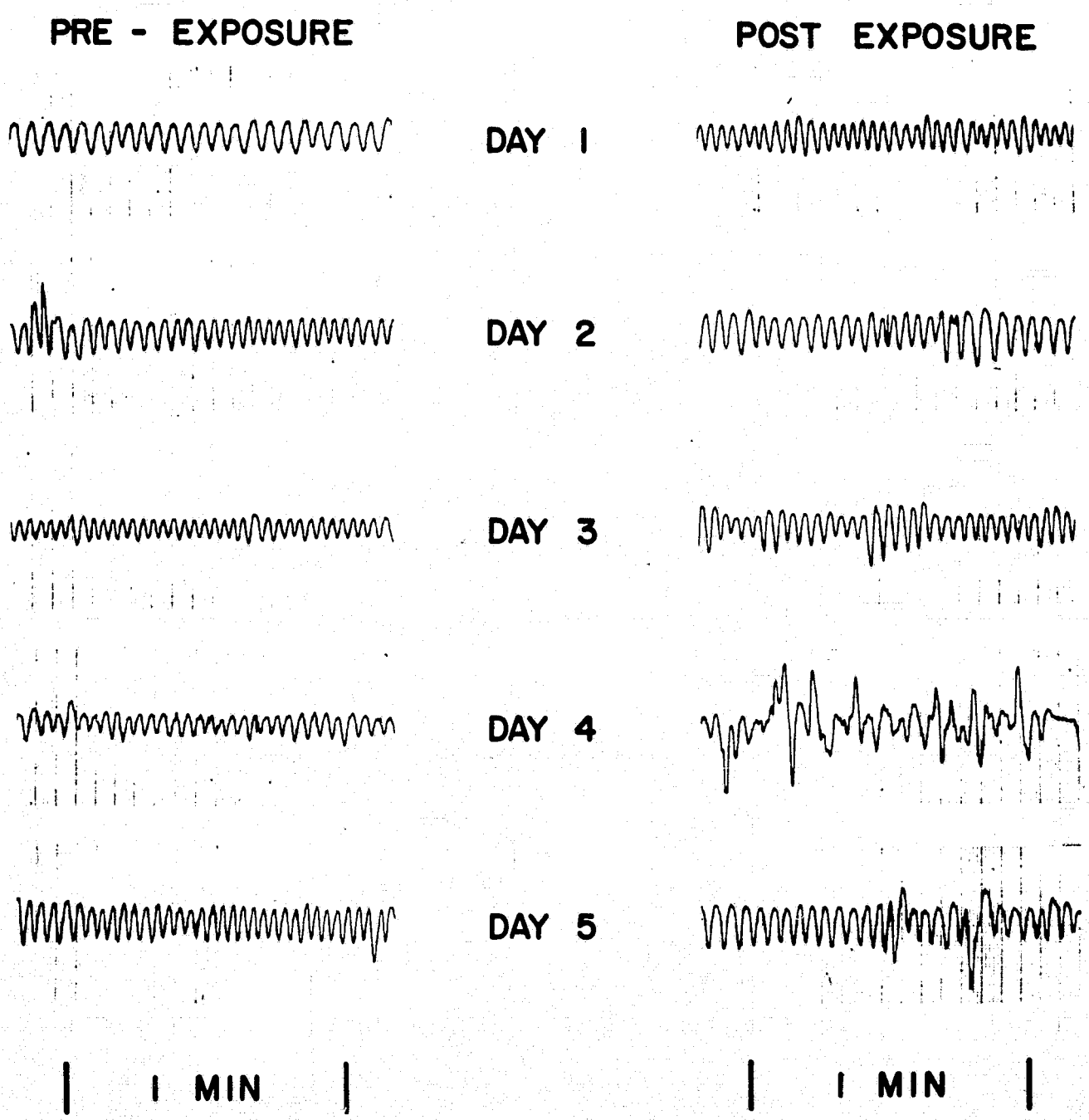
PRE - EXPOSURE
POST EXPOSURE
DAY 1
DAY 2
DAY 3
DAY 4
DAY 5
1 MIN
1 MIN

Fig. 39

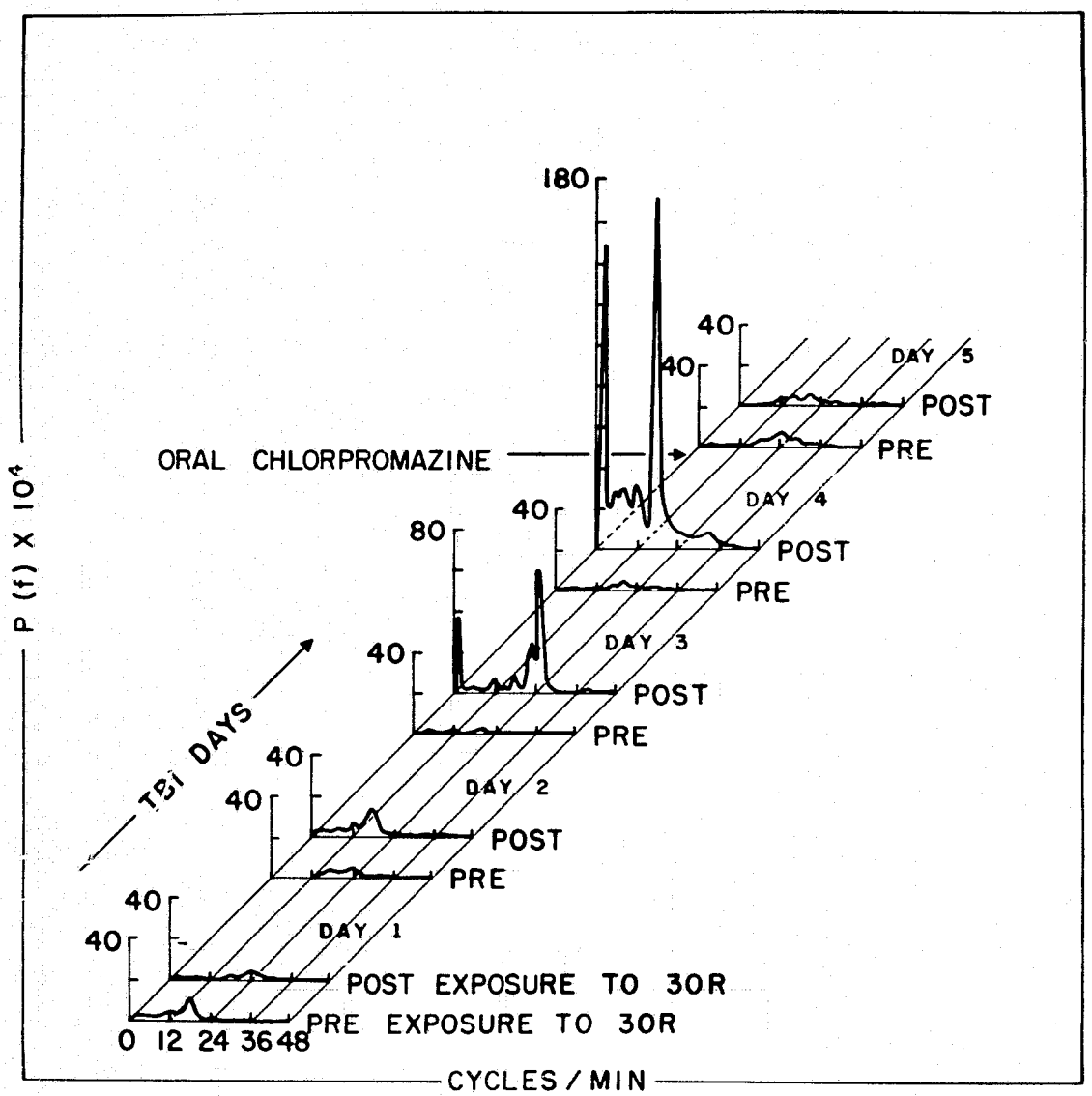
180
40
40
DAY 5
POST
PRE
ORAL CHLORPROMAZINE
DAY 4
40
80
POST
PRE
DAY 3
40
POST
PRE
40
40
DAY 2
POST
PRE
40
40
DAY 1
POST EXPOSURE TO 30R
PRE EXPOSURE TO 30R
P (f) X 10⁴
TBI DAYS
0 12 24 36 48
CYCLES / MIN

Fig. 40

TABLE 12

Patient Evaluation of GI Distress that Followed Treatment with 30 R (1.5 R/min) Daily for 5 Days

Accumulated Exposure	Described GI Distress
Post 30 R	None
Post 60 R	Mild
Post 90 R	Moderate
Post 120 R	Severe
Post 150 R	Mild

with the strip chart traces and the changes in their power spectral reductions. There is (Fig. 40) a progressive increase in the shift of pulmonary impedance waves to lower frequency and higher aplitude and power as radiation exposure accumulates. The patient reported that recovery from the postexposure nausea, reflected by these changes, occurred 2-8 hrs later. The relative absence of symptoms and pathologic pulmonary-impedance patterns and power spectra also correlated, as seen in Figs. 39 and 40, for day 5. The daily pretreatment pulmonary impedance traces and their power spectra are remarkably uniform and normal, substantiating, apparently, the patient's claim that symptoms of radiation sickness were absent at those times.

The comparison of dose rate effects was enhanced by the fact that the patient who received the fractionated radiation therapy (see above) returned for additional radiation treatment but the exposure (150 R) was protracted (1.5 R/hr) over a 5-day period. Pulmonary impedance strip chart traces recorded before, during, and immediately after the therapeutic irradiation period indicate that respiratory alterations occurred prior to and early into treatment and consisted primarily of high amplitude (deep) breathing (Fig. 41). Power spectra of pulmonary-impedance waveforms (Fig. 42) reflect these findings and show that no significant pulmonary alterations occurred throughout exposure after the initial changes. No low-frequency components are present in the power spectra obtained in relation to this dose protraction, however, low frequency shifts did occur in this same patient when the exposure (150 R) was fractionated (see above). These findings are interpreted as being due to psychologically-induced

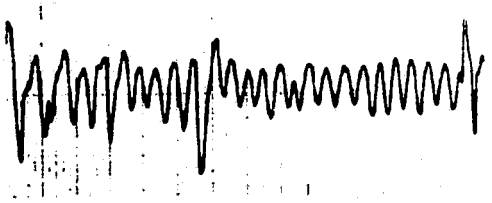

BEFORE TREATMENT

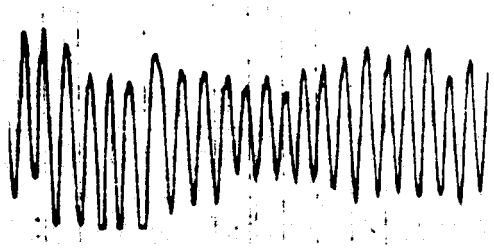

EARLY TREATMENT (6 R)

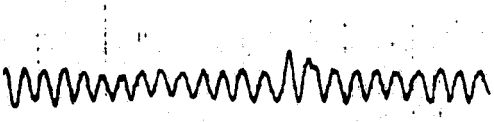

MID - TREATMENT (75 R)

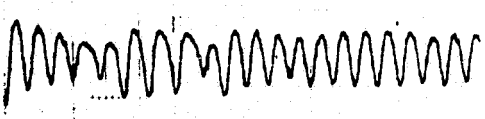

LATE TREATMENT (130 R)

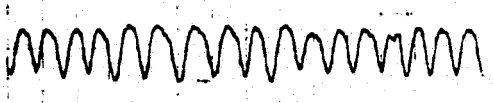

POST TREATMENT

Fig. 41

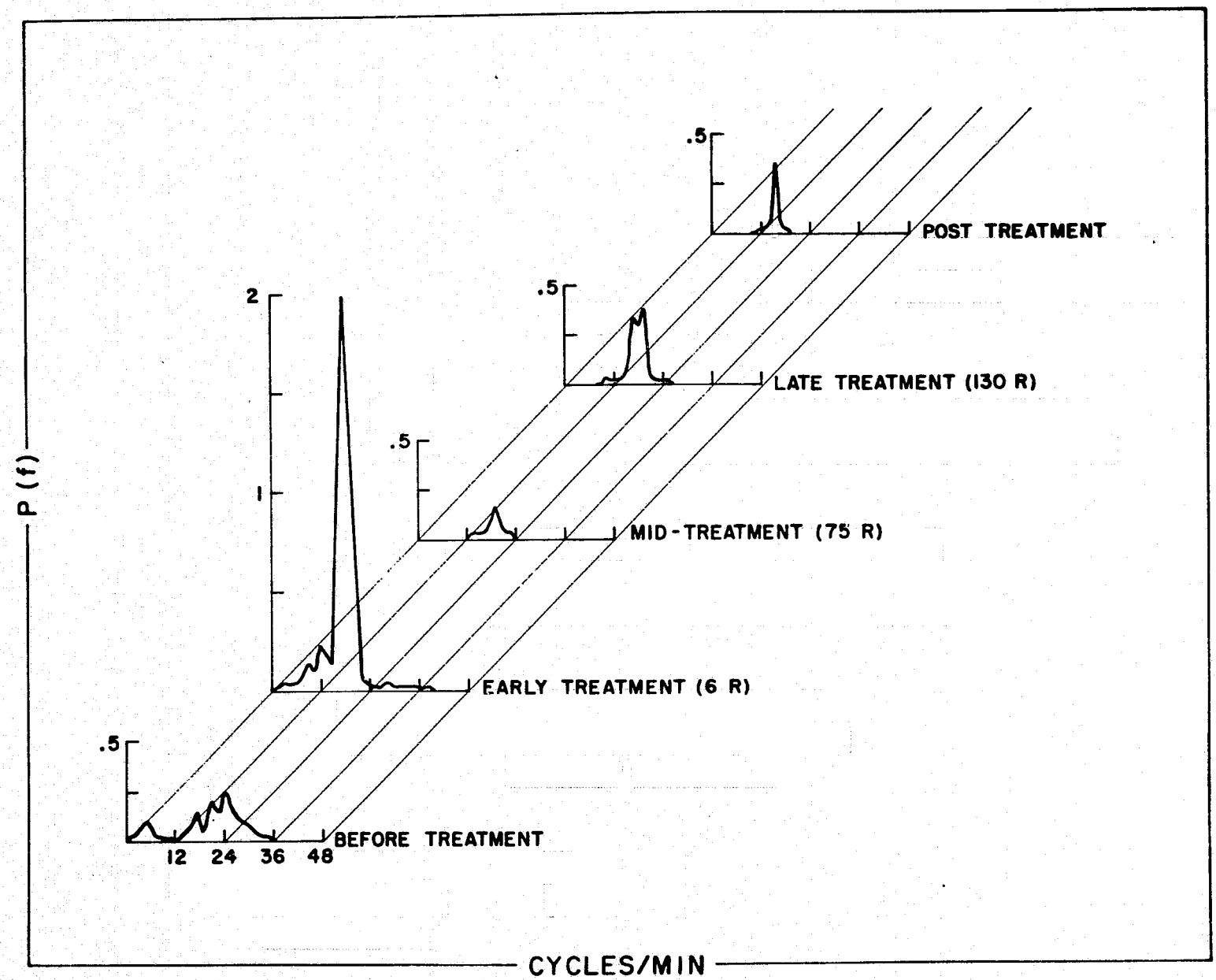
P (f)
.5
POST TREATMENT
.5
LATE TREATMENT (130 R)
2
1
.5
MID-TREATMENT (75 R)
EARLY TREATMENT (6 R)
.5
BEFORE TREATMENT
12
24
36
48
CYCLES/MIN

Fig. 42

nausea related to the severe nausea experienced previously by this same patient when given fractionated irradiation therapy six months prior. The fractionated exposure (150 R) which induced nausea in this experiment is well below the 300 rad dose (single exposure) previously reported by Lushbaugh, et al. (Rad. Res. 30(7): 398) that resulted in a mean vomiting-onset time of 144 ± 66 min. While this particular patient may have a low radiation-induced GI distress threshold, the dose rate influence on the human radiation prodrome is illustrated.

In order to compare radiation and pharmacologically induced gastrointestinal distress, we obtained power spectra of pulmonary impedance waveforms from a normal male volunteer, aged 22, who was administered an emetic (ipecac). Power spectra of these pulmonary traces are shown in Fig. 43 and illustrate shifts to high-power, low-frequency components at those times when the subject experienced severe nausea (17-20 min) and when emesis occurred (49-52 and 57-60 min, respectively). These data demonstrate similar respiratory phenomena occurred regardless of its means of induction. The quantity of analog data obtained in this experiment encouraged us to modify the computer program to afford greater data reduction. This modification is based on the fact that the area under a pulmonary impedance power spectrum is the total variance in terms of amplitude and frequency of respiration. This single number can be computed and used as a one-dimensional expression of the level of respiratory efforts.

When this number is plotted as it changes with time a continuous graph is produced of the variance in respiratory effort throughout the

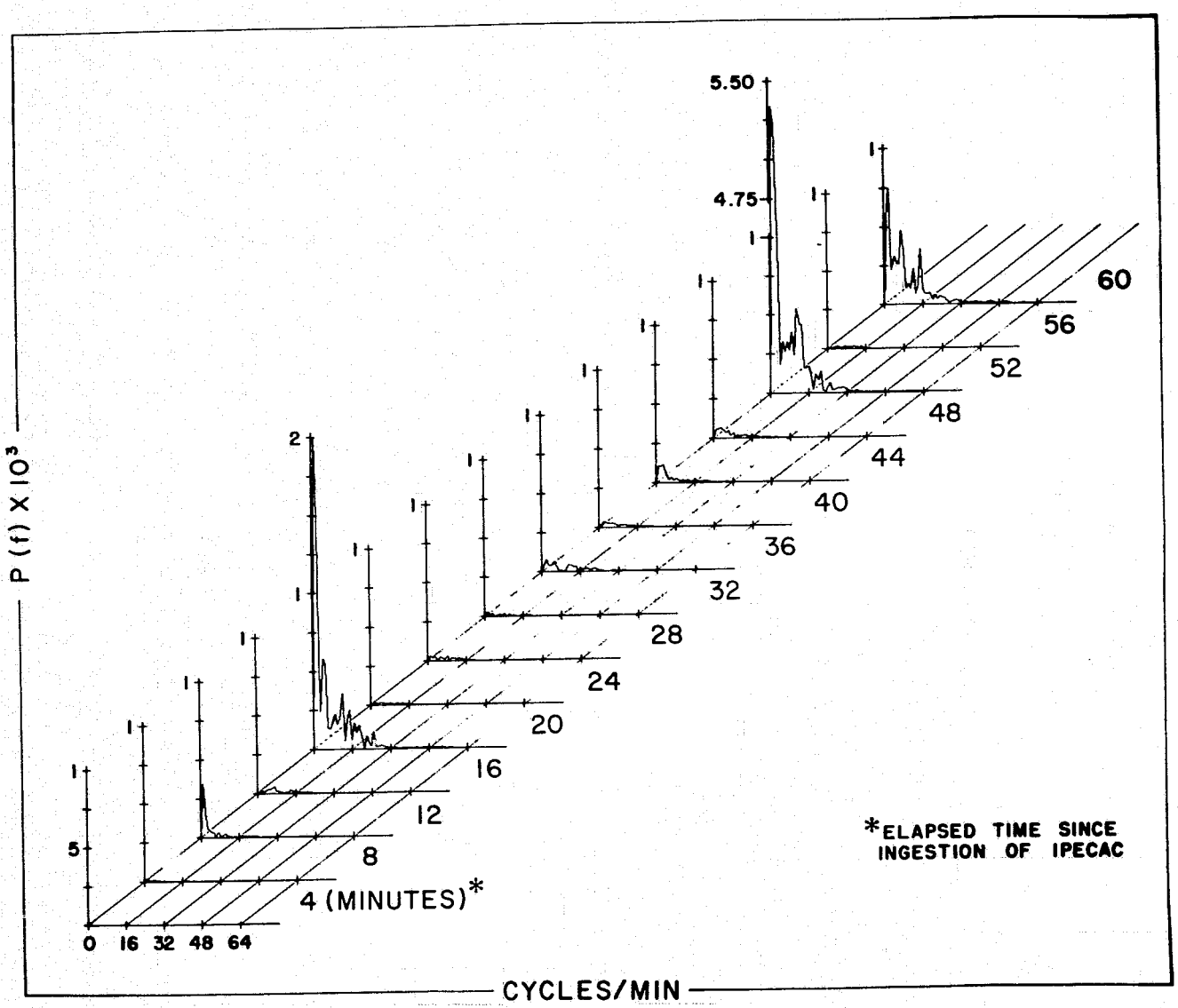
P (f) X 10³
5.50
4.75
5
1
2
0 16 32 48 64
CYCLES/MIN
4 (MINUTES)*
8
12
16
20
24
28
32
36
40
44
48
52
56
60
*ELAPSED TIME SINCE INGESTION OF IPECAC

Fig. 43

monitoring period. This new method requires one-half the previous computing time; the output consists of two indices (a mean and the variance of the power spectrum) that can be used without graphing the individual power spectrum. In this case, the mean is the average transthoracic voltage as measured by the impedance pneumography coupler, while the variance is directly proportional to the area under the power spectrum. The power spectrum of the pulmonary impedance waveform is not graphed in this new system unless requested by the investigator or clinician. In addition, this new method provides separate analysis of each of four consecutive minutes of pulmonary impedance data instead of one combined analysis of four minutes of data. An average mean and average variance (four 1-minute data periods /4) also is provided. We have defined the minute-by-minute variance as the continuous variance and its average over four minutes as the average variance.

Data obtained from the volunteer with pharmacologically induced GI distress (see above) and analyzed by the new method are shown in Fig. 44. Increased continuous variance corresponds exactly to the minute with the occurrence of severe nausea (18th minute) and emesis (50th and 59th minute). These changes in respiratory function are also well protrayed by the average variance which tends to smooth the data without losing fidelity. Inferences drawn from data analyzed by both the old and new methods were the same; that is, periods of gastrointestinal distress were accompanied by high-power, low-frequency shifts in the power spectra.

Again, plotting only the average variance, the radiation prodromal syndrome is also well demonstrated in the physiological data taken at

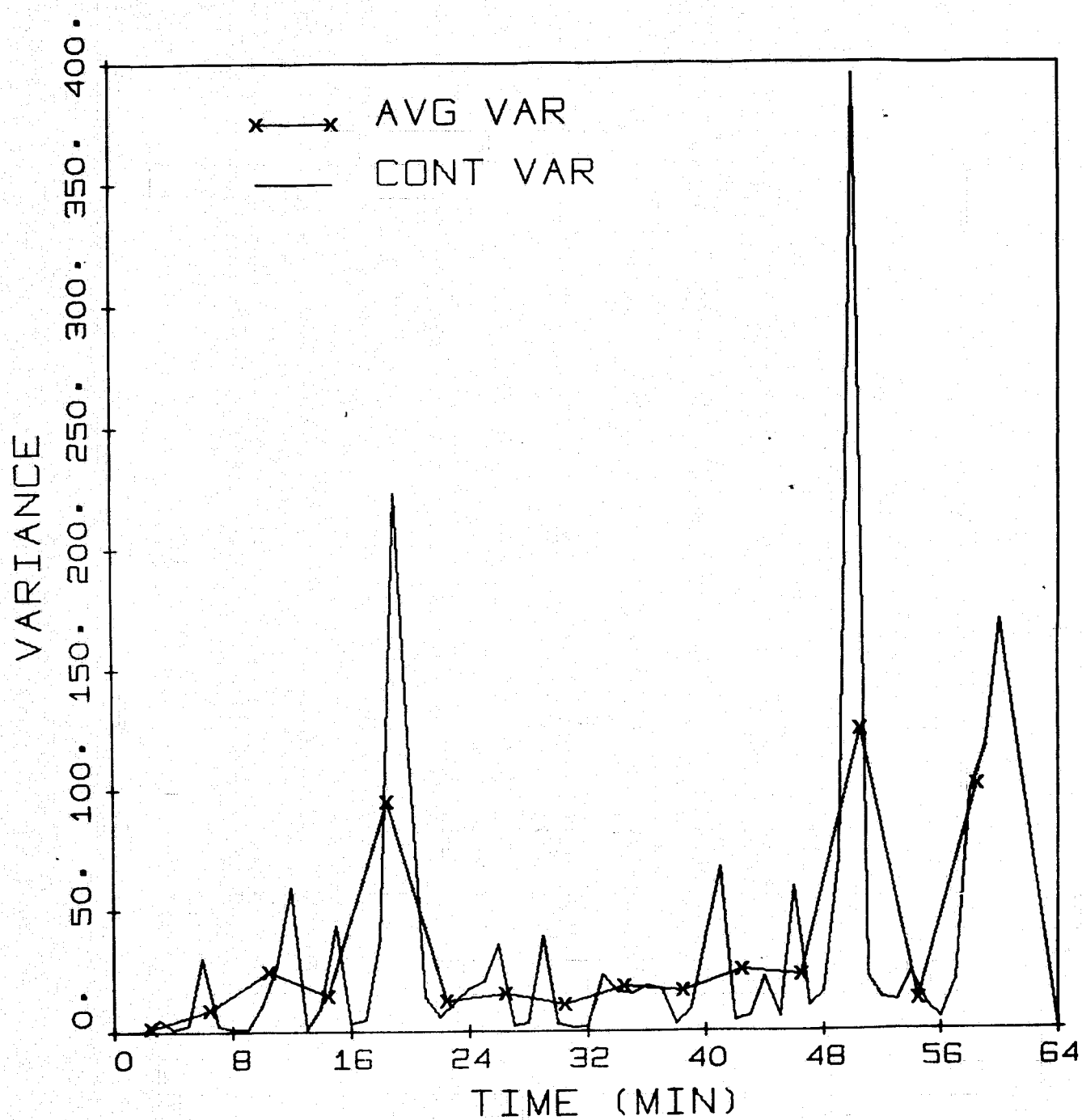
AVG VAR
CONT VAR
VARIANCE
0.
50.
100.
150.
200.
250.
300.
350.
400.
0
8
16
24
32
40
48
56
64
TIME (MIN)

Fig. 44

various times over several days before and after irradiation preparatory to bone marrow transplantation. Figure 45 shows data from a patient who received 500 R (40 R/min) total body gamma irradiation. Average variance of the pulmonary impedance was very stable over a period 10 days before and during irradiation. However by 50 min postirradiation the patient demonstrated a shift in this variance that correlated with nausea and emesis. The changes subsided within 24 hr and did not return as indicated by 12-15 hrs of pulmonary impedance data collection on each of four consecutive days postirradiation. In another patient who received 500 rads (694 R, 38 R/min) prior to bone marrow transplantation no nausea or vomiting was experienced and pulmonary impedance power spectra analysis confirmed the lack of these signs and symptoms, that is, a relatively constant average variance was recorded over several days pre- and postirradiation. The only significant increase was during a severe chill and atrial fibrillation beginning about 3 hrs postirradiation and continuing for some 4 hrs. The patient was, however, heavily sedated with thorazine just prior to receiving the 500 rads.

We also had the opportunity to determine the effect of accidental radiation-induced nausea and vomiting on pulmonary impedance in a young, health male (aged 31 yrs) who received 260 rem (350 R/min) total body gamma irradiation. Physiological monitoring commenced 4 hr postirradiation and periods of amplified average variance of the pulmonary impedance correlated well with nausea and emesis (Fig. 46). (The accident victim had vomited several times before the initiation of physiological monitoring.) Continuous monitoring of the physiological status of this accident victim revealed that during periods of sleep

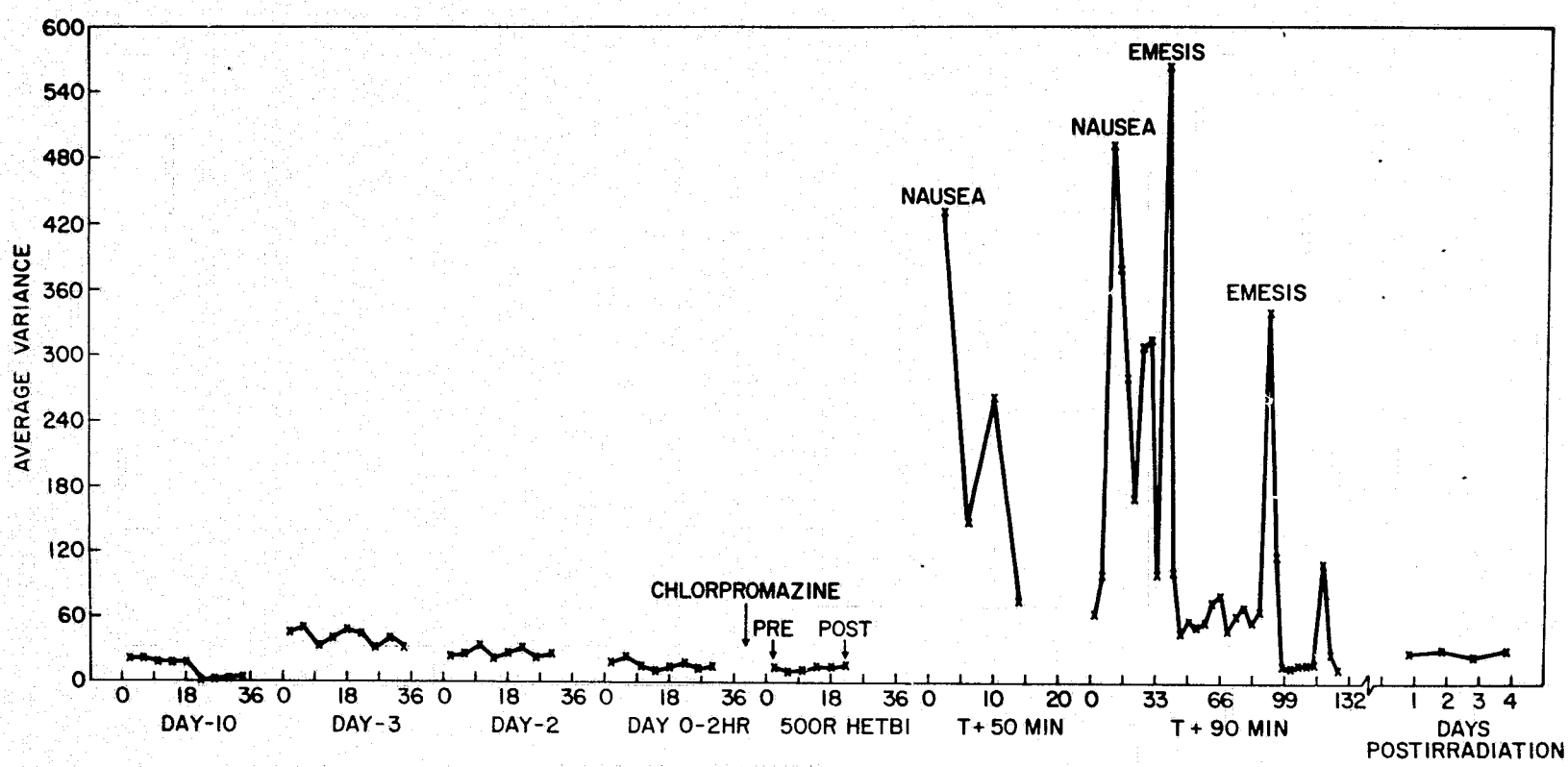
AVERAGE VARIANCE
600
540
480
420
360
300
240
180
120
60
0
NAUSEA
NAUSEA
EMESIS
EMESIS
CHLORPROMAZINE
PRE
POST
0 18 36 0 18 36 0 18 36 0 18 36 0 18 36 0 10 20 0 33 66 99 132 1 2 3 4
DAY-10
DAY-3
DAY-2
DAY 0-2HR
500R HETBI
T+50 MIN
T+90 MIN
DAYS
POSTIRRADIATION

FIG. 45

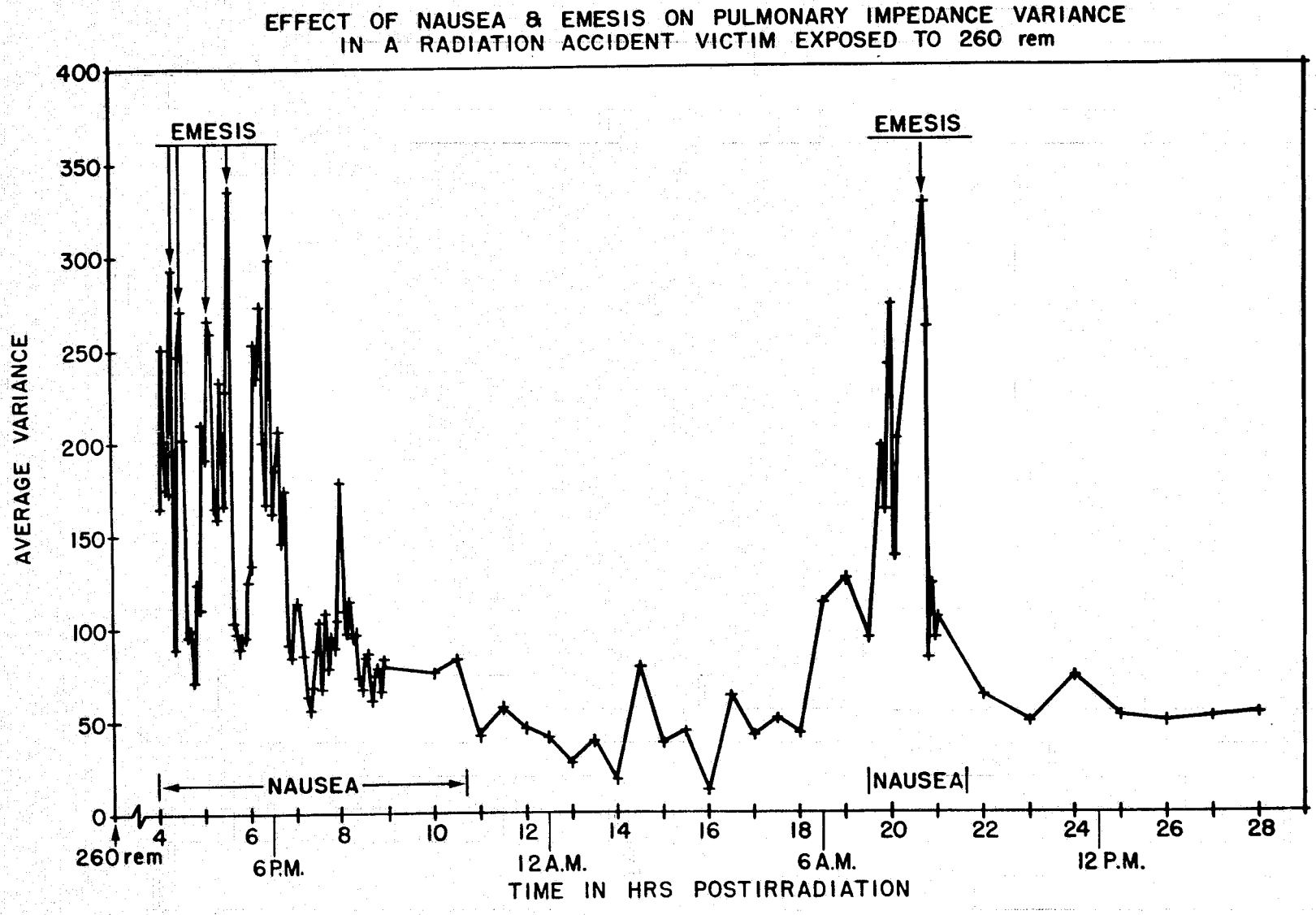
EFFECT OF NAUSEA & EMESIS ON PULMONARY IMPEDANCE VARIANCE
IN A RADIATION ACCIDENT VICTIM EXPOSED TO 260 rem
AVERAGE VARIANCE
400
350
300
250
200
150
100
50
0
EMESIS
EMESIS
NAUSEA
NAUSEA
4
6
8
10
12
14
16
18
20
22
24
26
28
260 rem
6 P.M.
12 A.M.
6 A.M.
12 P.M.
TIME IN HRS POSTIRRADIATION

Fig. 46

the variance diminished, spiking when the victim roused, and increased significantly upon awakening the following morning. Emesis again occurred when breakfast was brought into the patient's room although nothing was eaten. By 24 hrs postirradiation nausea and vomiting had subsided.

These data on pharmacologically-induced, therapeutic and accidental radiation-induced nausea and vomiting demonstrate inordinately well the capability of pulmonary impedance power spectral analysis to reflect periods of gastrointestinal distress.

Physical Performance.

A. Controlled Exercise Stress in Irradiated Man.

Having successfully measured radiation-induced gastrointestinal distress using pulmonary impedance power spectral analysis, we attempted, using this same system, to measure radiation-induced fatigue. It is common knowledge that both therapy patients and accident victims experience post-irradiation episodes of easy fatiguability. However, descriptions of this easy fatiguability have only been qualitatively described and shown to vary greatly with respect to subjective severity and duration. We attempted to detect and quantitatively measure this easy fatiguability using changes in pulmonary impedance waveform as previously described. All subjects (normal volunteers and therapy patients) participating in these exercise studies were fully informed of the procedures, their experimental nature, risks involved, etc. before rendering their consent as described by the U. S. Department of Health, Education and Welfare and review by our Human Use Committee on an annual basis.

In evaluating the performance decrement effects of total body irradiation, we first determined that the stress of exercise modified

pulmonary impedance in a way that power spectral analysis could measure. Normal (non-leukemic) volunteers exercised, under controlled conditions, on a bicycle ergometer for specific periods at standard workloads and were monitored before, during, and after exercise stress. Postexercise monitoring was generally continued for at least 30 min following cessation of exercise. Typical results, shown in Fig. 47, are from a volunteer exercising against a workload of 60 watts, pedaling at a speed of 50 RPM for 8 min. Increased respiratory demand, reflected by deep, high frequency breathing, during and immediately following exercise is indicated by increases in both continuous and average variances of the power spectrum. The continuous variance plot indicates that periods of deep breathing cycled with periods of normal breathing approximately every 5 min. The average variance plot likewise reflected increased respiratory demand after exercise.

To compare the response of irradiated men and unirradiated volunteers, normal males (aged 30 to 40 yrs) were monitored during controlled bicycling at workloads comparable to those used for patients. In a typical study, each of five normal males, who had not had previous experience with bicycle ergometry, exercised under controlled ergometry two or three times weekly for four consecutive weeks. The results in Fig. 48 show that normal man typically responds to moderate exercise by an increase in pulmonary impedance (as measured by its average variance). A decrease in the evaluation of pulmonary impedance during controlled work developed progressively during the first week and a half after which the exercise-induced response was relatively constant, probably due to adaptation to the exercise workloads. This effect is similar to

AVG VAR
CONT VAR
VARIANCE
0.0
15.0
30.0
45.0
60.0
75.0
90.0
105.0
120.0
EXERCISE
0
5
10
15
20
25
30
35
TIME (MIN)

Fig. 47

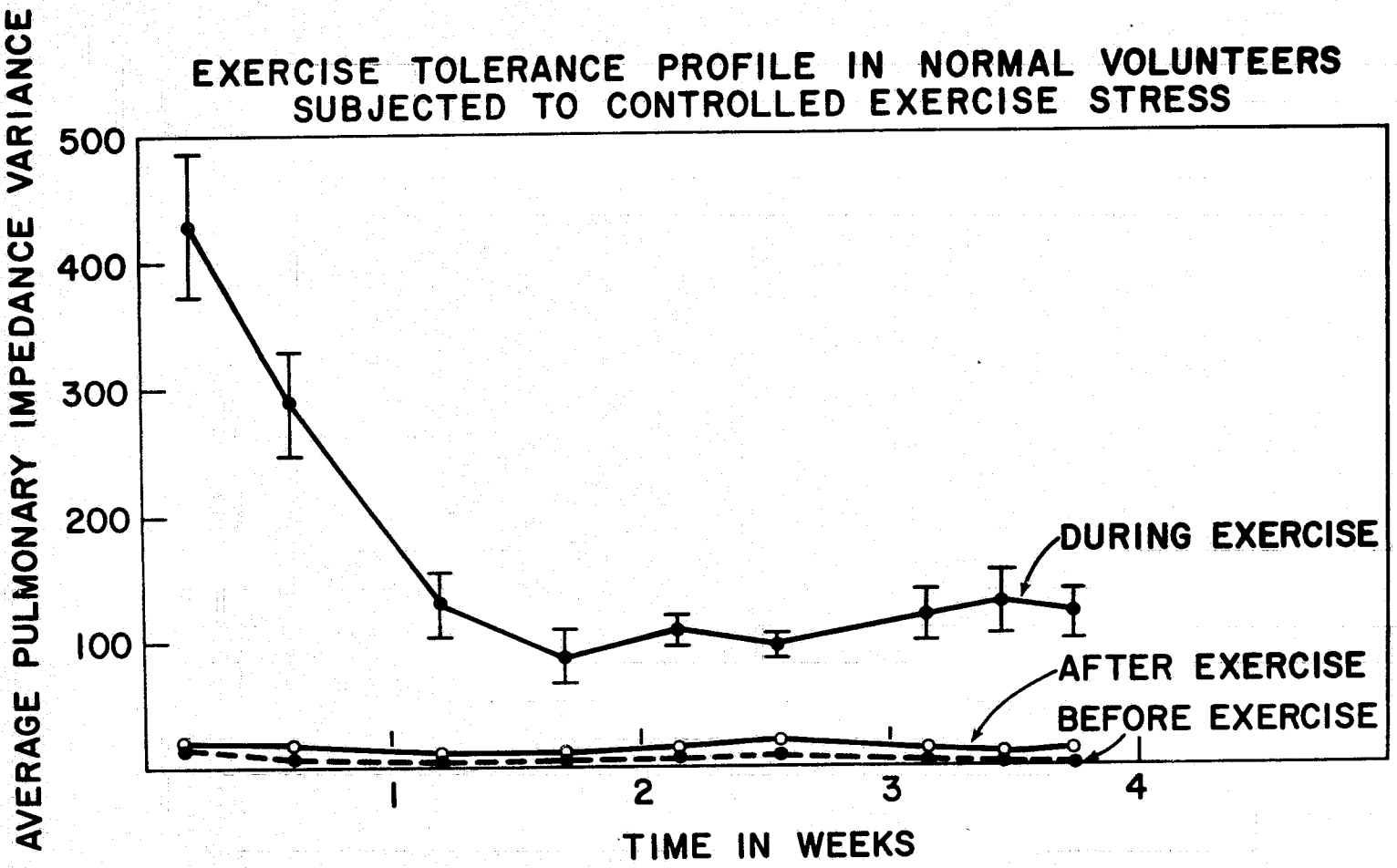
EXERCISE TOLERANCE PROFILE IN NORMAL VOLUNTEERS
SUBJECTED TO CONTROLLED EXERCISE STRESS
AVERAGE PULMONARY IMPEDANCE VARIANCE
500
400
300
200
100
1
2
3
4
TIME IN WEEKS
DURING EXERCISE
AFTER EXERCISE
BEFORE EXERCISE

Fig. 48

"training" but differs in that training would probably require 8 to 10 weeks during which the work levels would be progressively increased. All normal persons monitored showed this decrease during their second and third exercise period (first week of controlled exercise testing). There were no significant changes in the pulmonary impedance measured prior to each exercise period or at ∿15 min postexercise over the one month test period.

The pulmonary impedance variance generated by controlled exercise stress differed in one significant way from the induced by gastro-intestinal distress. That is, during exercise stress the variance is due to high frequency (<20 cpm) breathing while that induced by GI distress is primarily due to low frequency (>10 cpm), breath holding respiration. This basic difference thus allowed our system of analysis to recognize and descriminate (under laboratory conditions) between GI distress and exercise stress.

Following these initial studies, pulmonary impedance was measured in selected patients exercising on the ergometer before, during, and after total-body irradiation therapy. Only patients in chronic states of their disease without malaise of other symptoms of distress, were monitored in this study. Patients exercised at submaximal work levels comparable to nonirradiated volunteers, determined by preexposure tests to be within their capabilities. They were not in the radiation field during the exercise test period. Increased respiratory demand after exercise in irradiated patients was similar to that of the non-irradiated test subjects. However, the increase was amplified after radiation exposure was illustrated in typical performance profiles from

two therapy patients (Figs. 49 and 50). Fatiguability increased (performance decrement) on the third day postirradiation and appeared to subside within 10 days to two weeks.

We have defined these periods of increased respiratory effort (amplified impedance) as diminished exercise capacity (DEC). A comparison of pulmonary impedance data from therapy patients who participated in controlled exercise stress testing (and demonstrated DEC) with normal, control volunteers is shown in Fig. 51. When the response to exercise (variance during exercise stress) was normalized to pretreatment values, therapy patients began to adapt to submaximal stress loads, as did controls, but this adaptation was interrupted by exposure accumulation apparently in a dose rate dependent manner. Not all exercise-stressed therapy patients experienced DEC. Of 11 participating in controlled ergometry 8 responded with DEC and generally these were men as opposed to women even though workloads were comparable.

Our hypothesis that DEC is indicated by amplified pulmonary impedance variance (due to increased respiratory effort to perform at non-varying workloads) is supported by studies that demonstrate a direct relationship between work and impedance. That is, as workload on the ergometer is increased, respiratory effort increases and therefore pulmonary impedance. Furthermore, there appears to be a linear relationship between workload (up to subject's maximal efforts) and pulmonary impedance as illustrated in Fig. 52. These typical data were generated by alternate 2 min work/rest cycles and also illustrate cardiac rate changes. In light of the response of radiation therapy patients to controlled exercise stress, it is therefore possible that amplified

AVERAGE VARIANCE
0
10
20
30
40
50
60
70
80
0
20
40
DAY -1
DAY 1(24R)
DAY 1(29R)
DAY 3(82R)
DAY T+3
DAY T+10
EXERCISE TEST PERIODS (Min/Day [Accumulated Exposure])

Fig. 49

AVERAGE VARIANCE
0
10
20
30
40
50
60
70
80
0 24 48
DAY -1
0 24 48
DAY 1 (9R)
0 24 48
DAY 2 (36R)
0 24 48
DAY 3 (65R)
0 24 48
DAY -4 (97R)
0 24 48
DAY 5 (126R)
0 24 48
DAY T+4
72 0 24 48
DAY T+5
0 24 48
DAY T+10
EXERCISE TEST PERIODS (MIN/DAY [ACCUMULATED EXPOSURE])

Fig. 50

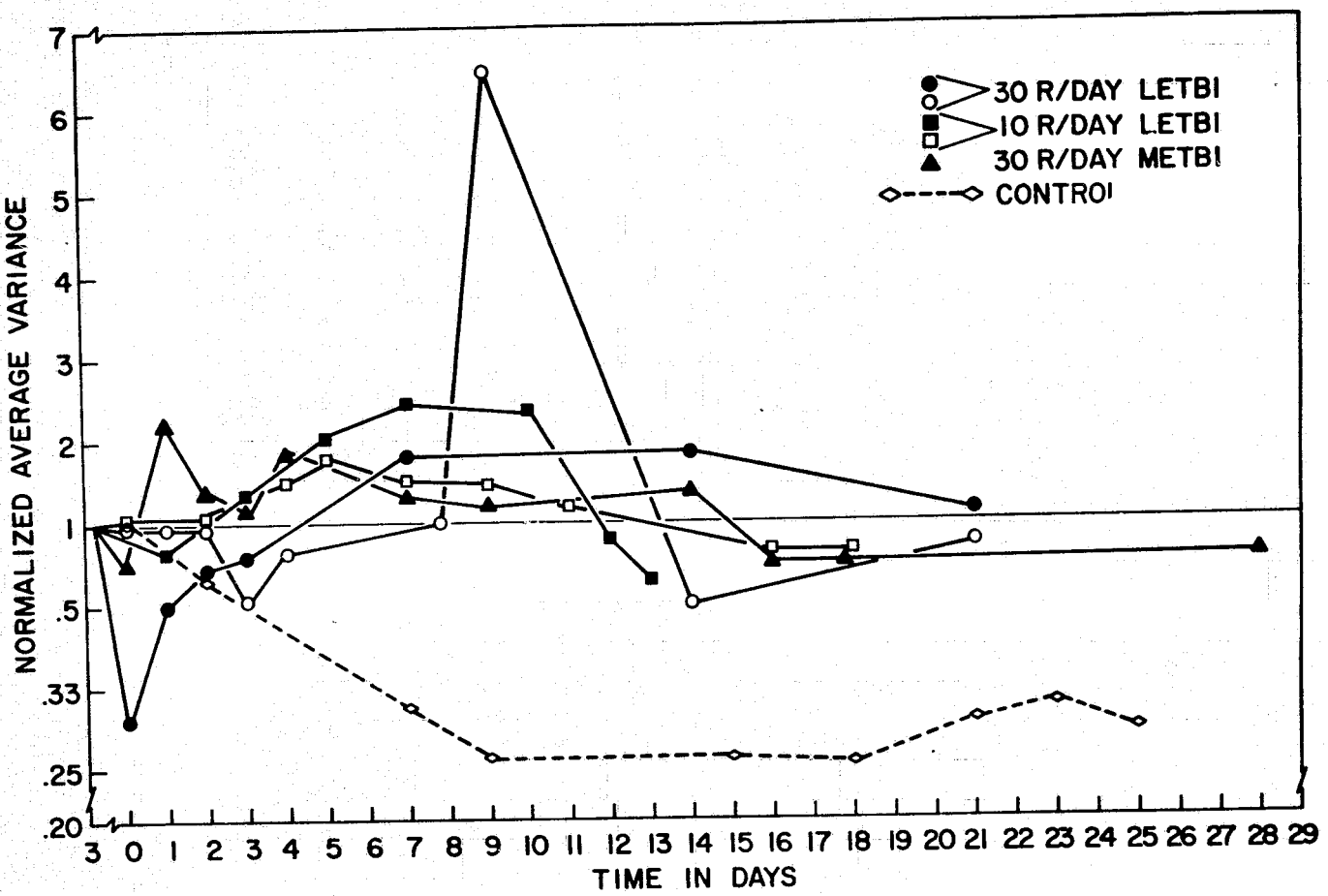
30 R/DAY LETBI
10 R/DAY LETBI
30 R/DAY METBI
CONTROI
NORMALIZED AVERAGE VARIANCE
7
6
5
4
3
2
1
.5
.33
.25
.20
3 0 1 2 3 4 5 6 7 8 9 10 11 12 13 14 15 16 17 18 19 20 21 22 23 24 25 26 27 28 29
TIME IN DAYS

Fig. 51

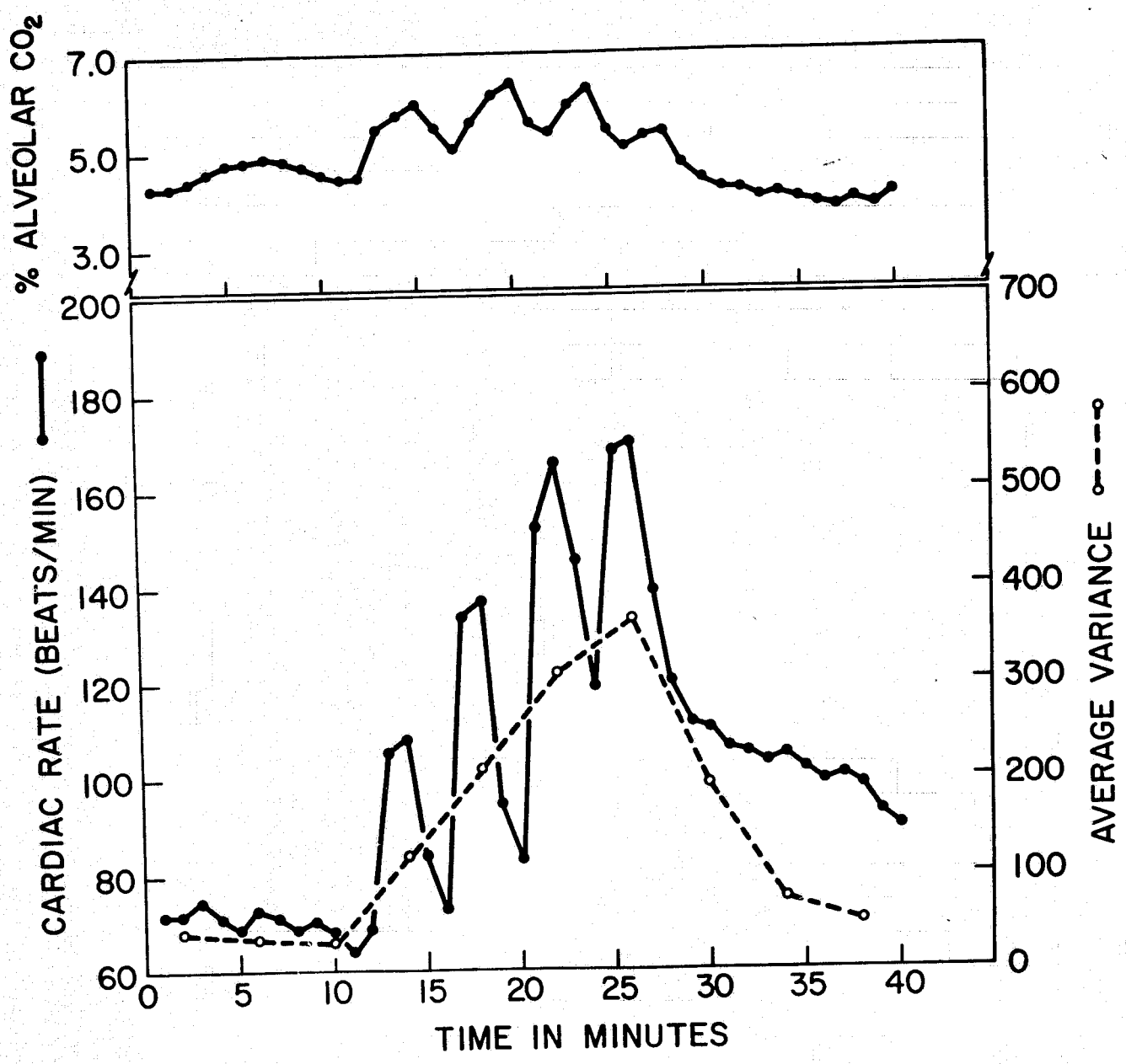
% ALVEOLAR CO_2
7.0
5.0
3.0
CARDIAC RATE (BEATS/MIN)
200
180
160
140
120
100
80
60
AVERAGE VARIANCE
700
600
500
400
300
200
100
0
0
5
10
15
20
25
30
35
40
TIME IN MINUTES

Fig. 52

pulmonary impedance during and after irradiation reflects a physiological deconditioning (DEC) to a non-varying workload. Although we did not solicit verbal opinions from these therapy patients (for fear of biasing the results) two of them did ask if the workload had been increased or decreased. In each case this inquisitiveness correlated to a significant increase or decrease in pulmonary impedance respectively.

A similar time-course study of radiation-induced performance decrement was made using this method after the accidental TBI of a man to 260 rem of ^{60}Co gamma rays for approximately 40 sec at 350 R/min. His estimated bone marrow depth dose, based on thermoluminescent dosimetry, was 115-155 rads. Pulmonary-impedance measurements during controlled exercise were obtained commencing three days postexposure and on a regular basis for a total of 60 days. Initially he exercised to his subjective tolerance against a workload of 50 watts. There was one minute of exercise on the third day but tolerance progressively increased to 30 min until on the 7th day postexposure the workload was doubled to 100 watts. At this exercise level, his exercise tolerance time remained relatively constant at $\sim$6 min. The zenith of variance in pulmonary impedance was reached within the first 6-8 min of each exercise test period. The results are summarized in Fig. 53. Decrement in performance occurred at days 7 through 13 and then at unpredictable times thereafter. Surprisingly, during the first week after exposure we failed to demonstrate any significant changes in the respiratory variance of this man even though he said he was exercising to tolerance. His subjective symptoms of fatigue were apparently not respiratory as in the radiation-induced fatigue of our irradiated patients. This observation suggested that radiation-induced fatigue was not always directly

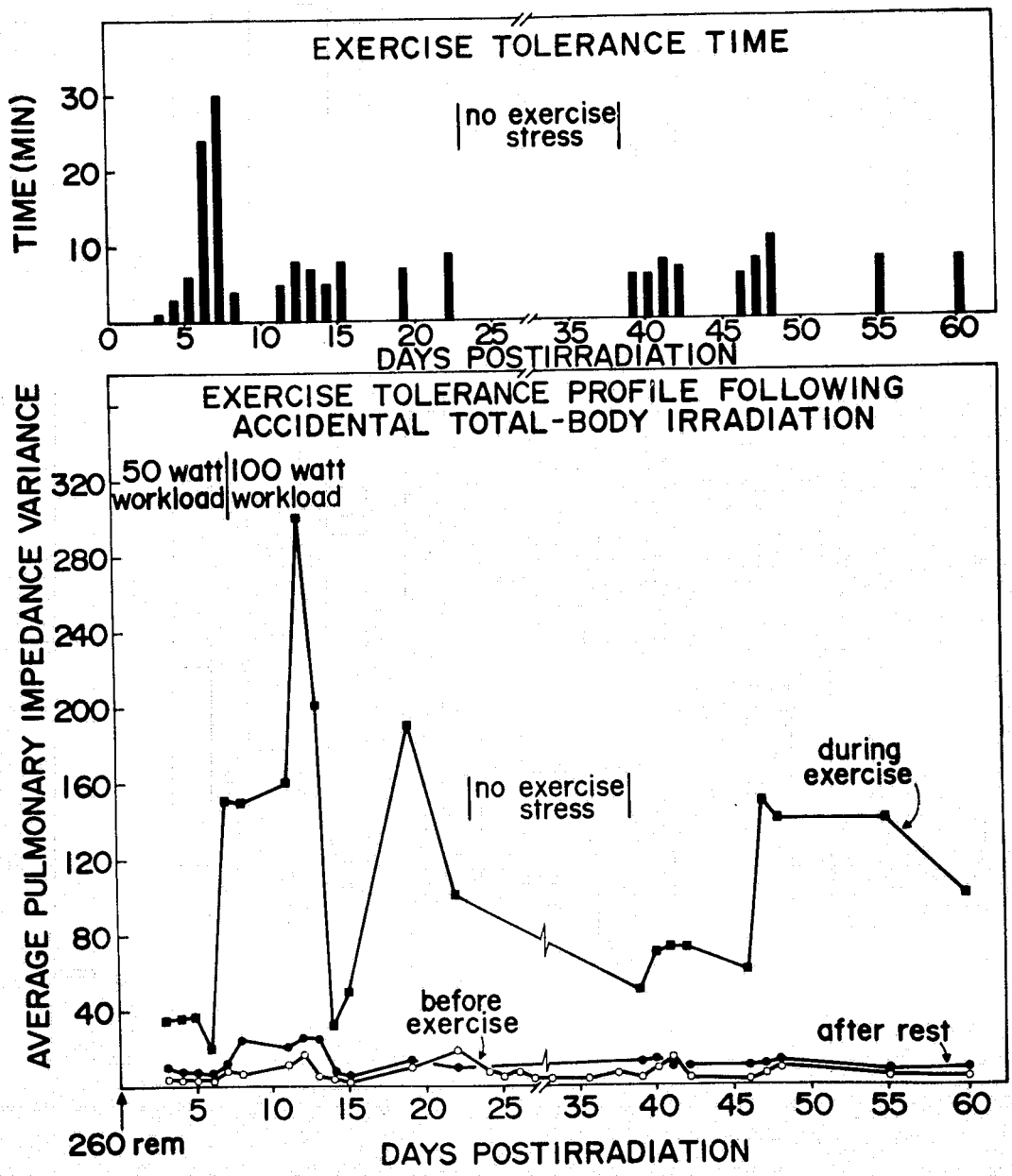
EXERCISE TOLERANCE TIME
TIME (MIN)
30
20
10
no exercise stress
0
5
10
15
20
25
35
40
45
50
55
60
DAYS POSTIRRADIATION
EXERCISE TOLERANCE PROFILE FOLLOWING ACCIDENTAL TOTAL-BODY IRRADIATION
AVERAGE PULMONARY IMPEDANCE VARIANCE
50 watt workload
100 watt workload
320
280
240
200
160
120
80
40
no exercise stress
during exercise
before exercise
after rest
260 rem
DAYS POSTIRRADIATION

Fig. 53

related to shifts in the pulmonary-impedance power spectra and their variance. Perhaps in persons in good physical condition respiratory reserves are too large for our system of exercise stress to elicit signs of performance decrement even though respiratory or vascular changes have been induced by irradiation. This dichotomy in our results may be explained on the basis of creatine phosphokinase studies in this accident victim. Following the first exercise period the serum level of this muscle enzyme rose significantly and remained high for a few days. When creatine phosphokinase levels returned to normal pulmonary impedance increased. It is unclear if creatine phosphokinase served as a "protective agent" against DEC. (These enzyme data are fully discussed in Chapter V, C.)

Irradiation therapy in the absence of exercise stress failed to cause any significant shift in pulmonary impedance variance when measured before, during, or after exposure. These basal, resting pulmonary impedance values are illustrated in Fig. 54. In patients subjected to both radiation and exercise stress there were some increases in basal resting pulmonary impedance during and shortly after therapy. Whether these basal changes were due to metabolic alterations, transient pulmonary edema or pulmonary vascular inflammation is not clear. Finally, these studies using pulmonary impedance waveform analysis demonstrate that this noninvasive and remote monitoring technique can qualitatively recognize radiation-induced DEC and that the performance changes measured thereby are significant but reversible in man accumulating up to ∿300 R.

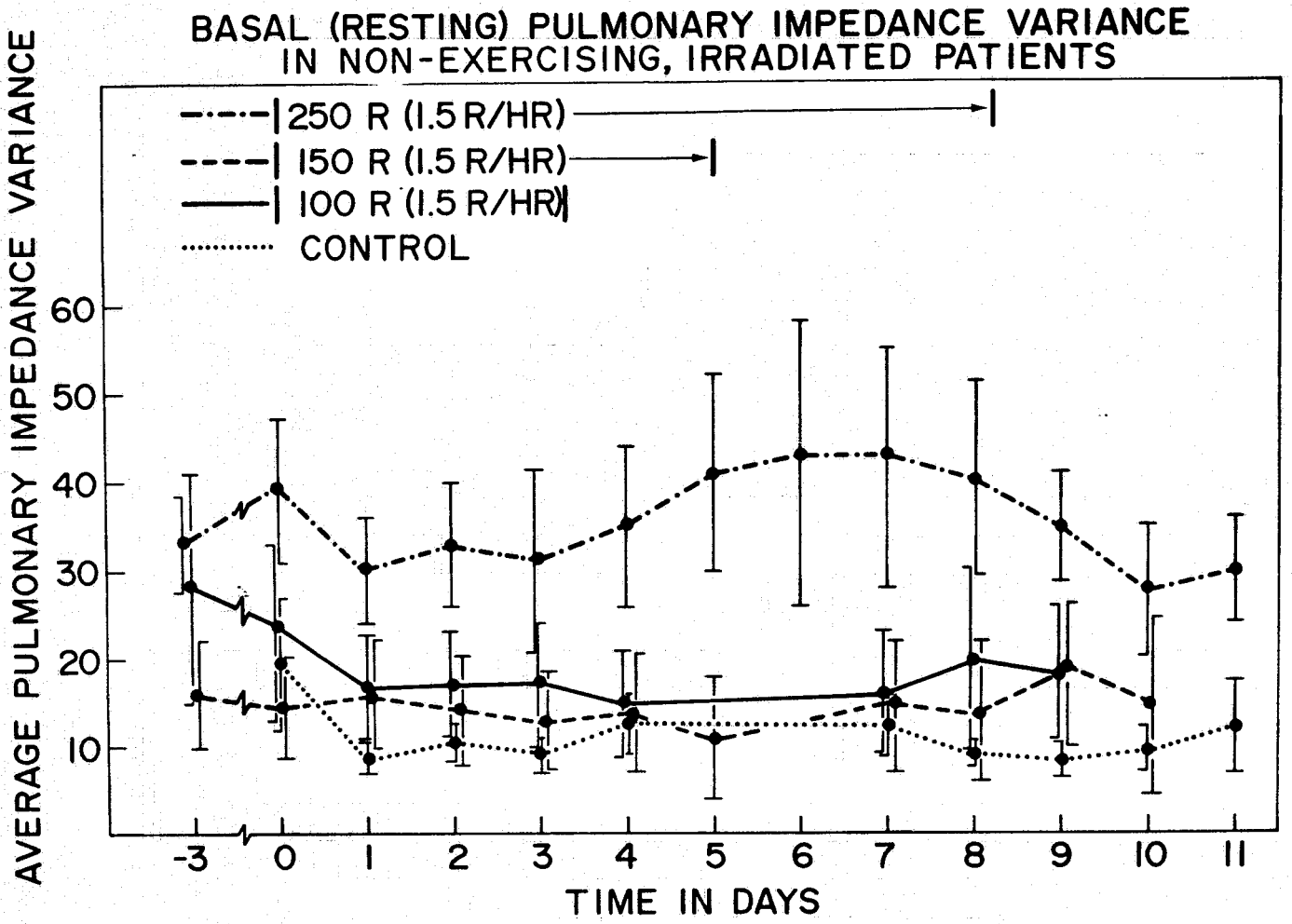
BASAL (RESTING) PULMONARY IMPEDANCE VARIANCE
IN NON-EXERCISING, IRRADIATED PATIENTS
250 R (1.5 R/HR)
150 R (1.5 R/HR)
100 R (1.5 R/HR)
CONTROL
AVERAGE PULMONARY IMPEDANCE VARIANCE
60
50
40
30
20
10
-3
0
1
2
3
4
5
6
7
8
9
10
11
TIME IN DAYS

Fig. 54

B. Controlled Exercise Stress in Irradiated Ponies

Many physiologic studies in the past involving man have demonstrated that in the event of unusual environmental stress (e.g., zero-G, total bed-rest) the exercise-conditioned man demonstrates a greater loss of exercise tolerance (more deconditioning) than the untrained individual. This phenomenon has been seen in NASA astronauts who demonstrated various levels of severe deconditioning upon return to earth gravity following extended manned-spacecraft missions.

A collaborative study was undertaken with the UT-AEC Comparative Animal Research Laboratory to determine in a large experimental animal the effect of conditioning exercises on the expected changes in pulmonary impedance waveform. Irradiated and nonirradiated Shetland ponies subjected to controlled exercise stress were used. These 12 ponies had been studied over a six year period beginning in 1966 to determine the effect of a prompt radiation exposure upon exercise tolerance and were scheduled now to be killed. In the previous study six ponies received 650 R TBI exposures of gamma radiation and six served as unirradiated controls; their pulmonary and cardiac rates and rectal temperature were measured and used to evaluate physiologic response to exercise and temperature stress. The results showed only that irradiated ponies did not dissipate body temperature normally when worked in hot environments (>85°) and no other well-defined physiologic effects of irradiation could be demonstrated.

In the current study we exposed eight of these ponies to 270 R at 30 R/day. The ponies were paired according to the following scheme, where the first number indicates prior irradiation and the second

number the exposure received in the current study: 0 + 0, 650 + 0, 0 + 270, 650 + 270. In addition, six of the twelve ponies were exercise conditioned for six weeks prior to irradiation (current study), the other six exercised only one week prior to irradiation. The exercise consisted of pulling a brake-loaded cart and is described later. Creatine phosphokinase data from these ponies (see Table 16, Chapter V) while quite variable, demonstrated again (as seen in our human studies) that irradiation and/or exercise stress result in increases in CPK levels. Animals that had received 650 R previously (with or without an additional 250 R or no additional irradiation or exercise conditioning) demonstrated the greatest change in CPK response, suggesting that some permanent biochemical lesion had resulted. The possible significance of this change is discussed later in relation to changes in pulmonary impedance variance in this group of ponies.

To measure the effects of exercise conditioning prior to irradiation and its effect on performance decrement, two of four teams of ponies were preconditioned six weeks prior to irradiation (270 R): the other two teams exercised under controlled conditions only one week prior to irradiation. One team of controls was exercise conditioned, the other was not.

Controlled exercise testing was accomplished using matched, trained teams of ponies accustomed to pulling a brake-loaded cart around a circular track. Each pony worked against a workload equal to a resistance of 3/4 horsepower for 30 min each human workday (M-F) for constant periods of time. In the preconditioned group of ponies, the total work period studied

was five weeks prior to and six weeks after irradiation; in the non-conditioned ponies, it was one week prior to and six weeks after irradiation.

In all ponies that participated in this study, the pulmonary-impedance variance data were similar to that seen in the normal man when subjected to controlled exercise testing. There was a general trend for the pulmonary-impedance variance to decrease (or remain relatively constant) over the conditioning period. In preconditioned ponies this gradual reduction in pulmonary-impedance variance was interrupted by the onset of TBI (30 R/1 -hr day), and was reflected by an increase in pulmonary-impedance variance. This increased variance in irradiated, preconditioned ponies was evident for three to four weeks postirradiation after which the variance values began to decrease. However, a similar shift in the pulmonary-impedance variance was noted in a preconditioned control pony that was forced to stand in its stall for 16 hrs/day to simulate the postural restriction of the ponies during their irradiation. This result suggests that the mechanism for irradiation-induced fatigue may be similar to that physiologic response induced by the prevention of supine rest (16-hr duration) in the pony.

When compared to preconditioned ponies, pulmonary-impedance variance of non-preconditioned ponies did not appear to be as severely affected by TBI. Indeed, non-preconditioned ponies did not, as a group, demonstrate an increased pulmonary-impedance variance postirradiation, with the exception of one animal that showed significantly increased variance during the nine-day irradiation period. As in the preconditioned control pony, non-preconditioned controls demonstrated

increased pulmonary-impedance variance in response to standing 16 hrs/day. These data are summarized in Figs. 55, 56, and 57.

No definite correlations were found in pulmonary-impedance variance data of these ponies that would indicate that a permanent physiologic lesion was present as a result of the 650 R exposure five years prior to the current study (270 R). The results do, however, suggest that exercise preconditioning may lower the radiation threshold for increased fatigability. This influence of preconditioning may be important in light of the demanding preflight conditioning and the phenomenon of postflight cardiovascular deconditioning noted in NASA manned-space-flight personnel.

At the end of the study all ponies were killed and necropsied to permit evaluation of the extent of any vascular radiation effects. Specimens of lungs, kidneys, testes, and skin were studied histologically for this purpose. Lung and kidney were chosen to study late radiation effects and testes to evaluate the levels of acute damage and subsequent repair of the effects of the two exposures. The skin was studied to determine whether Brown's*observation that irradiated ponies were relatively heat intolerant during exercise might be related to damage induced in sweat-gland structure.

Objectivity was obtained in this histologic study by coding all slide preparations so that individual ponies and their irradiation histories were not identifiable. After all the histologic appraisals were finished, a diagnostic interpretation was made as to whether or not the changes seen were related to any irradiation, 650 R only, 270 R only, three months or six weeks prior to necropsy, and 270 R in combination

*Dr. Dan Brown, D.V.M., formerly with UT-CARL.

EFFECT OF FORCED STANDING (16 HR./DAY) AND CONTROLLED EXERCISE STRESS ON PULMONARY IMPEDANCE IN TRAINED SHETLAND PONIES

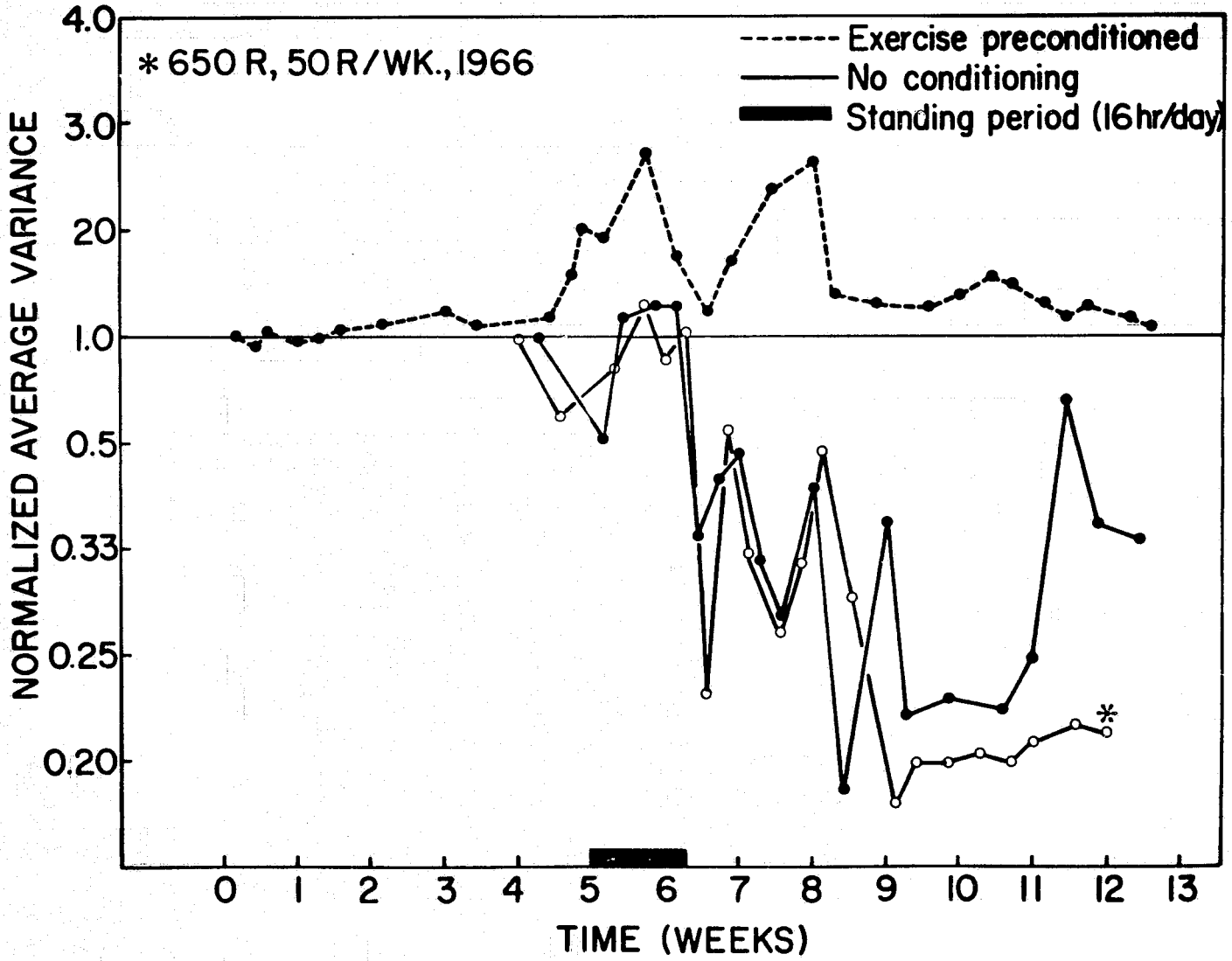

Fig. 55

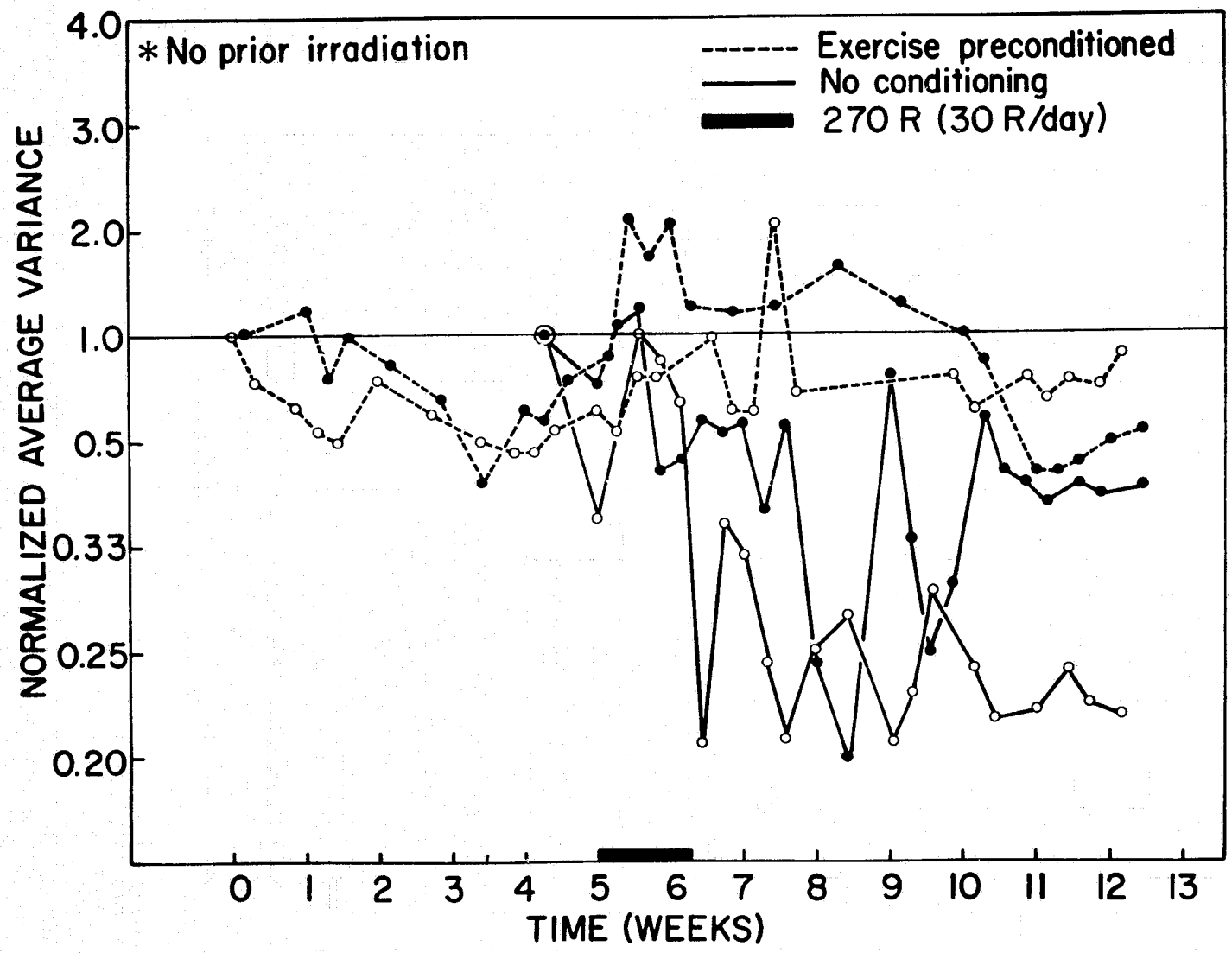
EFFECT OF TOTAL-BODY IRRADIATION*(270 R, 30R/DAY) AND CONTROLLED EXERCISE STRESS ON PULMONARY IMPEDANCE IN TRAINED SHETLAND PONIES
* No prior irradiation
Exercise preconditioned
No conditioning
270 R (30 R/day)
NORMALIZED AVERAGE VARIANCE
4.0
3.0
2.0
1.0
0.5
0.33
0.25
0.20
0 1 2 3 4 5 6 7 8 9 10 11 12 13
TIME (WEEKS)

Fig. 56

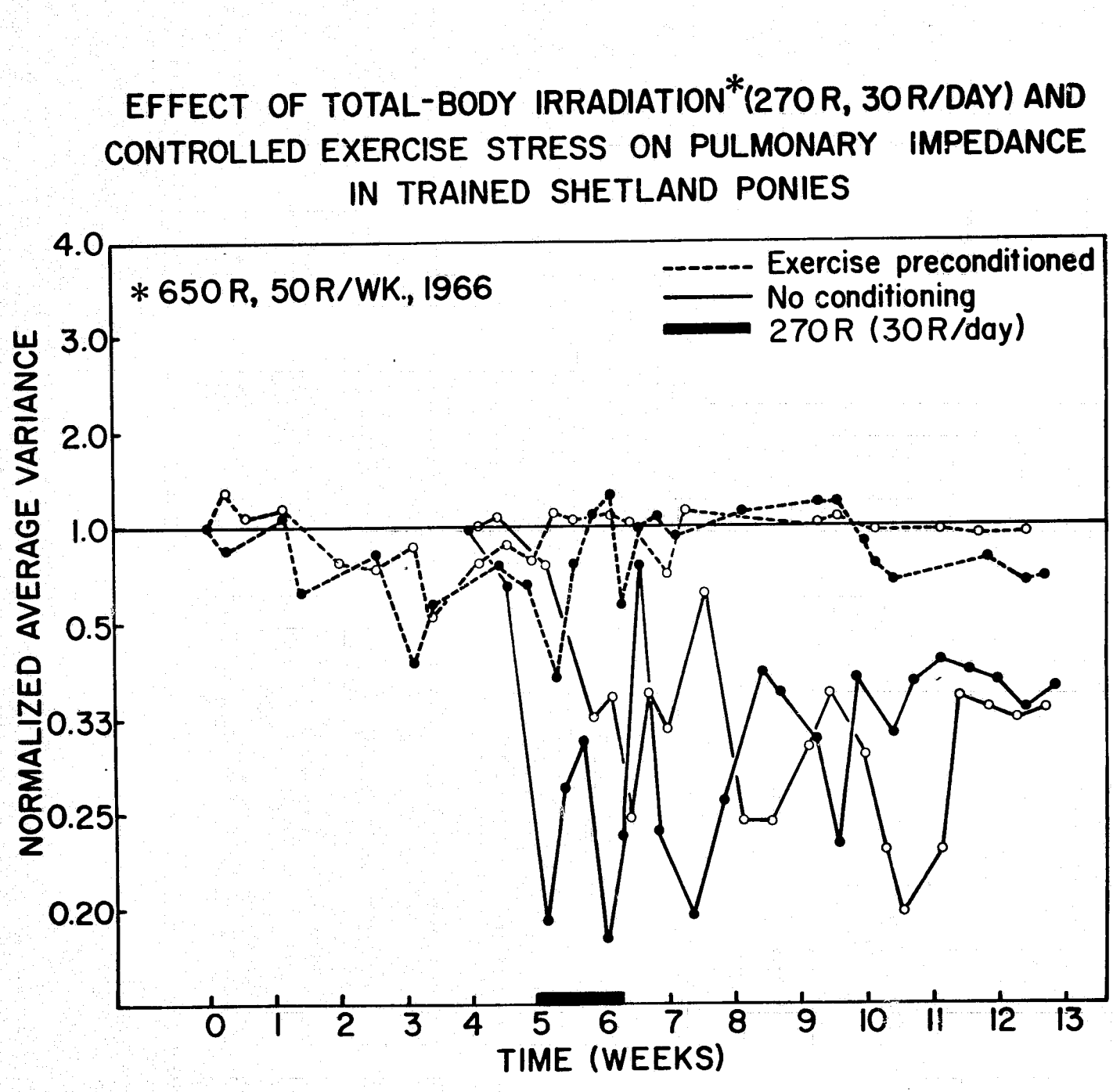
EFFECT OF TOTAL-BODY IRRADIATION*(270 R, 30 R/DAY) AND CONTROLLED EXERCISE STRESS ON PULMONARY IMPEDANCE IN TRAINED SHETLAND PONIES
* 650 R, 50 R/WK., 1966
Exercise preconditioned
No conditioning
270 R (30 R/day)
NORMALIZED AVERAGE VARIANCE
4.0
3.0
2.0
1.0
0.5
0.33
0.25
0.20
0 1 2 3 4 5 6 7 8 9 10 11 12 13
TIME (WEEKS)

Fig. 57

with the previous 650 R exposure. This appraisal and its interpretation were then decoded and compared with the actual histories of the ponies. The results of this study, in summary, were as follows.

Changes seen in pulmonary alveolar-wall collagen and glomerular and arteriolar vasculature did not correlate with either the degree of change in individual physiologic response to exercise or with the irradiation history. In the one pony in which the histologic changes in lung and kidney were extreme and obviously due to radiation, the animal could not be tested physiologically because he was lame. Remarkably, only three instances of unquestionable pulmonary and late renal vascular effects related to the irradiation experience of the animal were found. In the kidneys of most ponies the relation of vascular changes to irradiation was obscured by the presence of changes typical of intercurrent or chronic interstitial nephritis or chronic pyelonephritis. In the lungs, the unfortunate presence of chronic bronchiolar inflammation and peribronchial lymphoid infiltration in most ponies made evaluation of minimal degrees of alveolar sclerosis impossible.

The histologic appraisal of the changes in the testes, however, correlated directly with the irradiation histories. The ponies that had received only 650 R exposure had prominent foci of regeneration of testicular tubular germinal epithelium scattered among severely atrophic tubules. Those that had received a recent second exposure of 270 R, in addition to the 650 R, had lost these regenerative foci, while those with no previous exposure and only a recent 270 R exposure showed germinal epithelial atrophy without accompanying tubular sclerosis.

The unirradiated ponies had histologically normal testes. Of purely histologic interest, one pony had an adenomatous focal epithelial change that could be interpreted as being neoplastic, and several others had such an extreme focal increase in interstitial cells (Leydig) that doubt was cast on the validity for this species of the widely held radiopathological concept that the histologic increase in these cells after irradiation is apparent and not real. This increase in Leydig cells was most extreme in those animals that received the smaller more recent exposures.

Although the sections of skin were all taken from the same anatomical locus in all animals, the number of sweat glands in them was highly variable and did not correlate with radiation history.

The negative results of this histologic study strengthened our belief that the changes we have been finding in the exercise tolerance of irradiated men reflect reversible metabolic rather than irreversible anatomical changes.

2. Cardiac Rate/Oxygen Consumption

While our studies of pulmonary impedance power spectral analysis proved useful in assessing levels of radiation-induced GI distress and diminished exercise capacity, we continued to search for other physiologic indicators that were more tried and tested for measuring changes in stress response. Two such physiologic parameters, particularly for measuring exercise stress responses, are cardiac rate and respiratory gas analysis. Cardiac rate analysis was primarily confined to exercise stress testing and not to periods of GI distress since few significant changes were noted in patients experiencing radiation-induced nausea and vomiting. Those cardiac rate alterations during nausea and vomiting

were generally sinus rhythm in nature resultant from parasymphatic (vagal) looping accompaning low frequency, deep breathing. In only one nonexercise stress, irradiated patient did we record significant alterations in cardiac rate. This occurred during atrial fibrillation in the early postirradiation hours in a man exposed to 694 R (500 rads) whole-body gamma irradiation prior to bone marrow transplantation. Over a period commencing abour four hours postirradiation and continuing for two-three hours, the cardiac rate increased from 85 to 185 beats/minute. This patient had previously experienced atrial fibrillation and this current episode was controlled by conventional chemotherapy.

Efforts to correlate cardiac rate, pulmonary impedance, and expired (alveolar) CO_2 changes during exercise stress showed (Table 13) good data fit. However, pulmonary impedance was subject to minor motion artifacts as we had discovered earlier in ergometric testing. Periods of controlled stress were characterized by increases in pulmonary impedance variance, cardiac rate, and expired CO_2 as would be expected during increased respiratory demand. Figure 58 graphically illustrates the relationship between pulmonary impedance and alveolar CO_2 concentration in another study. Finally, with the acquisition of a system for measuring O_2 consumption rates, we attempted to correlated O_2 consumption (VO_2) with pulmonary impedance variance. Figure 59 shows typical results of this VO_2: impedance correlation. This correlation can be obtained only when the investigator is reasonably sure that no motion artifacts are present in the pulmonary impedance waveform. Thus, these correlations of pulmonary impedance variance with cardiac rate, CO_2 production, and O_2 consumption indicated that impedance measurements could provide meaningful,

TABLE 13

Relationship Between Pulmonary Impedance, Alveolar CO_2 and Cardiac Rate in a Normal Volunteer Exercising on a Bicycle Ergometer

Monitoring period	Pulmonary impedance variance	Ratio	
		CO_2/ basal CO_2	Heart rate/ basal heart rate
Preexercise*	41	1.00	1.00
During exercise	497	1.45	1.70
End exercise + 4 min	301	1.25	1.20
End exercise + 8 min	61	1.01	1.13
End exercise + 12 min	58	1.00	1.12
End exercise + 16 min	46	1.00	1.07
End exercise + 20 min	64	1.00	1.08
End exercise + 24 min	51	1.00	1.08
End exercise + 28 min	65	1.00	1.05

*Data measured at 5 min prior to bicycle ergometry (50 watt workload).

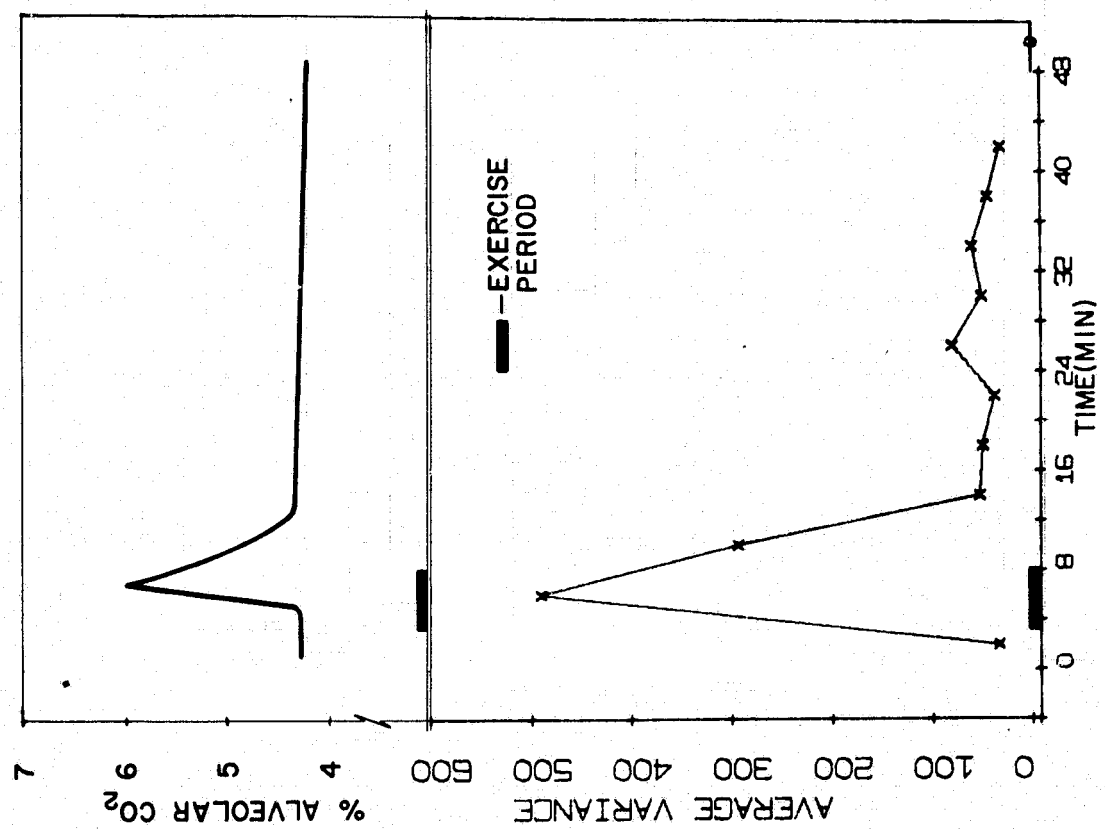
% ALVEOLAR CO_2
7
6
5
4
AVERAGE VARIANCE
600
500
400
300
200
100
0
EXERCISE PERIOD
0
8
16
24
32
40
48
TIME(MIN)

Fig. 58

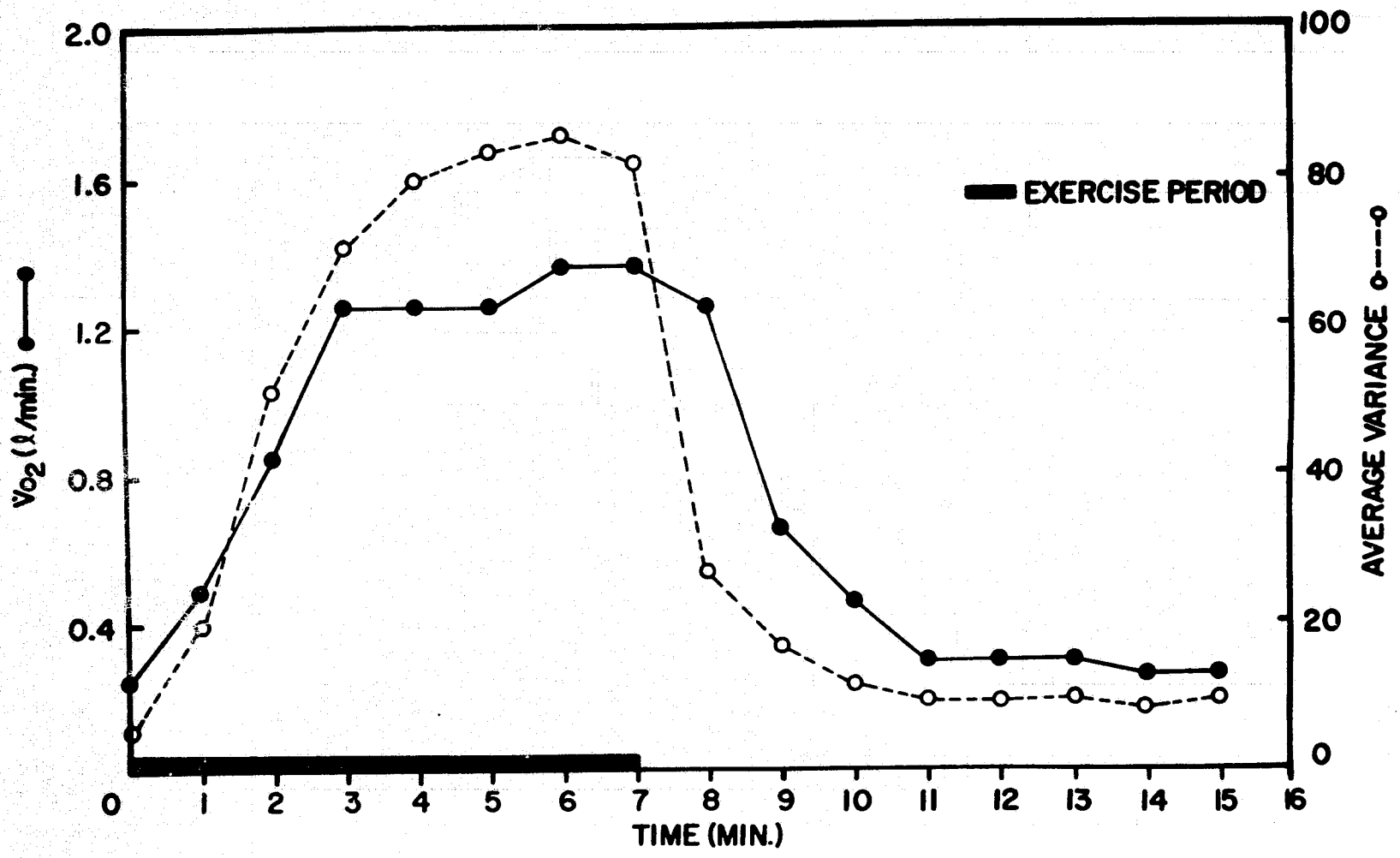
2.0
1.6
1.2
0.8
0.4
V_{O_2} (l/min.)
100
80
60
40
20
0
AVERAGE VARIANCE
EXERCISE PERIOD
0 1 2 3 4 5 6 7 8 9 10 11 12 13 14 15 16
TIME (MIN.)

Fig. 59

remotely monitored, physiologic information regarding human physical performance postirradiation. Notwithstanding, we continued to search for more useful methods of assessing radiation-induced performance decrement. Since VO_2 is the most common parameter used to assess physical status and response to exercise, we studied VO_2 in a patient exposed to 100 R (0.8 R/hr, 16 R/20 hr day) and controlled exercise stress. This patient, male, aged 44 years, had been recently diagnosed to be in the early stages of lymphosarcoma and was otherwise in very good physical condition. Performance was measured in response to a submaximal workload of 612 kilopound meter/min.* During the six days of irradiation therapy the patient responded to controlled ergometry with an increasing maximal cardiac rate (up 14%) although the workload remained constant. Following ceasation of irradiation therapy, the maximal cardiac rate returned to preirradiation levels over a 5-day period and the patient demonstrated a slight tendency toward training over an intermittant stress period of about 2-1/2 months. These cardiac rate data were used to predict maximal O_2 consumption (VO_2 max) using the method of Astrand (21). When corrected for age and sex these predicted VO_2 max data indicated a decrease from 2.32 liters/min (preirradiation) to 1.83 liters/min when 100 R were accumulated (Fig. 60). There was no significant change in the actual VO_2 (612 Kpm) required to perform at the submaximal workload. Actual O_2 consumed during all 26 exercise testing periods was well within the expected values. When averaged for all 26 controlled, submaximal exercise test periods the VO_2 measured (1.64 ± 12l/min) was well within the expected values as reported by the World Health Organization (22). Thus, it would seem that any radiation

*1 watt = 6.12 Kpm

Fig. 60

EFFECT OF TOTAL-BODY IRRADIATION ON CARDIAC RATE AND PREDICTED $\dot{V}o_2$ MAXIMUM DURING CONTROLLED EXERCISE STRESS IN MAN (age 44 years)

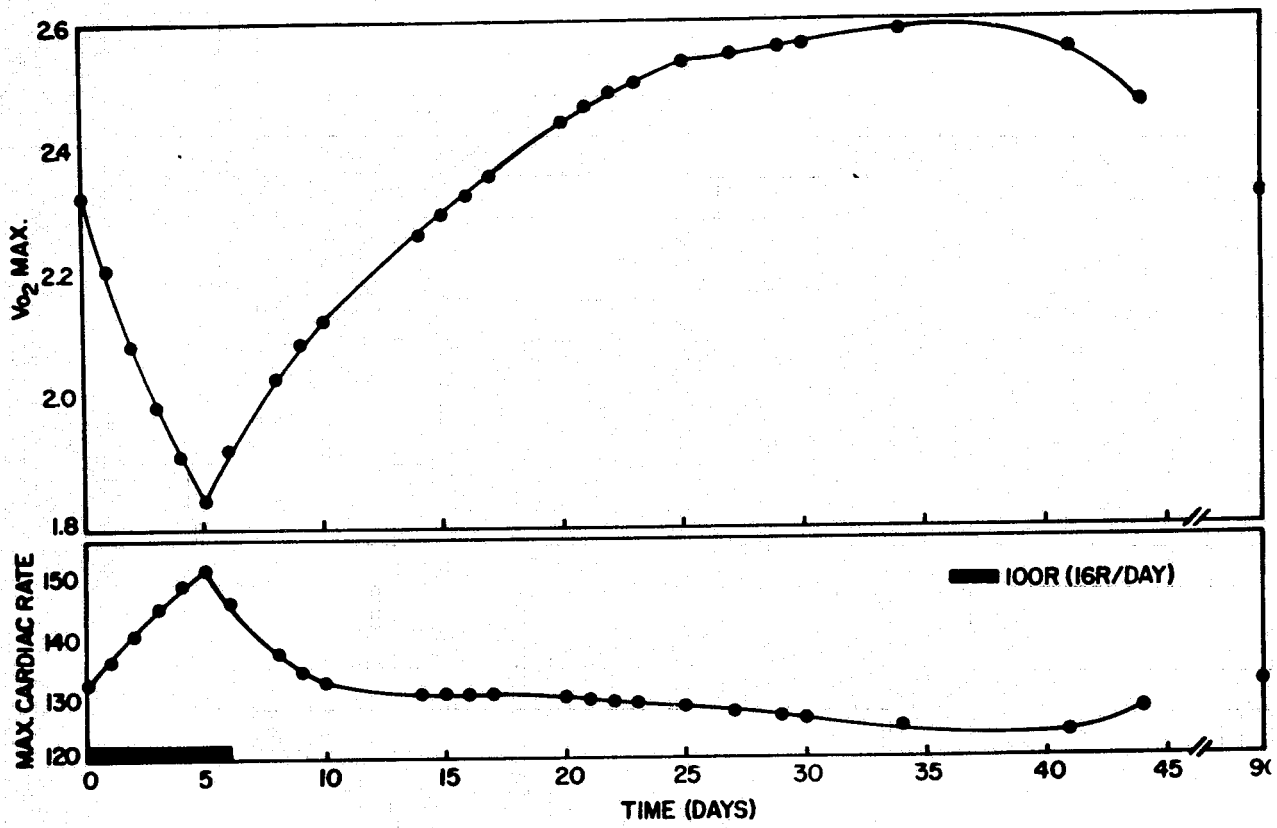

affect experienced by this patient was not at the tissue level of actual O_2 consumption but in the ability of the cardiovascular system to supply oxygen to the active muscles. This hypothesis is supported by the mode of death (irreversible hypotension) seen in radiation accident victims who receive very high exposures (>5000 R). It would appear that the threshold for cardiovascular deconditioning is quite low and the effect of whole-body exposures appreciably less than 5000 R are transient and completely reversible.

In attempting to model these O_2 consumption data from the irradiated patient we found a remarkable similarity between irradiation effect and data reported by Saltin et al. (23) for bedrest studies. Saltin's study demonstrated inordinately well the effects of 21 days bedrest on trained and untrained male volunteers. Following the three-week bedrest period, these volunteers experienced a fall in stroke volume, cardiac output, maximal oxygen consumption, and an increase in cardiac rate to perform at the same workload used prior to bedrest. Our data are compared to those obtained by Saltin and are summarized in Table 14. We included data from a normal, healthy control male matched by age, body build, and weight to the therapy patient.

These data prompted us to retrospectively study cardiac rate alterations in therapy patients who had or had not previously participated in controlled exercise stress testing. Maximal cardiac rates recorded during the final minute of an exercise stress period were compared for pre- and postexposure differences. Although the exercise protocols used in these stress tests did not conform exactly (in length of stress time in some cases) to those usually associated with oxygen

TABLE 14

COMPARISON OF CARDIOVASCULAR DECONDITIONING AS A RESULT OF BED REST* OR TOTAL-BODY IRRADIATION

21-day Bed Rest Study		100 R (16 R/day)	Control for Irradiation Study (workload 612 Kpm/min)
Cardiac rates†			
1. Pretreatment	129	132	120
2. End of treatment	154	151	120 (measured on 6th consecutive day of stress testing)
Oxygen Consumption (VO_2 max)			
1. Pretreatment	3.3 l/min	2.3 l/min§	2.8 l/min
2. End of treatment	2.4 l/min (↓27%)	1.8 l/min (↓22%)	2.8 l/min
3. Recovery time	∿9 days¶	11 days	-

* Saltin, et al.
† Measured at 600 Kpm/min in bed rest study, 612 Kpm/min in irradiation study.
§ Predicted from submaximal workload (612 Kpm/min.
¶ Untrained individuals only.

consumption studies, we used these cardiac rates to predict oxygen consumption again according to the methods of Astrand. These data, summarized in Table 15, revealed that maximal cardiac rates increased four to fourteen percent in therapy patients exposed to total body irradiation up to 250 R. The response did not seem to be dose or dose rate dependent and not all patients demonstrated significant increases in cardiac rates. Likewise, the maximal cardiac rate in a man accidentally exposed to 250 R total body irradiation increased 15% during repetitive controlled exercise stress. Significant increases in cardiac rates were not noted in patients exposed to irradiation up to 250 R but not subjected to physical stress. At stress loads similar to those patients were subjected to a group of control males demonstrated a decrease of 11% in maximal cardiac rates.

These results suggested that radiation-induced cardiovascular deconditioning (CVD) might be responsible for increased cardiac rates recorded during these stress sessions and support the hypothesis that radiation-induced "easy-fatiguability" may be revealed symptomatically only when the irradiated person is stressed physically. They do not, however, provide any information concerning whether or not these physiologic phenomena would be additive to those previously experienced by astronauts during prolonged low G activity.

TABLE 15

EFFECT OF TOTAL-BODY THERAPEUTIC OR ACCIDENT IRRADIATION ON CARDIAC RATE DURING CONTROLLED EXERCISE STRESS (UPRIGHT ERGOMETRY) AND MAXIMAL AEROBIC CAPACITY

IRRADIATION PROTOCOL	MAXIMUM CARDIAC RATE	MAXIMAL AEROBIC CAPACITY*
10R/Day (1.5R/Hr)	↑∿11% (3-5)†	down 22%
30R/Day (1.5R/Hr)	↑∿ 7% (1 week post)	down 10%
30R/Day (1.5R/Min)	↑∿ 4% (2)	down 10%
16R/Day (0.8R/Hr)	↑∿14% (5)	down 26%
Accidental Irradiation -260R (350R/Min)	↑∿15% (5, 2 week)	down 19%
Control (normal males)	↓∿11% (2-4 week)	up 19%
Control (patients not subjected to stress; 100-250R, 1.5R/Hr)	↓↑1-2%	

†Time in days to reach peak response after initiation of irradiation insult

*Extrapolated from submaximal work loads

CHAPTER V

ANCILLARY CLINICAL LABORATORY AND EXPERIMENTAL STUDIES

A. Red Cell Size Relation to Radiation Effect on Erythroblasts in Man and Mouse

Studies in experimental hematology use radioactive cell-labels in characterizing changes in the hematopoietic organ after irradiation and also employ modern electronic cell sizing and counting apparatus for detecting end points for radiation effects.

We investigated the usefulness of electronic cell-sizing in clinical and experimental hematology. Our studies were classified as (1) clinical and experimental applications and (2) experimental observations on the nature of the electronic two-peak red blood cell (RBC) population phenomenon.

The system used to accomplish these studies is described in detail in a previous publication. Briefly, the components of the system are built around the Coulter Counter, Model B, and its associated glass transducing assembly consisting of the aperture tube, electrodes, mercury liquid volume measurement device and pump. The pulses, formed as each cell is driven through the aperture by differential pressure, are taken off the Coulter electronics just before reaching the Coulter oscilloscope circuit. They are sorted and stored by a 400-channel pulse-height analyzer appropriately altered to accept the characteristically slowly rising pulses that are produced. Each stored pulse is simultaneously counted by a pre-set Coulter until 100,000 cell volumes are measured and the analysis automatically terminated.

The accumulation of "cells" of the same volume in each analyzer channel is displayed "live" on an oscilloscope screen. At the end of an

analysis, a photograph is made of the resulting frequency-distribution curve for the purpose of a visual record and the data are automatically typewritten for later computation. For clinical purposes the ratio of mean channel number to mean cell volume as derived from the hematocrit and red blood cell count and determined statistically with a large number of observations, is a sufficiently accurate means of calibration. This determination is accomplished as shown in Fig. 61 by graphing for each blood sample the hematocrit-derived MCV, and the electronically determined mean channel. Where extremely precise measurements are desired and apertures small in diameter are usable, Dow latex particles of bacterial size (0.87-1.31 micron diameter) can be employed. After this conversion factor has been determined, it can be used to transpose channel number to cubic microns providing the experimental and electronic conditions are kept constant.

Preliminary studies demonstrated the reliability of the hematocrit determined MCV and electronic MCV. These studies in neonatal mice are demonstrated in Fig. 62. Initial studies also demonstrated this capability of electronic MCV determinations to monitor RBC changes induced by total-body irradiation therapy and Methotrexate therapy. These thereapeutic data are shown in Figs. 63 and 64.

In clinical hematology the technique was used to: (a) in routine diagnostic work-up of new patients to approaise the status of their erythron and (b) during therapy of RBC diseases to gauge the rate of return of RBC size distribution in polycythemia rubra vera (PRV) after radiation therapy. These techniques of RBC sizing for clinical hematology were extended by studies of new patients and in long-term patients after repeated therapeutic trials over long periods. The results substantiated our tentative conclusions that remission induced in PRV by irradiation and

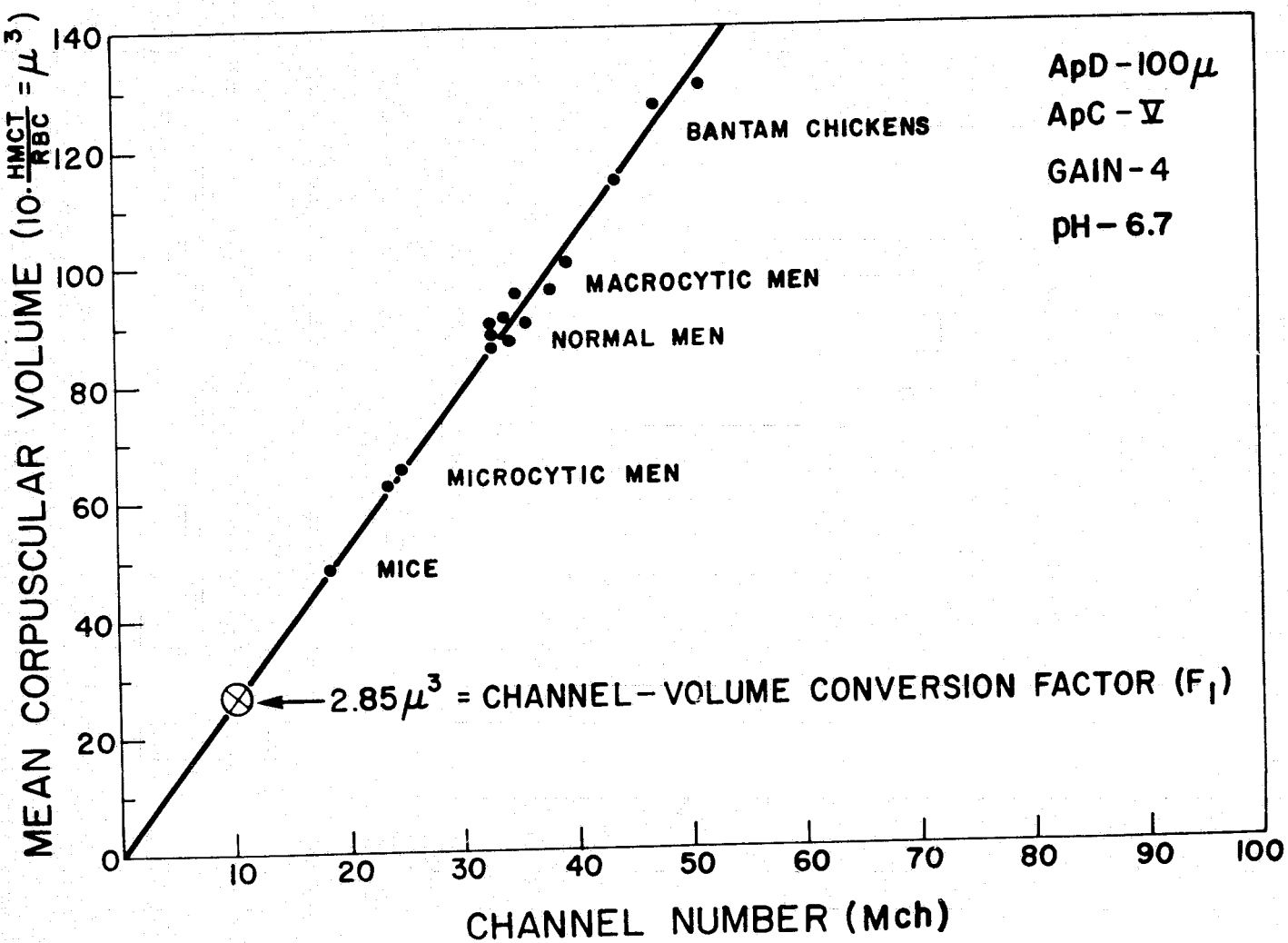
MEAN CORPUSCULAR VOLUME ($10 \cdot \frac{HMCT}{RBC} = \mu^3$)
CHANNEL NUMBER (Mch)
ApD - 100μ
ApC - V
GAIN - 4
pH - 6.7
BANTAM CHICKENS
MACROCYTIC MEN
NORMAL MEN
MICROCYTIC MEN
MICE
2.85μ³ = CHANNEL-VOLUME CONVERSION FACTOR (F1)
0
20
40
60
80
100
120
140
10
20
30
40
50
60
70
80
90
100

Fig. 61

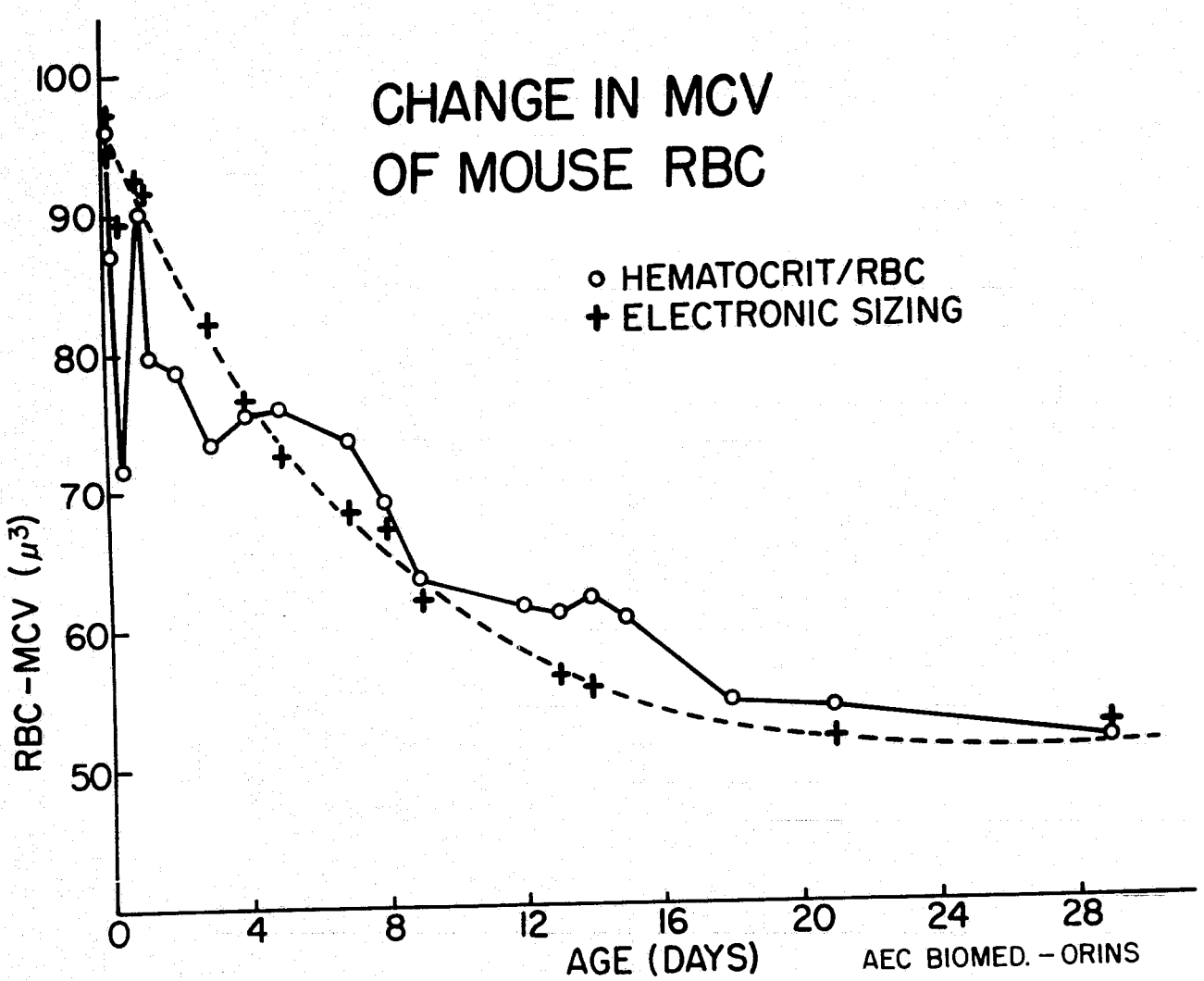
CHANGE IN MCV
OF MOUSE RBC
o HEMATOCRIT/RBC
+ ELECTRONIC SIZING
RBC-MCV (μ3)
100
90
80
70
60
50
0
4
8
12
16
20
24
28
AGE (DAYS)
AEC BIOMED. – ORINS

Fig. 62

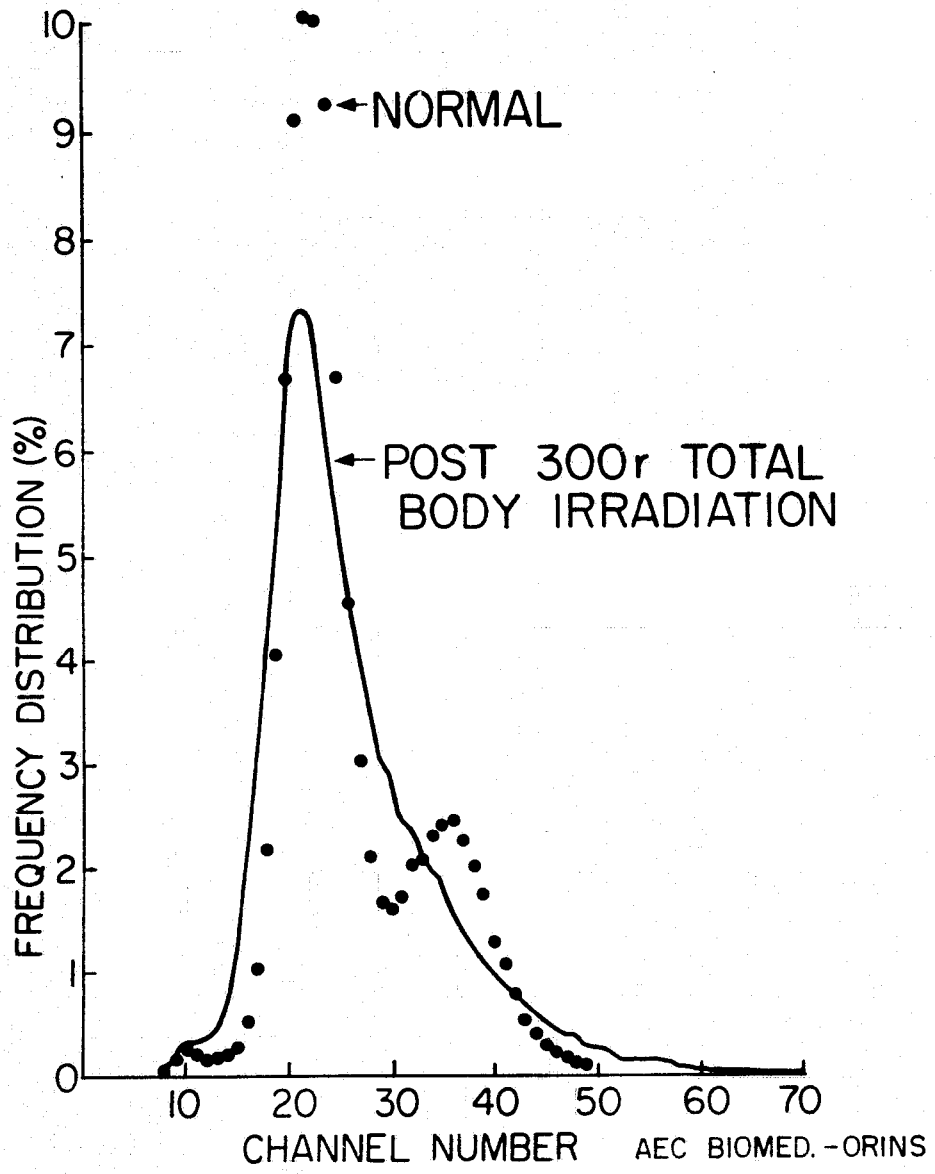
NORMAL
POST 300r TOTAL BODY IRRADIATION
FREQUENCY DISTRIBUTION (%)
CHANNEL NUMBER
AEC BIOMED. - ORINS

Fig. 63

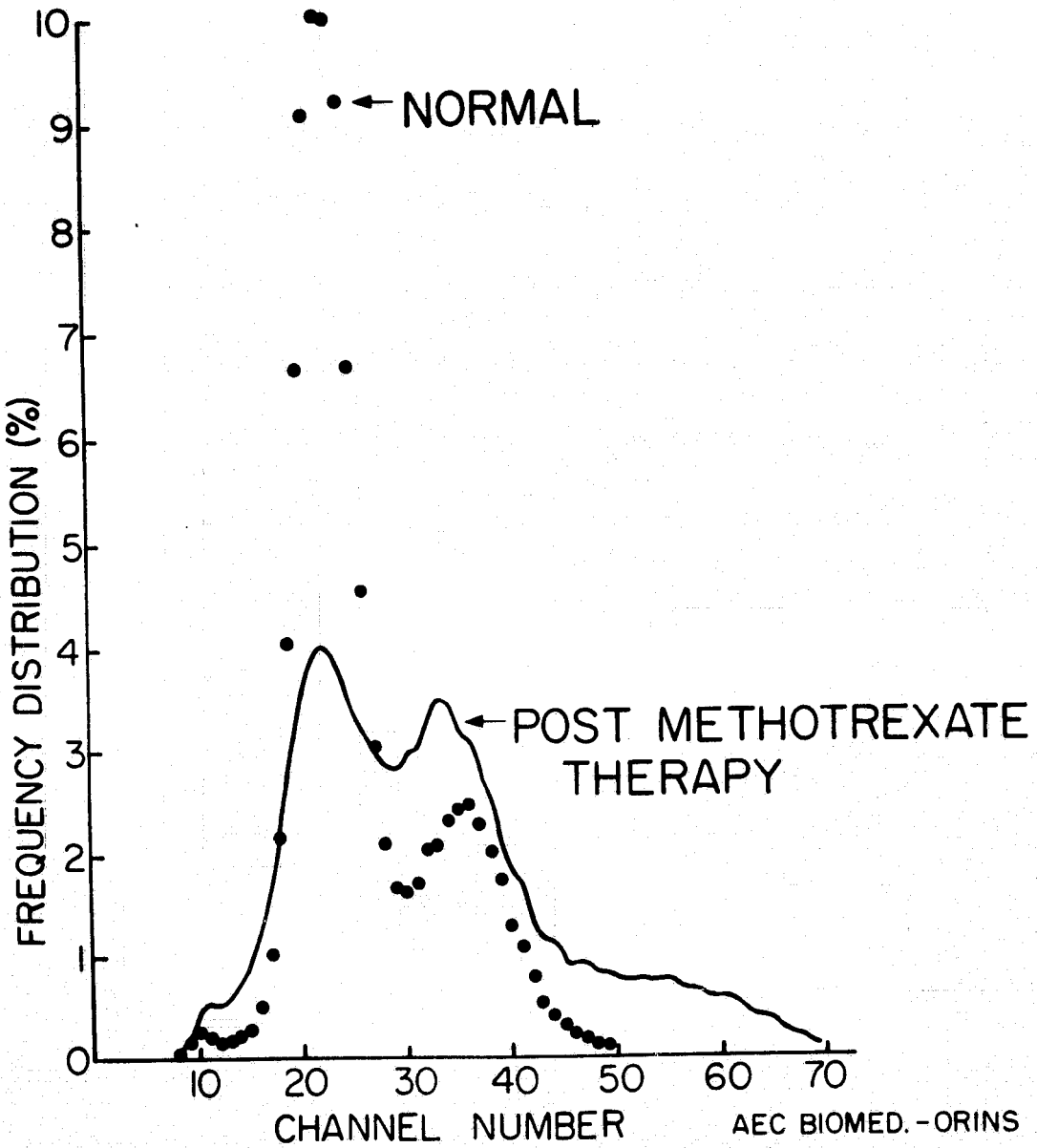
NORMAL
POST METHOTREXATE THERAPY
FREQUENCY DISTRIBUTION (%)
CHANNEL NUMBER
AEC BIOMED.-ORINS
0
1
2
3
4
5
6
7
8
9
10
10
20
30
40
50
60
70

Fig. 64

other methods of suppressing erythropoiesis was accomplished by the production of new RBC's of normal size. As these cells with a life expectancy of 120 days were delivered into the blood and old microcytic cells were removed, the initial abnormal sized RBC distribution changed progressively toward a normal one. Whether or not a completely normal size profile is obtained, however, depends on the duration of the period during which red cell production rate and iron stores are in balance; if iron deficiency is present (because of intestinal hemorrhage, for example) and goes untreated, iron stores are adequate for only a short time and production of microcytes soon begins and reverses the trend toward normal in the RBC size profile. In other blood dyscrasias with suppressed RBC production and iron stores normal or above, we found no abnormality in RBC size distribution and total body radiation exposures were not followed by change in RBC size.

In experimental radiation therapy and hematology, we used this technique to measure the macrocytosis of mice chronically irradiated at low dose rates where colonies of stem cells are formed in the spleen and abnormal hemoglobin is produced. The macrocytic shift in RBC size distribution correlates well, temporally, with splenic stem-cell colony proliferation and abnormal hemoglobin production but not with splenic stem-cell colony formation without proliferation. This finding suggests that when these colonies proliferate under stress they form macrocytes containing abnormal hemoglobins. This correlation allows electronic RBC sizing to be used for selecting irradiated mice for biochemical hemoglobin assay. Results of these studies on stem cell colony formation in irradiated mice will be discussed in considerable detail in Section D of this chapter.

Our electronic cell-sizing apparatus, appropriately set upper and lower analyzer gates, was also used to exclude agglutinated RBC masses from being counted in studies of the rate of replacement of an irradiated human recipient's own RBC by new RBC from transplanted bone marrow. Since the size distributions of the two RBC populations (donor versus recipient) differed, we could also follow the growth of the new RBC mass by obtaining sequential RBC size distribution studies. These seemed to correlate well with the findings of the in vitro hemagglutinin system, but were not as easily quantitated in percentages.

Studies on the nature of the well-defined two-peaked distribution of electronic pulses generated from normal blood when the electrical current is high (>1.0 but <3.0 microamps) helped justify our use of high currents in practice because it allowed us to differentiate RBC of two or more different model sizes easier than lower currents do. Sometimes we wished to compare the RBC of two persons with different MCV's by mixing a sample from each and comparing the two-peaked size distribution visually; the presence of two bloods in the sample was more clearly demonstrable with a high current than with a small one.

While there are numerous explanations for the presence or absence of two peaks dependent upon current, none have been shown experimentally to hold true under all the conditions of our measurements. Most explanations are based on physical theory and mathematical solutions rather than direct experimentation. The latest purports to show that the two peaks result from tumbling of some of the saucer-shaped red blood cells in the flow through the sensing volume of the aperture tube. We showed experimentally that this explanation is inadequate. When glutaraldehyde was buffered and in less than 2.5% concentration, it can fix RBC rapidly (within 15 min)

without microscopically detectable alteration in their size or shape. With 4% formalin in saline similar RBC fixation without distortion is obtained in 18 hours. We sized unfixed RBC suspensions and those fixed in these two solutions during periods in which all the variable parameters of the electronic sizing system were kept constant. By the time the RBC membrane became "fixed" the two-peaked distribution was not obtained even though the fixed RBC's were still disc shaped and just as capable of tumbling as unfixed cells. We believe that the two-peaked RBC size distribution results from alterations in the amount of intracellular fluid in the RBC caused by an effect of the electrical current on the ionic charges of the living, pliable RBC membrane that affects the sodium-ion water transfer pump. The single direct experiment that proved our explanation, however, continued to elude us. We attempted to gain more clues by using the well-known progressive chemical alterations that occur in blood-bank blood stored in acid citrate dextrose solution. Here the selective permeability of the RBC membrane decreases progressively and transport of substances across it depend finally only on Donnan state of equilibrium. The amount of intra-RBC sodium rises progressively over a 30-day period and mean corpuscular volume increases as the RBC swell. We obtained electronic RBC size distributions of blood from nine patients with PRV drawn into ACD at intervals over 30- to 70-day periods of storage at 40°F (Fig. 65). While the changes observed in cell volume were progressive, they were not linear with time, being slow at first and gradually becoming more rapid. These studies answered a practical question: How soon after a blood sample is drawn from a patient must the RBC sample be sized if in vitro changes are to be avoided? Sizes or distribution in the specimens did not change significantly during the first five days, but

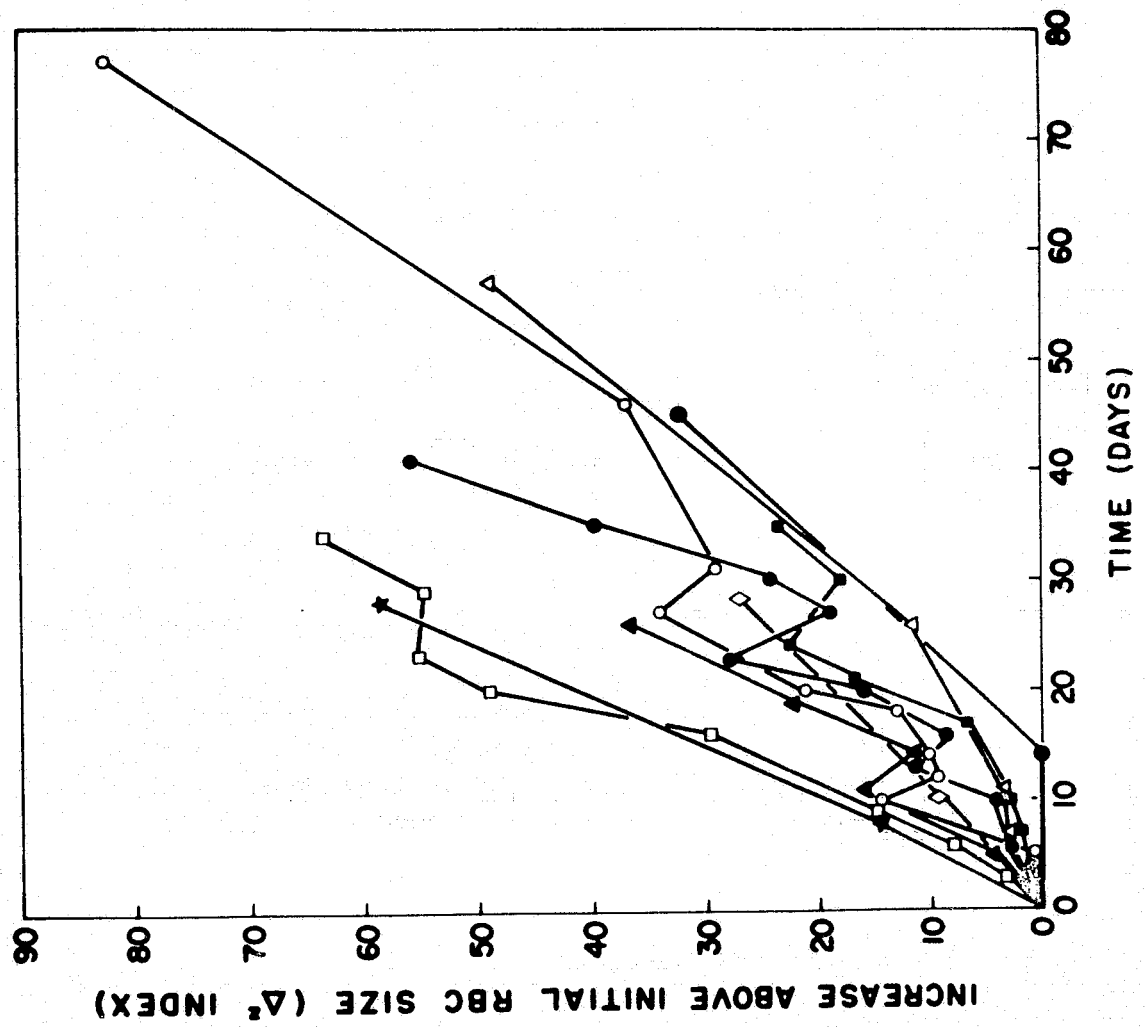
INCREASE ABOVE INITIAL RBC SIZE (Δ² INDEX)
TIME (DAYS)
0
10
20
30
40
50
60
70
80
90

Fig. 65

after that, all the RBC size distributions shifted progressively toward the right as the cells swelled. In Fig. 65 the squared difference index for the consecutively determined RBC size distributions of these bloods are shown. The index of zero can be assigned to each bottle of blood at the beginning of each experiment because the initial size distribution of each blood served as its own reference point for comparison with subsequent measurements of the same (aging) sample. On comparing the repeated frequency distribution histograms of these samples with the originals one sees that the higher peak comprised of the smaller cells in the initial RBC distribution became progressively lower, broader, and shifted further to the right (large size), finally merging with the original low, broad peak of large RBC. These changes logically fit our hypothesis: that passage through electrical current alters the cell membrane charge so that sodium and water leave the cell, making the cell shrink; that small cells with relatively little water and sodium show the greatest proportional shrinkage induced by electrical current while large cells swollen with water and comparatively rich in sodium are decreased least in relative size. Because passage time through the high density current in the aperture tube is constant, only a constant amount of sodium and water can be removed per passage. This is relatively faster and is a greater percentage of the total present initially in small dense cells. After blood bank storage RBC imbibe sodium and water when their ability to glycolyze fails in parallel with a fall in high energy phosphates; the amount imbibed is limited only by the cell membrane and all cells of the same individual swell toward this limit, hemolyzing when it is exceeded. Consequently, the RBC remaining in the bottle becomes more alike in sodium and water content and size; the proportional effect of the current upon

the cells decreases and the differentiation of the RBC size into two peaks of distribution becomes progressively poorer.

These studies suggested that electronic RBC sizing might be useful in studying the pliability of RBC membranes and their hemolytic fragility as well as variations in size of individuals in total RBC population variations. In addition it would seem feasible to use this system to rapidly detect undesirable changes in normal blood during blood bank storage. This might have an advantage over other methods because of its simplicity and the rapidity with which results can be interpreted.

B. Anti-proteolysis Radiation Effect and Dose Rate Dependence

Measurements to evaluate the effects of various therapeutic regimes generally rely excessively on quantitation of subjective symptoms. Commonly, such evaluations depend on a battery of chemical determinations and peripheral blood counts. The latter still reveals the most about how the hematologic patient is responding, for example, to total body irradiation. Their prognostic, as well as diagnostic value, is high but in many of the diseases we study and attempt to treat, the blood cell values are highly pathological and define the disease, but may obscure reaction to the disease or to concurrent infections. The pretreatment levels of specific cells in patients with the same disease, for example, chronic lymphocytic leukemia, also vary so much from patient to patient that therapeutically-induced responses are difficult to compare. It would be desirable to have additional reference measurements that would be normal in healthy people, but progressively abnormal as a person becomes ill and approaches death; the pathologic results in this measurement should subside toward normal when clinical management is successful or spontaneous recovery occurs. The study reported here was useful as an objective measure of cell substance in the blood with levels related to hematopoietic functions.

The importance of serum trypsin-inhibitor (TI) levels in health and disease is highly speculative. Numerous teleologic reports suggest that TI plays a role in promoting normal growth processes by limiting random, nonspecific proteolysis and that its most important role is in protecting the pancreas and the small intestine from undesirable tryptic autodigestion. Measurement of serum trypsin-inhibitor levels has been useful in clinical laboratory only in pancreatic disease where its correlation with clinical status has been established.

The results reported here were obtained by measuring TI levels using the serum and plasma of all persons who had some other measurement made on samples of their blood in the Medical Division laboratories. Experimental design was limited to that required for making the determinations. After all the measurements were completed, the sources of the serum samples were identified by disease and clinical condition and the results graphed in relation to calendar date. Those measurements from the same patient were connected by lines to see how the levels changes as the disease progressed or was arrested.

The amount of trypsin inhibitor was determined by measuring the amount of hydrolysis of α-N-Benzoyl-L-Arginine ethyl ester (BAEE) obtained under standard conditions by 0.653 units of trypsin with and without 10 microliters of serum present. The method was modified and adapted in our laboratory.

As shown in Fig. 66, normal persons and patients without serious disease, or without symptoms of a previously established malignant disease, had similar TI levels around the normal mean of 32.5 TI units/ml, ranging up to ∿45 units and down to ∿units. Patients hospitalized because of uncontrollable progression of such diseases as acute and chronic myelocytic

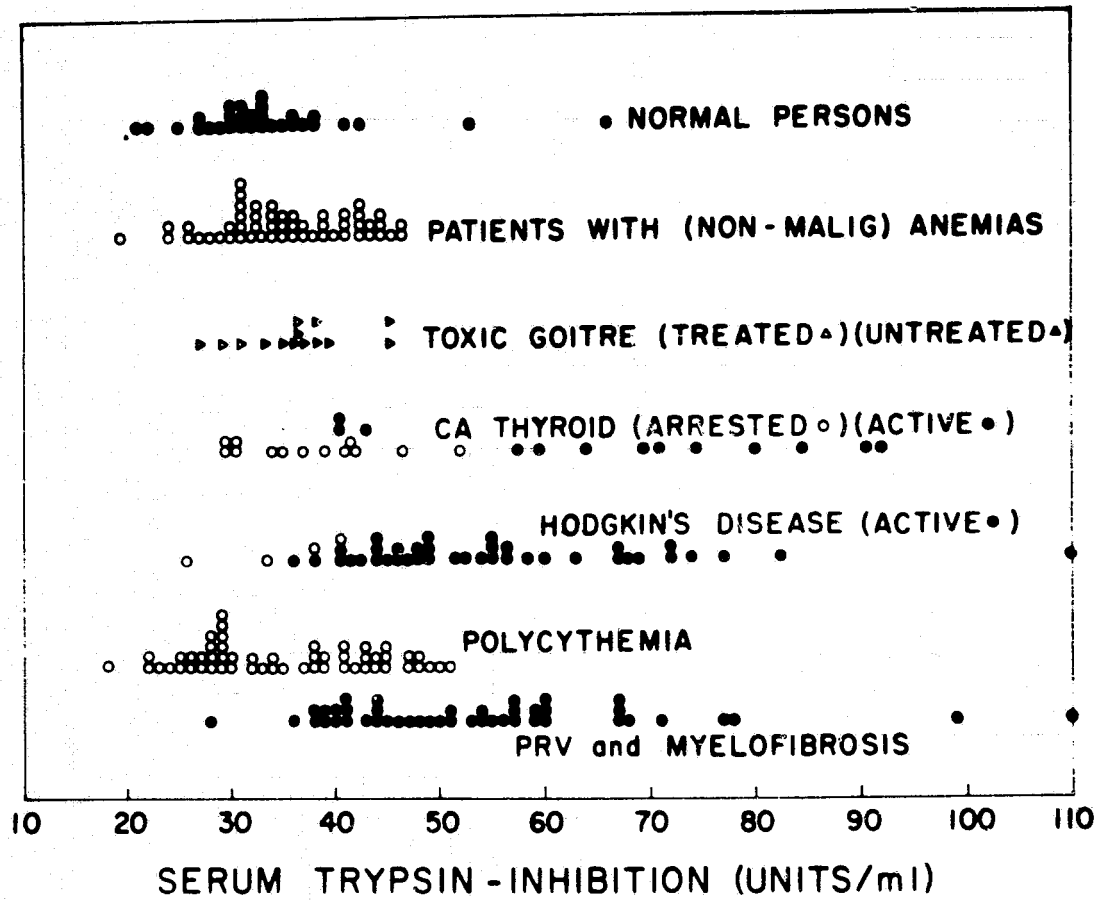
NORMAL PERSONS
PATIENTS WITH (NON-MALIG) ANEMIAS
TOXIC GOITRE (TREATED▲)(UNTREATED▲)
CA THYROID (ARRESTED○)(ACTIVE●)
HODGKIN'S DISEASE (ACTIVE●)
POLYCYTHEMIA
PRV and MYELOFIBROSIS
10
20
30
40
50
60
70
80
90
100
110
SERUM TRYPSIN-INHIBITION (UNITS/ml)

Fig. 66

and lymphocytic leukemia, myelomas, lymphomas, myelofibrosis, Hodgkin's disease, and carcinomas had levels commonly above 50 units, and those who died of their disease during this time had progressively rising levels occasionally in excess of 90 units (∿3 x average normal). Several persons with persistent values above 60 units have survived but have been difficult therapeutic problems. Two patients who died of vascular accidents associated with their malignant disease process or its therapy, were the only ones to succumb with approximately normal levels.

Metastatic spread of epithelial neoplasms has been reported to be accompanied by a progressively rising TI preceding death; an example is shown in Fig. 67.

We also saw this premortem rise in patients who died from Hodgkin's disease and myelofibrosis. However, such a rise is not always irreversible; a patient with malignant plasmocytoma, who had had moderately elevated TI levels for about two months, developed rapidly rising values paralleling a similar rapid increase in blood urea nitrogen (BUN) and oliguria. Intensive cytotoxic chemotherapy produced a return to normal TI values over a two-week period. The TI value remained normal during the rest of the study period of one month, during which the patient was relatively symptom free. Similar reductions of TI values have followed radiation and chemotherapy in other patients. It is not yet clear whether Prednisone has an effect on TI levels; it seems so far that corticosteroid therapy is accompanied by TI levels in the 50 to 60 unit range but this correlation has not been sufficiently studied. In chronic lymphcoytic leukemia (CLL) and polycythemia vera, when active disease was present but life was not immediately threatened, TI levels were often found to be much less than normal (20 down to 10 units).

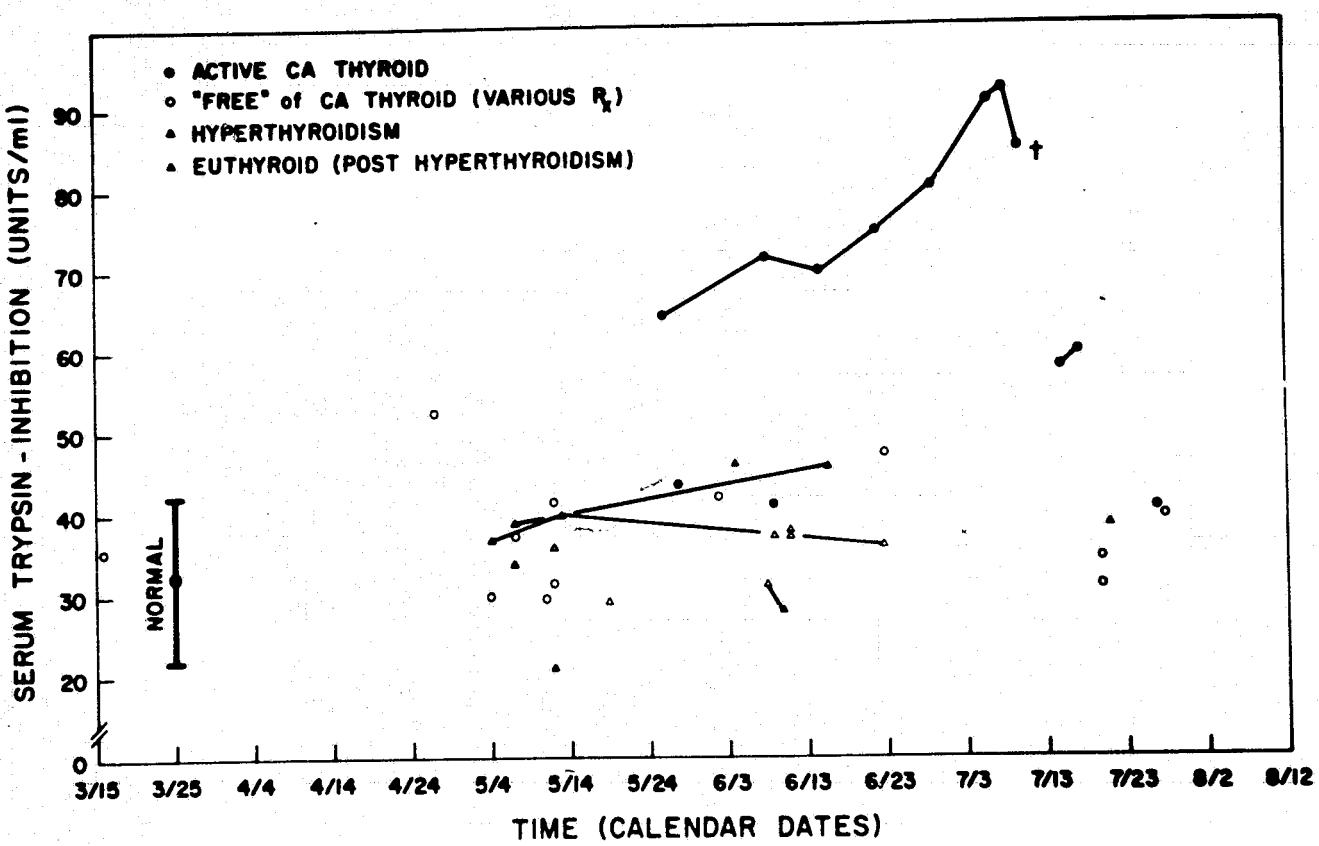
ACTIVE CA THYROID
"FREE" of CA THYROID (VARIOUS Rx)
HYPERTHYROIDISM
EUTHYROID (POST HYPERTHYROIDISM)
SERUM TRYPSIN - INHIBITION (UNITS/ml)
NORMAL
0
20
30
40
50
60
70
80
90
†
3/15
3/25
4/4
4/14
4/24
5/4
5/14
5/24
6/3
6/13
6/23
7/3
7/13
7/23
8/2
8/12
TIME (CALENDAR DATES)

Fig. 67

The clinical significance of this observation eludes us since the patients with CLL and acute leukemia who died during this observation period developed abnormally high TI levels shortly before death in spite of initially low base lines.

Later, the effect of total body irradiation on TI levels was studied in laboratory animals and in humans exposed to a wide dose range of therapeutic irradiations. Ten to 15-week-old BL/6 mice were exposed to ^{60}Co total-body irradiation at a rate of 40 R/min. Total exposures ranged from 250 R to 1000 R. Trypsin inhibitor determinations began at three hours postirradiation and were complete at 21 days postirradiation.

Mice given 250 R TBI had normal TI levels (1.84 µg/µl) through six hours postirradiation which gradually decreased to ∿68% of normal at 72 hr with no sign of recovery. The groups of mice receiving 500 R, 750 R, or 1000 R TBI all showed substantially lower TI capacity by three hours postirradiation, with the 750 R group having only 27% of normal at this earliest time. In all of these groups, the initial suppressed level was followed by fluxuations in the TI levels marked by recoveries to almost normal levels and further decreases to a minimum of 17% normal (750 R group). Neither amplitude nor rate of the changes in TI were dose-dependent, and we saw no real return to normal TI levels in these groups within our study period.

Finally, we measured TI levels in 10 patients who received 100-694 R TBI as partial therapy for CGL, CLL, or PRV. Fifteen normal persons had a mean TI capacity of 0.89 µg trypsin inhibited per µl plasma (S.D. = ± 0.11 µg/µl) ranging from 0.70 to 1.17 µg/µl. All of the diseased humans had TI levels above the upper limits of normals. With low level radiotherapy (1.5 R/hr) most patients demonstrated a rapid moderate depression and

recovery in TI levels, sometimes followed by a slight overshoot. Practically no change in TI capacity occurred during METBI (1.5 R/min) radiotherapy. The levels of TI after radiotherapy commonly correlated with the patient's overall hematological response, modified by secondary clinical developments. These data are graphically represented in Figs. 68 and 69.

During the course of multiple varied disease phases and concommitant therapeutic manipulations which these metastatically diseased patients received, their TI levels frequently changed apparently in response to many different stimuli. These included, in addition to irradiation, administration of drugs, blood, or plasma, decreased urinary output and electrolyte imbalance, changes in blood chemical levels, and presence of acute GVH disease. Our study of the relation of TI levels in malignant disease, and the effect of TBI, indicates that the level of this protein is increased with worsening of clinical status, is decreased with clinical improvement, is acutely increased during many infections, and is affected to a quite limited extent by exposures to gamma radiation levels described herein.

C. Effect of Irradiation on Serum Creatinine Phosphokinase Levels

Exposure to ionizing radiation, particularly total-body irradiation, results in a variety of in vitro biochemical changes dependent on dose and dose rate. Some familiar examples include circulating levels of serum iron, lactic acid dehydrogenase (LDH), and trypsin inhibitor (TI). Our efforts to find data to correlate biochemical/physiological changes with altered pulmonary impedance changes in irradiated patients led us to initiate clinical chemical determinations of serum creatine phosphokinase (SCPK) in control volunteers and patients. This particular enzyme (CPK) was chosen

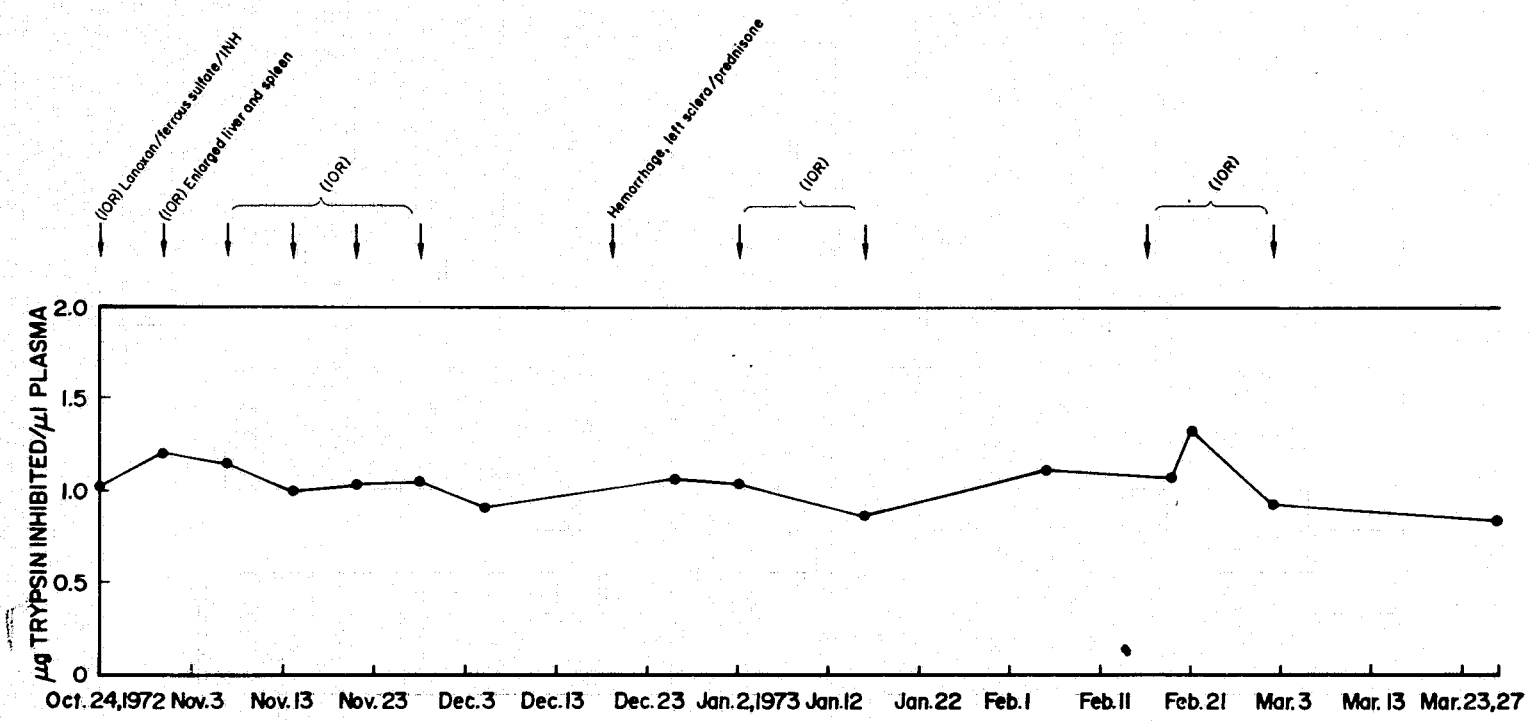
(10R) Lanoxan/ferrous sulfate/INH
(10R) Enlarged liver and spleen
(10R)
Hemorrhage, left sclera/prednisone
(10R)
(10R)
μg TRYPSIN INHIBITED/μl PLASMA
2.0
1.5
1.0
0.5
0
Oct. 24,1972
Nov. 3
Nov. 13
Nov. 23
Dec. 3
Dec. 13
Dec. 23
Jan. 2,1973
Jan. 12
Jan. 22
Feb. 1
Feb. 11
Feb. 21
Mar. 3
Mar. 13
Mar. 23,27

Fig. 68

COAP-Gut sterilization
Sore throat
Thorazine-atrial fibrillation-694R
Marrow transplantation
Macular erythema-methotrexate
Diarrhea-poor appetite-rash
Marrow hypocellular
CNS involvement-failing liver-fever-diarrhea
Dark purple erythema
Cough-cyanosis-anxiety-urine output decreased
Left lung-90% collapse
Liver enlarged-fever-diarrhea-hypothorax
Thoracentesis
4+ possible Coombs
Pulmonary congestion
μg TRYPSIN INHIBITED/μl PLASMA
2.0
1.5
1.0
0.5
0
Mar. 22
Apr. 1
Apr. 11
Apr. 21
May 1
May 11
May 21
May 31
June 10
June 20
June 30
July 10
July 20

Fig. 69

because of its relationship to muscle physiology, particularly its relationship with rapid production of ATP during increased physical activity.

Creatine phosphokinase (CPK) is responsible for the following reaction in muscular tissue:

creatine phosphate + adenosine dephosphate $\longleftrightarrow$ CPK

creatine + adenosine triphosphate

with ATP being the primary source of energy for the contraction process.

Our initial efforts to measure SCPK were directed to a radiation accident victim (previously mentioned) who received ∿260 rem (350 rem/min) cobalt irradiation. The SCPK levels on the day of the accident (day 0) and the following day were 25 mU/ml and within the normal expected range as determined by a UV (366 nm) assay method available through the Boehringer Mannheim Corporation, New York. Controlled exercise stress testing was initiated, following complete cessation of prodromal symptoms, three days postirradiation. On day 4, the SCPK level was 343 mU/ml and on day 5, 455 mU/ml, a 13.7 and 18.2 times increase, respectively when compared to preexercise values. Eight days postirradiation the SCPK levels returned to normal and remained within normal ranges throughout the remaining monitoring period as shown in Fig. 70. It is not clear from these results if the exercise stress testing on day 3 was responsible for the significant rise in SCPK or why the level suddenly dropped back to normal levels although exercise testing continued. However, when SCPK levels were elevated changes in pulmonary-impedance variance were minimal (see Chapter IV) even though the victim's tolerance to stress was minimal. Whether or not irradiation enhanced the response to exercise-induced hypoxia or caused a dumping of CPK into circulation remains obscure.

NORMAL = 0-50 (MU/ML)
CPK (MU/ML)
0
60
120
180
240
300
360
420
480
0
6
12
18
24
30
36
42
48
TIME (DAYS)

Fig. 70

Results of SCPK determination in the accident victim led us to begin measurement of CPK levels in irradiated patients exposed to a variety of exposures and exposure rates, normal volunteers, and irradiated laboratory animals (mice and Shetland ponies). The effect of exercise stress on SCPK levels was likewise evaluated.

All persons (patients and normal volunteers) demonstrated significant increases in serum creatine phosphokinase levels when subjected to controlled exercise stress and/or irradiation. Serum creatine phosphokinase levels (shown in Fig. 71) in normal volunteers exercising under submaximal stress conditions showed increases in this enzyme comparable to those for exercising men reported in recent literature (24). Generally, SCPK levels rose two to two-and-one-half times the preexercise levels and although they remained elevated throughout the four-week test period, they appeared to be returning to normal during the fourth week, possibly indicating an adaptation to the constant workload.

Next, serum creatine phosphokinase levels were determined in (1) irradiated patients who did not exercise and (2) patients who were similarly exposed and tested by controlled exercise. In nonexercising patients exposed to 100 R (30 R/day, 1.5 R/hr) significant increases in enzyme activity occurred during the exposure periods. The enzyme activity returned to normal within two weeks after exposure in all but one patient studied (Fig. 72). Similar changes in SCPK activity occurred in nonexercising patients exposed to 150 R in LETBI (Fig. 73). Only one of the patients exposed to 100 or 150 R failed to demonstrate the rise in SCPK levels. In nonexercising patients receiving fractionated exposures (10 R/day, LETBI) SCPK levels rose significantly in those receiving 150 R but not in one who received only 100 R (Fig. 74). This increase in SCPK activity was not evident until a

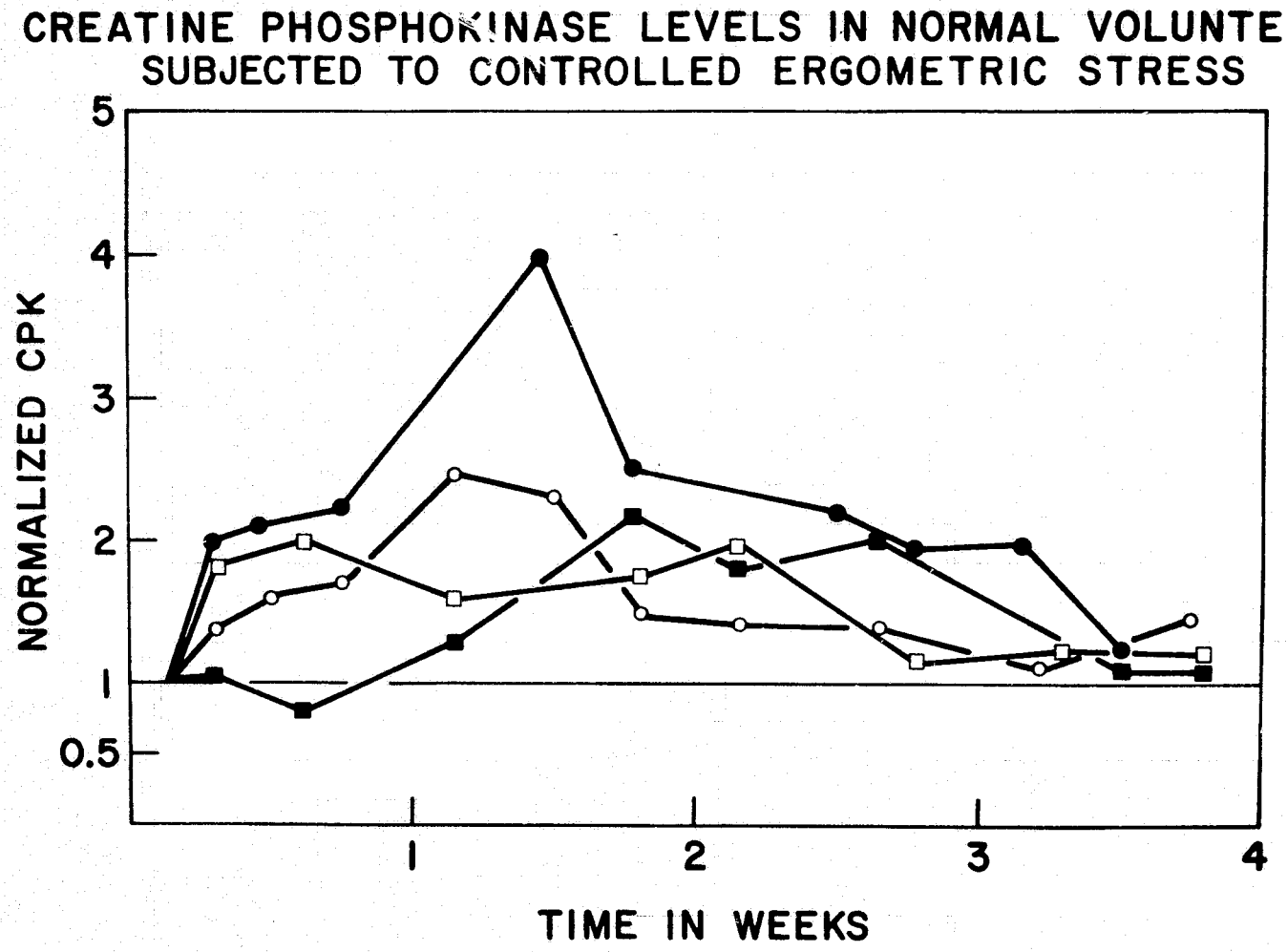
CREATINE PHOSPHOKINASE LEVELS IN NORMAL VOLUNTEERS
SUBJECTED TO CONTROLLED ERGOMETRIC STRESS
NORMALIZED CPK
5
4
3
2
1
0.5
1
2
3
4
TIME IN WEEKS

Fig. 71

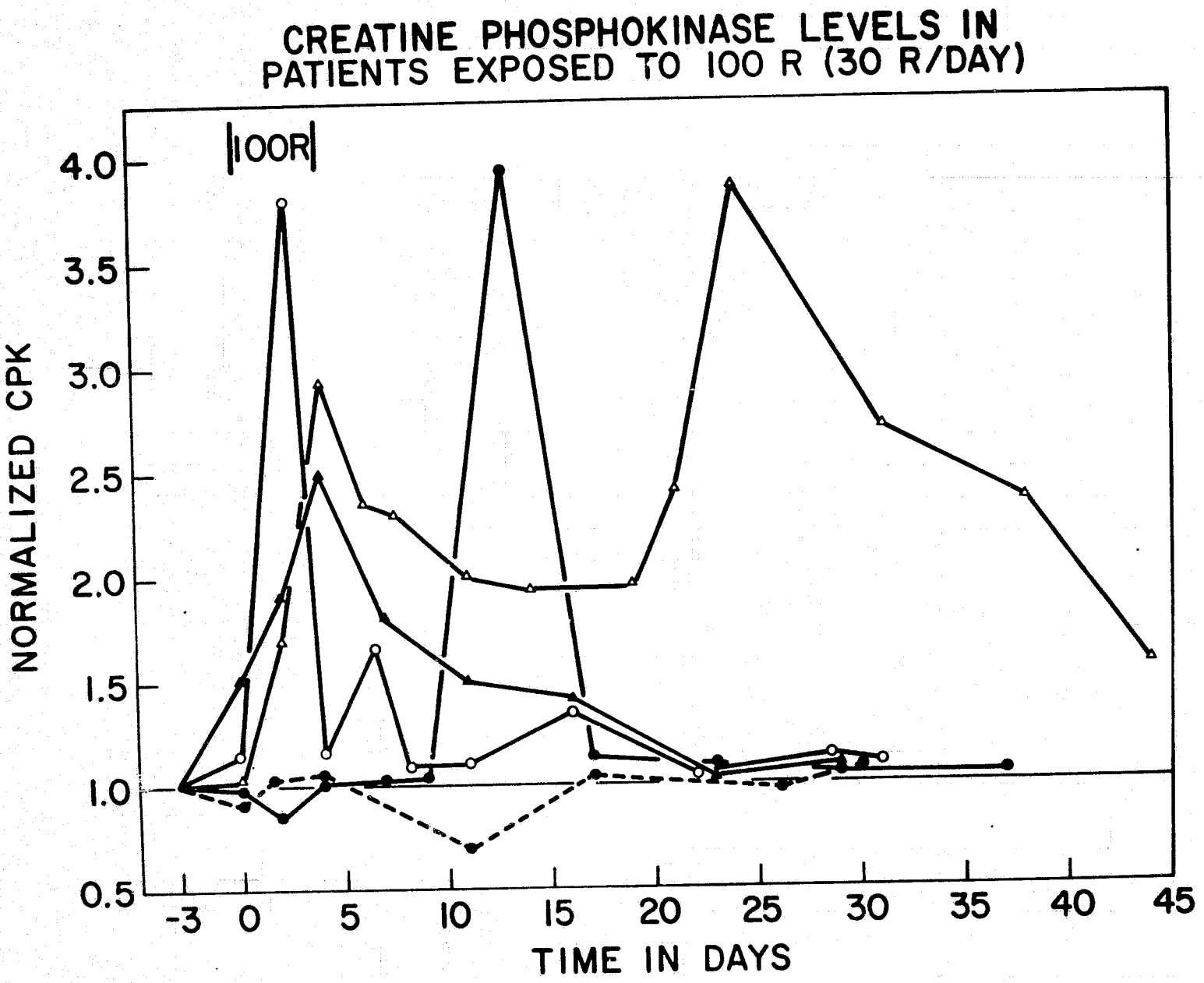
CREATINE PHOSPHOKINASE LEVELS IN
PATIENTS EXPOSED TO 100 R (30 R/DAY)
100R
NORMALIZED CPK
4.0
3.5
3.0
2.5
2.0
1.5
1.0
0.5
-3
0
5
10
15
20
25
30
35
40
45
TIME IN DAYS

Fig. 72

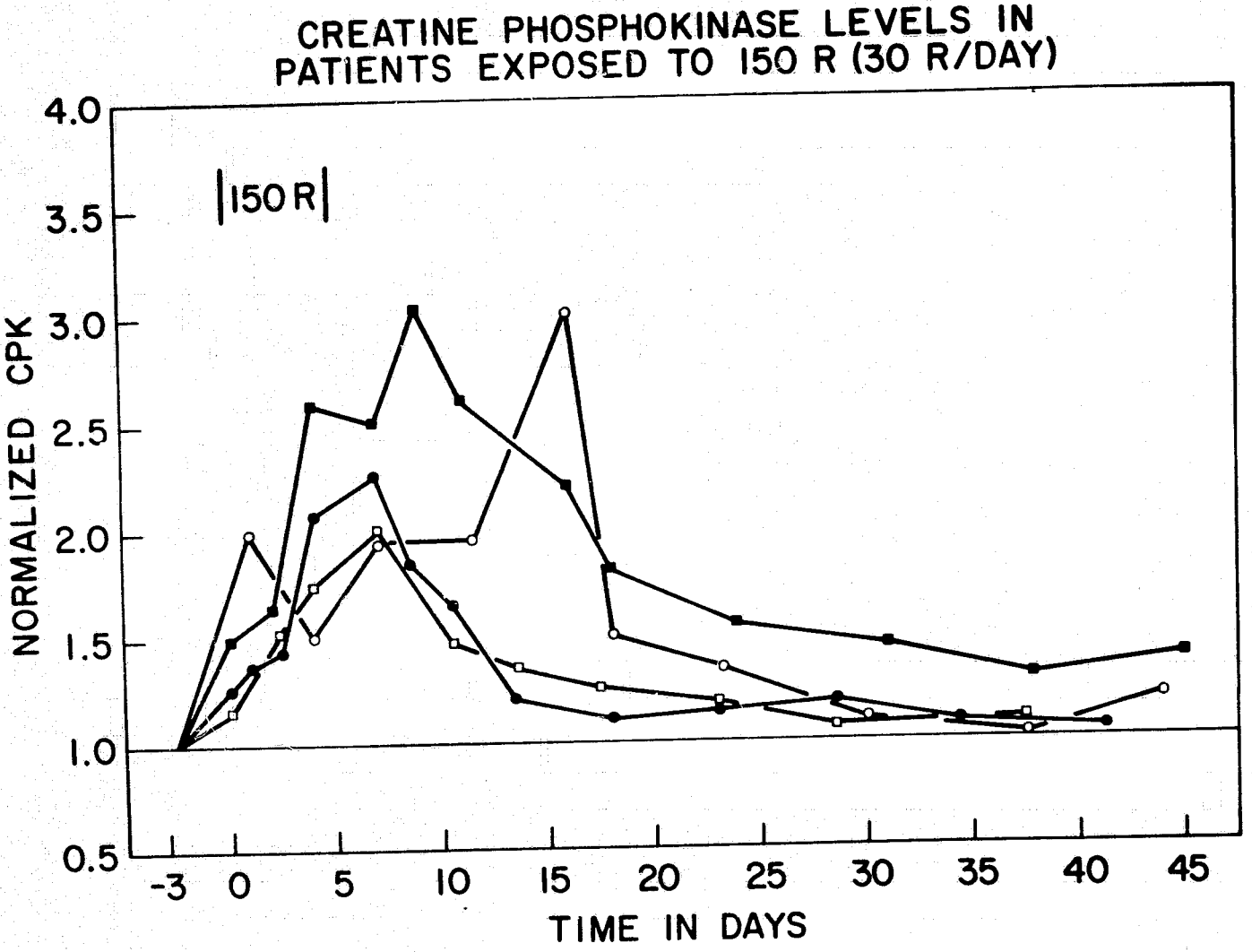
CREATINE PHOSPHOKINASE LEVELS IN
PATIENTS EXPOSED TO 150 R (30 R/DAY)
150 R
NORMALIZED CPK
4.0
3.5
3.0
2.5
2.0
1.5
1.0
0.5
-3
0
5
10
15
20
25
30
35
40
45
TIME IN DAYS

Fig. 73

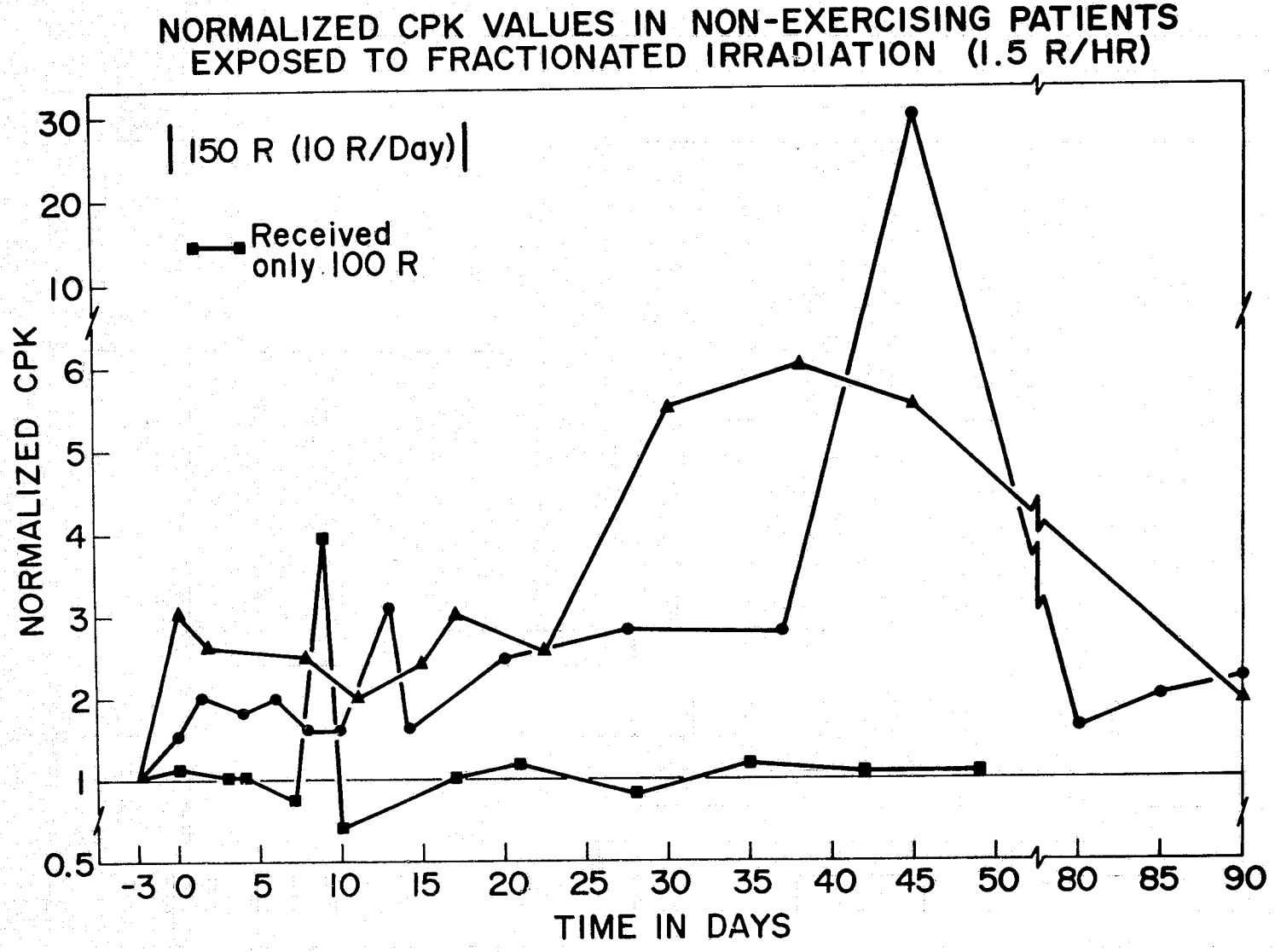
NORMALIZED CPK VALUES IN NON-EXERCISING PATIENTS
EXPOSED TO FRACTIONATED IRRADIATION (1.5 R/HR)
150 R (10 R/Day)
Received
only 100 R
NORMALIZED CPK
30
20
10
6
5
4
3
2
1
0.5
-3
0
5
10
15
20
25
30
35
40
45
50
80
85
90
TIME IN DAYS

Fig. 74

few days (<1 week) after irradiation and was much higher than in patients with similar but protracted exposures. A similar disparity between fractionated and protracted therapy and their affect on SCPK (Fig. 75) was noted in a patient who received both therapeutic protocols (6 months apart). Therapeutic exposures of 250 R and 792 R (Figs. 76 and 77, respectively) likewise resulted in elevated SCPK levels but not to any greater extent than did lower exposures. Exposures of mice ($C3BF_1$) to 450 R (3.36 R/min) resulted in SCPK levels (Fig. 78) similar to those seen in irradiated humans as did protracted exposures of 30 R/day (total exposure of 270 R) in exercising Shetland ponies (see Table 16).

Efforts to correlate SCPK levels with periods of diminished exercise capacity (DEC) in humans was possible in only one therapy patient, other than the radiation accident victim, and revealed that DEC was not evident when CPK levels were elevated (Fig. 79).

Our limited data on changes in SCPK levels suggest that some relationship exists between exercise response and energy output levels that are creatine-phosphokinase dependent. It is not yet clear which is cause and effect. For example, in one patient DEC, during fractionated (10 R/day) irradiation therapy, was followed by a significant increase in SCPK and then by recovery from radiation-induced fatiguability (Fig. 79). We feel that the increase in circulating SCPK level may be a systemic response to stress that feeds back to prevent or delay fatiguability, but further studies will be required before any such role can be substantiated.

These CPK studies reinforce our opinion that an irradiated patient does not respond to controlled exercise in the same way that normal unirradiated man does. The differences noted in irradiated patients could be

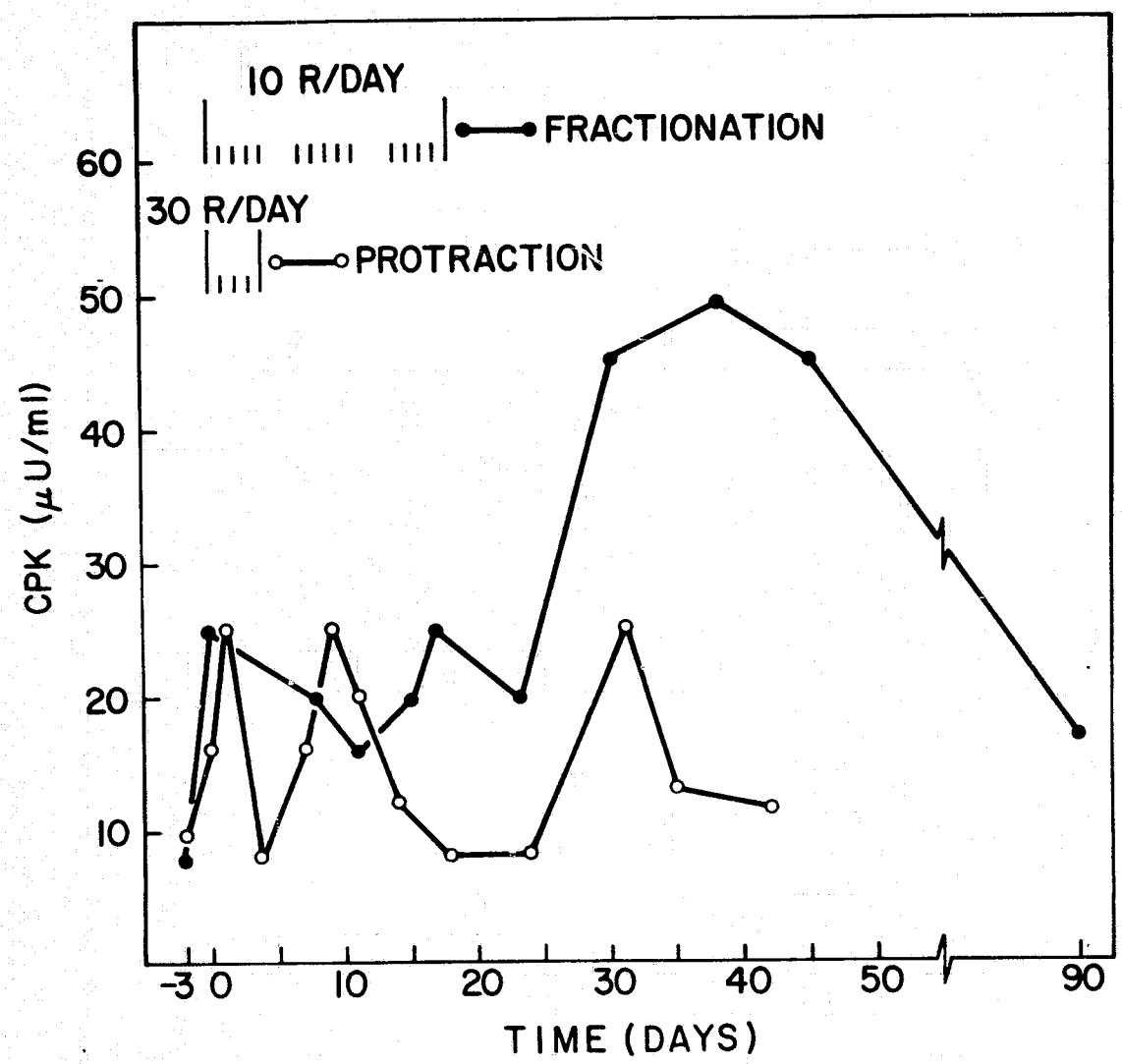
10 R/DAY
FRACTIONATION
30 R/DAY
PROTRACTION
CPK (μU/ml)
60
50
40
30
20
10
-3
0
10
20
30
40
50
90
TIME (DAYS)

Fig. 75

NORMALIZED CPK VALUES IN A PATIENT EXPOSED TO 250R TOTAL-BODY IRRADIATION (1.5R/HR)

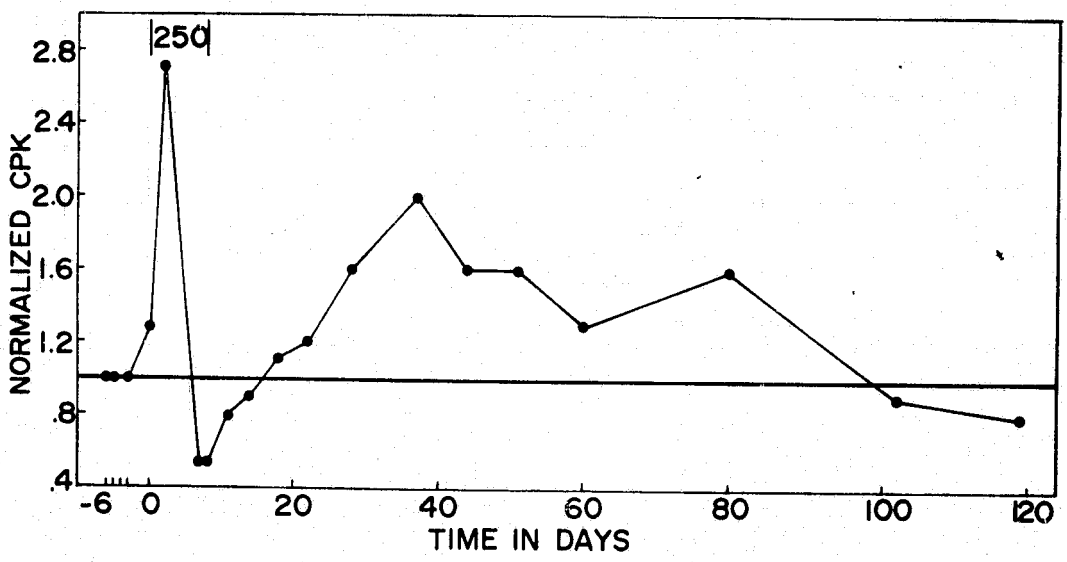

Fig. 76

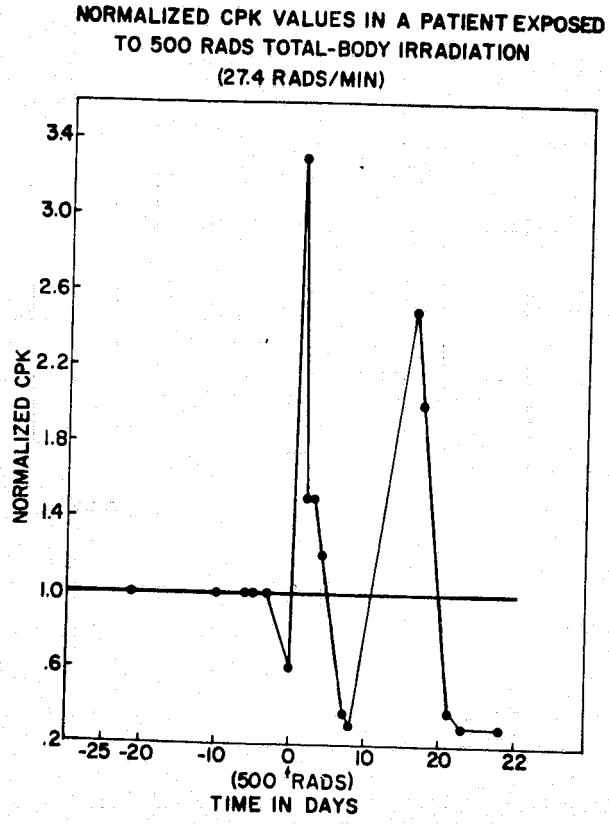
NORMALIZED CPK VALUES IN A PATIENT EXPOSED
TO 500 RADS TOTAL-BODY IRRADIATION
(27.4 RADS/MIN)
NORMALIZED CPK
3.4
3.0
2.6
2.2
1.8
1.4
1.0
.6
.2
-25 -20 -10 0 10 20 22
(500 RADS)
TIME IN DAYS

Fig. 77

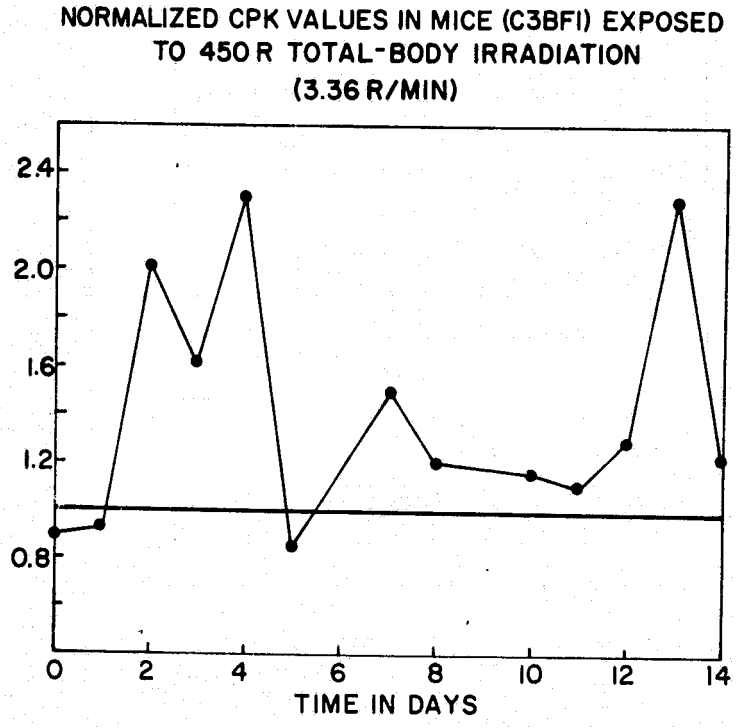
NORMALIZED CPK VALUES IN MICE (C3BFI) EXPOSED
TO 450 R TOTAL-BODY IRRADIATION
(3.36 R/MIN)
2.4
2.0
1.6
1.2
0.8
0
2
4
6
8
10
12
14
TIME IN DAYS

Fig. 78

TABLE 16

CREATINE PHOSPHOKINASE (CPK) LEVELS IN PONIES
EXPOSED TO 270 R TOTAL-BODY GAMMA IRRADIATION

↓ < 1/2 previous weeks level
→ steady state
↑ > 2 X previous weeks level

270 R ↓

0 + 0 *1-Preconditioning	→	→	↑	↓	→	↑	→	↑	→	→	↓	→		
1-No Conditioning					↓	↑	↓	→	→	→	→	↑	→	↓
650 + 0 1-Preconditioning	→	→	→	→	→	↑	→	↓	↑	↓	→	→		
1-No Conditioning					→	↑	→	↓	↑	↑	→	→	↓	↓
0 + 270 2-Preconditioning	↓	→	→	↑	↓	↑	→	→	→	→	→	→		
2-No Conditioning					↓	↑	↑	↓	↑	↓	→	↑	↑	→
650 + 270 2-Preconditioning	→	↑	↑	↓	↓	↑	↓	→	↑	↓	→	→		
2-No Conditioning					↑	↑	↓	→	↓	→	↑	↑	↑	↓
	1	2	3	4	5	6	7	8	9	10	11	12	13	14

TIME IN WEEKS

*Number of animals in each respective treatment.

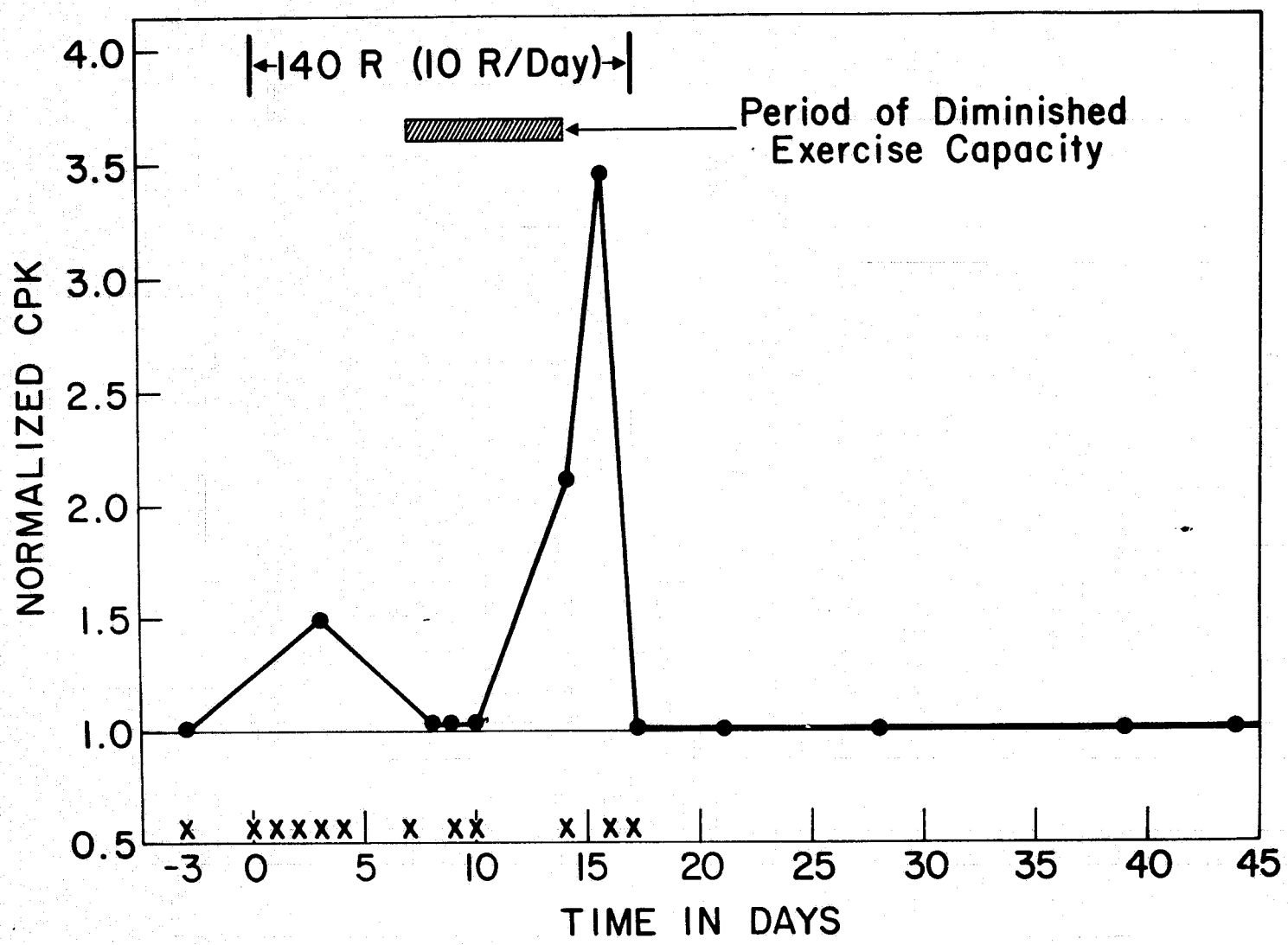
140 R (10 R/Day)
Period of Diminished Exercise Capacity
NORMALIZED CPK
4.0
3.5
3.0
2.5
2.0
1.5
1.0
0.5
-3
0
5
10
15
20
25
30
35
40
45
TIME IN DAYS

Fig. 79

due to their disease state but this seems highly unlikely since (1) none of the patients studied were acutely ill and (2) the patients tended to demonstrate degrees of DEC proportional to their irradiation exposure.

D. Low-Dose-Rate Radiation Lethality Syndrome - Human Extrapolations

Many models for lethality due to radiation exposure exist for man. While these models are quite variable with regard to LD_{50} estimations, we anticipated that our studies in humans exposed to therapeutic irradiations would add to the existing data base. This data base has generally been constructed from lower animal extrapolations based upon damage to the gastrointestinal (GI) tract and the bone marrow.

In parallel to our studies in man, we made experimental studies in mice to determine the accumulation rates of gastrointestinal and marrow damage when we used the discontinuous METBI fractionated daily exposures and the continuous LETBI exposures. Mice were used because of the approximately equal dosage to marrow and all parts of the gut from the same exposure field whose strength was easily determined by thermoluminescent dosimetry. Multiple cellular replicating systems were studied in them simultaneously to see whether the length of the radiation-free interval would allow their more rapidly repairing systems to negate the greater damaging effect of the higher dose rate. The same daily dose level was studied with C57 and Blk 6 Cum mice irradiated continuously at 0.8, 1.6, and 3.2 R/hr in LETBI and others pair-irradiated with identical doses per day delivered at about 4.0 R/min. Multiple criteria for determining GI and bone marrow repair levels were used: intestinal crypt mitotic index, intestinal weight, histopathology of necropsy sections, peripheral blood-cell counts and morphology, splenic weight, formation of endogenous erythroblast colonies in the spleen,

^{3}H-thymidine incorporation in replicating cells and testicular weight. These data were correlated with changes in total body weight and after-survival times in relation to accumulated dose. Two ages of mice were used: 50-day-old (radiosensitive) mice, and 120-day-old (radioresistant) mice.

Our findings did not support our initial thesis that the mouse would withstand the fractionated high-dose-rate daily exposures better than the continuous low-dose-rate ones. The germinal epithelium of the mouse testis and the white blood cell levels proved too radiosensitive to show any evidence of repair in either system of exposure at the dose rates used. Changes in intestinal length, weight, and crypt mitoses, on the other hand, seemed to indicate equal levels of good repair. Significant differences in response were found in changes in total body weight (Fig. 80), RBC indices and size distribution, spleen weight (Fig. 81), and numbers of endogenous erythroblast colonies, and in mean-after-survival times. At a dose (35 R/day) that was half that critical for the adult (70 R/day) the young mice showed these responses to a pronounced extent.

Obviously, more data was needed for the lowest exposure groups, while data from the other two exposure levels show that almost all deaths were due to erythroblastic failure to replenish RBC lost through senescence. As anemia developed, progressive loss in total body weight occurred. Splenic size increased and then decreased as endogenous splenic erythroblastic clones arose and disappeared. Red blood cell sizing showed that these abortive splenic colonies were correlated in time with the appearance of macrocytic red cells that approached mouse fetal RBC in size. No deaths due to infection were found even though all mice had severe leukopenia and thrombocytopenia at all these expose levels and patterns. In addition,

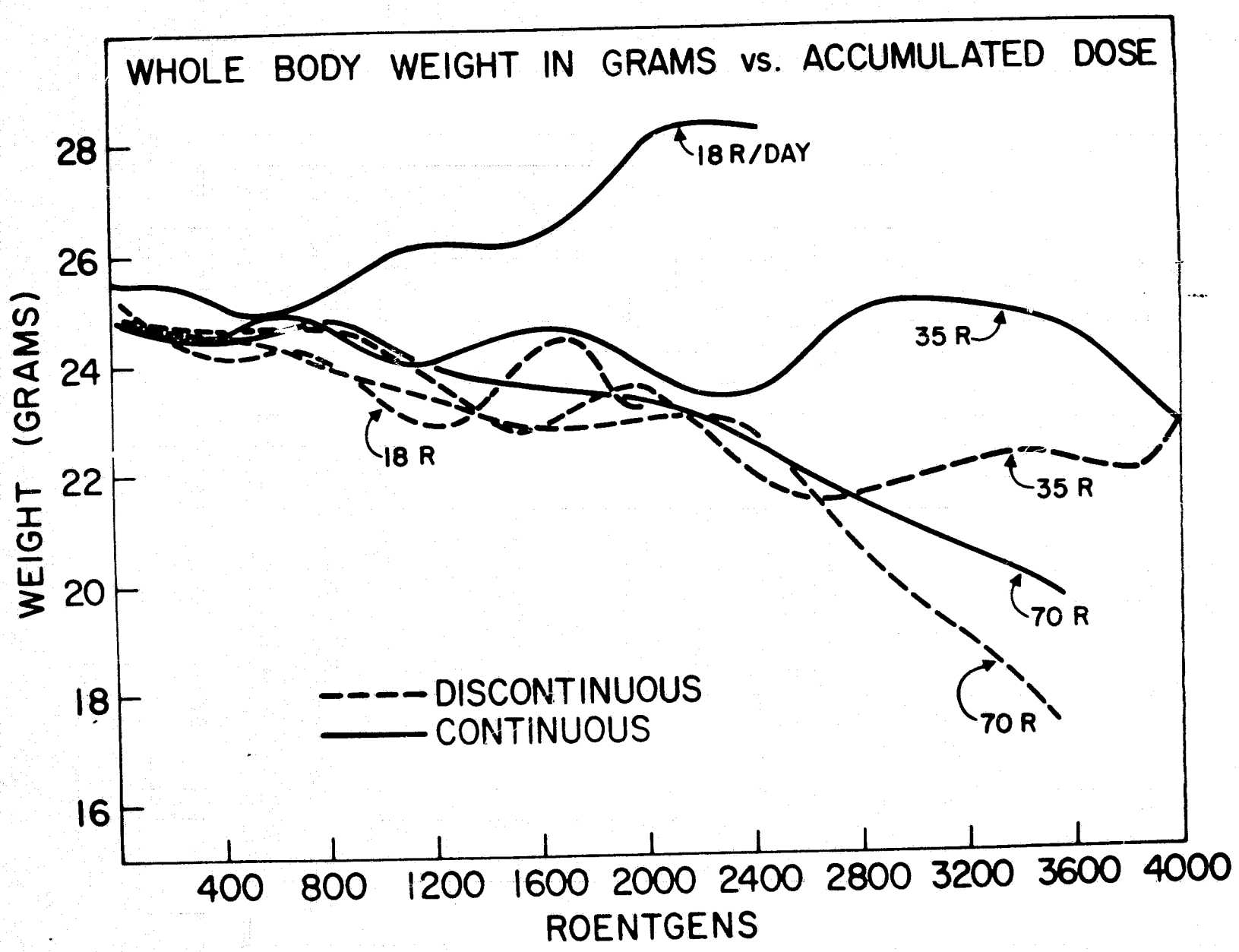
WHOLE BODY WEIGHT IN GRAMS vs. ACCUMULATED DOSE
WEIGHT (GRAMS)
28
26
24
22
20
18
16
18 R/DAY
35 R
18 R
35 R
70 R
70 R
DISCONTINUOUS
CONTINUOUS
400
800
1200
1600
2000
2400
2800
3200
3600
4000
ROENTGENS

Fig. 80

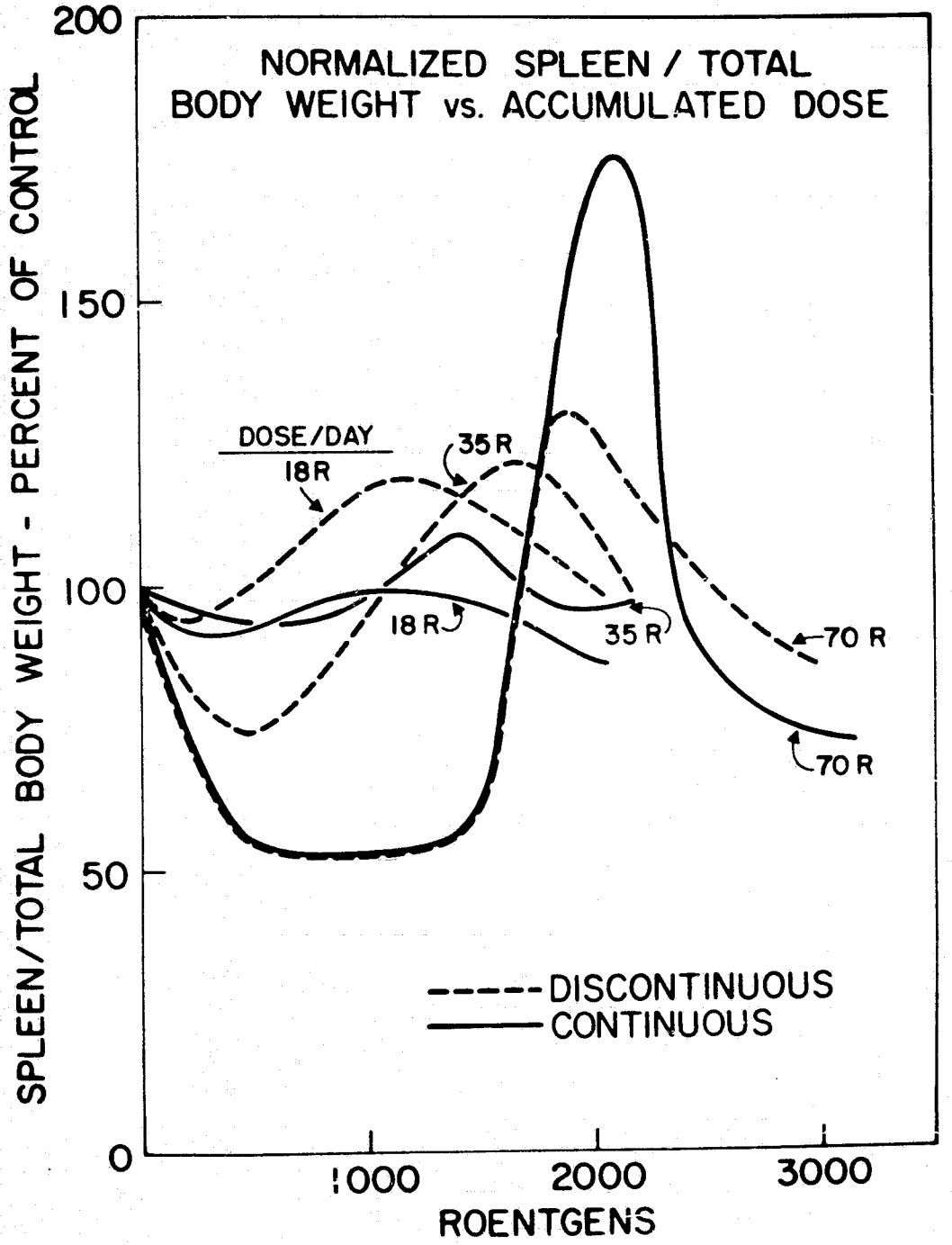
NORMALIZED SPLEEN / TOTAL
BODY WEIGHT vs. ACCUMULATED DOSE
SPLEEN/TOTAL BODY WEIGHT - PERCENT OF CONTROL
200
150
100
50
0
1000
2000
3000
ROENTGENS
DOSE/DAY
18R
35R
18R
35R
70R
70R
DISCONTINUOUS
CONTINUOUS

Fig. 81

none had granulocytic myelopoietic hyperplasia as a measurable reparative response.

All signs of reparative responses and failures in these systems just described occurred at lower accumulated doses and elapsed times in the mice exposed to 35 and 70 R/day discontinuously at 4.0 R/min than in mice exposed to the same daily dose continuous at 1.5 R/hr.

The results of these early experiments seem to show that in the mouse, as well as in man, discontinuous radiation exposures at high dose rates are more deleterious than the same daily dose given continuously at a low dose rate. Since no differences are seen qualitatively in the repairing systems, it would seen that the lower continuous exposure causes less cellular damage by providing time between "hits" for intracellular repair to occur before the second hit. As a result, less lethal cellular damage results and less replication by surviving cells was demanded in the critical cellular system.

Our observations on changes in body weight suggested that the higher radiosensitivity of the young animal may be due to greater somatic growth demands for protein synthesis in addition to that of its smaller, still developing, stem-cell population as previously demonstrated by Yuhas and Storer. Such demands would be a drain on its smaller stem-cell pool while, conversely, adequate reparative cellular replication would retard muturation of other systems.

Next, we extended these observations to studying the onset time of splenic colony formation, the number and size of colonies found, and the corresponding changes in splenic weight.

C57 black 6/cum male mice were placed in irradiation groups under two regimens: (1) mice were irradiated continuously (20 to 24 hrs/day) at three

rates of exposure (0.8, 1.6, and 3.2 R/hr) and received 16-19, 32-38, or 64-77 R/day; (2) other mice were pair-irradiated at 3.6 R/min, daily receiving the three same total exposures per day. Animals were killed when they had assumulated specific doses. Spleens were weighed, fixed in Bouin's fixative, and colonies counted. Although it is usual procedure to ignore the small colonies all were counted. Small ones are difficult to count and their quantitation is less dependable than that of those greater than 1 mm in diameter but their appearance time is biologically significant.

In Fig. 82 these results are shown as spleen weight, time of spleen colony appearance (S), and time of large colony development (L) in relation to accumulated exposure in R. In mice exposed at 18 R/day, spleen weight decreased initially about 25% and then remained constant until approximately 2200 R had accumulated. Then spleen weight began increasing in mice exposed in both the continuous and discontinuous modes. Although the rate of increase in spleen weight was greater in continuously irradiated mice, formation of discrete colonies was not observed in them, but was seen at this time only in the discontinuously irradiated mice (2200 R).

At 35 R/day (the approximate human therapeutic exposure rate in LETBI) mice exposed in the continuous mode respond to an accumulated dose of 700 R with a 30% decrease in spleen size and with initiation of colony formation. Those exposed discontinuously respond dramatically to the same accumulated exposure as exhibitied by reduced spleen weight (50% of normal) and by the initiation of spleen colony formation. With both modes of irradiation at this daily rate, as well as at 70 R/day, increase in spleen weight was related to colony proliferation (L), not colony formation (S). Colony formation was begun during or immediately following the time of minimum spleen weight; maximum proliferation corresponded to greatest spleen weight.

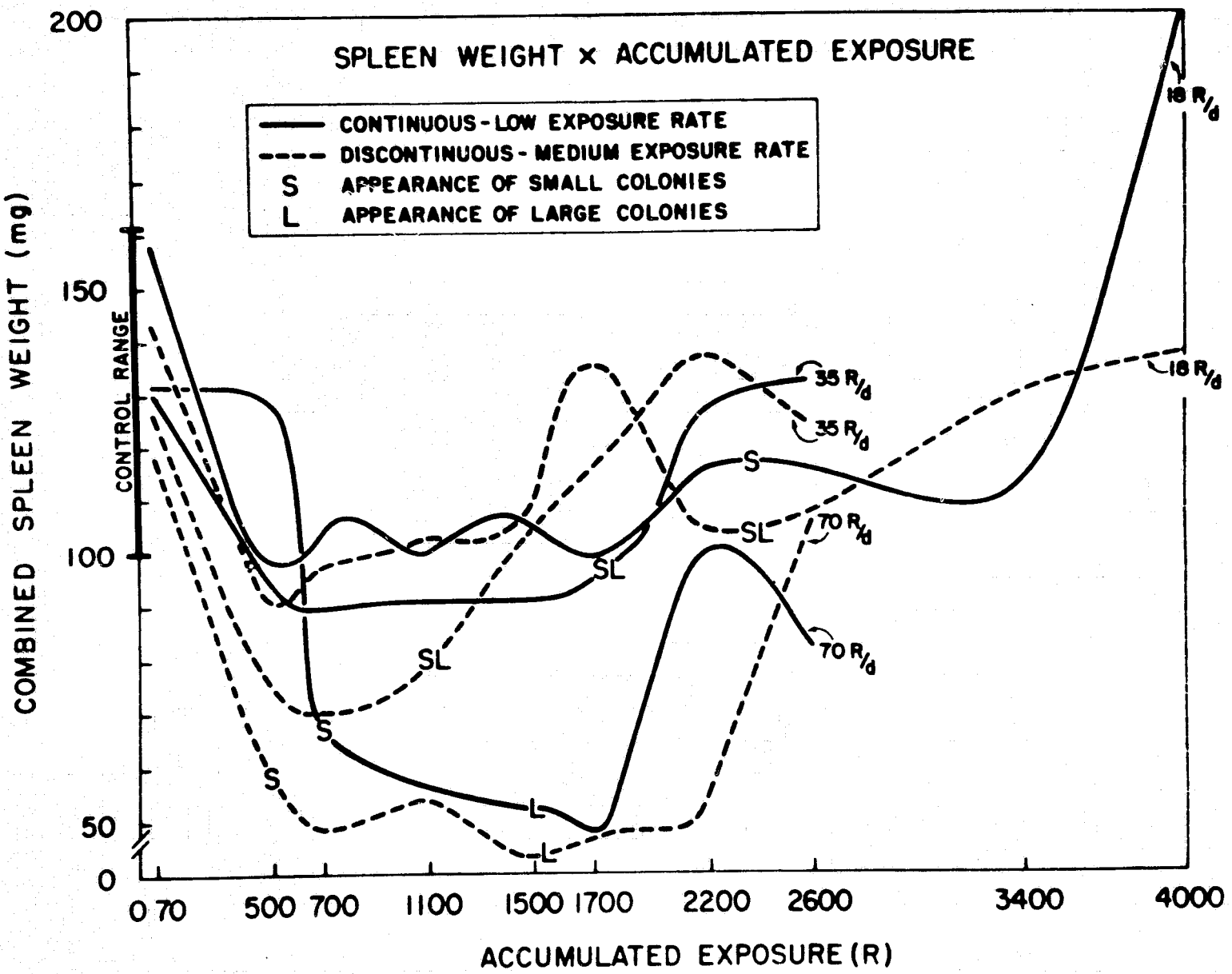
SPLEEN WEIGHT x ACCUMULATED EXPOSURE
CONTINUOUS - LOW EXPOSURE RATE
DISCONTINUOUS - MEDIUM EXPOSURE RATE
S APPEARANCE OF SMALL COLONIES
L APPEARANCE OF LARGE COLONIES
COMBINED SPLEEN WEIGHT (mg)
CONTROL RANGE
200
150
100
50
0
0 70
500 700
1100
1500 1700
2200
2600
3400
4000
ACCUMULATED EXPOSURE (R)
18 R/d
18 R/d
35 R/d
35 R/d
70 R/d
70 R/d
S
SL
SL
SL
S
S
L
L

Fig. 82

Spleen weight in 70 R/day mice never achieved the maximum values observed in the two lower exposure rate groups. Only at this highest exposure rate, however, did colonies become sufficiently large and numerous (up to 40/spleen estimated) to become confluent over the surface of the spleen. Mice exposed to 35 R/day in the discontinuous mode were the only other group that approached this degree of proliferation of spleen colonies.

We interpreted these results in terms of radiation damage and recovery to mean that: at 18 R/day, the rate of damage induction is depreciated by cellular repair mechanisms so that accumulated R "overestimates" residual damage. The level of accumulated residual damage does not induce formation and proliferation of splenic colonies until 2200 R or more have accumulated. Since this "turn on" occurs only in mice irradiated discontinuously, and since the delayed peak in spleen weight is greater in the continuously exposed mice, we assumed that residual damage has outweighed repair in the discontinuously exposed mice while in the continuous regimen repair had maintained at least an advantage over damage and may have even been producing a state of "over compensation."

At 35 R/day the rate of damage induction apparently exceeded reparability early (1100 R) and formation and proliferation of splenic colonies was a vigorous response to systemic demands for blood cell formation, a response which produces an abortive splenomegaly and macrocytosis of the RBC and which temporarily delays the onset of a lethal anemia.

At 70 R/day the reparative processes are quickly overwhelmed and damage accumulates sufficiently to elicit formation of spleen colonies almost at once (500 R) but their proliferation, as shown by the appearance of large colonies, is suppressed until 1500 R have accumulated. At this

level the 70 R/day mice began to exhibit the severe radiation-induced anemia which eventually was the main cause of death.

These results suggested that at low dose rates the physiologic level of hematopoietic damage depends upon dose rate and not dose, that recovery from such radiation damage was triggered by the rate at which residual or unrepaired damage was accumulated, and that endogenous stem-cell proliferation was also highly dose-rate dependent. Our findings concerning spleen colony formation and proliferation confirmed previous observations in which we compared the response of mice to continuous and discontinuous radiation using survival, splenic weight, and total body weight as endpoints. Mice in the discontinuous mode receive the radiation over a short period of time at a medium-exposure rate (3.6 R/min) and have a long radiation-free period during the day, while the mice in the continuous mode were exposed at a low-exposure rate and had a short or no radiation-free interval. Spleen colony formation and proliferation in mice irradiated in these two modes at 18 R, 35 R, and 70 R/day demonstrated that dose-rate effects predominate regardless of the length of radiation-free periods. Discontinuously irradiated mice exhibit damage earlier (spleen colony formation) and repair later (colony proliferation) than the continuously irradiated.

Thus, our data suggests the fact that because the rodent spleen has a tremendous capacity to increase its hematopoietic cell output, its role in the survival of mice and rats irradiated acutely (single large exposures) has been extensively studied. Although it was thought that removal of the spleen would hinder recovery of the blood-forming system, several investigators have shown that splenectomy not only does not reduce the acute $LD_{50/30}$ of rodents, but in some studies has been radioprotective. This is apparently due to the removal of the source of a splenic factor that inhibits

bone marrow mitotic activity necessary for recovery.

The importance of the spleen to survival of exposures to continuous irradiation has not been previously determined in mice. Several studies have been made elsewhere on adult rats given 50 to 85 R/day continuously up to total exposures of 4000 R. As in our mice, intact irradiated rats develop a massive splenic erythroid hyperplasia and marrow cellularity becomes progressively reduced. Because the postirradiation hematopoietic recovery patterns of intact and splenectomized rats are similar, the role of the spleen in tolerance to prolonged continuous irradiation was not definable. In another similar rat study, a difference was found in the recovery patterns of the mononuclears and platelets. The platelets response seemed to be improved by splenectomy and resulted in a greater mean-after-survival time when irradiation was at 84 rads/day. This increased survival was attributed to enhanced maintenance of the platelet counts in the splenectomized rats.

In our studies on the survival mechanisms of C57BL/6 male mice under continuous irradiation, sufficient numbers of splenectomized mice were irradiated at 0.8 R/hr, 1.6 R/hr, and 3.2 R/hr for statistically significant results. Daily exposures were 18.5, 37.0, and 70.0 R/day, respectively. Splenectomies were performed when the mice were ∿120 days old and irradiation started 30 days after surgery. In addition to mortality experiments where all animals are exposed until death, serial-sacrifice studies were performed on mice irradiated at 1.6 and 3.2 R/hr. These studies included measurement of ^{59}Fe-ferrokinetics, WBC and RBC counts, hematocrit, and hemoglobin. Platelet counts and WBC differentials were not made. Results of the mortality experiments are shown in Fig. 83. At the highest exposure

C-3

100
75
50
25
% MORTALITY
50
100
150
200
250
300
350
DAYS OF IRRADIATION
3.2 R/HR
SPLX
INTACT
1.6 R/HR
SPLX
INTACT
0.8 R/HR
SPLX
INTACT

Fig. 83

rate (3.2 R/hr) there was no different mean-after-survival (MAS) between splenectomized (MAS ∿58 days) and intact irradiation mice (MAS ∿58 days also) of similar age. A significant difference in survival was seen during the 1.6 R/hr exposures. The MAS (128 days) of the splenectomized mice was only 83% of that (155 days) of intact irradiated controls. Repetition of this experiment has confirmed this depression in survival rate. The MAS of the splenectomized mice in the second study was only 79% of that of intact mice. At our lowest exposure rate (0.8 R/hr) we found no significant difference in the survival times of intact (MAS ∿293 days) and splenectomized mice (MAS 298 days).

Thus, the radioprotective effect described after splenectomy and acute irradiation in mice and after splenectomy and continuous irradiation in rats was not found in our study using continuously irradiated C57BL/6 mice. To the contrary, splenectomy was detrimental to those irradiated at the 1.6 R/hr rate, which is the rate that produces the greatest splenic erythroblastic response. We analyzed histologic data to explain the inconsistency of the detrimental effect of splenectomy on the tolerance of mice for continuous radiation. Terminal histopathology of the mice in the mortality experiment at 1.6 R/hr consisted of an almost complete depletion of all hematopoietic elements in marrow of the splenectomized mice. Since the marrows of the intact mice contained myeloid and erythroid foci and the spleens of these mice often have significant hematopoietic foci, it is possible that the spleen is needed to reseed the marrow. The results obtained in the serial sacrifice experiments showed that the alterations of the peripheral RBC and WBC populations of the splenectomized mice coincide, both in time and magnitude, with those of their analogous intact irradiated

controls at both 1.6 and 3.2 R/hr, so we were unable to quantitate any effect of splenectomy on hematopoietic regenerative capacity in usual hematologic terms.

We had not previously studied lymphopoietic repair during low-dose-rate exposures, although it was well known that extensive lymphoid atrophy of all organs develops. We chose as a first approach to the problem of lymphoreticular repair to study the survival time patterns of several mouse strains under continuous irradiation at rates used clinically in total body irradiation therapy. We obtained lethality curves in relation to accumulated "doses" (R) in five strains of mice: $C3BF_1$, C57BL/6 Cum, C57BL/Cum, BALB/c, and AKR. Our studies on radiation suppression of erythropoiesis have been done principally on C57BL/6 Cum, because it is a long-lived radioresistant strain and upon C57BL/Cum, its radiosensitive parent strain. Our inclusion also of AKR strain mice was suggested by the recent study of Perkins et al. (25) who showed that the AKR mouse had an unusually low level of immuno-hematopoietic competence. This strain, well known for its 90% incidence of a virus-associated thymic lymphoma, has an exceedingly short (approximately 275 day) mean life span. It has a low resistance to promptly given single doses of radiation ($LD_{50/30}$ = ~600 R). For unknown reasons BALB/c is more radiosensitive even though much longer lived. Perkins et al. showed that the immunoincompetence of the AKR mouse is expressed in part by an inability to sustain the growth of exogenous colony-forming units in its spleen, a capability that we believe is required for compensatory erythropoiesis during continuous low-dose-rate irradiation. The AKR mouse seemed therefore to offer a unique opportunity in our system to study whether human therapy levels of irradiation would (1) alter the high lymphoma incidence of this

strain, (2) affect the leukemic process once it was initiated, and (3) decrease mean survival time by some process other than aplastic anemia. If the unusual immunoincompetence of this strain was worsened by irradiation, one might expect an earlier onset of thymic lymphoma in some animals along with a decrease in its incidence because of radiation-induced thymic destruction in others. Possibly also the reported immunoincompetence of this strain might be expressed as poor splenic production of endogenous erythroblasts with early death from aplastic anemia.

Fractionated doses of radiation (150 R at three weekly exposures) can shorten the latent period and increase the incidence of a similar leukemia in C57BL/6 mice and that 24 R/day (our lowest human therapeutic dose per day is approximately 10 R in LETBI) given to this mouse strain will increase the leukemia incidence from about 12% to about 60%. In AKR mice, however, previous studies of leukemogenesis have included leukemia induction time without alteration of the high incidence.

Two ages of AKR mice were available to us: 40-day-old females and "retired-breeder" females of uncertain age (about 120 days old). The two age groups were divided into three subgroups: unirradiated controls, irradiated mice at 1.6 R/hr or 37 R/day, and irradiated mice at 3.2 R/hr or 74 R/day. We observed the mice closely to obtain prompt necropsies for histologic study of the thymus, lungs, liver, spleen, and sternal bone marrow; yet about half were too autolyzed for histologic study but contributed data for determining the length of survival. Figure 84 is a graph of the percentage mortality of the AKR, C57BL/Cum, BALB/c, C57BL/6 Cum, and $C3BF_1$ strains under continuous irradiation at 1.6 R/hr, as a function of accumulated dose. The steeply rising curves of the other four strains stand in marked contrast with the slowly rising curve of the two age groups

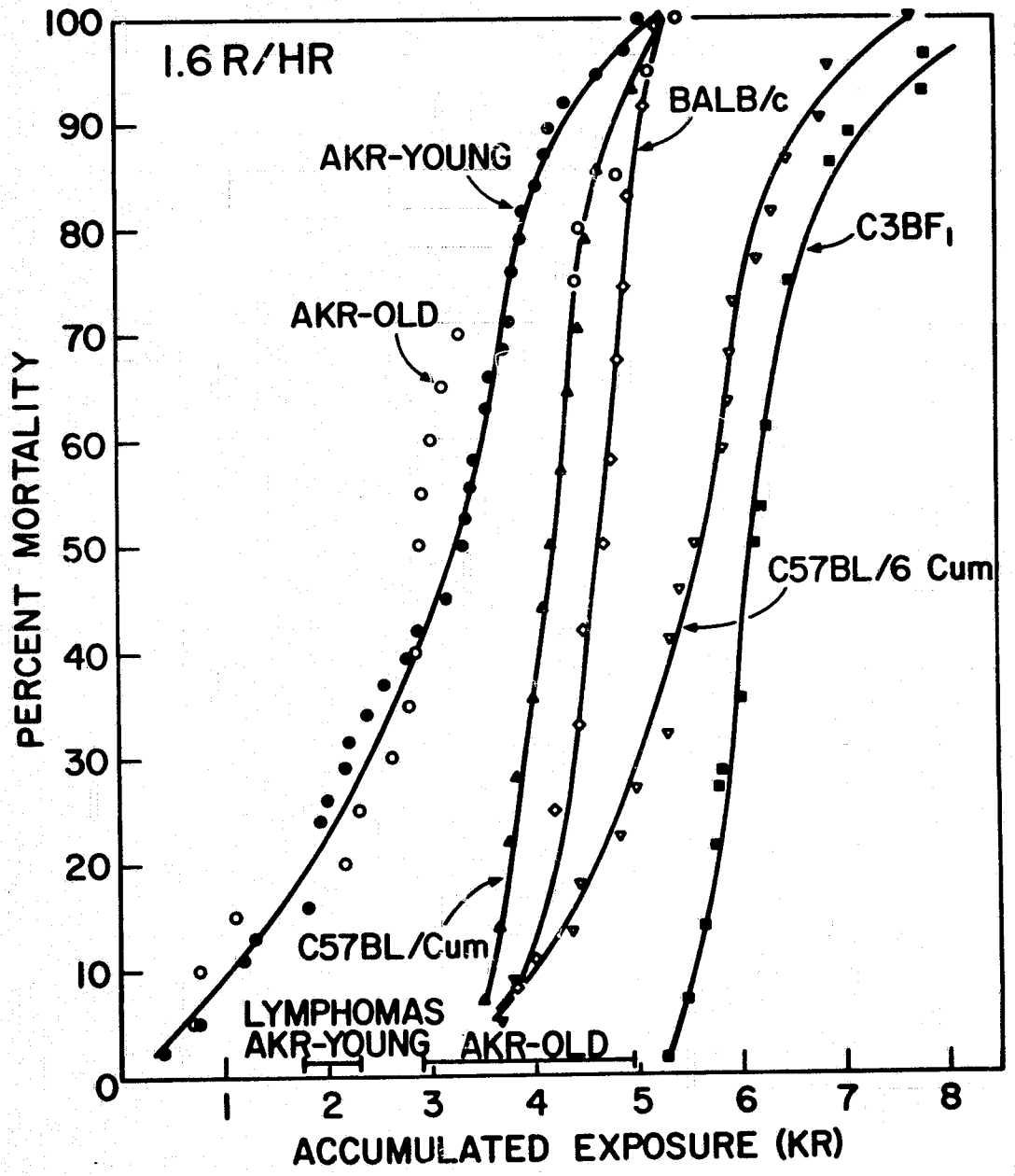
1.6 R/HR
AKR-YOUNG
BALB/c
C3BF1
AKR-OLD
C57BL/6 Cum
C57BL/Cum
LYMPHOMAS
AKR-YOUNG
AKR-OLD
PERCENT MORTALITY
ACCUMULATED EXPOSURE (KR)
0
10
20
30
40
50
60
70
80
90
100
1
2
3
4
5
6
7
8

Fig. 84

of AKR. At this low-dose-rate, surprisingly, there was no difference in apparent sensitivity between the 40-day-old and the "retired-breeder" AKR. This relatively slow rising curve for number of deaths per dosage-increment indicates a wide variance in radiosensitivity among different animals and suggests that more than one lethal mechanism may be operative. The first differentials of the other sigmoid curves are single-peaked distributions indicative of only one lethal process. The apparently sharp lower thresholds and the steepness of both seem to be related to homogeneity of the mice, here expressed as radiosensitivity. While the data are too few for mathematical differentiation of the AKR mortality curve, this irregularly rising line is roughly the sum of two separate subgroups of deaths that occur with peak incidences at quite different accumulated doses.

Gross anatomical and histologic studies in all groups were indicative of deaths occurring after more than 4000 R due to splenic and marrow atrophy.

The data from the histologic study of irradiated AKR mice at death were obtained for the young and adult groups exposed continuously at 1.6 and 3.2 R/hr. The data from 48 necropsies and histologic studies are summarized in Table 17 as percent incidence of lymphoma, thymic atrophy, lung adenosis and adenomas, complete splenic atrophy, and presence of splenic erythroblastic colonies. The approximate mean accumulated doses for the four groups are shown along with the average survival time. Unirradiated AKR mice have a mean life-span of about 275 days and their natural incidence of lymphoma is about 90% for females. Here the highest incidence of lymphoma was 40% and occurred in the adult mice at the lower exposure rate. We completely suppressed lymphoma in the 40-day-old mice exposed to 3.2 R/hr but this may simply mean that they did not live long enough to

TABLE 17

Incidence of Histopathologic Endpoints at Death
of AKR Mice from Continuous Irradiation at 1.6 and 3.2 R/hr

R/hr	Age (days)	MAD* (R)	Average survival time (days)	Lymphoma	Atrophy		Splenic erythroblastosis	Lung adenoma
					Thymus	Spleen		
				Percent				
1.6	40	3100	84 (124)†	17	82	53	39	44
1.6	120	3700	100 (∿220)	40	40	20	40	30
3.2	40	2600	35 (75)	0	100	77	23	55
3.2	120	2700	36 (∿150)	27	72	72	10	18

*MAD = accumulated dose at average survival time.

†Numbers in parentheses represent age at average survival time.

show it. The AKR mice of both age groups given 3.2 R/hr were the most radiosensitive that we have observed; mean accumulated dose at death was about 2600 R and complete thymic atrophy occurred within their 35-day survival period. Seventeen percent of these young mice irradiated at 1.6 R/hr developed lymphoma between 50 to 60 days of continuous irradiation, when they were 90 to 100 days old. The 27% of adult mice, on the other hand, that developed leukemia did so between accumulated doses of 1500 and 2500 R at 3.2 R/hr (20 to 34 days). However, accumulated doses between 2900 and 5000 R at 1.6 R/hr (78 to 135 days) were associated with the induction of lymphoma in 40%. Some of these late lymphomas could have been spontaneous rather than augmented by irradiation because these animals after 135 days of exposure were approaching their normal life span of 275 days. It is noteworthy that the thymus of only one mouse was nonleukemic and nonatrophic, in an adult female dying for unknown reasons after only 765 R with an apparently effective erythropoietic response of marrow and spleen. All other thymuses were either enlarged and lymphomatous or extremely small due to loss of lymphoid and histiocytic cells, sometimes with only the primitive epithelium remaining. This atrophy of the thymus was unrelated to presence or absence of a splenic erythropoietic response. Splenic erythropoiesis was quantitatively poor in all animals compared to similarly irradiated C57BL/6 Cum mice. When thymic lymphoma was present, its metastatic spread masked any normal splenic response to radiation-induced marrow damage. The reduced lymphoma incidence in the adult mice was not accompanied at the lower exposure rate by a decrease in induction time but was when they were exposed at the higher rate. The majority of mice at both ages and rates of exposure, that were free of lymphoma, appeared to die from complete marrow and splenic atrophy. For the first time in our experience in these

low dose rate studies, we noted that some of the early nonlymphomatous deaths were associated with bacteremias.

The occurrence of pulmonary adenomas (Table 17) was completely unexpected and, as far as we know from a cursory search of the literature, has not been reported in AKR mice even though this strain was derived originally from strain A mice having an extremely high incidence of these tumors. An atrophic thymus (or the absence of lymphoma?) seemed to be a necessary condition for this process to occur. Previously, others (26) have shown in young Swiss mice that after thymectomy there is an increase in both the spontaneous incidence of lung adenoma and the ease with which it is induced by carcinogens. This effect has been attributed to the impairment of immunocompetence that follows thymectomy and the observation may explain why the incidence of pulmonary adenomas was less in our adult AKR mice than in the young, since it is well known that thymic ablation has much less effect upon immune mechanisms in adult mice than in young ones. These lung tumors were minute and obviously just beginning to develop in many instances. Many would have been overlooked if only gross examinations had been made. In no instance were the tumors large enough to cause morbidity or death, although an occasional one filled a single lobe completely.

These observations at two dose rates of continuous radiation exposure suggest that: (1) AKR thymic lymphoma, if it develops during the treatment, is not suppressed by the irradiation, (2) if radiation-induced thymic atrophy develops quickly enough, leukemogenesis is prevented, and (3) radiation-induced thymic atrophy is similar to surgical thymectomy in releasing pulmonary-tumor formation from some normally constraining mechanism. The quantitative and qualitative differences in the responses of the two age groups probably reflect the well-known age differences in immunocompetence.

CHAPTER VI

A. List of Reports and Publications Generated by Program

1. Lushbaugh, C. C., Hofstra, R., Roth, R. E., and Andrews, G. A.: ED_{50} for Gastrointestinal Responses in Man. Radiation Res. 25: 114, May 1965 (abstract).

2. Andrews, G. A., Auxier, J. A., and Lushbaugh, C. C.: The Importance of Dosimetry to the Medical Management of Persons Accidentally Exposed to High Levels of Radiation. In Personnel Dosimetry for Radiation Accidents, IAEA, Vienna, August 1965.

3. Lushbaugh, C. C., Comas, F., Saenger, E. L., Jacobs, M.: Radiosensitivity of Man by Extrapolation from Studies of Total-body Irradiation of Patients (invited lecture, February 15, 1966). Radiat. Res. 27: 487-488, March 1966.

4. Andrews, G. A.: Treatment of Radiation Injury. J. Mississippi Med. Assoc. 7: 534-538, 1966.

5. Andrews, G. A., Lushbaugh, C. C., and Kniseley, R. M.: Proceedings of a Panel on Effects of Total-Body Irradiation in the Human Being. IAEA, Vienna, May 17, 1966.

6. Dalton, C. P. and Cloutier, R. J.: An Arrangement of Radioactive Sources for a Low-Exposure-Rate Total-Body Irradiation Facility. Physics in Medicine and Biology 12: 116, 1967.

7. Dalton, C. P. and Cloutier, R. J.: Source Arrangement for a Low-Exposure-Rate Total-Body Irradiation Facility for Man. USAEC Report ORINS-52, May 1, 1967, 205 pages.

8. Fanger, H. and Lushbaugh, C. C.: Radiation Death from Cardiovascular Schock Following a Criticality Accident: Report of a Second Death from a Newly Defined Human Radiation Death Syndrome. Arch. Path. 83: 446-460, May 1967.

9. Lushbaugh, C. C.: Editorial, Radiation and Shock. JAMA 200: 181, 1967.

10. Langham, W., editor: Space Radiation Study Panel: Radiobiologic Factors in Manned Space Flight. July 1, 1967.

    (1) Lushbaugh, C.C., Andrews, G. A., and Langham, W.: Prodromal Response, p. 76-90.

    (2) Conrad, R., Andrews, G. A., and Langham, W.: Hematologic Effects, p. 90-105.

    (3) Langham, W. and Lushbaugh, C. C.: Early Lethality, p. 105-124.

    (4) Thompson, J. and Andrews, G. A.: Chemical and Biological Protection, p. 218-230.

11. Lushbaugh, C. C., Comas, F., and Hofstra, R.: Clinical Studies of Radiation Effects in Man: A Preliminary Report of a Retrospective Search for Dose-Response Relationships in the Prodromal Syndrome. Radiat. Res. Suppl. 7: 398-412, November 1967.

12. Andrews, G. A.: Radiation Accidents and Their Management. Radiat. Res. Suppl. 7: 390-397, November 1967.

13. Lushbaugh, C.C.: Some Biological Endpoints of Dosimetric Value Derived from Clinical Data. In First International Symposium on Biological Interpretation of Dose from Accelerator Produced Radiation, March 13-16, 1967, E. J. Vallario, editor, DTIE CONF-670305.

14. Lushbaugh, C. C.: Recent progress in Assessment of Human Resistance to Total-Body Irradiation. In Proceedings of a Symposium Postattack Recovery from Nuclear War- Held at Fort Monroe, Virginia, November 6-9, 1967.

15. Lushbaugh, C. C., Comas, F., Edwards, C. L., and Andrews, G. A.: Clinical Evidence of Dose-Rate Effects in Total-Body Irradiation in Man. In The Proceedings of a Symposium on Dose Rate in Mammalian Radiation Biology, held April 29-May 1, 1968, Oak Ridge, Tennessee, CONF-680410.

16. Beck, W. L., Callis, E. L., and Cloutier, R. J.: Phantom Depth-Dose Measurements with Extruded LiF in a Low-Exposure-Rate Total-Body Irradiator. In Proceedings of the Second International Conference on Luminescence Dosimetry, September 23-26, 1968, USAEC Report CONF-680920, 1968, pp. 976-989.

17. Comas, F.V.: The Time Factor in Fractionated Irradiation of Mouse Skin. In The Proceedings of a Symposium on Dose Rate in Mammalian Radiation Biology, held April 29-May 1, 1968, Oak Ridge, Tennessee, USAEC Report, CONF 680410, pp. 18.1-18.12.

18. Comas, F. V., Andrews, G. A., and Nelson, B.: Spleen Irradiation in Secondary Hypersplenism. Amer. J. Roentgenol. 104: 668-673, 1968.

19. Lushbaugh, C. C., Comas, F. V., and Andrews, G. A.: Radiation Dose-Response Relations Derived from Clinical Data. Health Physics 15(2): 165-166, 1968 (abstract).

20. Bond, V.P., Osborne, J. W., Lesher, S., Lushbaugh, C. C., and Hornsey, S.: Panel Discussion on Mechanism of Intestinal Radiation Death. In Gastrointestinal Radiation Injury, Report of a symposium held at Richland, Washington, September 25-28, 1966. Excerpta Medica, March 1968, pp. 352-373.

21. Ur, A. and Lushbaugh, C. C.: Some Effects of Electrical Fields on Red Blood Cells and Electronic Red Blood Cell Sizing. Brit. J. Haemat. 15: 527-538, 1968.

22. Andrews, G. A.: The Therapeutic Use of Bone-Marrow Transplantation. In Proceedings of the International Conference on Leukemia-Lymphoma, Ann Arbor, 1967, edited by Chris J. D. Zarofonetic, Philadelphia, Lea and Febiger, 1968, pp. 423-432.

23. Lushbaugh, C. C.: Theoretical and Practical Aspects of Models Explaining "Gastrointestinal Death" and Other Lethal Radiation Syndromes. In Report of US/Japanese Symposium on Comparative Cellular and Species Radiosensitivity held in Kyoto, Japan, May 20-23, 1968. Edited by V. P. Bond, M. D. and Tsutomu Sugahara, M. D., Igaku Shoin Ltd., Tokyo, Japan, March 1969, pp. 288-297.

24. Lushbaugh, C. C., Frome, E. L., Davis, H. T., and Bibler, D. S.: The Power Spectrum of the Impedance Pneumograph: A Data Reduction System Producing an Analytical Parameter of Potential Clinical Usefulness. Aerospace Med. 40: 425-429, 1969.

25. Upton, A. C. and Lushbaugh, C. C.: The Pathological Anatomy of Total-Body Irradiation. In Atomic Medicine, 5th Edition. Charles F. Behrens and E. Richard King, editors, Williams and Wilkins Co., 1969.

26. Andrews, G. A., Kniseley, R. M., Vodopick, Helen, Bergner, P.-E. E., and Lushbaugh, C. C.: Hematologic Responses to Total-Body Irradiation, presented at Gesellschaft Fur nuclearmedizin, Wiesbaden, Germany, September 28, 1968.

27. Lushbaugh, C. C.: Reflections on Some Recent Progress in Human Radiobiology. In Advances in Radiation Biology, Vol. 3, edited by L. G. Augenstein, R. Mason, and M. Zelle, pp. 277-314, 1969.

28. Lushbaugh, C. C. and Auxier, J.: Reestimation of human LD_{50} Radiation Levels at Hiroshima and Nagasaki. Radiat. Res. 39, 526, 1969 (abstract).

29. Morris, A. C., Jr., Barclay, T. R., and Lushbaugh, C. C.: Monitoring Physiologic Response During Total-Body Irradiation Therapy. Second International Conference on Medical Physics, August 11-15, 1969, Boston, Mass. Phys. Med. Biol. 15: 192, 1970 (abstract).

30. Beck, W. L., Cloutier, R. J., Comas, F. V., and Lushbaugh, C. C.: Human Depth-Dose Estimates in Multidirectional Gamma-Ray Fields. Ibid. p. 144.

31. Upton, A. C., Cosgrove, G. E., and Lushbaugh, C. C.: The Induction of Glandular Carcinoma of the Stomach in Mice by Whole-Body Irradiation. US-Japan Conference on Experimental Carcinoma of the Glandular Stomach, Gann Monograph, 1970.

32. Corriil, L. S., Stokes, T. R., and Lushbaugh, C. C.: Accumulation Rates of GI and Marrow Damage in Pair-Irradiated Mice During Continuous and Fractionated Daily Exposures. Radiat. Res. 43, 271, 1970 (abstract).

33. Lushbaugh, C. C., Corrill, L. S., Stokes, T. R., Humason, G., and Lushbaugh, D.: Mouse Splenic Stem-Cell Response to Protracted Radiation Exposure. Radiat. Res. 43: 212-213, 1970 (abstract).

34. Cloutier, R. J. and Watson, E. E.: Radiation Dose from Radioisotopes in the Blood. In Medical Radionuclides: Radiation Dose and Effects. R. J. Cloutier, C. L. Edwards, and W. S. Snyder, editors. AEC Symposium Series No. 20, CONF-691212, 1970, pp. 325-346.

35. Balish, E., Pearson, T. A., and Chaskes, S.: Irradiated Humans: Microbial Flora, Immunoglobulins, Complement (C'3), Transferrin, Agglutinins, and Bacteriocidins. Radiat. Res. 43: 729, 756, 1970.

36. Comas, F. V., Edwards, C. L., and Vodopick, H.: Splenic Irradiation in Chronic Granulocytic Leukemia: Changes in Leukocyte Values. Radiat. Res. 42: 413-423, 1970.

37. Andrews, G. A., Balish, E., Edwards, C. L., Kniseley, R. M., and Lushbaugh, C. C.: Possibilities for Improved Treatment of Persons Exposed in Radiation Accidents. In Symposium on Handling of Radiation Accidents, IAEA-SM-119/56, 1970.

38. Ricks, Robert C., Lushbaugh, C. C., and Frome, E.: Changes in the Power Spectrum of the Impedance Pneumograph Trace During Radiation-Induced Gastrointestinal Distress in Man. Fed. Proc. 29(2): 451, 1970 (abstract).

39. Ricks, R. C. and Edwards, C. L.: The Effects of Dose Rate and Exposure Fractionation on Plasma Iron Kinetics in Rats and Man. Radiat. Red. 43: 240, 1970 (abstract).

40. Beck, W. L., Stokes, T. R., Cloutier, R. J., and Lushbaugh, C. C.: Dosimetry for Clinical Total-Body Irradiation. Am. Assoc. Phys. Med., Quart. Bull. 4: 2, 1970 (abstract).

41. Andrews, G. A., Comas, F. V., Edwards, C. L., Kniseley, R. M., Lushbaugh, C. C., and Vodopick, H.: Hematologic and Therapeutic Effects of Total-Body Irradiation (50R-100R) in Patients with Malignant Lymphoma, Chronic Lymphocytic and Granulocytic Leukemias, and Polycythemia. USAEC Report ORAU-112, 1970.

42. Andrews, G. A., Kniseley, R. M., Vodopick, H., Bergner, P.-E., and Lushbaugh, C. C.: Hematologic Responses to Total-Body Irradiation. In Radioisotope in Pharmakokinetik und klinischer Biochemie, F. K. Schattauer Verlag, Stuttgart-New York, pp. 517-527, 1970.

43. McDow, A. E., Jr. and Ricks, R. C.: Uses of a Time-Shared Computer in Quantitative Nuclear Medicine. In Proceedings of Symposium on Sharing of Computer Programs and Technology in Nuclear Medicine, Oak Ridge, 1971. USAEC Report CONF-710425, pp. 155-167.

44. Lushbaugh, C. C., Stokes, T. R., and Corrill, L. S.: Dose-Rate Dependence of Mouse Endogenous Splenic Colony Formation and Proliferation During Continuous and Fractionated Daily Irradiation at Low Exposure Rates. Radiat. Red. 47: 344, 1971 (abstract).

45. Ricks, R. C., Lushbaugh, C. C., McDow, E., and Frome, E.: Pulmonary-Impedance Power Spectral Analysis: A Facile Means of Detecting Radiation-Induced Gastrointestinal Distress and Performance Decrements in Man. Proc. Nat. Symposium on Natural and Manmade Radiation in Space. NASA TM X-2440, pp. 238-248, January 1972.

46. Yuhas, J. M., Stokes, T. R., and Lushbaugh, C. C.: Multifactorial Analysis of Human Blood Cell Responses to Clinical Total-Body Irradiation. Ibid., pp. 233-237.

47. Beck, W. L., Stokes, T. R., and Lushbaugh, C. C.: Dosimetry for Radiobiological Studies of the Human Hematopoietic System. Ibid., pp. 974-980.

48. Lushbaugh, C. C.: Predicted Levels of Human Radiation Tolerance Extrapolated from Clinical Studies of Radiation Effects. Ibid., pp. 398-415.

49. Lushbaugh, C. C. and Ricks, R. C.: Some Cytokinetic and Histopathologic Considerations of Irradiated Male and Female Gonadal Tissues. Proc. Symp. Mt. Sinai Cancer Clinic, 1970. University Park Press, 1972.

50. Ricks, R.C., Lushbaugh, C. C., and McDow, A. E., Jr.: Correlation of Heart Rate and CO_2 Production with Pulmonary Impedance During Exercise Stress in Man. Fed. Proc. 31: 311, 1972 (abstract 544).

51. Ricks, R. C., Lushbaugh, C. C., and McDow, A. E., Jr. Pulmonary Impedance Power Spectral Analysis: Its Correlation with Heart Rate and Expired CO_2 During Exercise Stress in Man. J. Assoc. Med. Instrum. 6: 186, 1972.

52. Stokes, T. R., Lushbaugh, D., Humason, G., and Lushbaugh, C. C. ^{59}Fe Studies on the Erythroblastic Response of Normal and Splenectomized Mice to Low Level Continuous Radiation. Radiat. Res. 51: 472-473, 1972 (abstract).

53. Beck, W. L., Cloutier, R. J., and Watson, E. E. Personnel Monitoring with Film and Thermoluminescent Dosimeters for High Exposures. Health Phys. 25: 421-425, 1973.

54. Cloutier, R. J., Watson, E. E., Rohrer, R. H., and Smith, E. M.: Calculating the Radiation Dose to an Organ. J. Nucl. Med. 14: 53-55, 1973.

55. Lushbaugh, C. C.: Human Radiation Tolerance. Chapter 10. In Space Radiation Biology and Related Topics. C. A. Tobias and P. Todd, eds., Academic Press, New York, 1973, pp. 475-522.

56. Lushbaugh, C. C.: Contribution to: HZE-Particle Effects in Manned Spaceflight. D. Grahn, ed. Radiobiological Advisory Panel, Committee on Space Biology, Space Science Board, National Research Council, Washington, National Academy of Sciences, 1973.

57. Lushbaugh, C. C.: Book Review: Manual on Radiation Haematology. A joint undertaking by IAEA and WHO, Technical Report Series No. 123, IAEA, Vienna, 1971. Health Phys. 24: 456, 1973.

58. Frome, E. L., Fredrickson, E. L., and Ricks, R. C.: Power Spectrum of the Respiratory System via the Pulmonary Impedance Pneumograph. In Proceedings of the 10th Biomathematics and Computer Science in the Life Sciences, Houston, Texas, 1973.

59. Beck, W. L., Stokes, T. R., and Lushbaugh, C. C.: Dosimetry for Total-Body Irradiation Therapy. In Health Physics in the Healing Arts, Seventh Midyear Topical Symposium, Health Physics Society, San Juan, Puerto Rico, December 1972. DHEW Publication (FDA) 73-8029, p. 423, 1973.

60. Cloutier, R. J. and Watson, E. E.: Radiation Doses from Nuclear Medicine Procedures. Ibid., pp. 71-78.

61. Ricks, R. C. and Lushbaugh, C. C.: Changes in Serum Creatine Phosphokinase (SCPK) Levels After Total-Body Irradiation. Aerospace Med., 1973.

62. Ricks, R. C. and Lushbaugh, C. C.: The Influence of ExerciseConditioning on the Performance Decrement Effects of Total-Body Irradiation. Health Phys. 27: 614, 1974 (abstract).

63. Ricks, R. C. and Lushbaugh, C. C.: Quantitation of Radiation-Induced Changes in Man. Rad. Res. 59: 39, 1974 (abstract).

64. Lushbaugh, C. C. and Yuhas, J. M.: Pathological Features of Radiation-Induced Murine Pulmonary Carcinomas and Their Metastases. Rad. Res. 59: 222, 1974 (abstract).

B. Medical Division Documented Computer Programs for NASA Study

These programs were written by Earl McDow, Edward Frome, Paulette Aarom, and Mona Smith and are available on request from the Computer Facility, Medical Division.

1. Greater Than Eight Days Nursing Notes Program - Summarizes the nurses notes for response to nausea, anorexia, and/or vomiting. A modification summarizes for less than eight day exposures.

2. Greater Than Eight Days Hematology Program - Lists data for WBC, platelets, and RBC for the period of exposure plus 45 days. A modification summarizes for less than eight day exposures.

3. Total Audit Program - Gives a general audit of the data in the Retrospective Studies Data Bank with respect to the number of patients, cases of exposure, males, females, etc. Modifications make audits of the groups of exposure such as greater than eight day exposure, less than eight day exposure, Heublein exposure, and single exposure.

4. Hematology Plot Program - Plots the WBC and platelet count values for a patient's period of exposure in linear and logrithmic form. Multiple plots are made for exposures of greater than 42 days.

5. Probit Analysis Program - Calculates the value for a and b in the equation $y = a + bx$, the probits, and the confidence limits for given input data. A plot is then made of the line and the confidence limits.

6. Identification Summary Program - Summarizes the identification data for the greater than and less than eight day exposure patients.

7. Diagnosis Addition Program - Adds the diagnosis codes to the already existing summary tapes.

8. Tape Correction Program - Makes any corrections to existing data bank tapes in maintenance of the data bank.

9. Nursing Notes Program for Portal Irradiation - Summarizes responses of anorexia, nausea, and vomiting for portal irradiation exposures.

10. Response Summary Program for Portal Irradiation - Writes to magnetic tape summary of positive nurses' notes responses and gives listing of all patient summaries.

11. Portal Irradiation - Weibull Function Program - Studies radiation sickness using the Weibull model. Calculates responses and nonresponses for each dose from 1 to 40 and calculates cumulative response. Does linear regression analysis using the Weibull model.

12. Portal Irradiation Frequency Program - Calculates the frequency of positive response to anorexia, nausea, and vomiting for each patient and groups the frequencies, calculates the pretreatment response frequencies, and does a grouping for all patients according to those frequencies.

13. POUSP - Plots the raw power spectra of the pulmonary impedance data in three dimension for publication.

14. VARPT - Plots the average variance of the pulmonary impedance waveform as a function of frequency in final form for publication.

15. ECOSV - Maintains the integrity of the digital output groups when used by multiple users.

16. GT8M0, GT8M1, GT8M2, GT8M3, GT8M4 - Plots the greater than eight day multiple exposure NASA data.

17. LMP1, LMP2, LMP3, LMP4, LMP5 - Formats the hematology data on the LETBI and METBI patients and plots various blood values as a function of time.

18. MDISK - Provides the FORTRAN user with a fast and easy method of assessing complete disk sectors within a disk data file. MDISK uses DISKN and provides both READ and WRITE functions on the file protected data files.

19. LETBI (PULM, RR, BTIME, LETB2) - A combination of INSKEL subroutines which handle the real time data acquisition from the LETBI console.

20. GHIST - Plots a histogram of the RR interval frequency table.

21. MTCLS and MTSET - Used to maintain on disk a current disk file of all LETBI tape numbers.

22. MPCOR - Plots on the IBM 1627 the total variance of the pulmonary impedance as a function of mean heart rate for each one minute interval and each average over 4 minutes.

23. PSPEC - Plots the percent frequency of the RR interval frequency table as a function of heart rate.

24. LETAN - Maintains the LETBI tape files and calculates the variables required by the investigator. This program is changed by adding additional subroutines as the desires of the researcher change.

25. MRDDF - Reads a requested record from the LETBI disk file LETBD and formats the data into array TBUF which is stored in COMMON for use by all other LETBI programs and written on tape for permanent storage of LETBI data.

26. SDIFF - Calculates differences between elements in an array vector. Used in the calculation of the power spectral estimates of the pulmonary impedance.

27. FAFT2 - Used by FTREA in the calculation of the Fourier transformation of an array X.

28. QRX1 - Provides access to the digital output points used to control the function lights on the LETBI console.

29. FTREA - Calculates the Fourier transform of a real valued series using the FFT alogrithm.

30. MVAR - Calculates the variance (low, medium, and high frequency), total average variance, and mean from the values in array PS.

31. IDXPN - Takes the digital identification data from the LETBI control box packed in five words and formats the data into seven words for inclusion in TBUF.

32. RHIS - Will expand two eight bit binary numbers packed in one word to two 16-bit words, i.e., /XXYY is expanded to /00XX and /00YY.

33. MLIST - Prints the results of the analysis of the pulmonary impedance and RR interval data.

34. MEANR - Calculates the number of observed events, the mean, and the standard deviation of the mean from a given frequency table. MEANR is used by the LETBI analysis program to calculate the number of heart beats, the mean RR interval, and the standard deviation of the mean interval.

35. ID99 - Removes all records with greater than 99 days exposure record from hematology tapes.

36. SERCH - Reads and selects from concatenated data sets all records of a chosen format; records data collectively on magnetic tape.

37. PRBIN - Selects required data according to a given method for a probit analysis from collected data.

38. MANLY - MANLY can perform two functions: If (1) the operator requests analysis of the LETBI data and (2) analysis has not been done on a set of data, MANLY does the analysis using the required subroutines and then writes the tape record (TBUF). If analysis has been done or is not desired, the subroutine writes the record with TBUF unchanged. When four data sets (1-4) have been analyzed, MANLY calculates the average RR and pulmonary values for four minutes and sets NSET=5 and writes TBUF (average values) on tape.

39. MPSA - Calculates the power spectral estimates of the pulmonary impedance data obtained from the LETBI data acquisition program.

40. MLOGL - Prints on the 1053 a log of the LETBI data processed.

CHAPTER VII

APPENDIX

A. List of Cooperating Institutions in Retrospective Studies

Hospitals Participating in Study

Albert Einstein Medical Center
Baylor University: Jefferson Davis Hospital
V.A. Hospital at Houston
Texas Medical Center
Burge Protestant Hospital
Cincinnati General Hospital
City of Hope Medical Center
Charity Hospital
Colorado General Hospital
Ellis Fischel State Cancer Center
Franklin Hospital
Jefferson Medical College
Long Beach Community Hospital
Los Alamos Hospital
Mary Imogene Bassett Hospital
Massachusetts General (McG) (LR)
M.D. Anderson Hospital
Medical College of Virginia
New York Memorial Hospital (CH) (N)
Oak Ridge Associated Universities Medical Division
Penrose Cancer Clinic
Peter Bent Brigham Hospital
Portland: Emanuel Hospital
Dr. Hyman's Clinic
Portland Medical Center
Princess Margaret Hospital
Providence Hospital
Rhode Island Accident
Spokane: Deaconess Hospital
Rockwood Clinic
Sacred Heart Hospital
Milo Harris Clinic
Swedish Hospital
Temple University
Thomas M. Fitzgerald Mercy
U.S. Naval Hospital
U. of California Medical School, S.F.
U. of Michigan
U. of Washington
V.A. Hospital at Denver
V.A. Hospital at Long Beach
V.A. Hospital at New Orleans
Vancouver: British Columbia Cancer Institute
Royal Columbian Hospital
Vancouver General Hospital
White Memorial Medical Center

B. List of Contributing Medical Division Staff Members

Medical	Paramedical	Computer
E. G. Ammerman	E. A. Anderson	Paulette Aaron
G. A. Andrews	Normal Asbury	Thomas Akin
Edward Bird	Mildred Bailey	Robert Beaver
F.V. Comas	Frances Banner	Linda Brown
C. L. Edwards	T. R. Barclay	Ed Frome
Dieter Emrich	W. L. Beck	Arthur Glaster
Kong-oo Goh	Per-Erik Bergner	Martha Hansard
F. A. Goswitz	Sarah Cecil	Janice Ishee
K. F. Hubner	Carol Chabot	Earl McDow
R. M. Kniseley	Kay Clayton	Daniel McFaddin
C. C. Lushbaugh	Martha Clevenger	Richard Queener
B. Nelson	R. J. Cloutier	Mona Smith
Etna Palmer	Shirley Colyer	Jimmie Sanders
Ryosaku Tanida	Lydia Corrill	
M. Van Woert	J. T. Crockett	
H. A. Vodopick	Evelyn Cunningham	
	Glenda Fritts	
	Dorothy Gaither	
Lucy Amburn	W. D. Gibbs	
Margie Bagley	J. H. Harmon	
Carol Bingham	Joyce Hewins	
Margaret Blackburn	Wanda Hodge	
Ervin Bobo	Harold Hodges	
Helen Brinker	Elizabeth Holloway	
Ruth Capshaw	Julia Hopper	
James Cozart	Mildred Hyp	
Mary Nell Craig	Gretchen Humason	
John Dean	Jane Kimbro	
Thelma Eden	Barbara LeClerc	
Eria Hartman	Kathryn Lore	
June Geldmeier	Willa Fae Loveday	
Mable Helton	Dorothy Lushbaugh	
Rita Holt	Kathryn McCulloch	
Rufus Jackson	Maryrose McGown	
Earl Jacobs	Jean McIntyre	
Sandra Landry	A. C. Morris	
Martha Laxton	Francine Pennington	
Bedford Mayott	Evalyn Repplinger	
Barbara Nance	Robert Ricks	
Benua Pack	Emily Roemer	
Garfield Porter	Elizabeth Rupp	
Naomi Presnell	Billie Ryan	
Mary Rogers	Evelyn Sipe	
Bernice Salley	Vivian Smith	
Lillie Simmons	T. R. Stokes	
Marilyn Smith	Katherine Stubbs	
Elaine Stoetzel	Mary Thomas	
Mary Sutliff	Mary Watkins	
Eugene Weaver	Allen Webb	
Martha Williams	Sondra Wilson	
Lillie Woods		

CHAPTER VIII

FIGURE LEGENDS

Fig. 1 The cumulative onset of anorexia for all patients, plotted on probability-log scales. The time scale represents treatment days, not number of fractions. In the probability scale is represented the percentage of patients who have had anorexia up to the designated day.

Fig. 2 The cumulative onset of anorexia for patients who were anoretic before irradiation (open circles) and for those who were not previously anoretic (closed circles). See legend on Fig. 1 for further details.

Fig. 3 The cumulative onset of nausea for all patients. See legend on Fig. 1 for details.

Fig. 4 The cumulative onset of nausea for patients who were nauseated before irradiation (open circles) and for those without previous nausea (closed circles). Shee legend of Fig. 1 for further details.

Fig. 5 The cumulative onset of vomiting for all patients. See legend on Fig. 1 for details.

Fig. 6 The cumulative onset of vomiting for patients who were vomiting before irradiation (open circles) and for those who previously did not vomit (closed circles). See legend on Fig. 1 for further details.

Fig. 7 Cumulative probability of onset of anorexia, nausea, and vomiting in patients receiving portal irradiation.

Fig. 8 Conditional probability of onset of anorexia, nausea, and vomiting in patients receiving portal irradiation.

Fig. 9 Conditional probability, in patients receiving portal irradiation, to become anorectic or nauseated or to vomit for the second time.

Fig. 10 Overall probability of three kinds of responses in patients receiving portal irradiation.

Fig. 11 Cutaway model of the ORAU total-body irradiation facility. "Radiation-safety" measurements with all sources "OFF."

Fig. 12 Entrance to maze into ORAU total-body irradiation room.

Fig. 13 Effect of beam-shaping filters.

Fig. 14 Gamma-energy spectrum vs. filter thickness. Increasing shades of darkness shows the introduction of a thicker filter series.

Fig. 15 Exposure attenuation curve.

Fig. 16 Cutaway diagram of low-exposure-rate total-body irradiation facility (LETBI) showing:

A. Concrete shielded radiation containment room.

B. Centrally positioned radiation exposure living room.

C. The remote control room for operation of the ^{60}Co sources (only sources numbers 1, 2, 5, 6, 7, C and F are shown), radiation exposure level supervision, nursing, and physiologic surveillance of the patient.

D. The on-line computer and data processing room.

Fig. 17 A simulated closed-circuit TV view of a patient in the radiation exposure living room (Fig. 16, room B) showing the two centrally placed studio couches and other furnishings.

Fig. 18 Drawing of the LETBI console. The source controls and radiation monitors are located to the left, the TV monitor and intercom are in the center panel, and the physiologic monitoring and recording sections are located to the right.

Fig. 19 Interfacing diagram showing the types of analog and digital signals flowing from the LETBI console to the IBM-1800 computer.

Fig. 20 LETBI console unit in operation. Progress of the patient's irradiation is being monitored by the operator and attending nurse.

Fig. 21 Block diagram for the physiologic monitor in the LETBI facility.

Fig. 22 Cutaway side view showing the arrangement of the monitoring and computing equipment for a radiation treatment.

Fig. 23 Electrode and amplifier block diagram showing the method of obtaining cardiac and respiratory signals from the same set of applied electrodes.

Fig. 24 Position of monitoring electrodes on a patient.

Fig. 25 Patient wearing the interconnecting webbed belt and the umbilical cord. The quick-disconnect assembly located about a foot down the umbilical cord permits the patient to use lavatory facilities in an adjacent room without having to disengage his electrodes.

Fig. 26 Electric field interference schematic.

Fig. 27 Magnetic field interference schematic.

Fig. 41 Pulmonary impedance tracings from patient exposed to 150 R (30 R daily) at 1.5 R/hr. Figures in parenthesis indicate accumulated R at time of pulmonary monitoring.

Fig. 42 Power spectra of pulmonary impedance waveforms obtained at specific intervals before, during, or immediate after exposure to 150 R (30 R/day) at 1.5 R/hr. Figures in parenthesis indicate accumulated R at time of pulmonary monitoring.

Fig. 43 Power spectra of pulmonary impedance waveforms obtained over a 1 hr time period in a normal volunteer following administration of an emetic (ipecac).

Fig. 44 Time series graph of average and continuous pulmonary impedance power spectral variances obtained over a 60 minute period in a normal subject following ingestion of ipecac.

Fig. 45 Effect of nausea and vomiting on pulmonary impedance in a female patient exposed to 500 R (40 R/min) total-body gamma irradiation prior to bone marrow transplantation.

HETBI same as VDRIF (high exposure rate total body irradiator).

Fig. 46 The effect of nausea and vomiting on pulmonary impedance in a radiation accident victim exposed to 260 rem total body gamma irradiation at the rate of 350 R/min.

Fig. 47 Changes in pulmonary impedance (power spectral) variance in a normal volunteer monitored electronically before, during, and after exercise on a bicycle ergometer.

Fig. 48 Graphic representation of normal man's response to controlled exercise on a bicycle ergometer. The progressive early reduction in average pulmonary-impedance variance during exercise is indicative of adaptation to the controlled ergometry. No significant changes are notable in the response before and after exercise.

Fig. 49 Average changes in pulmonary impedance (power spectral) variance during standard exercise periods obtained before, during, and after total body irradiation at 1.5 R/hr in a patient treated with 100 R for chronic leukemia. (Exercise load was 60 watts, 9 min duration.) In one each specific performance period the first data point represents the preexercise pulmonary impedance, followed by the exercise phase and subsequent recovery.

Fig. 50 Average pulmonary impedance (power spectral) variance for exercise periods obtained before, during, and after total-body irradiation at 1.5 R/hr in a patient treated with 150 R for idiopathic thrombocythemia. (Exercise load was 25 watts, 5 min duration.) On each specific performance period the first data point represents the preexercise pulmonary impedance followed by the exercise phase and subsequent recovery.

Fig. 51 Exercise-tolerance profiles from patients receiving protracted or fractionated irradiation therapy and who were subjected to controlled exercise stress. Each patient performed the same workload on successive trials. Results are normalized to preirradiation values and demonstrate the difference in the response of the normal, unirradiated and irradiated man to exercise stress. Normal man rapidly adapts to stress whereas the irradiated man shows periods of performance decrements dependent upon exposure.

Fig. 52 Composite graph illustrating the effects of a stepwise increase in exercise workload in pulmonary-impedance variance, cardiac rate, and alveolar CO_2 concentration. Test subject was normal male aged 32 years. Exercise period consisted of alternate 2-min work/rest cycles at 50-, 100-, 150-, and 200-watt workloads, respectively, as indicated by peaks in cardiac rate.

Fig. 53 Graphic representation of exercise tolerance profile and tolerance time in a normal man accidentally exposed to 260 rem gamma radiation. Due to thrombocytopenia no exercise stress was applied from days 23 through 38 although physiologic monitoring was continued.

Fig. 54 Pulmonary-impedance power-spectral analysis from nonexercising, irradiated patients before, during, and after protracted total body exposures. Except for patients receiving 250 R (whose higher variance may be due to splenomegaly) those exposed to 100 R or 150 R demonstrate little pulmonary-impedance change in the absence of controlled exercise stress.

Each subject was monitored in a sitting position for 15 min to assure basal physiologic conditions and then for periods up to 30 additional min. These data indicate that the performance-decrement effects of total body irradiation are not expressed until the individual is stressed (although only low levels of exercise are required).

Figs. 55, 56, 57 Changes in pulmonary impedance variance in Shetland ponies exposed to 270 R (30 R/16 hr day) whole body gamma irradiation. Half of the animals in each group were conditioned for 6 weeks prior to irradiation insult, the others were stressed for only one week to establish baseline data prior to irradiation. Controls were forced to stand to simulate conditions during irradiation in non-control groups.

Fig. 58 Graphic representation of the relationship between variance of pulmonary impedance and simultaneously measured alveolar CO_2 concentration in a normal male volunteer stressed under controlled exercise conditions. Data for CO_2 recorded breath-by-breath on a Beckman LB-2 medical gas analyzer and averaged every 15 sec. These data can be used to further determine the difference in exercise response between the irradiated and normal man.

Fig. 59 Graphic correlation between pulmonary impedance variance and oxygen consumption measured during submaximal exercise stress.

Fig. 60 Effect of total-body irradiation on cardiac rate and predicted maximal O_2 consumption during controlled exercise stress testing.

Fig. 61 Graphic correlation of hematocrit and mean analyzer channel number for various-sized RBC showing method of establishing the scaling factor for converting channel number to cubic microns.

Fig. 62 Graph showing progressive decrease in MCV of RBC of neonatal mice, comparing the hematocrit/RBC data with those obtained electronically.

Fig. 63 Normal frequency distribution curve of RBC volumes compared with those of the RBC of a patient nine days after 300 r total body gamma irradiation.

Fig. 64 Normal frequency distribution curve of RBC volumes compared with those of the RBC of a patient with folic acid blockade produced by Methotrexate.

Fig. 65 Graph showing the rates of increase in erythrocyte sizes in blood stored in ACD at 40°F for 30 to 75 days. The blood was obtained by phlebotomy during the course of therapy of nine patients with polycythemia. Initially all were microcytic. The increase in size is expressed by the squared difference index, a statistical measurement of the degree of difference between the initial and each new measurement.

Fig. 66 Histographic distributions of the serum trypsin-inhibitor levels found in 30 determinations in normal persons, 56 in patients with anemias but without hematopoietic malignancies, 15 in patients with active or inactive toxic goiter, 13 in 5 patients with active thyroid carcinoma, 13 in 10 patients whose thyroid carcinoma is arrested, 46 in 4 patients with active Hodgkin's disease, and 3 with Hodgkin's disease suppressed by therapy; and multiple determinations in 4 patients with myelofibrosis and 5 patients with polycythemia vera. All were measured in the same 5 consecutive calendar months. See text for further explanation.

Fig. 67 Graph of the serum trypsin-inhibitor measurements in patients with thyroid disease (shown in Fig. 66) according to the calendar dates of their measurement. The dots connected by lines represent measurements in the same patient. The mean normal value and two standard deviations of the mean are shown at 3/25. The cross designates the death of one patient.

Fig. 68 Serum trypsin-inhibitor levels in patient receiving periodic whole body irradiation therapy (10 R each treatment, 1.5 R/min).

Fig. 69 Serum trypsin-inhibitor levels in a patient who received 500 rads prior to bone marrow transplantation.

Fig. 70 Serum CPK enzyme levels obtained from a radiation accident victim exposed to 260 rem TBI.

Fig. 71 Serum creatine phosphokinase levels from four normal male volunteers performing in two or three controlled exercise periods per week over a one-month period. (Pulmonary-impedance response shown in Fig. 48.) Values are normalized to the pretest sample value. Results are typical for expected SCPK levels for nontrained individuals stressed at submaximal levels for shorter periods.

Fig. 72 Serum creatine phosphokinase levels in four nonexercise-stressed patients exposed to 100 R protracted irradiation therapy and normalized to preexposure levels. Although no exercise stress was administered, these patients responded as stressed; the radiobiological mechanism is not understood at this time.

Fig. 73 Serum creatine phosphokinase levels in four nonexercise-stressed patients exposed to 150 R protracted irradiation therapy and normalized to preexposure levels. The magnitude and timing of the response is similar to those seen when 100 R is administered (Fig. 72).

Fig. 74 Serum creatine phosphokinase levels in three nonexercise-stressed patients exposed to 100 R or 150 R fractionated irradiation therapy and normalized to preexposure levels. Individual responses are similar to those seen during protracted exposures.

Fig. 75 Serum CPK enzyme levels obtained from a nonexercising patient who received both protracted (150 R, 30 R/20-hr day) and fractionated (15 daily 10 R fractions) TBI.

Fig. 76 CPK values obtained from a patient exposed to 250 R TBI.

Fig. 77 CPK values obtained from a patient exposed to 500 rads prior to bone marrow transplant.

Fig. 78 CPK values obtained from $C3BF_1$ mice exposed to 450 R TBI.

Fig. 79 Graphic representation of the relationship between SCPK levels and DEC in a patient exposed to 140 R total body therapeutic irradiation and controlled exercise stress. Values for SCPK are normalized to preexercise levels. These isolated data indicate that rising creatine phosphokinase levels may reverse the physiological process responsible for radiation-induced fatigue. However, the mechanism is not explained by this limited data.

Fig. 80 Smoothed averages of the body weights of mice exposed discontinuously and continuously to total body irradiation with the same daily doses. In every instance the mice given their daily exposure quickly (3.7 R/min) lost weight more rapidly than those exposed for 22 hr/day.

Fig. 81 Smoothed averages of changes in splenic weight of mice during discontinuous (METBI) and continuous (LETBI) gamma irradiation. They are expressed as spleen/total-body-weight ratios to correct for the fluctuations in total-body weight shown in Fig. 80.

Fig. 82 Graphic illustration of spleen weight in mice correlated with accumulated exposure and colony formation.

Fig. 83 Cumulative percent mortality of splenectomized and intact C57BL/6 male mice irradiated continuously ($\sim$23 hr/day) at 0.8 R/hr, 1.6 R/hr, or 3.2 R/hr.

Fig. 84 Percent mortality as a function of accumulated dose for five strains of mice irradiated continuously (23 + hr/day at 1.6 R/hr).

BIBLIOGRAPHY

1. Mayneord, W. V. and Clarkson, J. R.: Energy Absorption. II, Part 1, Integral Dose When the Whole-Body is Irradiated. J. Radiol. 17: 151-157, 1944.

2. Wright H. Langham, ed., Radiobiologic Factors in Manned Space Flight. National Academy of Sciences, National Research Council, Publication No. 1487, 1967.

3. Lushbaugh, Clarence C. Human Radiation Tolerance. Chapter 10. In Space Radiation Biology and Related Topics. Academic Press, 1974. Cornelius A. Tobias and Paul Todd, editors.

4. Bergey, G. E., Sipple, W. C., Hamilton, W. A., and Squires, R. D.: A Quantitative Impedance Pneumograph. NADC-MR-6622, Naval Air Development Center, Johnsville, Pa., Aerospace Medical Research Dept., 10 November 1966, 33 p.

5. Geddes, L. A. and Hoff, H. E.: The measurement of physiologic events by electrical impedance. Am. J. Med. Electron. 3: 16-17, 1964.

6. Geddes, L. A., Hoff, H. E., Hickman, D. M., and Moore, A. G. The Impedance Pneumograph. Aerospace Med. 33: 28-33, 1962.

7. Pasquali, E.: Problems in Impedance Pneumography: Electrical Characteristics of Skin and Lung Tissue. Med. Biol. Eng. 5: 249-258, 1967.

8. Pacela, A. F.: Impedance Pneumography - A Survey of Instrumentation Techniques. Med. Biol. Eng. 4: 1-15, 1966.

9. Day, J. L. and Lippitt, M.W., Jr.: A Long-Term Electrode System for Electrocardiography and Impedance Pneumography. Psychophysiol. 1: 174-182, 1964.

10. Geddes, L. A., Hoff, H. E., Vallbona, C., Harrison, G., Spencer, W. A., and Canzoneri, J.: Numerical Indication of Indirect Systolic and Diastolic Blood Pressures, Heart and Respiratory Rate. Anestheosiol. 25: 861-866, 1964.

11. Geddes, L. A.: The Acquisition of Physiological Data. Int. Anesthesiol. Clin. 3: 379-405, 1965.

12. Montes, L. F., Day, J. L., and Kennedy, L.: The Response of Human Skin to Long-Term Space Flight Electrodes. J. Invest. Dermatol. 49: 100-102, 1967.

13. Day, J. L.: Review of NASA-MSC Electroencephalogram and Electrocardiogram Electrode Systems Including Application Techniques. NASA Technical Note, NASA TN D-4398, 1968.

14. Tukey, J. W.: Discussion, Emphasizing the Connection Between the Analysis of Variance and Spectrum Analysis. Technometrics 3: 191-219, 1961.

15. Davis, H. T. and Jones, R. H.: Tests for Time Series Based on the Periodogram. Johns Hopkins University, Technical Report No. 79, 1967.

16. Walter, D. O. and Adey, W. R.: Spectral Analysis of Electroencephalograms Recorded During Learning in the Cat, Before and After Subthalamic Lesions. Exp. Neurol. 7: 481-501, 1963.

17. Pacela, A. F.: Impedance Pneumography - A Survey of Instrumentation Techniques. Med. Biol. Eng. 4: 1-15, 1966.

18. Jenkins, G. M.: General Considerations in the Analysis of Spectra. Technometrics 3: 133-166, 1961.

19. Blackman, R. B. and Tukey, J. W.: The Measurement of Power Spectra. Dover Publications, Inc., New York, 1958.

20. Lushbaugh, C. C., Frome, E. L., Davis, H. T., and Bibler, D.S.: Power Spectrum of the Impedance Pneumograph: A Data Reduction System Producing an Analytical Parameter of Potential Clinical Usefulness. Aerospace Med. 40(4): 425-429, 1969.

21. Astrand, Per-Olof and Rodahl, Kaare: Appendix 1, Textbook of Work Physiology, McGraw-Hill Book Co., 1970.

22. Anderson, K. Lange, Shepard, R. J., and Denolin, H.: Chapter 8. Fundamentals of Exercise Testing. World Health Organization, Geneva, 1971.

23. Saltin, B., et al.: Response to Submaximal and Maximal Exercise After Bedrest and Training. Circulation 38(7): 1968.

24. Hunter, J. B. and Critz, J. B.: Effect of Training on Plasma Enzyme Levels in Man. J. Appl. Physiol. 31: 20-23, 1971.

25. Perkins, E. H. and Makinodan, T.: Defective Immunohematopoiesis in Young, Adult Mice of the Leukemia-Prone AKR Strain. J. Nat. Cancer Inst. 46: 845-859, 1971.

26. Trainin, N. and Linker-Israeli, M.: In Immunological Parameters of Host-Tumor Relationships. D. W. Weiss, ed., Academic Press, New York, 1971, p. 36.